Geochemical Evolution of Water in the Madison Aquifer in Parts of Montana, South Dakota, and Wyoming

U.S. GEOLOGICAL SURVEY PROFESSIONAL PAPER 1273-F

AVAILABILITY OF BOOKS AND MAPS OF THE U.S. GEOLOGICAL SURVEY

Instructions on ordering publications of the U.S. Geological Survey, along with prices of the last offerings, are given in the current-year issues of the monthly catalog "New Publications of the U.S. Geological Survey." Prices of available U.S. Geological Survey publications released prior to the current year are listed in the most recent annual "Price and Availability List." Publications that are listed in various U.S. Geological Survey catalogs (**see back inside cover**) but not listed in the most recent annual "Price and Availability List" are no longer available.

Prices of reports released to the open files are given in the listing "U.S. Geological Survey Open-File Reports," updated monthly, which is for sale in microfiche from the U.S. Geological Survey, Books and Open-File Reports Section, Federal Center, Box 25425, Denver, CO 80225. Reports released through the NTIS may be obtained by writing to the National Technical Information Service, U.S. Department of Commerce, Springfield, VA 22161; please include NTIS report number with inquiry.

Order U.S. Geological Survey publications **by mail** or **over the counter** from the offices given below.

BY MAIL

Books

Professional Papers, Bulletins, Water-Supply Papers, Techniques of Water-Resources Investigations, Circulars, publications of general interest (such as leaflets, pamphlets, booklets), single copies of Earthquakes & Volcanoes, Preliminary Determination of Epicenters, and some miscellaneous reports, including some of the foregoing series that have gone out of print at the Superintendent of Documents, are obtainable by mail from

U.S. Geological Survey, Books and Open-File Reports
Federal Center, Box 25425
Denver, CO 80225

Subscriptions to periodicals (Earthquakes & Volcanoes and Preliminary Determination of Epicenters) can be obtained ONLY from the

Superintendent of Documents
Government Printing Office
Washington, D.C. 20402

(Check or money order must be payable to Superintendent of Documents.)

Maps

For maps, address mail orders to

U.S. Geological Survey, Map Distribution
Federal Center, Box 25286
Denver, CO 80225

Residents of Alaska may order maps from

Alaska Distribution Section, U.S. Geological Survey,
New Federal Building - Box 12
101 Twelfth Ave., Fairbanks, AK 99701

OVER THE COUNTER

Books

Books of the U.S. Geological Survey are available over the counter at the following Geological Survey Public Inquiries Offices, all of which are authorized agents of the Superintendent of Documents:

- **WASHINGTON, D.C.**--Main Interior Bldg., 2600 corridor, 18th and C Sts., NW.
- **DENVER, Colorado**--Federal Bldg., Rm. 169, 1961 Stout St.
- **LOS ANGELES, California**--Federal Bldg., Rm. 7638, 300 N. Los Angeles St.
- **MENLO PARK, California**--Bldg. 3 (Stop 533), Rm. 3128, 345 Middlefield Rd.
- **RESTON, Virginia**--503 National Center, Rm. 1C402, 12201 Sunrise Valley Dr.
- **SALT LAKE CITY, Utah**--Federal Bldg., Rm. 8105, 125 South State St.
- **SAN FRANCISCO, California**--Customhouse, Rm. 504, 555 Battery St.
- **SPOKANE, Washington**--U.S. Courthouse, Rm. 678, West 920 Riverside Ave..
- **ANCHORAGE, Alaska**--Rm. 101, 4230 University Dr.
- **ANCHORAGE, Alaska**--Federal Bldg, Rm. E-146, 701 C St.

Maps

Maps may be purchased over the counter at the U.S. Geological Survey offices where books are sold (all addresses in above list) and at the following Geological Survey offices:

- **ROLLA, Missouri**--1400 Independence Rd.
- **DENVER, Colorado**--Map Distribution, Bldg. 810, Federal Center
- **FAIRBANKS, Alaska**--New Federal Bldg., 101 Twelfth Ave.

Geochemical Evolution of Water in the Madison Aquifer in Parts of Montana, South Dakota, and Wyoming

By JOHN F. BUSBY, L. NIEL PLUMMER, ROGER W. LEE, *and* BRUCE B. HANSHAW

GEOLOGY AND HYDROLOGY OF THE MADISON LIMESTONE AND ASSOCIATED ROCKS IN PARTS OF MONTANA, NEBRASKA, NORTH DAKOTA, SOUTH DAKOTA, AND WYOMING

U.S. GEOLOGICAL SURVEY PROFESSIONAL PAPER 1273-F

UNITED STATES GOVERNMENT PRINTING OFFICE, WASHINGTON : 1991

DEPARTMENT OF THE INTERIOR

MANUEL LUJAN, JR., *Secretary*

U.S. GEOLOGICAL SURVEY

Dallas L. Peck, *Director*

Library of Congress Cataloging-in-Publication Data

Geochemical evolution of water in the Madison Aquifer in parts of Montana, South Dakota, and Wyoming : geology and hydrology of the Madison Limestone and associated rocks in parts of Montana, Nebraska, North Dakota, South Dakota, and Wyoming / by John F. Busby ... [et al.].

p. cm.—(U.S. Geological Survey professional paper ; 1273–F)

Includes bibliographical references.

1. Hydrogeology—Madison Aquifer. 2. Water chemistry. I. Busby, John F. II. Series: Geological Survey professional paper : 1273–F.

GB1019.G46 1991

551.48'09786—dc20 90–28405

CIP

For sale by the Books and Open-File Reports Section, U.S. Geological Survey,
Federal Center, Box 25425, Denver, CO 80225

CONTENTS

ILLUSTRATIONS

TABLES

GEOCHEMICAL EVOLUTION OF WATER IN THE MADISON AQUIFER IN PARTS OF MONTANA, SOUTH DAKOTA, AND WYOMING

By JOHN F. BUSBY, L. NIEL PLUMMER, ROGER W. LEE, and BRUCE B. HANSHAW

ABSTRACT

The geochemical models BALANCE and WATEQF have been used to deduce the major chemical reactions controlling the ground-water chemistry in the Madison aquifer in parts of Montana, South Dakota, and Wyoming. Although the Madison aquifer extends into North Dakota, wells were not available in North Dakota from which an uncontaminated sample of water could be collected. The chemical system was assumed to be closed to mass transfer of carbon dioxide. The dominant reactions along each of the eight selected flow paths were found to be dedolomitization caused by the irreversible dissolution of anhydrite and the bacterially mediated reduction of sulfate. Some cation (calcium/sodium) exchange and halite dissolution were determined to occur along flow paths in central Montana.

After the geochemical models had been validated using carbon-13 data in an independent mass-balance calculation, the carbon-14 ages were adjusted for the contribution of sources and sinks of carbon. These carbon-14 ages were adjusted for incongruent dissolution by applying Rayleigh-distillation equations to the isotope fractionation. The adjusted carbon-14 ages were then used to calculate regional hydraulic conductivities, and these values agreed well with those obtained by a computer-based digital model of the ground-water flow simulation. The adjusted ages also were used to calculate apparent rates of reaction for dissolution of anhydrite, dolomite, and halite, reduction of sulfate, and calcite precipitation.

INTRODUCTION

This report describes the results of an investigation to determine the geochemical reactions controlling water chemistry in the Madison aquifer underlying the northern Great Plains in parts of Montana, South Dakota, and Wyoming (fig. 1). Although the Madison aquifer extends into North Dakota, little use is made of water from the aquifer in that State because of the large concentration of dissolved solids. For this reason, that part of the Madison aquifer underlying North Dakota was not investigated chemically and is excluded from this report. This investigation is part of a larger interdisciplinary study to describe the geohydrology of the Madison and associated aquifers.

In this report, the geohydrology of the Madison aquifer system is first summarized from information contained in reports by Sando (1976b), Peterson (1978, 1981), Thayer (1981), Brown and others (1982), MacCary and others (1983), and Downey (1984) in order to set the scene for understanding the geochemistry. Following the geohydrologic section, revisions of the WATEQF data base and speciation calculations based on WATEQF are discussed. Geochemical reactions in the Madison aquifer are then characterized using chemical and isotopic mass-balance techniques.

The mass-balance modeling was used to solve the inverse problem in geochemical modeling: determination of the chemical reactions controlling the water chemistry from the chemical and isotopic data. The program BALANCE (Parkhurst and others, 1982) was used to calculate the change, in moles, of selected minerals and gases entering and leaving the ground water between a point in the recharge area and a point downgradient along a flow path. If the determined mass transfer for a particular evolutionary set of reactions was thermodynamically consistent with the results of WATEQF and yielded calculated isotopic compositions in agreement with the field-measured values, that set of minerals and gases was considered to be a good representation of the geochemical reactions controlling the actual water chemistry.

After a viable model was derived, the results of this model were used to calculate an adjusted ^{14}C (carbon-14) age, following the method of Wigley and others (1978, 1979). The model-adjusted ^{14}C age was then used to calculate flow rates, regional hydraulic conductivities, and relative rates of chemical reactions.

ACKNOWLEDGMENTS

Many personnel of the U.S. Geological Survey have assisted in the preparation of this report. In particular, the authors have had helpful and thoughtful discussions with William Back, Tyler B. Coplen, Ruth Deike, Donald W. Fisher, Blair F. Jones, Leonard F. Konikow, and Donald C. Thorstenson (Reston, Va.). Discussions with

Robert O. Rye (Lakewood, Colo.) helped with the understanding of sulfur-isotope geochemistry.

Especially helpful were the comments of Joe S. Downey and Briant A. Kimball (both at Lakewood, Colo.) and William J. Steinkampf (Tacoma, Wash.). Field assistance of Joel D. Johnson (Charleston, W. Va.), Carole L. Loskot (Lakewood, Colo.), and Michael R. Plummer (Fairfax, Va.) is gratefully acknowledged. The computer support of George Fleming and David Stanley (Reston, Va.) was invaluable, as was the typing of Ana M. MacKay (Reston, Va.) and the editing and typing of Alicia A. Mitchell (Austin, Tex.). The drafting and redrafting of figures was well and cheerfully performed by Donald L. Leslie and John P. Maguire (both of Austin, Tex.). Graig C. Joy (Cheyenne, Wyo.) and Richard Feltis (Billings, Mont.) aided the work by providing copious amounts of well-completion data. Rochelle Rittmaster (Austin, Tex.) and Gary Mackey (Austin, Tex.) deserve credit for assistance in proofreading.

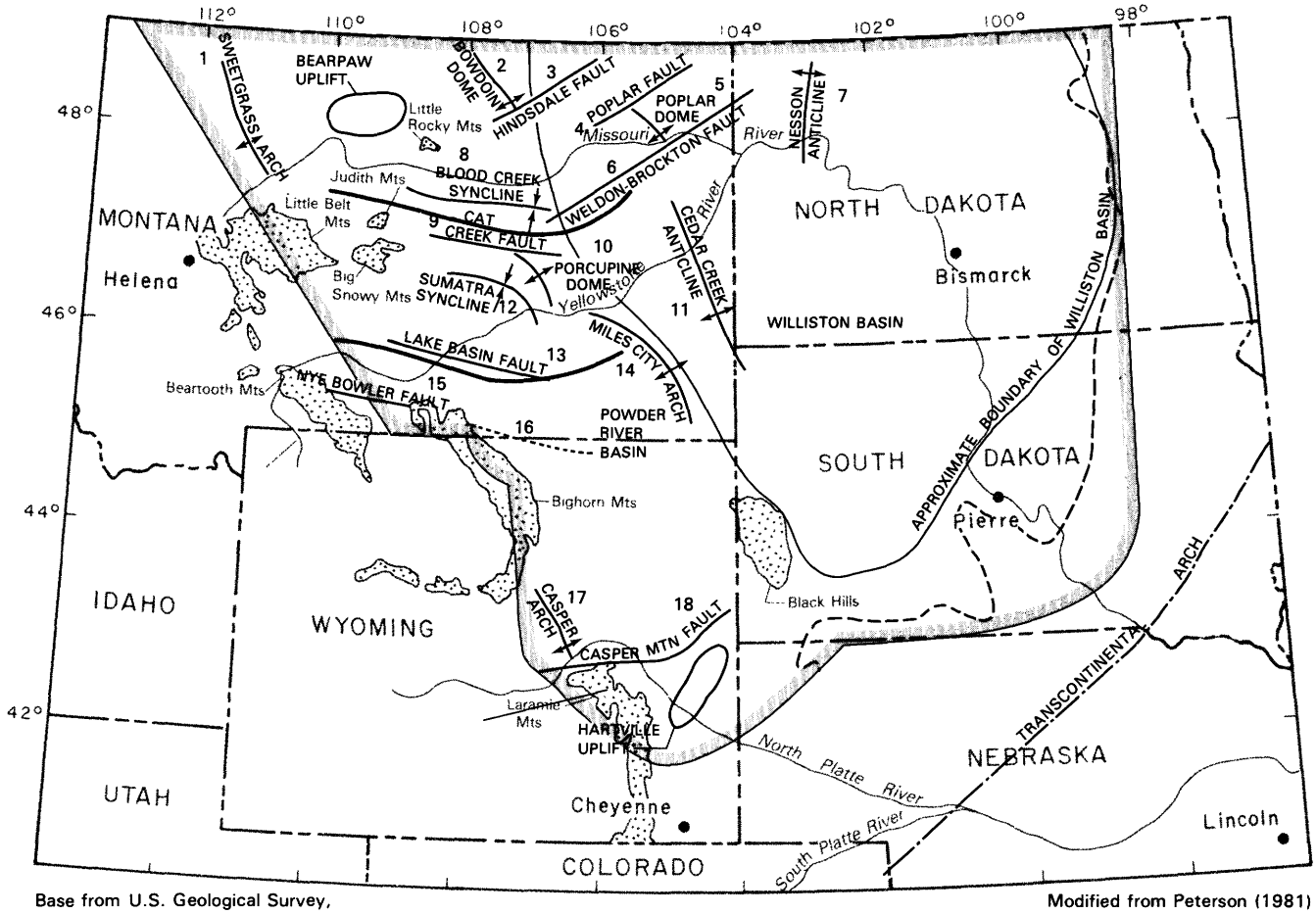

Base from U.S. Geological Survey, 1:7,500,000 map, 1970

Modified from Peterson (1981)

0 50 100 150 200 MILES
0 50 100 150 200 KILOMETERS

EXPLANATION

- MISSISSIPPIAN OR OLDER ROCKS—Exposed at land surface
- APPROXIMATE EASTERN LIMIT OF MADISON LIMESTONE
- BOUNDARY OF CENTRAL MONTANA TROUGH
- LINEAMENT—Probable extension of Nye Bowler fault zone
- 9 NUMBER USED TO IDENTIFY STRUCTURAL FEATURES IN OTHER FIGURES
- PROJECT AREA BOUNDARY

FIGURE 1.—Location of project area and major structural features.

DESCRIPTION OF PROJECT AREA

The climate of the project area is characterized as middle-latitude steppes occupying a transitional zone between arid lands to the west and more humid environments to the east. The annual precipitation of about 12 inches per year occurs mostly in the spring as rain when warm moisture-laden air from the gulf coast meets colder arctic air masses, and in the winter as snow resulting from arctic air masses moving across the region. Because much of the recharge to the aquifer system occurs in the spring as the result of snowmelt, a ground-water temperature of about 15 °C (degrees Celsius) has been used as one of the criteria for a recharge water.

The major physiographic features in the area include the Bighorn Mountains, the Laramie Mountains, the Little Rocky Mountains, the Big Snowy Mountains, the Hartville uplift, and the Black Hills (fig. 1). These highland features serve as the principal recharge areas to the Madison aquifer (Downey, 1984). Extensive undulating plains dissected by streams lie between the uplift areas and the regional discharge area for the aquifer system in eastern North and South Dakota.

GEOLOGIC SETTING

During the time in which the Mississippian Madison Limestone was deposited, the study area was a part of the cordilleran platform bordered on the west by the cordilleran miogeosyncline, which trended approximately north-south in Idaho and western Montana. Most of the sediment in the synclinal trough came from the Antler orogenic belt, which probably was an island arc to the west that underwent intermittent tectonism during the Paleozoic. The transcontinental arch located to the south of the project area was emergent but low-lying, and it sporadically contributed minor quantities of sediment that were spread thinly by marine currents across the platform. In general, during Mississippian time the cordilleran platform was a shallow-water, shelf-and-basin system that received predominantly carbonate and evaporite sediments in alternating cycles of transgression and regression of a sea lying to the west (Sandberg, 1961; Sando, 1968).

PALEOSTRUCTURE

Uplifted areas (fig. 1) were not regionally significant tectonic elements until late Paleozoic or early Mesozoic time (Agnew and Tychsen, 1965; Peterson, 1981) and had little influence on Mississippian sedimentation. Structural deformation during Mississippian time has been explained in terms of horizontal compression (Sales, 1968; Stone, 1969), vertical tectonics (Stearns and others, 1975), and wrench-fault tectonics (D.L. Brown, Frio Oil Company, Denver, Colo., written commun., 1978). Although the mechanics of deformation have little direct effect on the existing hydrologic system, there is general agreement that the current structure has been controlled by the preexisting structure of the Precambrian basement as modified by the Laramide orogeny. Several authors, including Sandberg (1962), Rose (1976), and Slack (1981), have suggested that the paleostructure in various parts of the study area has had a pronounced effect on the thickness and depositional environments of the sediments.

The major porosity zones in the Madison aquifer occur along paleostructures that are predominantly faults (fig. 2). The relation between the paleostructure and lithology is shown in figure 3. Although no trend in the type of lithofacies with paleostructure is apparent, changes in the type of lithofacies most commonly occur along structural elements.

STRATIGRAPHY

The Madison aquifer in this report is composed of the Madison Limestone or the Madison Group where divided, or stratigraphic equivalents. The Madison Group, from oldest to youngest, consists of the Lodgepole Limestone, the Mission Canyon Limestone, and the Charles Formation. The generalized correlation chart for Paleozoic rocks (table 1) shows the stratigraphic relation between the formations in the study area, and the data in table 2 relate to the stratigraphic intervals from which water samples were collected. The Lodgepole Limestone is a cyclic carbonate sequence consisting largely of fossiliferous to micritic dolomite and limestone units that are argillaceous and thinly bedded in most of the study area (Smith, 1972). The thickness of the unit ranges from 0 to more than 900 ft (feet) in the study area and averages about 300 ft.

The Mission Canyon Limestone grades from a coarsely crystalline limestone at its base to finer crystalline limestone with evaporite minerals near the top. The sequence contains one evaporite cycle and shares a second with the lower part of the overlying Charles Formation. Bedded evaporites are absent in most of Wyoming and South Dakota but occur in southeastern Montana. The evaporite deposits thicken in the central Montana trough, reaching their maximum areal extent in the Williston basin of North Dakota. The thickness of the Mission Canyon Limestone ranges between 0 and about 650 ft and averages about 300 ft.

The Charles Formation is the uppermost unit of the Madison Group. It is a marine evaporite sequence consisting of anhydrite and halite with interbedded dolomite, limestone, and argillaceous units. The thickness of the Charles Formation ranges from 0 to more than 295 ft with an average thickness of about 98 ft in the study area. Pre-Jurassic erosion has removed most of the Charles Formation in the western and southern parts of the study area.

Because the sulfate and carbonate rocks of the Madison Limestone are relatively soluble in water, the development of karst (solution) features is common. These complex and interconnected solution features developed in limestones under weathering conditions when the rocks were exposed at the land surface (figure 4). Sando (1974) describes ancient karst features, including enlarged joints, sinkholes, caves, and solution breccias, that developed in the Madison Limestone in north-central Wyoming. He further indicates that most of the open spaces were filled by sand and residual products reworked by a transgressive sea during Late Mississippian time. Large and extensive

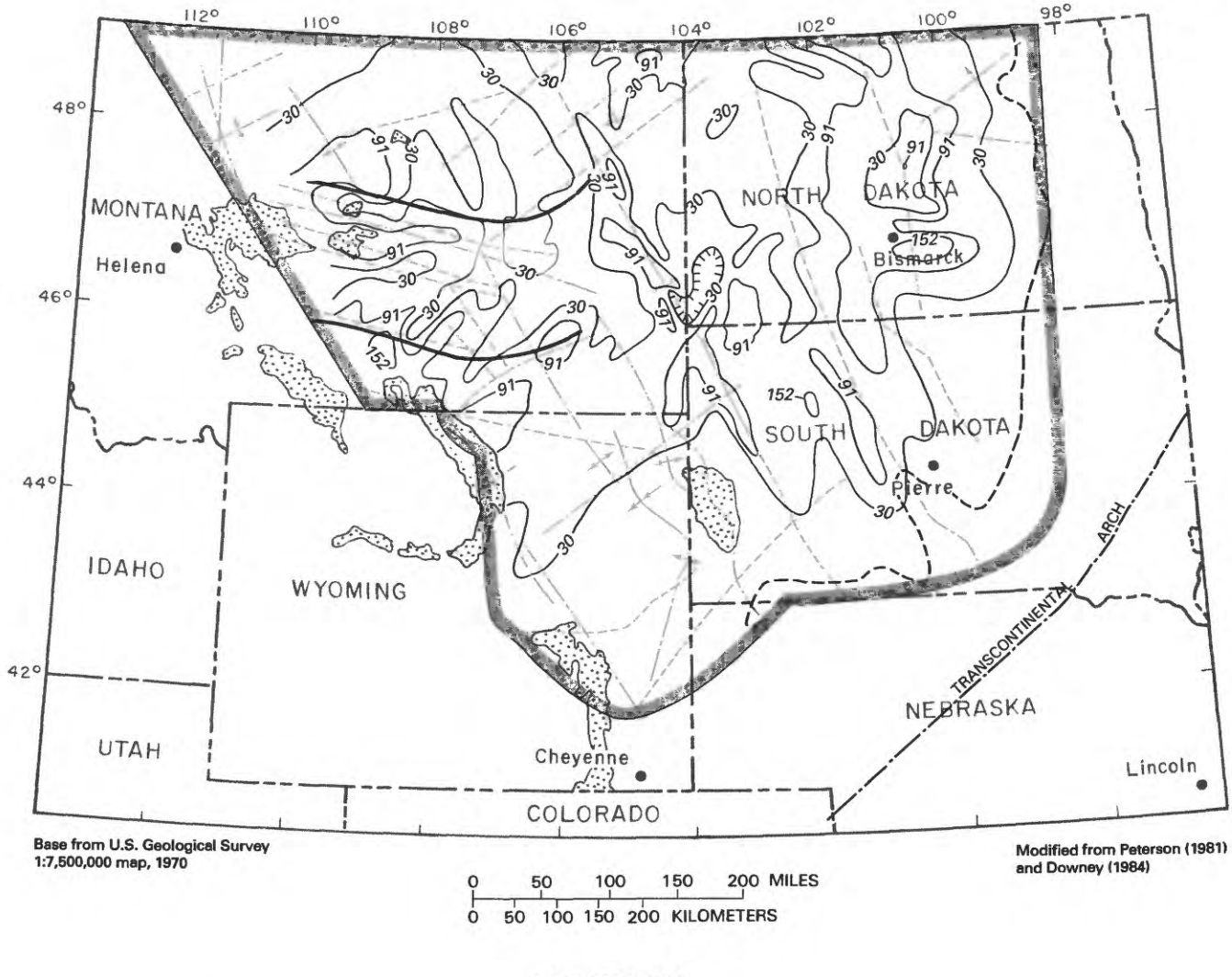

EXPLANATION

- MISSISSIPPIAN OR OLDER ROCKS—Exposed at land surface
- APPROXIMATE EASTERN LIMIT OF MADISON LIMESTONE
- BOUNDARY OF CENTRAL MONTANA TROUGH
- FAULT, PROBABLE FAULT, OR LINEAMENT
- ANTICLINE TREND OR DOME—Dashed line shows probable extension of feature
- STRUCTURAL TREND, ARCH, OR UPLIFT
- MONOCLINE
- 91 — LINE OF EQUAL THICKNESS OF ROCK WITH POROSITY EQUAL TO OR GREATER THAN 10 PERCENT—Interval 61 meters; hachures indicate area of closed low
- PROJECT AREA BOUNDARY

FIGURE 2.—Relation between paleostructure and porosity of Madison Limestone.

cave systems in outcrop areas of the Madison Limestone in the Bighorn Mountains and in the Black Hills are further evidence of the importance of the dissolution process in the development of secondary permeability in limestone units.

Overlying the Charles Formation in parts of Montana and South Dakota are rocks of Late Mississippian age belonging to the Big Snowy Group. The Big Snowy Group consists of, in ascending order, the Kibbey, Heath, and Otter Formations. These formations are composed mainly of shale and sandstone but also contain minor limestone beds. The Big Snowy Group is considered a confining unit of the underlying Madison aquifer (Downey, 1984).

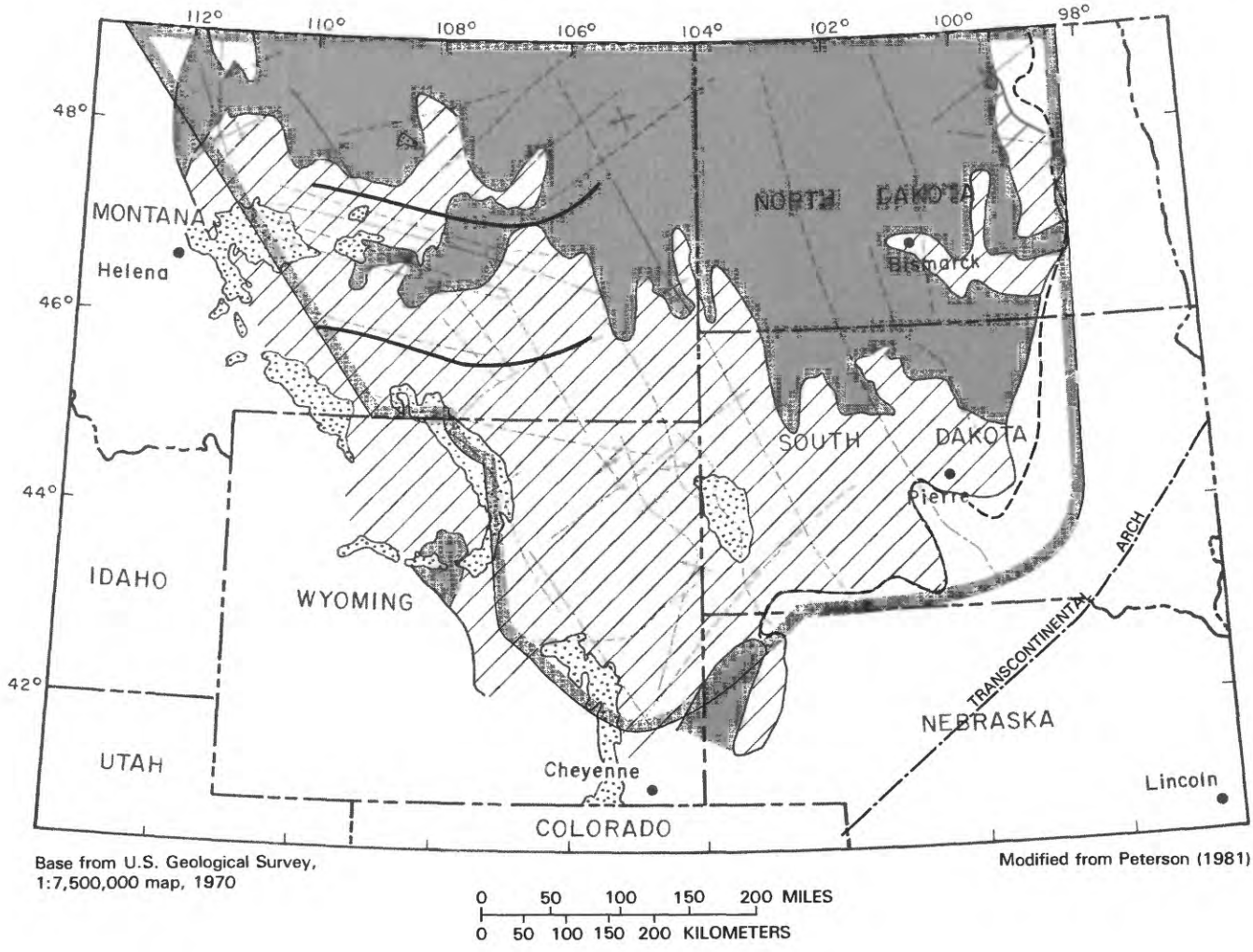

EXPLANATION

- MISSISSIPPIAN OR OLDER ROCKS—Exposed at land surface
- DOLOMITE FACIES OF MADISON LIMESTONE
- PRIMARY LIMESTONE AND SHALEY LIMESTONE FACIES OF MADISON LIMESTONE
- APPROXIMATE EASTERN LIMIT OF MADISON LIMESTONE
- BOUNDARY OF CENTRAL MONTANA TROUGH
- FAULT, PROBABLE FAULT, OR LINEAMENT
- ANTICLINE TREND OR DOME—Dashed line shows probable extension of feature
- STRUCTURAL TREND, ARCH, OR UPLIFT
- MONOCLINE
- PROJECT AREA BOUNDARY

FIGURE 3.—Relation between paleostructure, lithology, and thickness of Madison Limestone.

TABLE 1.—*Generalized correlation chart of Paleozoic rocks*

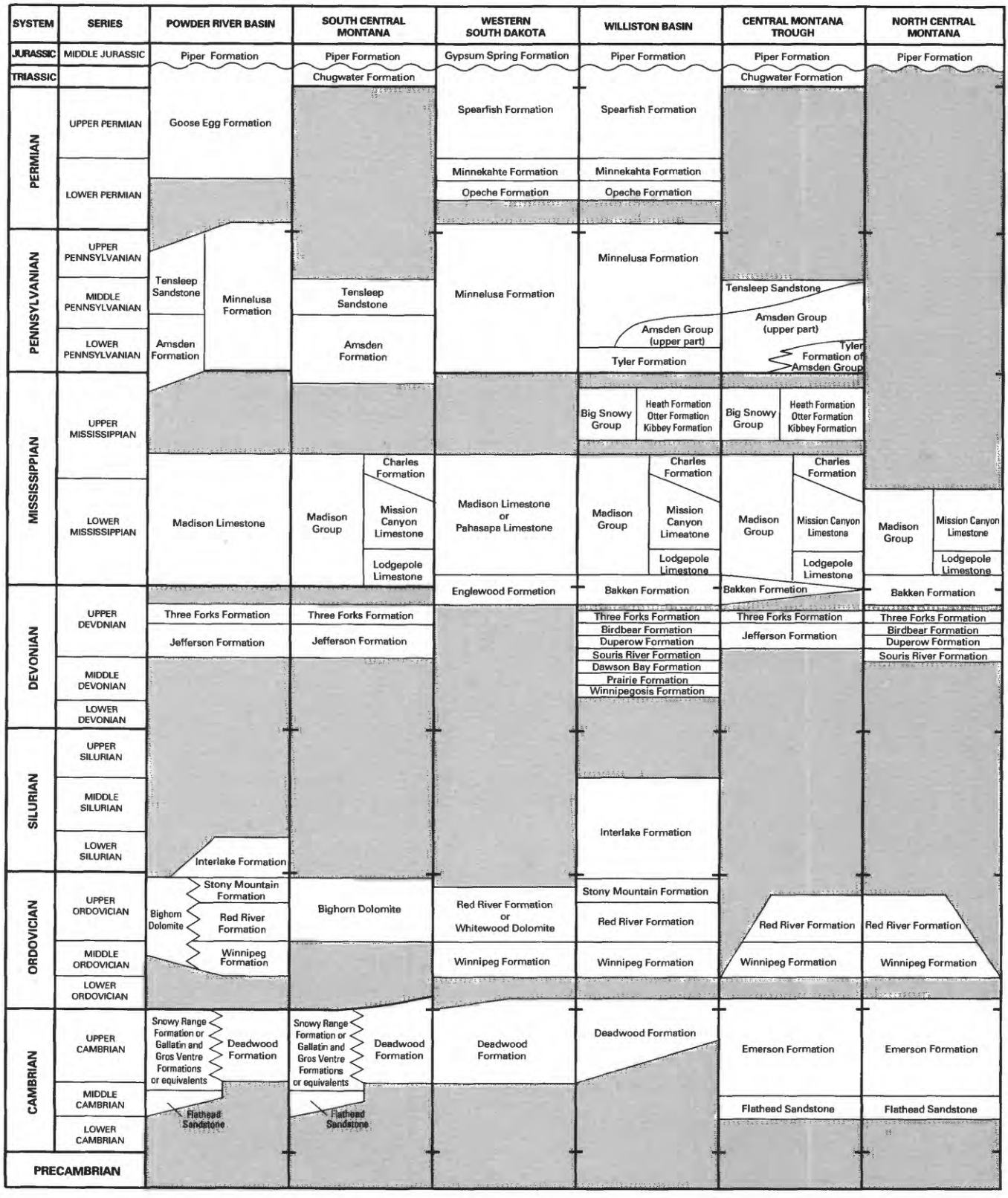

TABLE 2.—*Wells and springs sampled and source of water*

[The legal description (for example 02N 27E 35AAB01) is the location of the well based on the rules set forth in the ordinance of May 20, 1785, "The establishment of the rectangular survey system"]

Well or spring number [1]	Name	Legal description [2]	Total depth (feet)	Interval sampled (feet)	Water-yielding unit
		MONTANA			
2	Gore Hill	20N 03E 28CDAD	755	679–699	Madison Limestone
3	Great Falls High School	20N 04E 07BDAC	426	400–426	Madison Limestone
4	Bozeman Fish Hatchery	01S 06E 34BCDA	200	115–200	Madison Limestone
5	Bough Ranch	22N 06E 09DDAB	1,299	1,266–1,299	Madison Limestone
6	McLeod Warm Spring	03S 13E 34ABAB	spring	--	Madison Limestone
7	Big Timber Fish Hatchery	01N 14E 15DAAA	spring	--	Madison Limestone
8	Hanover Flowing Well	16N 16E 22DCC	751	--	Mission Canyon Limestone
9	Vanek Warm Spring	17N 18E 09BCAA	spring	--	Mission Canyon Limestone
10	Lewistown Big Spring	14N 19E 05ABCC	spring	--	Madison Limestone
11	Bluewater Spring	06S 24E 09BCAA	spring	--	Madison Limestone
12	Landusky Spring	25N 24E 32DABC	spring	--	Mission Canyon Limestone
13	Lodgepole Warm Spring	26N 25E 24BCDB	spring	--	Mission Canyon Limestone
14	HTH No. 3	02N 27E 35AABO1	7,175	4,373–4,422	Mission Canyon Limestone
15	Keg Coulee	11N 32E 24ADCD	--	6,457–6,516	Mission Canyon and Lodgepole Limestones
16	Texaco C115X	11N 32E 15ABC	6,768	6,079–6,768	Mission Canyon Limestone
17	Sumatra	11N 32E 24ADCD	6,854	6,152–6,854	Mission Canyon Limestone, Charles Formation, and Lodgepole Limestone
18	Sleeping Buffalo	32N 32E 35CDBD	3,199	3,130–3,199	Mission Canyon Limestone
19	Sarpy Mine	01N 37E 26BDDD	--	--	-
20	Mysse Flowing Well	12N 39E 09AACA	5,102	5,039–5,102	Mission Canyon Limestone
21	Colstrip	02N 41E 34BADA	9,337	7,795–8,340	Mission Canyon and Lodgepole Limestones
22	Moore	10N 43E 21CDCA	flowing well	--	Mission Canyon Limestone
23	Ranch Creek	09S 53E 22ABAC	7,260	7,169–7,260	Madison Limestone
24	Belle Creek	08S 54E 21ADAD	7,190	6,991–7,190	Madison Limestone
26	Gas City	14N 55E 27CDDB	7,598	7,434–7,598	Mission Canyon Limestone
27	Buckhorn Exeter	11N 31E 36AA	6,519	6,174–6,335	Madison Limestone
		SOUTH DAKOTA			
1	Kosken	42N 26W 34ABCD	--	2,661–2,936	Madison Limestone
2	McNenney	02N 01E 21BBC	220	144–220	Madison Limestone
3	Provo	10S 02E 03	3,845	--	Madison Limestone
4	Rhoads Fork	02N 02E 15	flowing well	--	Madison Limestone
5	Spearfish	06N 02E 10D	879	650–879	Pahasapa Limestone
6	Fuhs	05N 03E 28BACBB	551	548–551	Madison Limestone
7	Delzer No. 1	12N 03E 28BACCB	4,557	--	-
8	Delzer No. 2	12N 03E 32ACBAC	5,453	--	-
9	Cascade Spring	08S 05E 20	spring	--	-
10	Evans Plunge	07S 05E 24BAAA	spring	--	Madison Limestone
11	Kaiser	06S 05E 23	--	689–781	Pahasapa Limestone
12	Jones Spring	04N 05E 23	spring	--	-
13	Black Hills Cemetery	05N 07E 08	--	--	Pahasapa Limestone
14	Streeter Ranch	06S 06E 15AACC	938	928–938	Pahasapa Limestone
16	Cleghorn Spring	01N 07E 08	spring	--	Madison Limestone
17	Lien	02N 07E 18BCA	3,921	--	Pahasapa Limestone
18	Ellsworth AFB	02N 08E 13BDC	4,436	--	Pahasapa Limestone
19	Philip	01N 20E 01ACDD	4,009	3,783–4,009	Mission Canyon Limestone
20	Dupree	13N 21E 31BDDA	4,501	--	Lodgepole Limestone
21	Hamilton	08N 23W 26CDA	3,760	--	Madison Limestone
22	Hilltop Ranch	05N 24E 17CBBD	--	3,379–4,101	Madison Limestone
23	Eagle Butte	12N 24E 17CBDD	4,324	--	Madison Limestone
24	Midland	01N 25E 06CAA	3,320	3,166–3,320	Madison Limestone
25	Murdo	01S 26E 36ACA	3,314	--	Madison Limestone
26	Prince	05N 27E 22CD	2,838	2,700–2,746	Madison Limestone
27	Bean	09N 03E 20CDD	3,510	3,199–3,510	Pahasapa Limestone

TABLE 2.—*Wells and springs sampled and source of water*—Continued

Well or spring number [1]	Name	Legal description [2]	Total depth (feet)	Interval sampled (feet)	Water-yielding unit
		WYOMING			
1	Mock Ranch	57N 87W 21DBC01	1,594	--	Madison Limestone
2	Denius No. 1	58N 87W 32BA	--	--	Lodgepole Limestone
3	Denius No. 2	58N 87W 32BAB	--	942–3,143	Lodgepole Limestone
4	Denius No. 3	58N 87W 32BB	--	--	Lodgepole Limestone
5	Hole in the Wall	41N 84W 20BAC	432	--	Madison Limestone
6	Storey Fish Hatchery	53N 84W 13BDC	764	--	Madison Limestone
7	Mobil	49N 83W 27DDA	1,112	--	Madison Limestone
8	Conoco No. 44	41N 81W 09CDA	--	2,680–2,880	Madison Limestone
9	Shidler	40N 79W 31BCA	6,155	5,141–6,155	Madison Limestone
10	MKM	39N 78W 26CDC	7,178	6,391–7,178	Madison Limestone
11	Conoco No. 175	33N 75W 20AAC	--	8,845–9,154	Madison Limestone
12	Barber Ranch Spring	32N 74W 03CBD	1,467	--	-
13	Devils Tower	53N 65W 18BBD	479	450–479	Madison Limestone
14	HTH No. 1	57N 65W 15DA	4,341	2,431–2,595	Upper Mission Canyon Limestone
15	Upton	48N 65W 25CC	3,159	2,900–3,159	Lower Charles Formation
16	Coronado No. 2	46N 64W 13CCA	4,521	4,085–4,521	Madison Limestone
17	Osage	46N 63W 15BD	3,071	2,684–3,071	Madison Limestone
18	JBJ	44N 63W 26CAC	6,880	6,476–6,880	Madison Limestone
19	Seeley	46N 62W 18BDC	2,677	2,349–2,677	Madison Limestone
20	Voss	45N 61W 28AB	2,738	2,467–2,738	Madison Limestone
21	Newcastle	45N 61W 33AB01	2,637	2,618–2,637	Madison Limestone
22	Self	45N 60W 07CA	3,596	3,169–3,596	Madison Limestone
23	Martens Madison	45N 60W 04BDA	--	640–718	Madison Limestone
24	Mallo Camp	47N 60W 04BDA	spring	--	Madison Limestone
25	Ranch A	50N 60W 1BC	--	--	Madison Limestone

[1]Missing well numbers indicate that the well initially bearing that number was deleted after the report was in process. Wells were deleted when errors were found in the analysis, when it was learned that the well drew water from more than one source, or when the well was not completed in the formation thought.

[2]The legal description (for example, 02N 27E 35AAB01) is the location of the well based on the rules set forth in the ordinance of May 20, 1785, "The establishment of the rectangular survey system."

DEPOSITIONAL ENVIRONMENT

According to Sando (1976b), the deposition of the Mississippian System occurred in a set of three cycles of major transgression and regression. Each of the three cycles is divided into phases of minor transgression and regression. The Madison Limestone or Group was deposited during cycle 1 as described by Sando (1976b). Cycle 1 deposition was followed in cycle 2 by a period of epeirogenic uplift and erosion that marked the end of Madison deposition.

During much of Mississippian time most of the study area was covered by a alternately transgressive-regressive warm shallow sea (Sando, 1976b), termed the "knee-deep" environment by Hanshaw (B.B. Hanshaw, U.S. Geological Survey, written commun., 1985). This environment was conducive to prolific biologic productivity, sediment accumulation, and the development and preservation of shoals and reefs. Many of these small reefs and associated oolite- and crinoid-bank shoals formed lagoons that had restricted inflow from the sea.

Extensive dolomitization occurred on the shelf environment, and the lagoonal system served as centers for anhydrite precipitation. As the seas regressed, precipitation of halite occurred (Kinsman, 1969; Hanshaw and others, 1971).

Evidence of more restricted areas or areas with a more rapid rate of evaporation, probably during regressive phases of the cycles, is the accumulations of bedded evaporites found in the Williston basin and the Central Montana trough (fig. 5). These shallow-water depositional environments grade both laterally and vertically from shallow-marine carbonate and evaporite facies to deep-water facies. The Big Snowy Group was deposited during subsidence of the Central Montana trough and Williston basin. Regression of the sea from these restricted basins resulted in the deposition of extensive anhydrite and some halite.

FIGURE 4.—Solution karst features developed in Mission Canyon Limestone at Mission Canyon, near Hayes, Montana.

MINERALOGY

MAJOR MINERALS

The major minerals in the Madison Limestone are calcite ($CaCO_3$), dolomite [$CaMg(CO_3)_2$], and anhydrite ($CaSO_4$) (Thayer, 1981; R.G. Deike, U.S. Geological Survey, written commun., 1984). Minor quantities of goethite (FeOOH), hematite (Fe_2O_3), and quartz (SiO_2) also are common.

R.G. Deike (written commun., 1984) also reported the presence of talc [$Mg_3Si_4O_{10}(OH)_2$], fluorite (CaF_2), and chalcedony (SiO_2) in the Osagean interval penetrated by well HTH No. 1 and amphibole in the Meramecian interval penetrated by the same well. Thayer (1981) reported one example of dedolomite (calcite pseudomorphic after dolomite) in well HTH No. 1. The most common clay minerals in the system are kaolinite [$Al_2Si_2O_5(OH)_4$] and illite [$K_{0.6}Mg_{0.23}Al_{2.3}Si_{3.5}O_{10}(OH)_2$], for example, some of which is in a mixed layer of illite-smectite. Smectites, such as a calcium montmorillonite [$Ca_{0.17}Al_{2.33}Si_{3.67}O_{10}(OH)_2$], for example, also occur but in quantities subordinate to those of other clay minerals.

RELATION OF MINERALOGY TO WATER CHEMISTRY

The most common mechanism operating in the Madison aquifer is the incongruent dissolution of calcite caused by the dissolution of anhydrite and dolomite. The paucity of dedolomite reported by Thayer (1981) probably is due to a kinetic control preventing its formation. Although secondary calcite commonly is observed, it is not pseudomorphous after dolomite (dedolomite). Because the stoichiometry of the incongruent dissolution of calcite caused by the dissolution of anhydrite and dolomite is consistent with the formation of dedolomite, the term "dedolomitization" has been applied to this reaction, even in the absence of mineral phase "dedolomite," for the sake of brevity.

HYDROLOGY

REGIONAL GROUND-WATER FLOW

Downey (1984) developed a digital simulation model of the hydrologic system with two major aquifers and two confining units as shown in figure 6. The results of his simulation are shown in figure 7.

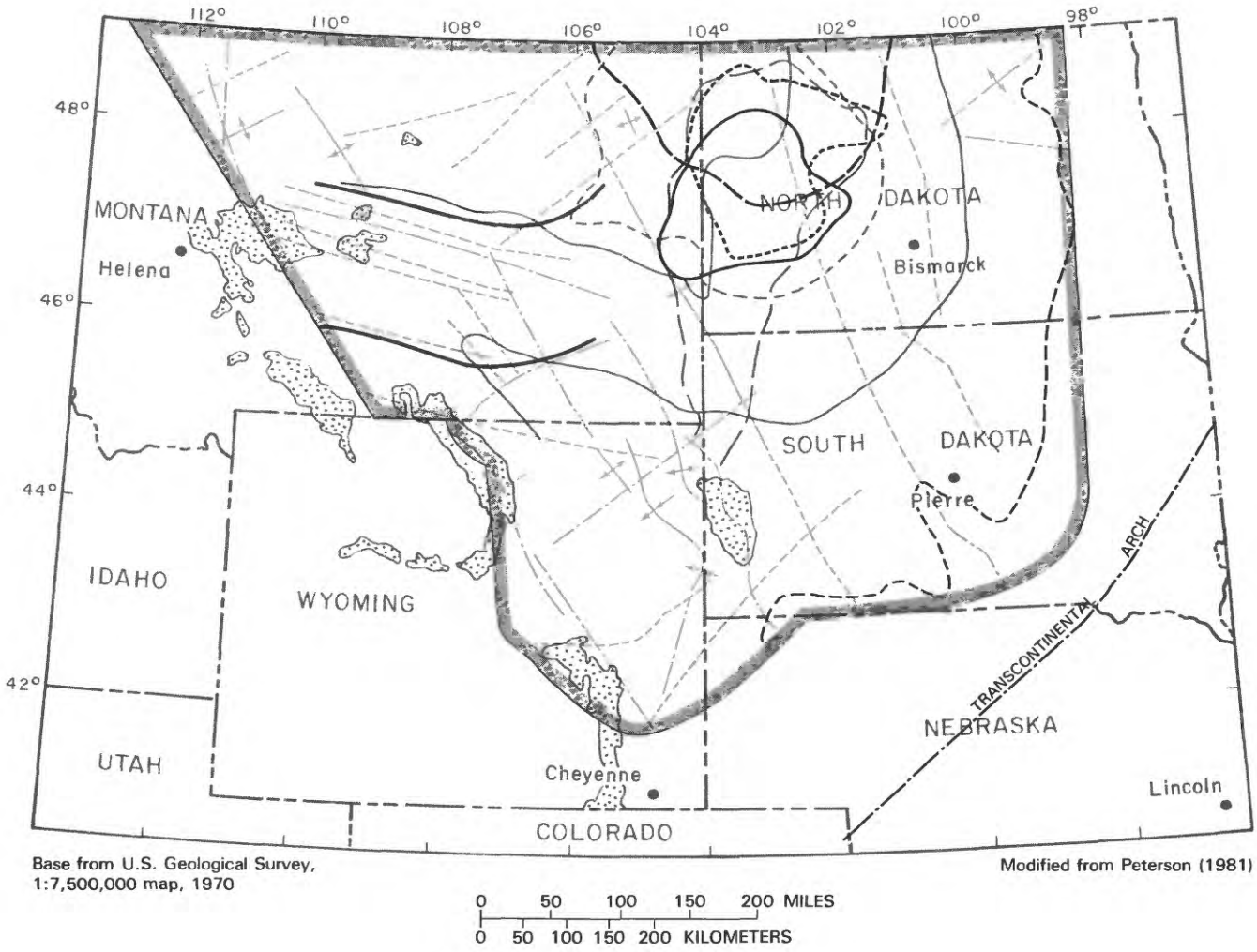

EXPLANATION

- MISSISSIPPIAN OR OLDER ROCKS—Exposed at land surface
- APPROXIMATE EASTERN LIMIT OF MADISON LIMESTONE
- BOUNDARY OF CENTRAL MONTANA TROUGH
- FAULT, PROBABLE FAULT, OR LINEAMENT
- ANTICLINE TREND OR DOME—Dashed line shows probable extension of feature
- STRUCTURAL TREND, ARCH, OR UPLIFT
- MONOCLINE
- LIMIT OF DUNHAM SALT OF INFORMAL SUBSURFACE USAGE, JURASSIC
- LIMIT OF PINE SALT OF INFORMAL SUBSURFACE USAGE, TRIASSIC
- LIMIT OF OPACHE SALT OF INFORMAL SUBSURFACE USAGE, PERMIAN
- LIMIT OF CHARLES SALT OF INFORMAL SUBSURFACE USAGE, MISSISSIPPIAN
- LIMIT OF ANHYDRITE IN THE MIDDLE PART OF THE MADISON LIMESTONE, MISSISSIPPIAN
- LIMIT OF PRAIRIE SALT OF INFORMAL SUBSURFACE USAGE, DEVONIAN
- PROJECT AREA BOUNDARY

FIGURE 5.—Extent of halite and anhydrite in Madison Limestone and in younger and older rocks.

Downey (1984) found that the Madison aquifer functioned as a confined aquifer system with recharge in the western highlands and a general direction of flow toward the northeast. Major discharge areas for the aquifer system are along the subcrop of the Madison Limestone in east-central South Dakota and eastern North Dakota, and in the saline lakes in northern North Dakota and saline springs and seeps in the Canadian province of Alberta (Grossman, 1968; Downey, 1984).

Recharge entering the ground-water flow system in the Black Hills follows two general paths. One component flows north along the front of the Black Hills and then to the east in response to structural and hydrologic control. The other component flows south along the front of the Black Hills and then to the east, also in response to structural and hydrologic control. Very little water recharged from the Black Hills enters the Madison aquifer system in the Powder River basin of Wyoming.

The same general situation occurs for recharge waters entering the Madison aquifer from the Bighorn Mountains. Waters entering the northern end of the Bighorn Mountains flow to the east, whereas waters entering along the flanks of the mountains are diverted to the north by structural features along the eastern front of the mountain range.

Lower Cretaceous	Upper boundary
Pennsylvanian, Permian, Triassic, Jurassic, and Charles Formation of Mississippian age	Confining layer
Lodgepole and Mission Canyon Limestones of the Madison Group	Madison aquifer
Silurian–Devonian formations and Bakken Formation of Mississippian age	Confining layer
Red River, Stonewall, Stony Mountain, Winnipeg, and upper Deadwood Formations of Cambrian to Ordovician age	Cambrian–Ordovician aquifer
Precambrian	Lower boundary

FIGURE 6.—Relation between geologic units and units used in simulation model.

As shown in figure 7, little recharge to the ground-water flow system occurs from the Laramie Mountains, and the recharge that does enter the system in this region moves toward the center of the Powder River basin.

A map (fig. 8) relating concentration of dissolved solids to geologic structure indicates a significant control of the dissolved-solids distribution by the geologic structure. The area in east-central Montana bounded by the Cat Creek fault and Porcupine dome shows a large dissolved-solids concentration, indicating a possible retardation of flow by geologic structure emanating from the Big Snowy Mountains. The high dissolved-solids concentration could also be the result of the availability of soluble material in the aquifer material. In eastern Wyoming the set of anticlines and minor faults along the western front of the Black Hills diverts recharge north and south around the Black Hills and away from the Powder River basin of Wyoming. In southern Wyoming the Casper Mountain fault and Casper arch appear to retard flow north from the Laramie Range.

LEAKAGE

The possibility of significant crossformational leakage into the Madison aquifer from underlying Cambrian-Ordovician strata was considered during formulation of the geochemical models and rejected. This conclusion was based on the hydrologic modeling results of Downey (1984, 1986), which show that vertical hydraulic conductivity between the Cambrian-Ordovician and Madison aquifers is less than 10^{-6} ft/d throughout the study area. This compares to horizontal hydraulic conductivities within the Madison aquifer ranging from approximately 1 to 10 ft/d. This comparison indicates that on a regional scale crossformational leakage between the Madison and Cambrian-Ordovician aquifers can be disregarded.

ESTIMATION OF REGIONAL HYDRAULIC CONDUCTIVITY

The regional hydraulic conductivity (K_{14C}), in feet per second, was estimated from the ^{14}C data after adjustment of the data for reaction as explained in the section "Carbon-14 Ages."

The flow paths used in this analysis (fig. 9) were selected to be orthogonal to the potentiometric surface, with the exception of those in southern Wyoming, where the flow lines were selected to follow the dissolved-solids gradient.

The calculation of regional hydraulic conductivity (K_{14C}) based on the work of Hanshaw and others (1964) uses the Darcy equation in the form

$$K = \frac{v\theta}{\Delta h/\Delta l}, \qquad (1)$$

where

K is the hydraulic conductivity, in feet per second;
v is the average linear flow velocity, in feet per second;
θ is the porosity, dimensionless;
Δh is the change in hydraulic head, in feet; and
Δl is the length of the flow path, in feet.

The value of K_{hyd}, (the regional hydraulic conductivity) was calculated by dividing the transmissivity, obtained by either aquifer tests or model simulation, by the aquifer thickness. Both the thicknesses and transmissivities were distance-weighted averages along the length of the flow path.

The values for the hydraulic conductivities (K_{14C})

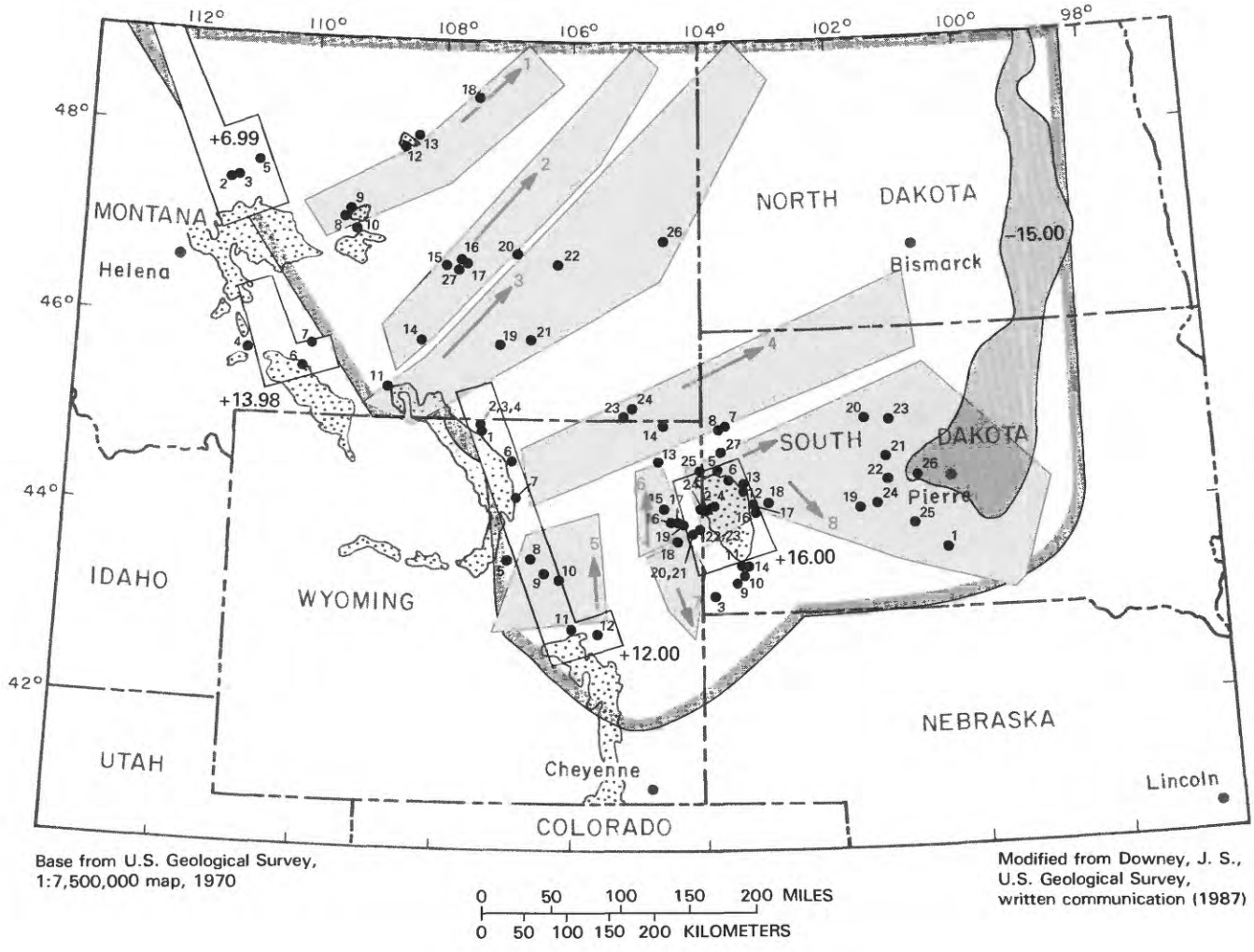

EXPLANATION

MISSISSIPPIAN OR OLDER ROCKS—Exposed at land surface

-15.00 AREA OF GROUND-WATER DISCHARGE—Number is discharge, in cubic feet per second

+13.98 AREA OF GROUND-WATER RECHARGE—Number is recharge, in cubic feet per second

4 OUTLINE OF FLOW PATH—Arrow shows principal direction of flow. Numbers in box are those of flow path

22 WELL REPRESENTS CONTROL POINTS USED IN GEOCHEMICAL MODEL—Number is identification number of well

PROJECT AREA BOUNDARY

NOTE: Wells not within flow path were used for recharge

FIGURE 7.—Recharge rates, flow paths, flow directions, and discharge rates used in analysis of geochemical data.

derived from the calculated flow velocity on the basis of ^{14}C age and an assumed porosity of 3 percent and for the hydraulic conductivities (K_{hyd}) derived from analysis of the transmissivity maps (fig. 29) developed by Downey using a computation-based digital model are shown in table 3 (Downey, 1984). The differences between the values derived from the two different methods are within the range of values typical of carbonate aquifer systems

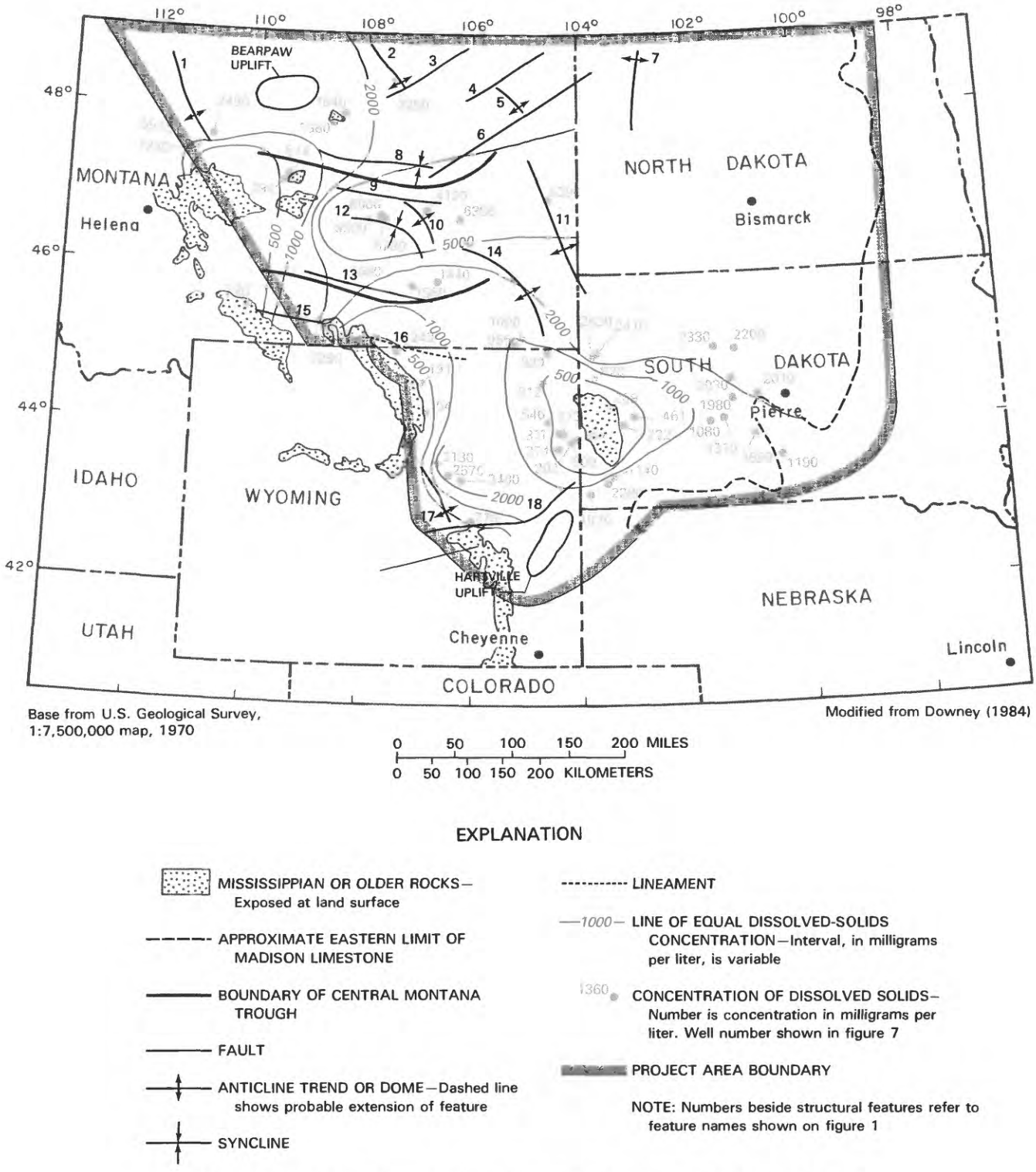

FIGURE 8.—Relation between geologic structure and concentration of dissolved solids.

and show a remarkable consistency between the two sets of data, with the worst case being within a factor of 8. The K_{14C} values range from 1.12×10^{-6} to 29.87×10^{-6} ft/s (feet per second), a factor of about 30 and a reasonable range for carbonate aquifers. The larger values at Dupree (well No. 20), Eagle Butte (well No. 23), Kosken (well No. 1), and Prince (well No. 26) in South Dakota along flow path 8 are measured from near a zone of greater permeability postulated by Downey (1986).

The smallest values of regional hydraulic conductivity (K_{14C}) calculated on the basis of ^{14}C age are found along flow path 5 in Wyoming, an area expected to have received detrital material from the transcontinental arch during deposition (Sando, 1976b).

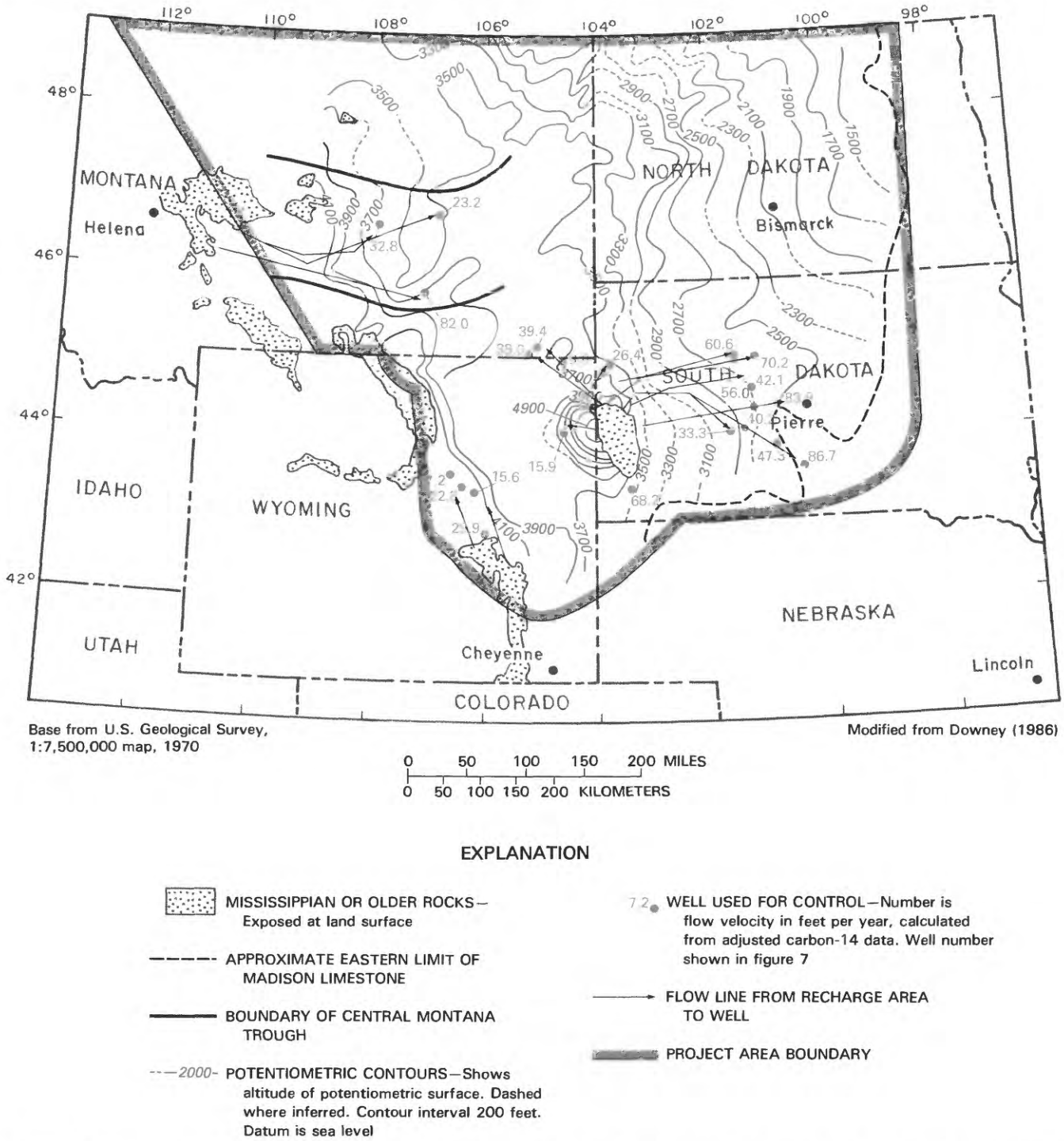

FIGURE 9.—Ground-water flow velocity based on adjusted carbon-14 ages, flow lines from recharge area to well, and potentiometric surface.

TABLE 3.—*Comparison of hydraulic-conductivity values calculated from ground-water flow velocities based on adjusted carbon-14 ages with those calculated from digital simulation (Downey, 1984)*

[ft, feet; mi, miles; ft/yr, feet per year; ft/s, feet per second; porosity of 3 percent assumed]

Well	Well No.	State	Flow path	Change in hydraulic head (ft)	Horizontal flow length (mi)	Hydraulic gradient (x10-3)	Carbon-14 age (x10^3 yr)	Velocity (ft/yr)	Hydraulic conductivity (in ft/s x 10-6) based on:	
									Carbon-14 age	Digital simulation
Keg Coulee	15	Mont.	2	3,002	143	3.98	23.0	32.8	7.85	6.07
Sarpy Mine	19	Mont.	3	3,002	174	3.27	11.2	82.0	23.86	3.29
Mysse Flowing Well	20	Mont.	3	3,097	99	5.92	22.5	23.2	3.73	3.48
HTH No. 1	14	Wyo.	4	1,260	40	5.97	7.3	28.9	4.61	7.81
Ranch Creek	23	Mont.	4	1,260	68	3.51	9.2	39.0	10.58	7.09
Belle Creek	24	Mont.	4	1,260	68	3.51	9.1	39.4	10.69	7.45
Delzer No. 2	8	S.Dak.	4	1,499	28	10.14	5.6	26.4	2.48	6.96
Conoco No. 175	11	Wyo.	5	1,631	43	7.02	7.6	29.9	4.05	7.14
MKM	10	Wyo.	5	1,001	62	3.06	21.0	15.6	4.85	4.26
Shidler	9	Wyo.	5	1,001	50	3.79	11.6	22.8	5.71	4.36
Conoco No. 44	8	Wyo.	5	1,001	31	6.12	22.6	7.2	1.12	4.69
Upton	15	Wyo.	6	1,125	25	8.52	8.3	15.9	1.78	6.20
Evans Plunge	10	S.Dak.	7	1,499	31	9.16	2.4	68.2	7.08	7.15
Kosken	1	S.Dak.	8	2,539	174	2.76	10.6	86.7	29.87	5.45
Philip	19	S.Dak.	8	2,241	106	4.00	16.8	33.3	7.92	3.54
Midland	24	S.Dak.	8	2,342	124	3.58	16.3	40.2	10.67	6.23
Murdo	25	S.Dak.	8	2,500	130	3.64	14.5	47.3	12.38	4.56
Hilltop Ranch	22	S.Dak.	8	2,500	106	4.47	10.0	56.0	11.91	5.18
Prince	26	S.Dak.	8	2,552	124	3.90	7.8	83.9	20.47	4.26
Hamilton	21	S.Dak.	8	2,434	106	4.35	13.3	42.1	9.20	3.54
Eagle Butte	23	S.Dak.	8	2,500	149	3.18	11.2	70.2	21.0	5.74
Dupree	20	S.Dak.	8	2,402	124	3.67	10.8	60.6	15.71	4.00

ERROR ANALYSIS OF REGIONAL HYDRAULIC CONDUCTIVITY

The major sources of error in hydraulic-conductivity values derived from ^{14}C data, as suggested by L.F. Konikow (U.S. Geological Survey, written commun., 1984), were in the flow-path lengths, hydraulic-head changes, and porosities used.

To these suspected sources of error should also be added the error in the measurement of the unadjusted ^{14}C age of the water [±500 yr (years)]; errors in the geochemical model, including the choice of plausible phases; inadequacies in the thermodynamic data; and assumptions regarding the temperature dependence of the equilibrium constant. Using the well at Keg Coulee (well No. 15 in Montana) as an example and assuming the validity of all chemical data, the effect of other errors can be calculated if the range of the errors is known.

For the purposes of this exercise, the error in hydraulic-head change (Δh) is assumed to be ±20 percent, error in length of flow path (Δl) to be ±20 percent, error in porosity (θ) to be ±70 percent, and error in the unadjusted ^{14}C age to be ±500 yr.

Let Δh = 3,002 ft − 600 ft = 2,402 ft;
Δl = 143 mi + 29 mi = 172 mi;
θ = 0.03 + 0.021 = 0.051; and
^{14}C = 23,000 yr − 500 yr = 22,500 yr before present.

The hydraulic gradient becomes $\frac{\Delta h}{\Delta l} = 2.64 \times 10^{-3}$, the velocity becomes 40.4 ft/yr, and the calculated hydraulic conductivity is 14.5×10^{-6} ft/s, a net relative error of about 86 percent compared with the original estimate of 7.85×10^{-6} ft/s.

Using the set of minimum-value assumptions,

Δh = 3,602 ft,
Δl = 114 mi,
θ = 0.009, and
^{14}C = 23,500 yr before present,

the hydraulic gradient is 5.98×10^{-3}, the velocity is 25.61 ft/yr, and the calculated hydraulic conductivity is 4.07×10^{-6} ft/s, a net relative error of 48.2 percent compared

with the original estimate of 7.85×10^{-6} ft/s. Although the error in the calculation of the hydraulic conductivities depends on the error ranges chosen for the porosity, length of flow path, hydraulic gradient, and age, this exercise does indicate the relation between the errors in the parameters.

The effect of differences in the choice of mass-transfer models may be investigated by comparing the results of Back and others (1983), which are based on a model using only the incongruent dissolution of calcite for the evolution of water chemistry from the recharge area to the well at Midland (well No. 24 in South Dakota), with the model (along the same flow path) incorporating both the incongruent dissolution of calcite and sulfate reduction. Using the values of Δl and Δh from this study and $\theta = 0.03$, the calculated K_{14_C} from the data of Back and others (1983) for the well at Midland is 5.64×10^{-6} ft/s, a relative error of 89 percent compared with the value of 10.67×10^{-6} ft/s calculated using the reaction model described in this report.

GEOCHEMISTRY

SAMPLE COLLECTION

The selection criteria used in choosing a well or spring for sampling were (1) a record of the well or spring had to be available, (2) the sample had to represent a point source in some member of the Madison Group, and (3) the well or spring had to be free of contamination.

Samples were collected for measurement of major and minor elements using the methods described in Brown and others (1970). The analytical results for all data collected by the Madison aquifer study are reported in Busby and others (1983). Only the subset of those data judged useful in the geochemical model is presented in this report. Field determinations were made for pH, alkalinity, temperature, and specific conductance following the methods of Wood (1976).

Samples were collected for the analysis of the radioactive isotopes ^{14}C and tritium and the stable isotope ratios $\delta^{13}C$, δD, and $\delta^{18}O$ using the methods described in Busby and others (1983). The collection of samples for the analysis of $\delta^{34}S$ was changed from that used by Busby and others (1983) and is described below.

SULFUR ISOTOPES—SULFIDE PHASE

Although the odor of hydrogen sulfide (H_2S) was detected in many of the wells sampled by Busby and others (1983), $\delta^{34}S$ was measurable in the sulfide phases in only one sample. Possible reasons for this are (1) coprecipitation of carbonate could have resulted in an inordinately large sample bulk on the filter, leading the field personnel to the false conclusion that an adequate quantity of sulfide had been collected; (2) analytical error; or (3) oxidation of sulfide by dissolved oxygen introduced during transfer of the sample from the filter plate to the sample bottle.

It was judged that the likelihood of such a large number of analytical errors was remote, and a careful review of the sampling procedure revealed no obvious error. The possibility of a judgment error in estimating the quantity of the sulfide phase collected or of oxidation by occluded water was not amenable to testing.

In an attempt to eliminate suspected causes, L. Niel Plummer and Eurybiades Busenberg (U.S. Geological Survey, written commun., 1982) performed a set of experiments on sulfide stabilities. The investigation resulted in the following procedure:

1. The field-determined concentration of sulfide was used to calculate the quantity of cadmium acetate ($Cd(CH_3CO_2)_2$) required to precipitate the sulfide present, and then a large excess of cadmium acetate was added to a 10-L (liter) carboy.
2. The carboy was filled with water, and concentrated hydrochloric acid (HCl) was added to decrease the pH to about 4.0.
3. The carboy was capped, shaken well, and allowed to stand until precipitation appeared complete.
4. After precipitation, the carboy was again shaken and its contents transferred into a stainless-steel kettle and filtered under nitrogen pressure through a 0.1-μm (micrometer) millipore filter. After filtration, the filter was removed and placed in an actinic glass bottle, which was then sparged with nitrogen.
5. The bottle was wrapped with foil, retightened, and sealed with paraffin prior to shipment to the laboratory.

Although this procedure was a marked improvement, problems remain. Successful determinations of $\delta^{34}S$ of dissolved sulfide were made for only 70 percent of the samples, indicating the need for further improvement of the sampling procedure.

SULFUR ISOTOPES—SULFATE PHASE

The sampling procedure for $\delta^{34}S$ of dissolved sulfate was modified for convenience. The new procedure involved precipitation of the sulfate from an acidified (HCl) 200-mL sample of water with barium chloride ($BaCl_2$) and filtration through a 0.45-μm filter using a syringe pump.

FIELD PROCEDURES

In addition to the field procedures reported by Busby and others (1983), dissolved sulfide was also determined in the field using the methylene-blue method with a Hach model DR-2 spectrophotometer. The procedure followed was that described in the Hach Chemical Company

manual for analysis of water and waste water (Hach Chemical Co., 1982). The results determined in the field and from duplicate samples submitted to the U.S. Geological Survey laboratory in Arvada, Colorado, are shown in table 4. The sulfide concentrations determined by the methylene-blue method are consistently less than those determined using the iodometric method used by the U.S. Geological Survey laboratory.

TABLE 4.—*Comparison of field- and laboratory-determined sulfide data*

[Field—Data determined in the field using a Hach model DR-2 spectrophotometer as a detector for methylene-blue determination of sulfide. Laboratory—Data determined by the U.S. Geological Survey laboratory in Arvada, Colorado, using an iodometric titration; mg/L, milligrams per liter]

Well	Well number	Flow path	Concentration of dissolved sulfide determined in: Field (mg/L)	Laboratory (mg/L)
Sleeping Buffalo	18	1	0.04	0.3
Delzer No. 1	7	4	.04	.2
Delzer No. 2	8	4	.17	1.8
Evans Plunge	10	7	.03	.3
Murdo	25	8	.14	.7
Streeter Ranch	14	--	.02	.3
Dupree	20	8	1.0	19
Hilltop Ranch	22	8	.07	.9
Midalnd	24	8	.02	.3
Kosken	1	8	.13	.7
Philip	19	8	.01	.3
Bean	27	8	.04	.2
Fuhs	6	8	.05	.5
Black Hills Cemetery	13	8	.02	.2
Kaiser	11	8	.03	.1
Prince	26	8	.12	.6

RESULTS OF PREVIOUS WORK

The major conclusions in the report by Busby and others (1983) were the following:

1. Deuterium and oxygen-isotope ratios are consistent with present-day meteoric waters, and no uncorrected ^{14}C age greater than 30,000 yr was measured.
2. The major geochemical mechanisms controlling the water quality are (*a*) dissolution of anhydrite, (*b*) incongruent dissolution of dolomite, and (*c*) bacterially mediated sulfate reduction.
3. The precipitation of calcite in the well-bore caused by the large loss of CO_2 in wells with temperatures greater than 60 °C may result in diminished well capacity. This statement is not supported by the present study, however.
4. There is significant leakage from the overlying Pennsylvanian and Permian sedimentary rocks in the vicinity of Midwest, Wyoming. This leakage was thought to be caused by withdrawal of water from the Madison aquifer for secondary recovery of petroleum from sedimentary rocks of Cretaceous age. This statement is not supported by the present study.

MODELING STRATEGY FOR MASS-TRANSFER MODELS

Because the chemical data generally met the criteria for the saturation-sufficient case of Plummer and others (1983), mass-balance models of hypothesized reactions were used to predict the quantity of material transferred to or from the solid phase. Because sulfate reduction was evident, the mass balance on $\delta^{34}S$ for the sulfide and sulfate phases was included in the system of reactions. The direction of the predicted mass transfers was compared for consistency with the results from WATEQF (Plummer and others, 1976); if, for example, the mass-transfer model predicted the dissolution of calcite, but results from WATEQF indicated the system to be oversaturated with respect to calcite, the mass-balance model was not consistent with the results of WATEQF. Therefore, the concept of dissolution of calcite was eliminated.

The model results were then partially validated using the possible mass-balance models to predict the fractionation of $\delta^{13}C$. If a model shows a substantial lack of agreement between the observed and predicted values of $\delta^{13}C$, other reactants and (or) products need to be considered. Thus, through this elimination process, reaction models (that is, particular sets of reactants and products) may be identified that are consistent with all the chemical and isotopic data, and those that are not are shown to be invalid.

DEFINITION OF FLOW PATHS FOR MASS-TRANSFER MODELS

The ground-water flow paths used in this report generally were along flow lines selected to agree with the direction of flow as determined from the potentiometric surface of the Madision aquifer (fig. 7). Flow path 5 in southern Wyoming is an exception to this generality. The potentiometric gradient is orthogonal to the gradient in dissolved solids. Because pressure heads in this area were determined from drill-stem test data with rather large error ranges, the direction of increasing concentration of dissolved solids was chosen to indicate the direction of flow.

DEFINITION OF RECHARGE CHEMISTRY

The chemical composition of rainfall and snowmelt were not used to define the recharge water; instead the chemistry of waters near the beginning of the flow path, waters that had passed through the soil zone but had not interacted significantly with the rock matrix, were used to define the chemistry of the recharge water.

With one exception, all waters chosen to represent recharge met at least four of the following criteria: (1)

TABLE 5.—*Recharge waters selected for use in geochemical models of the Madison Limestone*

[°C, degrees Celsius; mg/L, milligrams per liter; TU, tritium units]

Spring or well	Spring or well number	State	Flow path	Temperature (°C)	Sulfate (mg/L)	Carbon-14 (percent modern)	Tritium (TU)
Lewistown Big Spring	10	Mont.	1	10.6	140.0	35.8	0.8
Bozeman Fish Hatchery	4	Mont.	2	8.6	23.0	84.1	115
Big Timber Fish Hatchery	7	Mont.	2	10.7	27.0	103.9	124
Mock Ranch	1	Wyo.	3	10.8	8.1	57.7	35.4
Denius No. 1	2	Wyo.	3	9.0	22	8.4	19.8
Mock Ranch	1	Wyo.	4	10.8	8.1	57.7	35.4
Storey Fish Hatchery	6	Wyo.	4	8.0	3.2	88.8	107
Mobil	7	Wyo.	4	7.1	7.7	62.2	56.7
Denius No. 1	2	Wyo.	4	9.0	22.0	8.4	19.8
Hole in the Wall	5	Wyo.	5	8.2	6.2	87.4	.5
Barber Ranch Spring	12	Wyo.	5	15.7	34	83.7	53.0
Mallo Camp	24	Wyo.	6	7.7	1.8	92.9	--
Rhoads Fork	4	S.Dak.	6	5.7	3.1	92.9	62.2
Rhoads Fork	4	S.Dak.	7	5.7	3.1	92.9	62.2
Kaiser	11	S.Dak.	8	15.0	14	81.1	27.7
Jones Spring	12	S.Dak.	8	12.9	5.8	100.0	276
Cleghorn Spring	16	S.Dak.	8	11.6	23	91.6	182

The well or spring had to be located in a recharge area; (2) temperature, measured at the wellhead or spring outlet, had to be less than or equal to the mean annual air temperature of 15 °C; (3) sulfate concentration had to be less than 100 mg/L; (4) the unadjusted ^{14}C value had to be at least 50 percent modern; and (5) the tritium value had to be greater than 10 TU (tritium units).

Criteria for the recharge water selected for the modeling effort are shown in table 5. The Lewistown Big Spring (well No. 10 in Montana) failed to meet all but the temperature criterion but was retained because it was the only site along flow path 1 that at least met one of the criteria.

EQUILIBRIUM-SPECIATION CALCULATIONS

In order to investigate thermodynamic controls on the water composition, equilibrium-speciation calculations were made using WATEQF (Plummer and others, 1976). These calculations provide a saturation index (*SI*) of minerals that may be reacting in the system. The *SI* of a particular mineral is defined as

$$SI = \log IAP/K_T, \quad (2)$$

where

IAP is the ion activity product of the mineral; and

K_T is the thermodynamic equilibrium constant adjusted to the temperature of the given analysis.

The *SI* is greater than zero for oversaturation and less than zero for undersaturation. Before the speciation and *SI* calculations could be made, several revisions and updates were made to the thermodynamic data base of WATEQF, as outlined in table 6. These changes were necessary because the previous thermodynamic data for the carbonate system were reliable to 50 °C, whereas the waters in many wells completed in the Madison aquifer have temperatures of 80 °C and higher.

The chemical data presented in tables 7 and 8 are from Busby and others (1983). The results from WATEQF calculations are summarized in table 9. These include *SI*'s of calcite, aragonite ($CaCO_3$), dolomite, gypsum, anhydrite, siderite ($FeCO_3$), strontianite ($SrCO_3$), celestite ($SrSO_4$), and barite ($BaSO_4$), as well as the calculated in situ log P_{CO_2} (partial pressure of carbon dioxide). In calculating the saturation state of siderite, it was assumed that the total dissolved iron was in the ferrous state.

Uncertainties in *SI*'s occur because of uncertainties in mineral and aqueous thermodynamic data used in the model, different degrees of analytical accuracy, and errors in pH caused by the more rapid outgassing of carbon dioxide from the higher temperature waters (table 9). As a result, some judgment is required in interpreting the *SI*'s. Generally a tolerance of ± 0.1 can be assigned to the *SI* of calcite, aragonite, gypsum, and anhydrite; ± 0.2 for the *SI* of dolomite, celestite, and strontianite; and much larger uncertainties on the order of ± 0.5 to the *SI* of barite and siderite. Because the solubilities of barite and, to some

TABLE 6.—*Summary of revised thermodynamic data*

[ΔH_r°, standard enthalpy of reaction in kilocalories per mole at 298.15 kelvins and 1 atmosphere pressure; K, equilibrium constant; T, temperature in kelvins]

		ΔH_r°	log K	Analytical expression	Reference
Reaction (species):					
$Ca^{2+} + HCO_3^- = CaHCO_3^+$		4.11	1.095	$\log K_{CaHCO_3^+} = 1209.120 + 0.31294T - 34765.06/T - 478.782 \log T$	(1)
$Ca^{2+} + CO_3^{2-} = CaCO_3^\circ$		3.556	3.224	$\log K_{CaCO_3^\circ} = -1228.732 - 0.299444T + 35512.75/T + 485.818 \log T$	(1)
$CO_2(g) = CO_2(aq)$		-4.776	-1.468	$\log K_H = 108.3865 + 0.01985076T - 6919.53/T - 40.45154 \log T + 669365/T^2$	(1)
$CO_2(aq) + H_2O = H^+ + HCO_3^-$		2.177	-6.352	$\log K_1 = -356.3094 - 0.06091964T + 21834.37/T + 126.8339 \log T - 1684915/T^2$	(1)
$HCO_3^- = H^+ + CO_3^{2-}$		3.561	-10.329	$\log K_2 = -107.8871 - 0.03252849T + 5151.79/T + 38.92561 \log T - 563713.90/T^2$	(1)
$Sr^{2+} + HCO_3^- = SrHCO_3^+$		6.05	1.18	$\log K_{SrHCO_3^+} = -3.248 + 0.014867T$	(2)
$Sr^{2+} + CO_3^{2-} = SrCO_3^\circ$		5.22	2.81	$\log K_{SrCO_3^\circ} = -1.019 + 0.012826T$	(2)
$Sr^{2+} + SO_4^{2-} = SrSO_4^\circ$		1.6	2.55	--	(3)
Reaction (minerals):					
$CaSO_4 = Ca^{2+} + SO_4^{2-}$	Anhydrite	-4.3	-4.384	--	(4)
$CaCO_3 = Ca^{2+} + CO_3^{2-}$	Aragonite	-2.589	-8.336	$\log K_A = -171.9773 - 0.077993T + 2903.293/T + 71.595 \log T$	(1)
$BaSO_4 = Ba^{2+} + SO_4^{2-}$	Barite	6.141	-9.978	—	(5)
$CaCO_3 = Ca^{2+} + CO_3^{2-}$	Calcite	-2.297	-8.480	$\log K_C = -171.9065 - 0.077993T + 2839.319/T + 71.595 \log T$	(4)
$SrSO_4 = Sr^{2+} + SO_4^{2-}$	Celestite	.228	-6.578	$\log K_{Cel} = 73.415 - 3603.341/T - 29.8115 \log T$	(6)
$CaMg(CO_3)_2 = Ca^{2+} + Mg^{2+} + 2CO_3^{2-}$	Dolomite	-9.436	-17.09	--	(7)
$CaSO_4\ 2H_2O = Ca^{2+} + SO_4^{2-} + 2H_2O$	Gypsum	-.028	-4.602	$\log K_G = 82.090 - 3853.936/T - 29.8115 \log T$	(8)
$FeCO_3 = Fe^{2+} + CO_3^{2-}$	Siderite	-6.14	-10.57	—	(9)
$SrCO_3 = Sr^{2+} + CO_3^{2-}$	Strontianite	-.40	-9.271	$\log K_{Stront} = 155.0305 - 7239.594/T - 56.58638 \log T$	(2)

(1) Plummer and Busenberg (1982).
(2) Busenberg and others (1984).
(3) Smith and Martell (1976).
(4) Log K of Harvie and Weare (1980) adjusted to be consistent with log K_G ΔH_r° from Parker and others (1976).
(5) Parker and others (1976).
(6) Calculated from the data of Gallo (1935) for $SrSO_4$ precipitated as given by Linke and Seidell (1965) and consistent with $SrSO_4^\circ$ data of Smith and Martell (1976).
(7) Robie and others (1978).
(8) Calculated from the data of Marshall and Slusher (1966) using the aqueous model of WATEQF.
(9) Log K of Smith (1918) recalculated using aqueous model of WATEQF at 30 °C. Adjusted to 25 °C using ΔH_r° from Parker and others (1976).

extent, celestite and gypsum depend on the crystallinity of the solid phase, it is sometimes possible to interpret seemingly constant levels of undersaturation or oversaturation as uncertainties in the thermodynamic data, rather than as actual indications of nonequilibrium.

The *SI* values of aragonite, calcite, dolomite, and gypsum as a function of dissolved-sulfate concentration are shown in figures 10–13. As dissolved sulfate increases, the waters approach gypsum saturation (fig. 13). Although gypsum is not known to occur in the Madison Limestone, thermodynamic calculations based on gypsum are more reliable that those for anhydrite as a result of the availability of high-quality solubility data (table 6).

The slight oversaturation of many waters with calcite (fig. 11) could be due to pH error (Pearson and others, 1978), with the increase in pH at higher temperatures due to the increased outgassing of carbon dioxide (CO_2) during field measurement of pH (table 7). Significant pH error is, however, discounted, as the pH measurements were made in a closed flow cell to minimize the effects of CO_2 outgassing, and the effect of the expected increase in pH with temperature is not apparent in figure 14.

TABLE 7.—*Chemical and temperature data used in modeling (cations)*

[°C, degrees Celsius; all constituent concentrations are in milligrams per liter; letter in front of flow-path number indicates whether the spring or well was used as recharge (R) or on the flow path (F); Ca, calcium; Mg, magnesium; Na, sodium; K, potassium; Ba, barium; Fe, iron; Li, lithium; Mn, manganese; Sr, strontium]

Spring or well	Spring or well number	State	Flow path	Temperature (°C)	pH	Ca	Mg	Na	K	Ba	Fe	Li	Mn	Sr
Lewistown Big Spring	10	Mont.	R1	10.6	7.58	75	28	2.4	0.9	0.0	0.04	0.02	0.00	0.98
Hanover Flowing Well	8	Mont.	F1	20.4	7.63	84	29	2.8	1.2	.0	.01	.02	.00	1.6
Vanek Warm Spring	9	Mont.	F1	19.6	7.40	130	40	3.6	1.3	.0	.03	.02	.00	2.5
Landusky Spring	12	Mont.	F1	20.4	7.24	260	99	41	9.2	.0	.03	.08	.00	4.9
Lodgepole Warm Spring	13	Mont.	F1	31.6	7.08	260	96	79	12	.0	.02	.14	.01	5.6
Sleeping Buffalo	18	Mont.	F1	40.9	7.00	510	120	310	26	.0	.44	.34	.02	11
Bozeman Fish Hatchery	4	Mont.	R2	8.6	7.84	50	17	1	.6	.0	.10	.00	.00	.14
Big Timber Fish Hatchery	7	Mont.	R2	10.7	7.64	51	16	9.2	2.9	.0	.01	.00	.00	.40
McLeod Warm Spring	6	Mont.	F2	24.6	7.40	71	23	1.5	1.4	.0	.00	.00	.00	.49
Sumatra	17	Mont.	F2	83.7	6.61	220	34	1,800	130	.1	.02	3.80	.14	12
Keg Coulee	15	Mont.	F2	61.7	6.50	350	53	1,500	120	.1	.39	3.50	.08	13
Texaco C115X	16	Mont.	F2	84.7	6.40	320	52	1,700	150	.0	.05	4.4	.05	13
Mock Ranch	1	Wyo.	R3,	10.8	7.50	56	20	.4	.6	.2	.02	.00	.00	.20
Denius No. 1	2	Wyo.	R3,	9.0	7.60	40	29	.6	1.1	--	.09	.00	.02	.17
Colstrip	21	Mont.	F3	97.5	6.52	220	28	140	67	.0	.34	.57	.01	9.0
Sarpy Mine	19	Mont.	F3	83.0	6.70	320	51	48	49	.2	.56	.33	.02	11
Gas City	26	Mont.	F3	91.5	6.61	370	61	1,400	110	.2	.1	1.5	.02	15
Bluewater Spring	11	Mont.	F3	14.3	7.29	530	67	71	2.7	.2	.01	.05	.01	5.6
Moore	22	Mont.	F3	86.9	6.67	380	68	1,700	130	.2	.02	2.3	.01	15
Mysse Flowing Well	20	Mont.	F3	63.0	6.61	450	110	730	99	.2	.02	2.1	.01	11
Storey Fish Hatchery	6	Wyo.	R4	8.0	7.30	52	15	1.4	.5	.0	--	.01	.00	.07
Mobil	7	Wyo.	R4	7.1	7.31	32	19	2.2	1.0	.0	.09	.00	.07	.09
HTH No. 1	14	Wyo.	F4	46.2	6.99	180	44	36	7.6	.2	5.8	.04	.16	4.5
Ranch Creek	23	Mont.	F4	52.7	6.94	190	46	38	8.0	.0	.02	.04	.02	4.8
Belle Creek	24	Mont.	F4	56.2	7.01	200	48	38	8.0	.2	.05	.04	.01	4.7
Delzer No. 1	7	S.Dak.	F4	22.8	7.51	510	110	36	35	.1	7.9	.09	.15	12
Delzer No. 2	8	S.Dak.	F4	55.6	6.77	550	110	45	12	.1	5.7	.06	.06	11
Hole in the Wall	5	Wyo.	R5	8.2	7.25	35	32	1.6	.6	.0	.03	.01	.00	.10
Barber Ranch Spring	12	Wyo.	R5	15.7	7.46	56	19	8.3	2.6	.0	.02	.01	.01	.4
Conoco No. 175	11	Wyo.	F5	65.0	7.07	110	25	77	9.8	.1	2.4	.15	.30	1.6
MKM	10	Wyo.	F5	88.1	6.71	290	41	760	69	.1	6.9	.87	.15	6.0
Shidler	9	Wyo.	F5	56.0	7.08	300	49	490	35	.0	2.4	.39	.24	4.6
Conoco No. 44	8	Wyo.	F5	32.2	7.17	240	61	380	25	.1	.87	.36	.02	3.4
Mallo Camp	24	Wyo.	R6, R7	7.7	7.60	57	24	1.3	.7	--	--	.00	.00	--
Rhoads Fork	4	S.Dak.	R6, R7	5.7	7.35	66	23	.9	.6	--	--	--	--	.07
Seeley	19	Wyo.	F6	13.0	7.30	66	27	1.3	1.2	.1	.02	.00	.00	.25
Coronado No. 2	16	Wyo.	F6	39.8	7.16	56	27	1.8	1.7	.0	--	.00	.00	.38
Newcastle	21	Wyo.	F6	25.0	7.20	64	29	2.6	1.7	--	--	--	--	.38
Osage	17	Wyo.	F6	23.4	7.20	70	27	2.1	1.4	--	--	--	--	.32
Upton	15	Wyo.	F6	25.7	7.12	88	41	2.6	2.2	.0	--	.00	.00	2.9
Devils Tower	13	Wyo.	F6	17.1	7.20	110	38	3.7	1.5	.0	.03	.01	.00	--
Voss	20	Wyo.	F7	26.1	7.30	63	29	2.6	1.7	.0	--	.00	.00	.39
Self	22	Wyo.	F7	29.5	7.30	73	31	2.5	2.1	.0	.02	.01	.02	.61
JBJ	18	Wyo.	F7	45.1	6.70	73	22	11	4.8	.0	--	.03	.22	6
Evans Plunge	10	S.Dak.	F7	30.5	6.90	210	41	86	11	--	--	--	--	2.9
Cascade Spring	9	S.Dak.	F7	20.0	6.89	540	83	27	5.2	--	--	--	--	6.2
Jones Spring	12	S.Dak.	R8	12.9	7.20	71	22	1.5	.6	--	.00	--	--	.12
Kaiser	11	S.Dak.	R8	15.0	7.40	47	18	9.7	2.9	.1	.08	.01	.03	.24
Cleghorn Spring	16	S.Dak.	R8	11.6	7.41	42	19	4.9	2.7	--	--	--	--	.10
Lien	17	S.Dak.	F8	11.9	7.41	46	25	2.4	1.8	.1	.01	.00	.00	.14
McNenney	2	S.Dak.	F8	11.5	7.18	87	24	2.1	1.4	--	--	--	--	.89
Ellsworth AFB	18	S.Dak.	F8	49.0	7.01	91	33	4.9	3.7	--	--	--	--	.94
Fuhs	6	S.Dak.	F8	10.7	7.21	88	63	5.8	3.6	.0	.01	.01	.00	.50
Kosken	1	S.Dak.	F8	63.5	6.68	240	48	27	11	--	--	--	--	4.6
Philip	19	S.Dak.	F8	68.0	6.65	220	58	18	7.3	--	--	--	--	4.5
Midland	24	S.Dak.	F8	71.0	6.69	270	66	25	9.7	--	--	--	--	5.5
Murdo	25	S.Dak.	F8	59.1	6.68	300	65	46	13	0.0	1.4	0.07	0.05	6.6
Hilltop Ranch	22	S.Dak.	F8	66.0	6.70	360	77	85	13	.0	.86	.17	.11	8.0
Prince	26	S.Dak.	F8	57.0	6.67	410	83	72	20	.2	.42	.12	.02	9
Hamilton	21	S.Dak.	F8	58.5	6.66	420	90	34	15	.0	3.0	.02	.05	9.2

TABLE 7.—*Chemical and temperature data used in modeling (cations)*—Continued

Spring or well	Spring or well number	State	Flow path	Temperature (°C)	pH	Ca	Mg	Na	K	Ba	Fe	Li	Mn	Sr
Eagle Butte	23	S.Dak.	F8	54.7	6.84	390	110	60	28	.0	3.0	.11	.09	11
Dupree	20	S.Dak.	F8	56.5	6.82	390	94	110	49	.0	.30	.23	.04	12
Gore Hill	2	Mont.	--	14.0	7.13	170	76	130	13	.0	1.0	.33	.02	3.2
Great Falls High School	3	Mont.	--	13.1	7.40	96	37	32	3.9	.0	.08	.06	.02	1.1
Bough Ranch	5	Mont.	--	17.9	7.06	320	200	150	20	.0	.18	.30	.02	8.6
HTH No. 3	14	Mont.	--	51.8	6.80	490	100	95	39	.0	.97	.40	.46	9.5
Buckhorn Exeter	27	Mont.	--	80.0	6.40	380	66	1,600	120	--	.5	--	.04	--
Provo	3	S.Dak.	--	60.0	6.97	110	30	200	18	--	--	--	--	2.2
Spearfish	5	S.Dak.	--	13.2	7.39	52	23	2.1	1.1	--	--	--	--	0.15
Black Hills Cemetery	13	S.Dak.	--	12.4	7.28	55	23	2.3	1.3	.3	.02	.00	.00	.33
Streeter Ranch	14	S.Dak.	--	42.2	7.61	40	15	9.2	2.3	.0	.02	.01	.00	..28
Bean	27	S.Dak.	--	41.5	7.10	160	51	14	5.0	.0	.04	.02	.00	3.3
Denius No. 2	3	Wyo.	--	8.3	7.55	55	16	.6	.5	.0	.01	.00	.00	.11
Denius No. 3	4	Wyo.	--	8.5	7.69	74	30	1.9	.0	.0	.01	.01	.02	.55
Martens Madison	23	Wyo.	--	15.0	7.50	61	26	2.7	2.0	--	--	.00	.01	--
Ranch A	25	Wyo.	--	12.2	7.26	120	30	2.6	1.4	.0	--	.00	.00	1.1

TABLE 8.—*Chemical data used in modeling (anions)*

[Letter in front of flow-path number indicates whether the spring or well was used as recharge (R) or on the flow path (F); Cl, chloride; SO_4, sulfate; HCO_3, bicarbonate; H_2S, hydrogen sulfide; B, boron; Br, bromide; F, fluoride; PO_4, orthophosphate; H_4SiO_4, silicic acid]

Spring or well	Spring or well number	State	Flow path	Cl	SO_4	HCO_3	H_2S (field)	H_2S (laboratory)	B	Br	F	PO_4	H_4SiO_4
Lewistown Big Spring	10	Mont.	R1	1.8	140	190	--	--	0.03	0.0	1.1	0.00	6.7
Hanover Flowing Well	8	Mont.	F1	1.5	170	200	--	--	.03	.0	1.4	.00	8.9
Vanek Warm Spring	9	Mont.	F1	2.4	330	200	--	--	.06	.0	1.5	.00	9.3
Landusky Spring	12	Mont.	F1	19	970	210	--	--	.21	.1	1.6	.00	12
Lodgepole Warm Spring	13	Mont.	F1	67	990	200	--	--	.41	.2	1.7	.00	16
Sleeping Buffalo	18	Mont.	F1	190	2,000	150	0.04	0.3	1.0	.6	3.3	.00	18
Bozeman Fish Hatchery	4	Mont.	R2	1.1	23	220	--	--	.01	.0	.2	.00	4.8
Big Timber Fish Hatchery	7	Mont.	R2	2.8	27	230	--	--	.04	.0	3.9	.00	16
McLeod Warm Spring	6	Mont.	F2	1.1	120	190	--	--	.01	.0	.6	.00	11
Sumatra	17	Mont.	F2	2,300	1,200	330	--	46	6.8	12	4.9	.00	9.1
Keg Coulee	15	Mont.	F2	2,000	1,300	340	--	57	6.1	11	5.2	.00	55
Texaco C115X	16	Mont.	F2	2,100	1,400	360	--	132	7.9	12	5.4	.01	58
Mock Ranch	1	Wyo.	R3, R4	.5	8.1	250	--	--	.23	.0	.2	.00	6.3
Denius No. 1	2	Wyo.	R3, R4	.7	22	240	--	--	.01	.0	.7	.00	7.8
Colstrip	21	Mont.	F3	96	740	140	--	4	.67	.6	4.7	.00	69
Sarpy Mine	19	Mont.	F3	21	960	140	--	2.9	.34	.1	4.5	.03	49
Gas City	26	Mont.	F3	1,900	1,300	390	--	54	4.7	.1	4.7	.06	58
Bluewater Spring	11	Mont.	F3	2.4	1,500	220	--	--	.17	.0	1.4	.06	13
Moore	22	Mont.	F3	2,400	1,500	300	--	19	3.3	6.9	5.4	.00	56
Mysse Flowing Well	20	Mont.	F3	630	1,900	320	--	8.8	3.2	2.4	4.2	.00	36
Storey Fish Hatchery	6	Wyo.	R4	1.4	3.2	220	--	--	.01	--	.1	.03	6.8
Mobil	7	Wyo.	R4	.9	7.7	190	--	--	.01	.0	.2	.00	9.3
HTH No. 1	14	Wyo.	F4	54	460	210	--	--	.09	.2	2.8	.03	30
Ranch Creek	23	Mont.	F4	56	480	210	--	--	.09	.1	3.3	.09	33
Belle Creek	24	Mont.	F4	57	520	210	--	--	.09	.2	3.6	.00	32
Delzer No. 1	7	S.Dak.	F4	25	1,600	110	.04	.2	.14	.1	3.1	.00	17
Delzer No. 2	8	S.Dak.	F4	67	1,700	170	.17	1.8	.17	.2	3.6	.00	29
Hole in the Wall	5	Wyo.	R5	1.3	6.2	260	--	--	.02	.0	.2	.03	6.7
Barber Ranch Spring	12	Wyo.	R5	4.4	34	230	--	--	.02	.1	.3	.06	19
Conoco No. 175	11	Wyo.	F5	70	340	120	.08	--	.20	.4	1.4	.00	19
MKM	10	Wyo.	F5	1,200	920	130	.07	--	.89	3.5	4.4	.00	59
Shidler	9	Wyo.	F5	620	970	110	.12	--	.43	1.9	3.5	.00	32
Conoco No. 44	8	Wyo.	F5	490	840	220	.30	--	.36	4.3	3.0	.03	24
Mallo Camp	24	Wyo.	R6, R7	1.0	1.8	300	--	--	.00	--	.1	.00	12
Rhoads Fork	4	S.Dak.	R6, R7	.4	3.1	310	--	--	--	--	.1	--	8.8

TABLE 8.—*Chemical data used in modeling (anions)*—Continued

Spring or well	Spring or well number	State	Flow path	Cl	SO_4	HCO_3	H_2S (field)	H_2S (laboratory)	B	Br	F	PO_4	H_4SiO_4
Seeley	19	Wyo.	F6	.8	17	300	--	--	.01	.0	.3	.03	12
Coronado No. 2	16	Wyo.	F6	.8	28	280	--	--	.01	--	.2	.02	14
Newcastle	21	Wyo.	F6	1.2	47	290	--	--	--	--	.3	--	12
Osage	17	Wyo.	F6	.7	50	300	--	--	--	--	.4	--	11
Upton	15	Wyo.	F6	0.8	170	280	--	--	--	--	1.2	--	12
Devils Tower	13	Wyo.	F6	2.6	210	270	--	--	.00	--	.5	.06	11
Voss	20	Wyo.	F7	1.7	43	310	--	--	.01	--	.3	.06	12
Self	22	Wyo.	F7	2.1	86	280	--	--	.01	.0	.6	.00	13
JBJ	18	Wyo.	F7	7.6	200	100	--	--	.04	--	1.4	.00	4.5
Evans Plunge	10	S.Dak.	F7	110	550	230	.03	.3	--	--	1.1	--	23
Cascade Spring	9	S.Dak.	F7	31	1,500	240	--	--	--	--	1.6	--	15
Jones Spring	12	S.Dak.	R8	.5	5.8	340	--	--	.03	--	.1	.00	8.4
Kaiser	11	S.Dak.	R8	3.7	14	230	.03	.1	.03	.1	.5	.00	10
Cleghorn Spring	16	S.Dak.	R8	2.2	23	200	--	--	--	--	.0	--	11
Lien	17	S.Dak.	F8	1.5	14	240	--	--	.02	.1	.2	.00	11
McNenney	2	S.Dak.	F8	.6	100	260	--	--	--	--	.3	--	12
Ellsworth AFB	18	S.Dak.	F8	1	200	200	--	--	--	--	.6	--	21
Fuhs	6	S.Dak	F8	3.9	200	340	.05	.5	.02	.0	.2	.00	12
Kosken	1	S.Dak.	F8	40	680	130	.13	.7	.00	.2	1.7	--	39
Philip	19	S.Dak.	F8	22	640	160	.01	.3	--	--	2.6	--	33
Midland	24	S.Dak.	F8	28	800	150	0.02	0.3	--	--	2.8	--	35
Murdo	25	S.Dak.	F8	61	860	150	.14	.7	0.10	0.3	2.6	--	33
Hilltop Ranch	22	S.Dak.	F8	160	1,200	130	.07	.9	.14	4.2	2.9	--	36
Prince	26	S.Dak.	F8	110	1,200	130	.12	.6	.18	.5	3.4	0.00	29
Hamilton	21	S.Dak.	F8	48	1,300	150	--	1.4	.13	.2	3.4	.03	31
Eagle Butte	23	S.Dak.	F8	63	1,300	180	--	.9	.25	.2	3.7	--	30
Dupree	20	S.Dak.	F8	120	1,400	160	1.0	19	.49	.4	3.6	--	34
Gore Hill	2	Mont.	--	110	570	340	--	.9	.51	.7	2.4	.00	15
Great Falls High School	3	Mont.	--	14	230	260	--	--	.09	.1	.9	.00	12
Bough Ranch	5	Mont.	--	64	1,600	260	--	8.2	.33	.3	3.2	0.00	9.7
HTH No. 3	14	Mont.	--	39	1,800	160	--	4.5	.37	.5	.7	.01	7.0
Buckhorn Exeter	27	Mont.	--	2,500	1,300	310	--	34	--	--	4.9	--	58
Provo	3	S.Dak.	--	270	310	180	--	--	--	--	1.3	--	30
Spearfish	5	S.Dak.	--	.6	8	270	--	--	--	--	.2	--	10
Black Hills Cemetery	13	S.Dak.	--	1.8	11	270	.02	.2	.01	.0	.3	.03	10
Streeter Ranch	14	S.Dak.	--	2.5	9	200	.02	.3	--	.0	.4	--	17
Bean	27	S.Dak.	--	17	450	190	.04	.2	--	.4	1.7	--	20
Denius No. 2	3	Wyo.	--	.3	3	240	--	--	.01	.0	.2	--	5.2
Denius No. 3	4	Wyo.	--	.6	43	310	--	--	.01	.0	.3	.00	8.9
Martens Madison	23	Wyo.	--	1.4	11	310	--	--	.03	.0	.3	.00	11
Ranch A	25	Wyo.	--	1.4	200	270	--	--	.03	.1	.3	.00	8

TABLE 9.—*Results of thermodynamic calculations*

[Letter in front of flow-path number indicates whether the spring or well was used as recharge (R) or on the flow path (F)]

Spring or well	Spring or well number	State	Flow path	Log P_{CO_2}	Saturation index: Calcite	Aragonite	Dolomite	Anhydrite	Siderite	Strontianite	Celestite	Barite
Lewistown Big Spring	10	Mont.	R1	-2.40	0.01	-0.15	-0.27	-1.80	-1.46	-1.37	-1.68	--
Hanover Flowing Well	8	Mont.	F1	-2.38	.25	.11	.35	-1.60	-1.75	-1.03	-1.45	--
Vanek Warm Spring	9	Mont.	F1	-2.17	.14	-.01	.06	-1.24	-1.58	-1.15	-1.09	--
Landusky Spring	12	Mont.	F1	-2.01	.15	.00	.20	-.70	-1.85	-1.18	-.60	--
Lodgepole Warm Spring	13	Mont.	F1	-1.80	.11	-.03	.22	-.61	-1.98	-1.22	-.58	--
Sleeping Buffalo	18	Mont.	F1	-1.81	.18	.04	.20	-.15	-.81	-1.21	-.22	--
Bozeman Fish Hatchery	4	Mont.	R2	-2.60	.19	.04	.01	-2.68	-.74	-1.82	-3.17	--
Big Timber Fish Hatchery	7	Mont.	R2	-2.37	.05	-.11	-.27	-2.59	-1.86	-1.53	-2.66	--

TABLE 9.—*Results of thermodynamic calculations*—Continued

Spring or well	Spring or well number	State	Flow path	Log P_{CO_2}	Saturation index							
					Calcite	Aragonite	Dolomite	Anhydrite	Siderite	Strontianite	Celestite	Barite
McLeod Warm Spring	6	Mont.	F2	-2.14	.02	-.13	-.10	-1.74	--	-1.72	-2.07	--
Sumatra	17	Mont.	F2	-.83	.18	.07	-.16	-.48	-1.76	-.88	-.37	.09
Keg Coulee	15	Mont.	F2	-.88	.05	-.07	-.26	-.38	-.77	-1.14	-.34	.41
Texaco C115X	16	Mont.	F2	-.68	.07	-.04	-.38	-.28	-1.64	-1.13	-.30	--
Mock Ranch	1	Wyo.	R3, R4	-2.20	-.01	-.16	-.33	-3.07	-1.65	-1.93	-3.49	.06
Denius No. 1	2	Wyo.	R3, R4	-2.32	-.11	-.26	-.25	-2.80	-.98	-1.94	-3.12	--
Colstrip	21	Mont.	F3	-.89	.12	.02	-.60	-.30	-.68	-1.10	-.36	--
Sarpy Mine	19	Mont.	F3	-1.20	.27	.16	-.00	-.18	-.41	-1.00	-.27	.60
Gas City	26	Mont.	F3	-.70	.56	.46	.52	-.20	-.94	-.66	-.25	.32
Bluewater Spring	11	Mont.	F3	-2.08	.37	.22	.09	-.38	-2.48	-1.19	-.47	1.70
Moore	22	Mont.	F3	-.88	.48	.37	.45	-.20	-1.71	-.74	-.24	.39
Mysse Flowing Well	20	Mont.	F3	-.94	.29	.17	.42	-.11	-1.93	-1.10	-.28	.92
Storey Fish Hatchery	6	Wyo.	R4	-2.06	-.32	-.48	-1.11	-3.51	--	-2.64	-4.31	--
Mobil	7	Wyo.	R4	-2.14	-.59	-.75	-1.35	-3.32	-1.39	-2.59	-3.78	--
HTH No. 1	14	Wyo.	F4	-1.57	.18	.05	.25	-.82	.79	-1.12	-.84	.88
Ranch Creek	23	Mont.	F4	-1.47	.23	.10	.33	-.75	-1.63	-1.09	-.80	--
Belle Creek	24	Mont.	F4	-1.52	.35	.22	.56	-.68	-1.13	-1.01	-.80	.77
Delzer No. 1	7	S.Dak.	F4	-2.57	.37	.23	.43	-.32	.52	-.89	-.17	1.26
Delzer No. 2	8	S.Dak.	F4	-1.41	.25	.13	.27	-.04	.38	-1.21	-.25	.76
Hole in the Wall	5	Wyo.	R5	-1.94	-.48	-.64	-.92	-3.41	-1.78	-2.48	-3.88	--
Barber Ranch Spring	12	Wyo.	R5	-2.17	-.02	-.17	-.29	-2.41	-1.61	-1.72	-2.65	--
Conoco No. 175	11	Wyo.	F5	-1.74	.07	-.04	-.04	-.94	.54	-1.50	-1.30	.28
MKM	10	Wyo.	F5	-1.21	.20	.10	-.22	-.32	.65	-1.27	-.63	.05
Shidler	9	Wyo.	F5	-1.90	.18	.05	.05	-.43	.20	-1.37	-.74	--
Conoco No. 44	8	Wyo.	F5	-1.85	.21	.07	.26	-.72	-.20	-1.29	-.86	.90
Mallo Camp	24	Wyo.	R6	-2.23	.12	-.04	-.06	-3.76	--	--	--	--
Rhoads Fork	4	S.Dak.	R6, R7	-1.98	-.09	-.25	-.60	-3.50	--	-2.49	-4.36	--
Seeley	19	Wyo.	F6	-1.91	-.05	-.20	-.31	-2.70	-1.73	-1.96	-3.12	-.12
Coronado No. 2	16	Wyo.	F6	-1.63	.08	-.05	.33	-2.31	--	-1.71	-2.79	--
Newcastle	21	Wyo.	F6	-1.76	-.02	-.16	-.02	-2.17	--	-1.81	-2.56	--
Osage	17	Wyo.	F6	-1.75	.01	-.13	-.06	-2.13	--	-1.89	-2.61	--
Upton	15	Wyo.	F6	-1.69	-.03	-.17	-.02	-1.57	--	-1.10	-1.24	--
Devils Tower	13	Wyo.	F6	-1.84	.00	-.15	-.21	-1.48	-1.68	--	--	.41
Voss	20	Wyo.	F7	-1.82	.12	-.02	.27	-2.21	--	-1.66	-2.59	--
Self	22	Wyo.	F7	-1.85	.16	.02	.36	-1.85	-1.39	-1.51	-2.14	--
JBJ	18	Wyo.	F7	-1.58	-.71	-.84	-1.44	-1.37	--	-1.46	-.83	--
Evans Plunge	10	S.Dak.	F7	-1.55	-.03	-.17	-.34	-.84	--	-1.53	-.97	--
Cascade Spring	9	S.Dak.	F7	-1.61	.10	-.05	-.30	-.33	--	-1.46	-.46	--
Jones Spring	12	S.Dak.	R8	-1.75	-.06	-.21	-.45	-3.13	--	-2.32	-3.90	--
Kaiser	11	S.Dak.	R8	-2.11	-.15	-.30	-.51	-2.86	-1.07	-1.94	-3.17	-.18
Cleghorn Spring	16	S.Dak.	R8	-2.19	-.30	-.45	-.79	-2.71	--	-2.40	-3.32	--
Lien	17	S.Dak.	F8	-2.12	-.19	-.34	-.48	-2.91	-2.03	-2.18	-3.41	-.14
McNenney	2	S.Dak.	F8	-1.86	-.17	-.32	-.74	-1.88	--	-1.65	-1.86	--
Ellsworth AFB	18	S.Dak.	F8	-1.57	.03	-.10	.12	-1.29	--	-1.64	-1.69	--
Fuhs	6	S.Dak.	F8	-1.79	-.09	-.25	-.18	-1.68	-2.22	-1.84	-1.92	.58
Kosken	1	S.Dak.	F8	-1.34	-.05	-.17	-.36	-.48	--	-1.52	-.73	--
Philip	19	S.Dak.	F8	-1.18	.03	-.09	-.09	-.51	--	-1.42	-.76	--
Midland	24	S.Dak.	F8	-1.24	0.13	0.01	0.04	-0.36	--	-1.34	-0.63	--
Murdo	25	S.Dak.	F8	-1.32	.01	-.11	-.17	-.38	-0.19	-1.39	-.56	--
Hilltop Ranch	22	S.Dak.	F8	-1.36	.06	-.05	-.12	-.20	-.44	-1.36	-.42	--
Prince	26	S.Dak.	F8	-1.40	-.01	-.13	-.25	-.21	-.88	-1.42	-.38	0.96
Hamilton	21	S.Dak.	F8	-1.32	.05	-.07	-.10	-.17	.03	-1.36	-.36	-.43
Eagle Butte	23	S.Dak.	F8	-1.45	.23	.11	.40	-.24	.24	-1.06	-.29	--
Dupree	20	S.Dak.	F8	-1.47	.17	.04	.18	-.20	-.83	-1.10	-.23	--
Gore Hill	2	Mont.	--	-1.71	.04	-.11	-.05	-1.08	-.34	-1.24	-.88	--
Great Falls High School	3	Mont.	--	-2.08	.05	-.10	-.11	-1.54	-1.18	-1.41	-1.52	--
Bough Ranch	5	Mont.	--	-1.78	.01	-.14	.11	-.56	-1.33	-1.17	-.29	--

TABLE 9.—*Results of thermodynamic calculations*—Continued

Spring or well	Spring or well number	State	Flow path	Log P_{CO_2}	Saturation index							
					Calcite	Aragonite	Dolomite	Anhydrite	Siderite	Strontianite	Celestite	Barite
HTH No. 3	14	Mont.	--	-1.50	.13	.01	.06	-.09	-.46	-1.33	-.29	--
Buckhorn Exeter	27	Mont.	--	-.66	.16	.05	-.11	-.27	-.64	--	--	--
Provo	3	S.Dak.	--	-1.51	.07	-.05	.06	-1.06	--	-1.35	-1.25	--
Spearfish	5	S.Dak.	--	-2.04	-.08	-.24	-.34	-3.08	--	-2.11	-3.62	--
Black Hills Cemetery	13	S.Dak.	--	-1.93	-.18	-.34	-.58	-2.94	-1.80	-1.89	-3.15	.21
Streeter Ranch	14	S.Dak.	--	-2.20	.30	.17	.68	-2.83	-.91	-1.48	-3.30	--
Bean	27	S.Dak.	--	-1.75	.15	.02	.28	-.90	-1.37	-1.22	-.96	--
Denius No. 2	3	Wyo.	--	-2.27	-.01	-.17	-.48	-3.55	-1.99	-2.16	-4.18	--
Denius No. 3	4	Wyo.	--	-2.31	.32	.16	.34	-2.32	-1.78	-1.27	-2.39	--
Martens Madison	23	Wyo.	--	-2.08	.17	.01	.17	-2.89	--	--	--	--
Ranch A	25	Wyo.	--	-1.93	.03	-.13	-.37	-1.51	--	-1.52	-1.56	.58

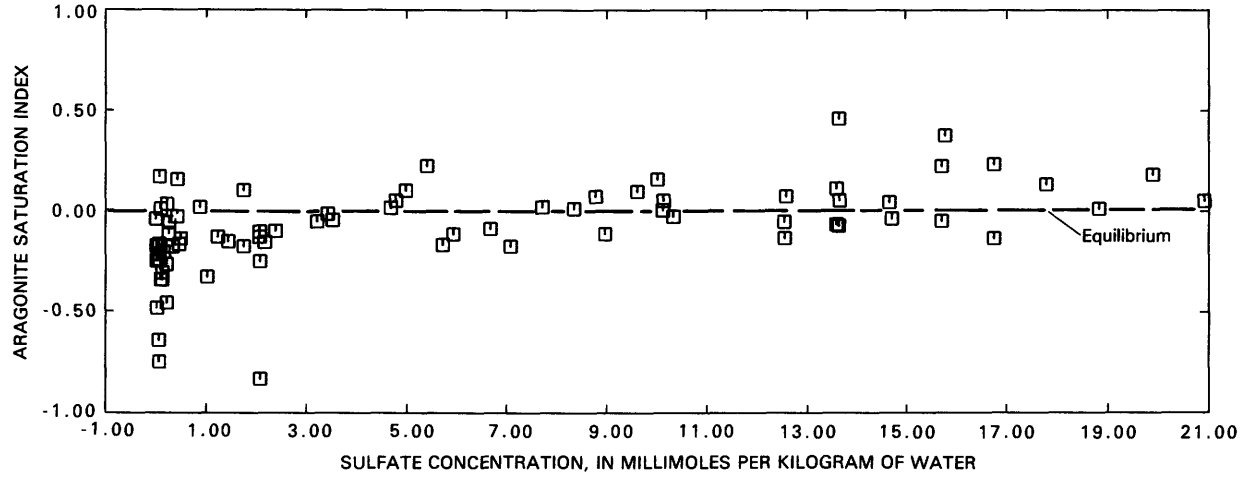

FIGURE 10.—Saturation indices of aragonite as a function of dissolved-sulfate concentration for all wells and springs sampled.

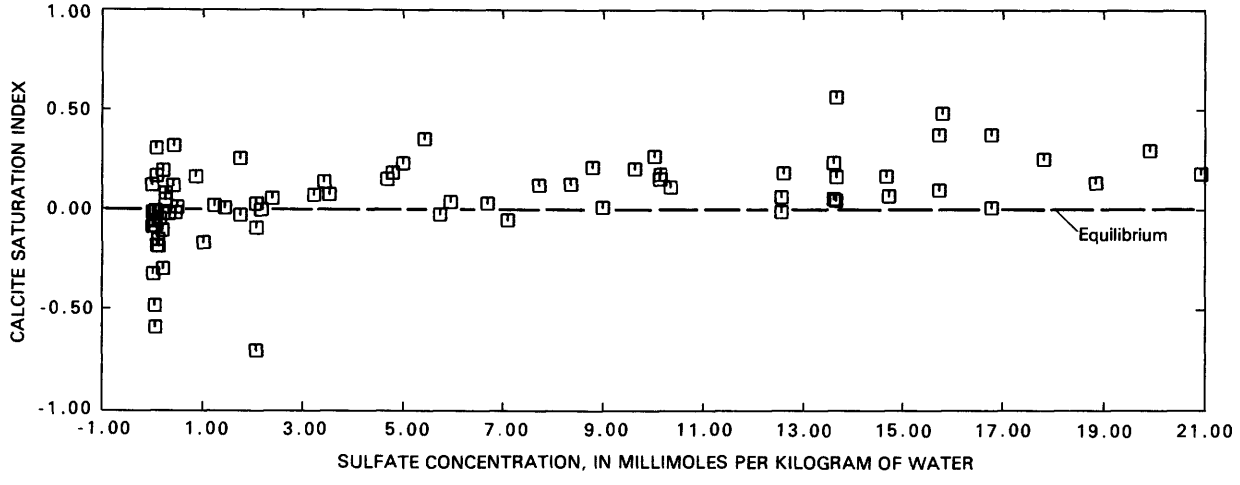

FIGURE 11.—Saturation indices of calcite as a function of dissolved-sulfate concentration for all wells and springs sampled.

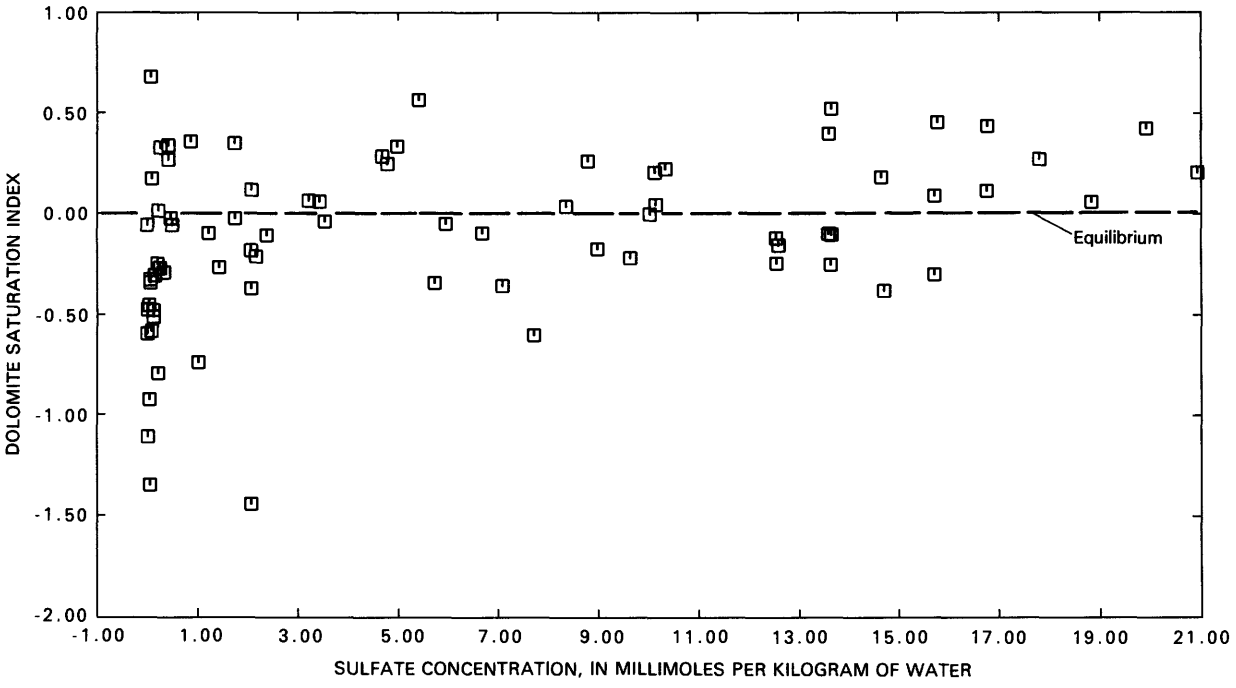

FIGURE 12.—Saturation indices of dolomite as a function of dissolved-sulfate concentration for all wells and springs sampled.

Alternatively, laboratory studies have shown that the presence of dissolved magnesium and higher temperatures favor precipitation of aragonite rather than calcite (Bischoff, 1968). Thus, under the in situ conditions, aragonite may be controlling the $CaCO_3$ solubility product rather than calcite. The X-ray diffraction analysis of samples of scale and travertine from the outlets of the flowing wells of Mysse (well No. 20 in Montana), Moore (well No. 22 in Montana), and Philip (well No. 19 in South Dakota) showed the presence of both calcite and aragonite, though aragonite was not noted in the subsurface by either Thayer (1981) or R.S. Deike, (U.S. Geological Survey, written commun., 1984).

The data in figure 12 show that, except for some waters with very small sulfate concentrations, waters in the Madison aquifer are saturated with dolomite. Because the solubility of dolomite as a function of temperature is not well known, the dolomite *SI* has been calculated using the thermodynamic data in table 6 by assuming a constant change in enthalpy (ΔH_r°) for the dissolution of dolomite throughout the entire range of temperature determined for the Madison aquifer and adjusting the equilibrium constant for the effects of temperature by using the Van't Hoff equation:

$$\log \frac{K_{DT}}{K_{298.15}} = \frac{-\Delta H_r^\circ}{R}\left(\frac{1}{T} - \frac{1}{298.15}\right), \quad (3)$$

where

K_{DT} is the equilibrium constant for dolomite dissolution;

$K_{298.15}$ is the equilibrium constant for dolomite dissolution at 298.15 K;

ΔH_r° is the standard enthalpy of the dissolution reaction at 1 atm pressure and 298.15 K;

R is the gas constant (0.08205 L-atm/mol·K); and

T is the final temperature, in kelvins.

If the waters from the Madison aquifer are in equilibrium with aragonite (or calcite) and dolomite, it is possible to derive more accurate expressions for the temperature dependence of the dolomite equilibrium constant from the field data.

The data in figure 15 show an increase in $\log(a\mathrm{Ca}^{2+}/a\mathrm{Mg}^{2+})$ with temperature corresponding to the following relation:

$$\log\left(\frac{a\mathrm{Ca}^{2+}}{a\mathrm{Mg}^{2+}}\right) = 1.907 + 0.0072T, \quad (4)$$

where

T is temperature, in kelvins; and

a is the activity of the specified ion.

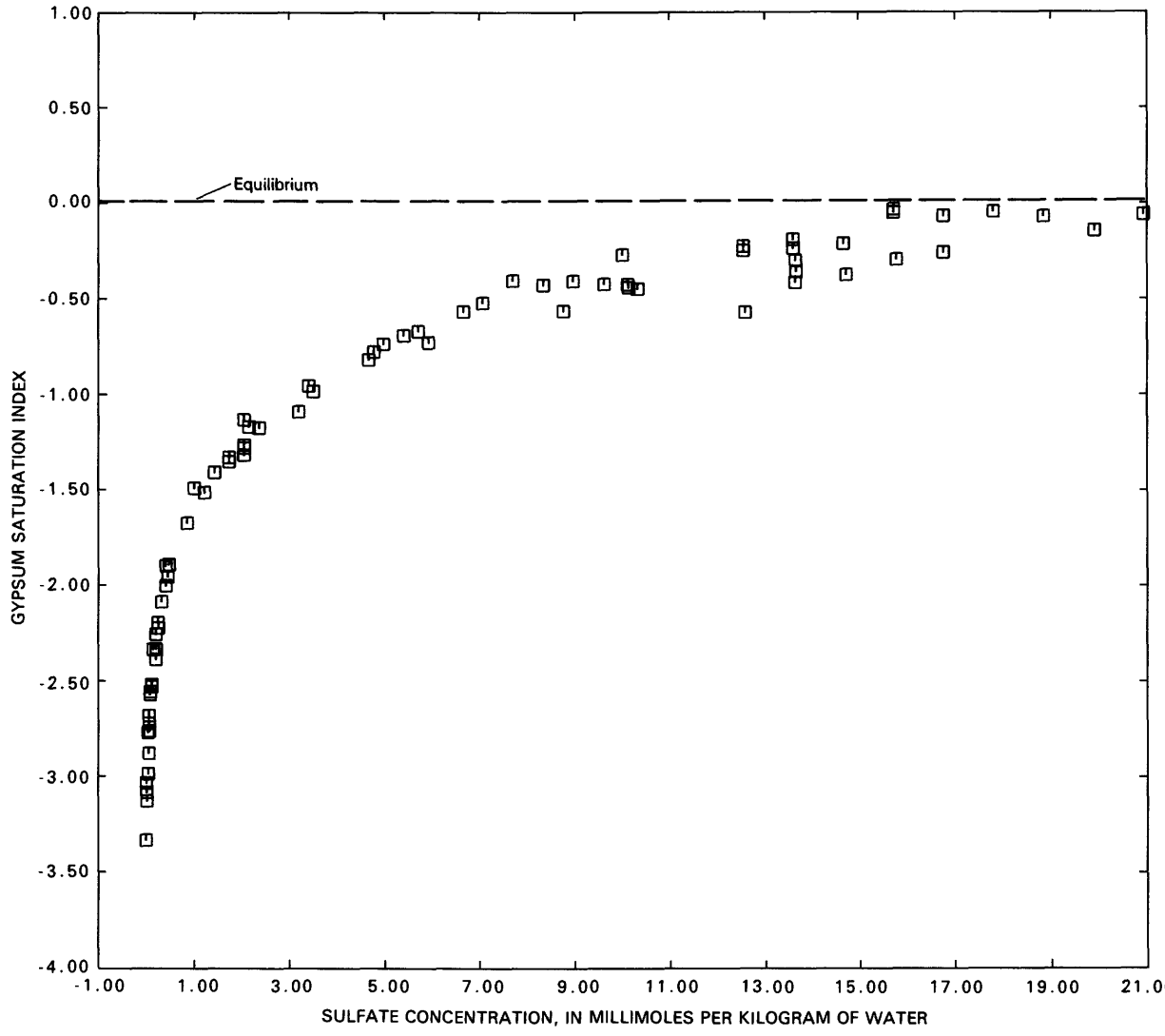

FIGURE 13.—Saturation indices of gypsum as a function of dissolved-sulfate concentration for all wells and springs sampled.

For water in equilibrium with aragonite (or calcite) and dolomite, equation 5 may be written from the following reactions:

$$2CaCO_3 = 2Ca^{2+} + 2CO_3^{2-} \quad 2\log K_A$$

$$Ca^{2+} + Mg^{2+} + 2CO_3^{2-} = CaMg(CO_3)_2 \quad -\log K_D$$

$$2CaCO_3 + Mg^{2+} = CaMg(CO_3)_2 + Ca^{2+} \quad 2\log K_A - \log K_D, \quad (5)$$

for which the equilibrium constant is

$$\log\left(\frac{a\mathrm{Ca}^{2+}}{a\mathrm{Mg}^{2+}}\right) = 2\log K_A - \log K_D \quad (6)$$

where the subscripts A and D denote aragonite and dolomite, respectively. Assuming that the dolomite is in equilibrium with aragonite and using the approximately linear relation for $\log (a\mathrm{Ca}^{2+}/a\mathrm{Mg}^{2+})$ from figure 15 with the aragonite equilibrium-constant expression from table 6, the temperature dependence of the dolomite equilibrium constant is approximately

$$\log K_D = 2\log K_A - \log \frac{a\mathrm{Ca}^{2+}}{a\mathrm{Mg}^{2+}}, \quad (7)$$

$$\log K_D = -342.05 - 0.163186T + 5806.586/T + 143.19\log T. \quad (8)$$

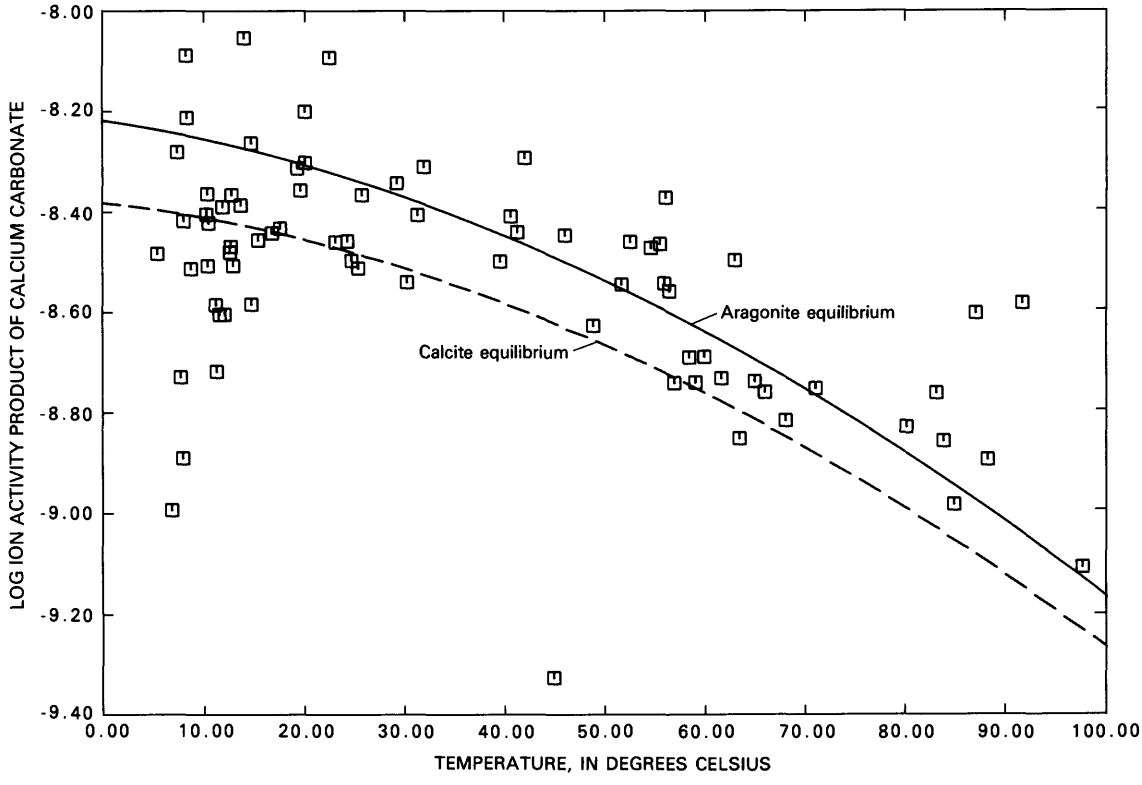

FIGURE 14.—Log of ion activity product of calcium carbonate as a function of temperature for all wells and springs sampled.

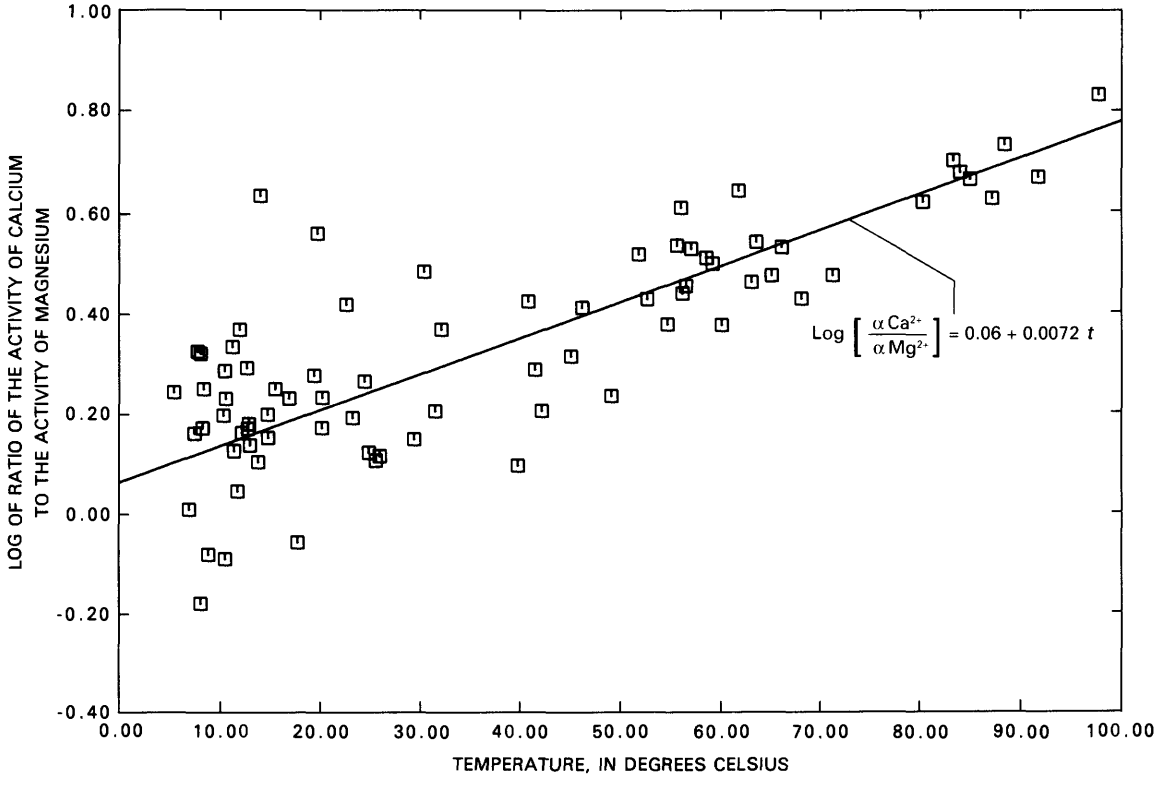

FIGURE 15.—Log of ratio of activity of calcium to activity of magnesium as a function of temperature (t, in °C) for all wells and springs sampled.

Alternatively, if the waters from the Madison aquifer are in equilibrium with calcite rather than aragonite, the equation becomes

$$\log K_D = -341.91 - 0.163186T + 5678.638/T + 143.19 \log T. \quad (9)$$

Application of the Van't Hoff equation to the data in table 6 leads to

$$\log K_D = -24.01 + 2062.035/T. \quad (10)$$

The data in figure 16 compare log K_D calculated from equations 8 to 10 and show that the Van't Hoff equation used in this report for calculation of the dolomite equilibrium constant probably is accurate to ± 0.1 log K at 60 °C, but that it may overestimate the value by as much as 0.4 log K units at 80 °C. If equations 8 or 9 more accurately describe the temperature dependence of the dolomite equilibrium constant, then the computed dolomite SI for waters at 80 °C, for example, should be increased by 0.2 to 0.4 SI units. The data in figure 17 show a trend toward undersaturation with respect to dolomite

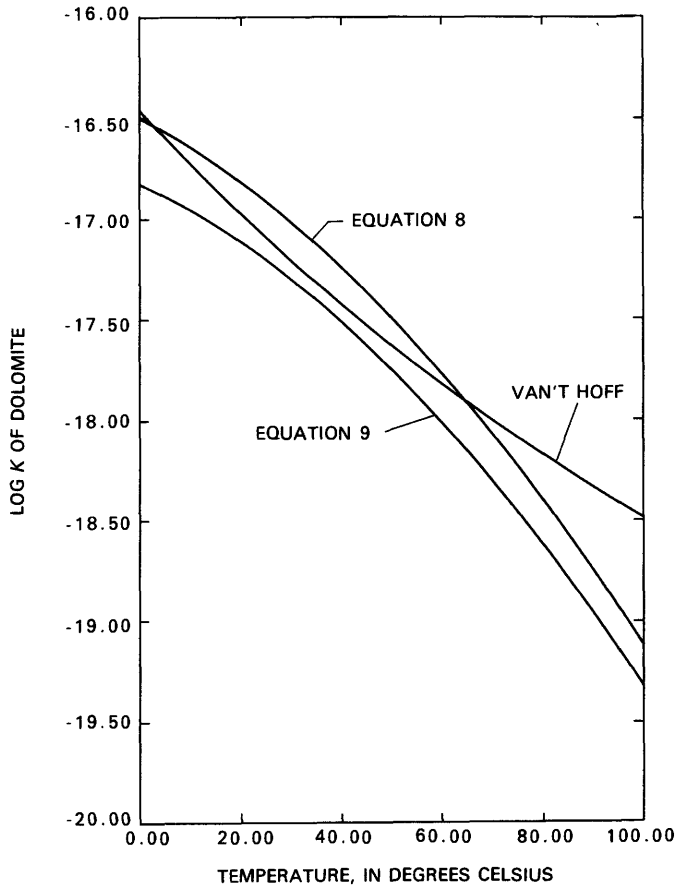

FIGURE 16.—Comparison of temperature dependence of log K dolomite as given by Van't Hoff equation and derived from assumption of aragonite-dolomite equilibrium (eq 8) and calcite-dolomite equilibrium (eq 9) as a function of temperature for all wells and springs sampled.

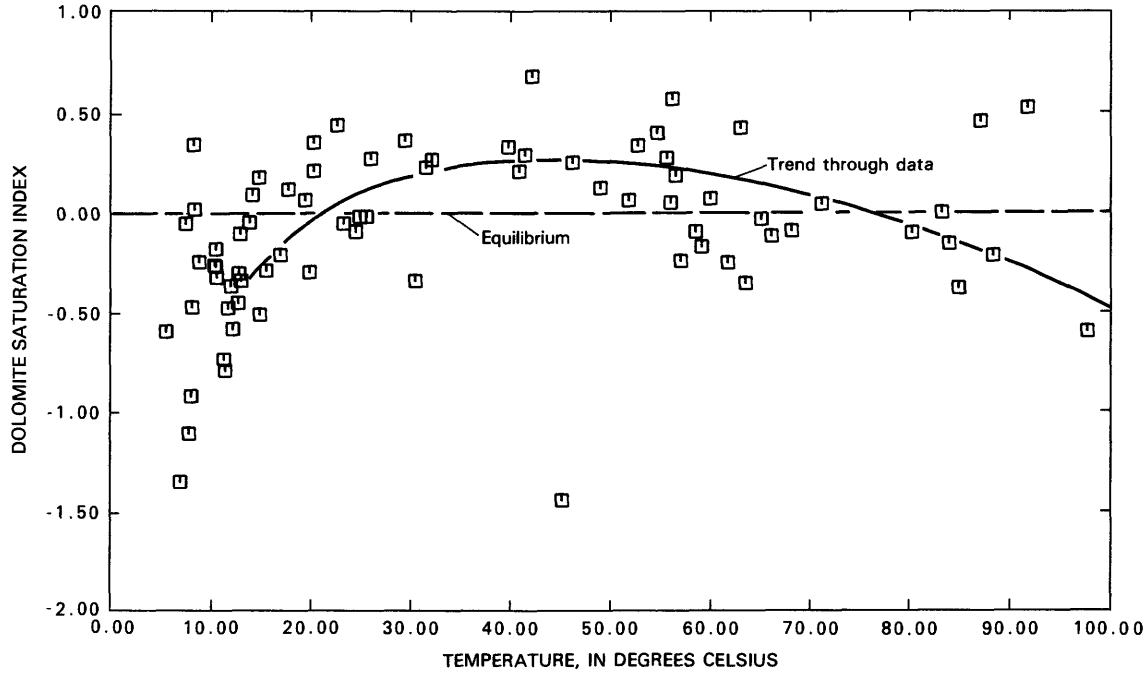

FIGURE 17.—Dolomite saturation index based on Van't Hoff equation as a function of temperature for all wells and springs sampled.

at higher temperatures based on the Van't Hoff approximation to log K_D (table 6). From the results of figure 16, this trend probably reflects the inappropriateness in using a constant ΔH_r^o at higher temperatures rather than undersaturation with respect to dolomite.

The data in figure 18 show that with increasing sulfate concentration the celestite *SI* approaches a constant value near −0.2 between 14 and 21 mmol/L (millimoles per liter) sulfate. This indicates saturation with a celestite phase slightly less soluble than that of the laboratory-precipitated celestite (Gallo, 1935) given in table 6.

An application of the Gibbs phase rule to the $CaCO_3$-$CaSO_4$-$SrSO_4$ system at constant temperature and pressure indicates that waters in equilibrium with calcite (or aragonite), gypsum, and celestite cannot also be in equilibrium with strontianite. For example, assume that a water is saturated with aragonite, gypsum, and celestite:

$$\log (a\mathrm{Ca}^{2+}\ a\mathrm{CO}_3^{2-}) = \log K_A,$$

$$\log (a\mathrm{Ca}^{2+}\ a\mathrm{SO}_4^{2-}) = \log K_G, \text{ and}$$

$$\log (a\mathrm{Sr}^{2+}\ a\mathrm{SO}_4^{2-}) = \log K_{Cel},$$

where the subscripts *A*, *G*, and *Cel* represent aragonite, gypsum (assuming unit activity of water), and celestite, respectively. The *SI* of strontianite is then dependent on

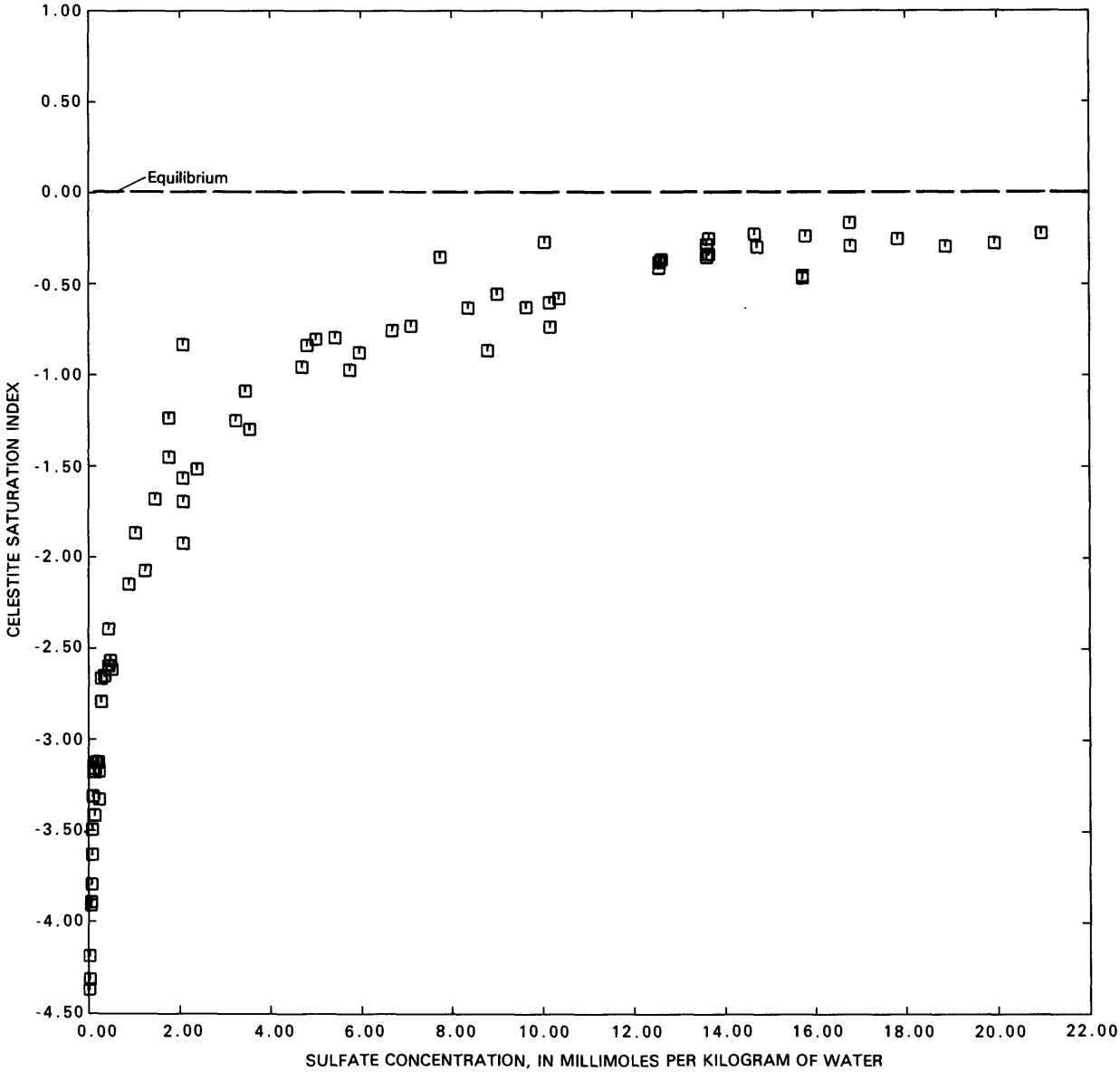

FIGURE 18.—Celestite saturation index as a function of dissolved-sulfate concentration for all wells and springs sampled.

the equilibrium constants of aragonite, gypsum, and celestite according to

$$SI_{St} = \log \frac{K_A K_{Cel}}{K_G K_{St}}, \quad (11)$$

where *St* represents strontianite, and the other terms are as defined above.

A constant level of undersaturation with respect to strontianite near −1.0 would be expected if the data in table 6 at 25 °C are substituted into equation 11. The data in figure 19 show that the strontianite *SI*, as a function of sulfate concentration, is near -1.2 ± 0.2 throughout the Madison aquifer, in agreement with equation 11. Based on this determination, if strontianite were present in the Madison aquifer, it would dissolve irreversibly, causing precipitation of celestite, calcite, and further dissolution of gypsum.

The results of the thermodynamic calculations in table 9 show considerable variation for barite and siderite, partly reflecting larger uncertainties in the analytical data for dissolved barium and iron. The calculations indicate, however, that most waters of the Madison aquifer are probably saturated or oversaturated with barite and undersaturated with siderite.

The data in figure 20 show that most of the waters are oversaturated with respect to quartz but either saturated or slightly undersaturated with respect to chalcedony throughout the temperature range.

In addition to providing *SI* information, the equilibrium-speciation calculations may yield information on other parameters of use during the modeling process. These include P_{CO_2} (table 9), the redox state of the water (*RS*) (Parkhurst and others, 1980), the total concentration of inorganic carbon (molal units), and a conversion of the total concentrations of the other analyzed elements to the molal scale. The molal-scale concentrations (mmol/kg of water) of the elements and redox state are summarized in table 10 for the average recharge water of each flow path and for each subsequent well on the flow path. These values were used in a mass-balance analysis of the reactions and are discussed after an examination of trends in the water-quality data.

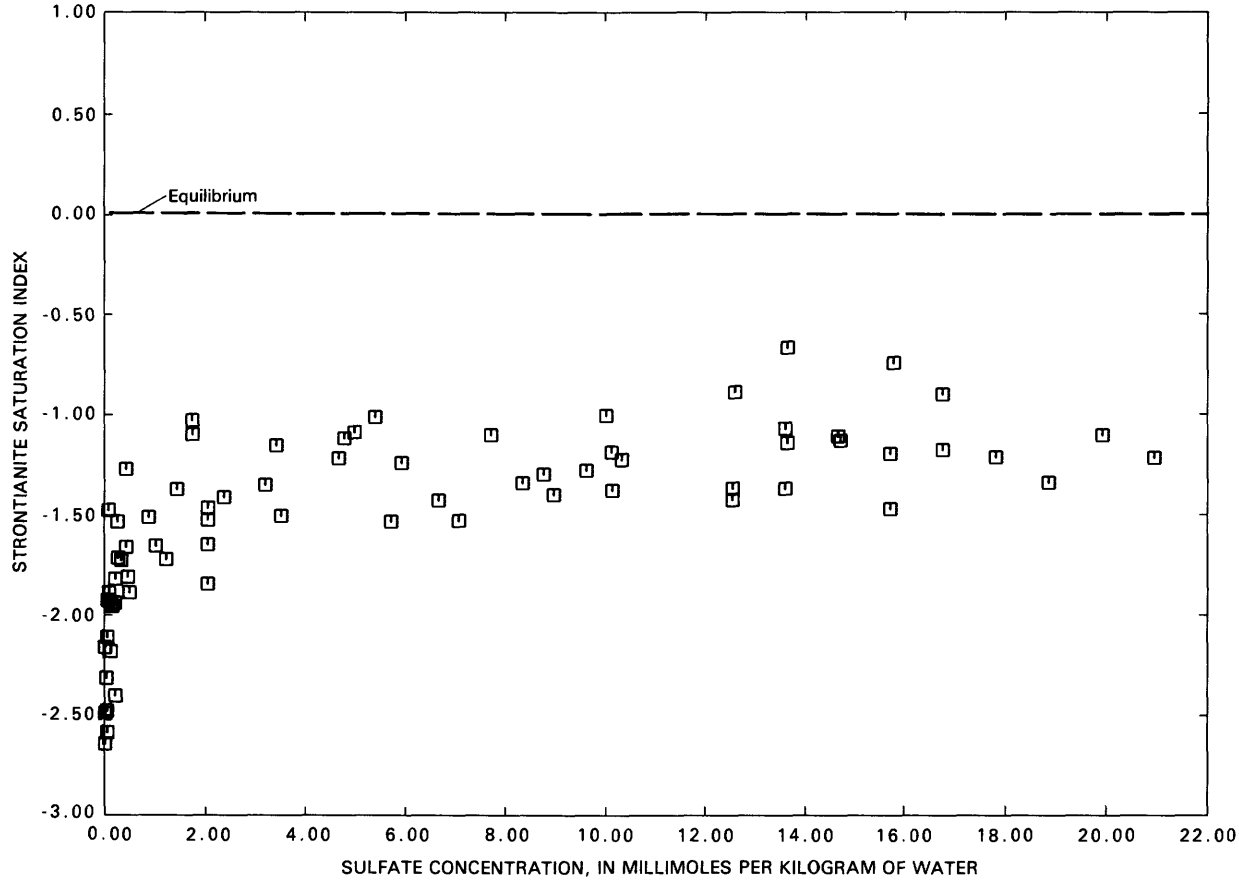

FIGURE 19.—Strontianite saturation index as a function of dissolved-sulfate concentration for all wells and springs sampled.

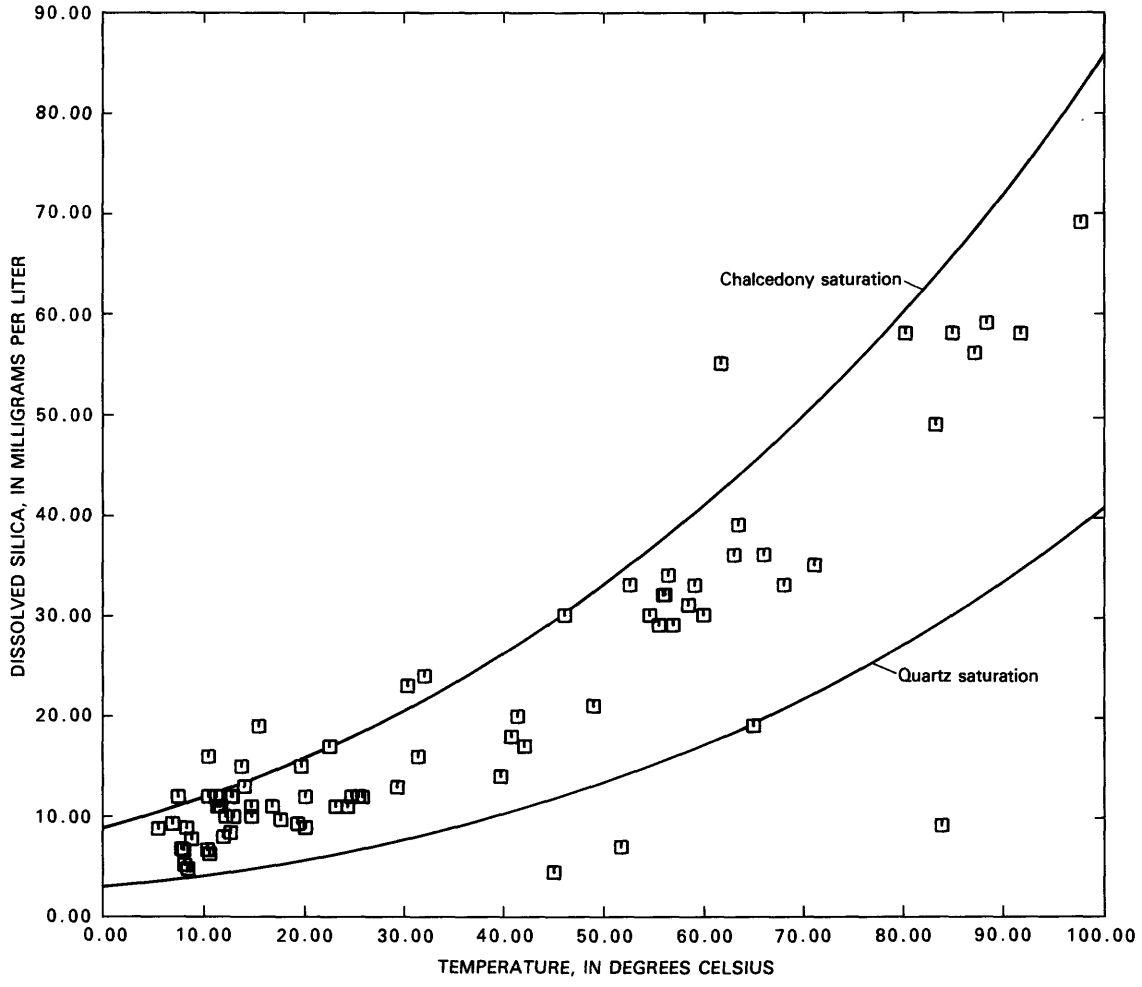

FIGURE 20.—Dissolved-silica concentration as a function of temperature for all wells and springs sampled.

TRENDS IN WATER-QUALITY DATA

Trends in the water-quality data as a function of dissolved sulfate are an indication of further reactions in the system. These trends also can indicate other reactions that need to be considered; for example, calcite and dolomite may be either dissolving or precipitating as a function of reaction progress, responding almost reversibly to the dissolution of anhydrite (a partial-equilibrium system).

In the preceding section, thermodynamic calculations were used to determine, from the saturation states, which minerals may react reversibly and which may react irreversibly in the Madison aquifer. Based on these calculations, it is likely that anhydrite dissolves irreversibly in most of the system, whereas the water remains at or near saturation with calcite and dolomite. It is appropriate then to choose total dissolved sulfate as a reaction-progress variable in examining trends in the water-quality data.

Changes in predominant cations and anions are depicted (on a mole percent basis) on the trilinear diagram in figure 21. No single flow path shows the entire evolutionary trend, but the combined eight flow paths have different segments of the overall reaction path. The evolutionary path for cations proceeds from a predominance of calcium and magnesium to sodium predominance.

The anions proceed from a predominance of bicarbonate to sulfate to chloride. This trend indicates that the major-element chemistry is initially determined by dissolution of calcite and dolomite followed by dissolution of anhydrite, and along several flow paths halite dissolution may be important.

There are distinct differences in the extent of reaction progress along each flow path as shown in separate trilinear diagrams (figs. 22–29). Flow paths 1, 4, 7, and 8 (figs. 22, 25, 28, and 29) begin as calcium-magnesium bicarbonate waters but are significantly affected by

TABLE 10.—*Total concentrations of the major elements and redox state used in mass-balance models*

[All constituent concentrations are in millimoles per kilogram of water; letter in front of flow-path number indicates whether the spring or well was used as recharge (R) or on the flow path (F); Ca, calcium; Mg, magnesium; Na, sodium; K, potassium; Cl, chloride; C, total dissolved inorganic carbon; S, total dissolved sulfide; SO_4, sulfate; Fe, total dissolved iron]

Spring or well	Spring or well number	State	Flow path	Ca	Mg	Na	K	Cl	C	S	SO_4	Fe	Redox state
Recharge No. 1	--	--	R1	1.87	1.15	0.10	0.02	0.05	3.31	--	1.46	0.0007	21.9
Hanover Flowing Well	8	Mont.	F1	2.10	1.19	.12	.03	.04	3.42	--	1.77	.0002	24.2
Vanek Warm Spring	9	Mont.	F1	3.25	1.65	.16	.03	.07	3.53	--	3.44	.0005	34.7
Landusky Spring	12	Mont.	F1	6.50	4.08	1.79	.24	.54	3.81	--	10.11	.0005	75.9
Lodgepole Warm Spring	13	Mont.	F1	6.50	3.96	3.44	.31	1.89	3.72	--	10.32	.0004	76.8
Sleeping Buffalo	18	Mont.	F1	12.77	4.95	13.53	.67	5.38	2.81	0.001	20.89	.0079	136.5
Recharge No. 2	--	--	R2	1.26	.68	.22	.04	.05	3.85	--	.26	.0010	16.9
McLeod Warm Spring	6	Mont.	F2	1.77	.95	.07	.04	.03	3.35	--	1.25	.0000	20.9
Sumatra	17	Mont.	F2	5.52	1.41	78.78	3.35	65.27	6.31	1.358	12.57	.0004	97.9
Keg Coulee	15	Mont.	F2	8.78	2.19	65.63	3.09	56.74	6.78	1.682	13.61	.0070	105.4
Texaco C115X	16	Mont.	F2	8.03	2.15	74.42	3.86	59.61	6.37	3.898	14.67	.0009	105.6
Recharge No. 3	--	--	R3	1.20	1.01	.02	.02	.02	4.30	--	.16	.0010	18.1
Colstrip	21	Mont.	F3	5.50	1.15	6.10	1.72	2.71	3.58	.118	7.72	.0061	60.3
Sarpy Mine	19	Mont.	F3	8.00	2.10	2.09	1.26	.59	2.99	.085	10.01	.0100	71.8
Gas City	26	Mont.	F3	9.28	2.52	61.24	2.83	53.90	7.54	1.594	13.61	.0018	108.6
Bluewater Spring	11	Mont.	F3	13.26	2.76	3.10	.07	.07	3.97	--	15.65	.0002	109.8
Moore	22	Mont.	F3	9.54	2.82	74.44	3.35	68.14	6.02	.561	15.72	.0004	117.2
Mysse Flowing Well	20	Mont.	F3	11.28	4.54	31.89	2.54	17.85	6.87	.259	19.86	.0004	146.1
Recharge No. 4	--	--	R4	1.12	.85	.05	.02	.02	4.05	--	.11	.0012	16.8
HTH No. 1	14	Wyo.	F4	4.50	1.81	1.57	.19	1.52	3.99	--	4.79	.1040	44.9
Ranch Creek	23	Mont.	F4	4.75	1.89	1.65	.20	1.58	4.05	--	5.00	.0004	46.2
Belle Creek	24	Mont.	F4	5.00	1.98	1.65	.20	1.61	3.95	--	5.42	.0009	48.3
Delzer No. 1	7	S.Dak.	F4	12.76	4.54	1.57	.90	.71	1.88	.001	16.70	.1418	107.9
Delzer No. 2	8	S.Dak.	F4	13.76	4.54	1.96	.31	1.89	3.45	.005	17.74	.1023	120.4
Recharge No. 5	--	--	R5	1.14	1.05	.22	.04	.08	4.45	--	.21	.0004	19.0
Conoco No. 175	11	Wyo.	F5	2.75	1.03	3.35	.25	1.98	2.23	.002	3.54	.0430	30.2
MKM	10	Wyo.	F5	7.26	1.69	33.17	1.77	33.97	2.81	.002	9.61	.1240	69.1
Shidler	9	Wyo.	F5	7.50	2.02	21.37	.90	17.53	2.00	.004	10.12	.0431	68.8
Conoco No. 44	8	Wyo.	F5	6.00	2.51	16.57	.64	13.85	3.98	.009	8.76	.0156	68.5
Recharge No. 6	--	--	R6	1.54	.97	.05	.02	.02	5.46	--	.03	.0000	21.9
Seeley	19	Wyo.	F6	1.65	1.11	.06	.03	.02	5.51	--	.18	.0004	23.0
Coronado No. 2	16	Wyo.	F6	1.40	1.11	.08	.04	.02	5.13	--	.29	--	22.2
Newcastle	21	Wyo.	F6	1.60	1.19	.11	.04	.03	5.34	--	.49	--	24.2
Osage	17	Wyo.	F6	1.75	1.11	.09	.04	.02	5.54	--	.52	--	25.2
Upton	15	Wyo.	F6	2.20	1.69	.11	.06	.02	5.25	--	1.77	--	31.6
Devils Tower	13	Wyo.	F6	2.75	1.56	.16	.04	.07	5.03	--	2.19	.0005	33.2
Recharge No. 7	--	--	R7	1.65	.95	.04	.02	.01	5.73	--	.03	.0000	23.1
Voss	20	Wyo.	F7	1.57	1.19	.11	.04	.05	5.56	--	.45	--	24.9
Self	22	Wyo.	F7	1.82	1.28	.11	.05	.06	5.00	--	.90	.0004	25.3
JBJ	18	Wyo.	F7	1.82	.91	.48	.12	.21	2.20	--	2.08	--	21.2
Evans Plunge	10	S.Dak.	F7	5.25	1.69	3.75	.28	3.11	4.59	.001	5.73	--	52.7
Cascade Spring	9	S.Dak.	F7	13.51	3.42	1.18	.13	.88	4.87	--	15.65	--	113.4
Recharge No. 8	--	--	R8	1.33	.81	.23	.05	.06	4.67	.001	.15	.0007	19.5
Lien	17	S.Dak.	F8	1.15	1.03	.10	.05	.04	4.31	--	.15	.0002	18.1
McNenney	2	S.Dak.	F8	2.17	.99	.09	.04	.02	4.96	--	1.04	--	26.0
Ellsworth AFB	18	S.Dak.	F8	2.27	1.36	.21	.09	.03	3.80	--	2.08	--	27.7
Fuhs	6	S.Dak.	F8	2.20	2.59	.25	.09	.11	6.41	.002	2.08	.0002	38.1
Kosken	1	S.Dak.	F8	6.00	1.98	1.18	.28	1.13	2.83	.004	7.09	--	53.8
Philip	19	S.Dak.	F8	5.50	2.39	.78	.19	.62	3.57	.000	6.67	--	54.2
Midland	24	S.Dak.	F8	6.75	2.72	1.09	.25	.79	3.26	.001	8.34	--	63.0
Murdo	25	S.Dak.	F8	7.50	2.68	2.00	.33	1.72	3.24	.004	8.97	.0251	66.7
Hilltop Ranch	22	S.Dak.	F8	9.00	3.17	3.70	.33	4.52	2.77	.002	12.52	.0154	86.2
Prince	26	S.Dak.	F8	10.25	3.42	3.14	.51	3.11	2.80	.004	12.52	.0075	86.3
Hamilton	21	S.Dak.	F8	10.50	3.71	1.48	.38	1.36	3.22	.041	13.56	.0538	94.2
Eagle Butte	23	S.Dak.	F8	9.75	4.53	2.62	.72	1.78	3.54	.027	13.56	.0538	95.6
Dupree	20	S.Dak.	F8	9.75	3.88	4.80	1.26	3.39	3.17	.029	14.61	.0054	100.2

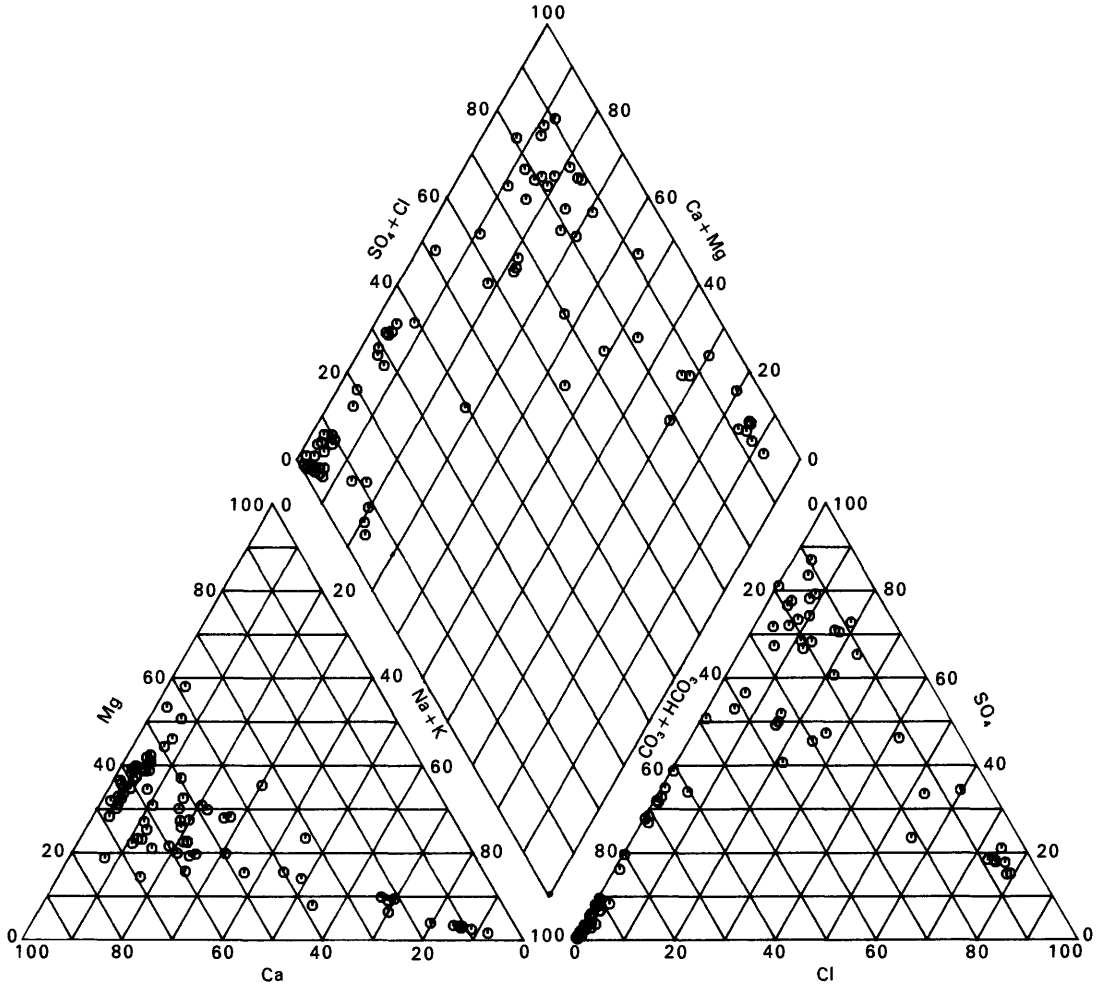

FIGURE 21.—Trilinear diagram showing chemical composition of water along all flow paths, in mole percent of cations and anions.

anhydrite dissolution. Flow paths 2, 3, and 5 (figs. 23, 24, and 26) are significantly affected by halite dissolution. Flow path 6 (fig. 27) is controlled predominantly by carbonate mineral reactions. Flow path 4 (fig. 25) represents a relatively mature water in which dissolution of anhydrite dominates over dissolution of the carbonate minerals. Although these waters are dominated by halite dissolution, they also show evidence of earlier evolution in the calcite-dolomite-anhydrite reaction system. For example, flow paths 3 (fig. 24) and 5 (fig. 26) begin with waters similar in composition to those at the end of flow paths 1 (fig. 22) and 8 (fig. 29), and the initial well on flow path 2 (fig. 23) predominantly is calcium-magnesium bicarbonate. It is expected that better well control along the beginnings of flow paths 2, 3, and 5 would show the full reaction path from predominantly $Ca>Mg:HCO_3$ to $Ca>Mg:SO_4>HCO_3$ to $Na>Ca>Mg:Cl>SO_4>HCO_3$ waters.

Because the trilinear diagrams only indicate changes in the relative proportions of cations and anions, more reaction information may be gained by examining actual changes in concentration as a function of reaction progress (sulfate concentration).

Systematic increases in both calcium and magnesium as sulfate increases are shown in figures 30 and 31. An increase in dissolved sulfate also corresponds with a general decrease in pH and an increase in P_{CO_2} (figs. 32 and 33).

These trends result from the dedolomitization reaction as discussed by Back and others (1983). Beginning with recharge water near saturation with calcite and dolomite, dissolution of anhydrite adds calcium to the ground water, causing precipitation of calcite. Calcite precipitation causes pH to decrease (fig. 32) (as a result of H^+ released from HCO_3^- in incorporation of CO_3^{2-} in calcite). The decrease in pH increases the proportion of carbonic acid

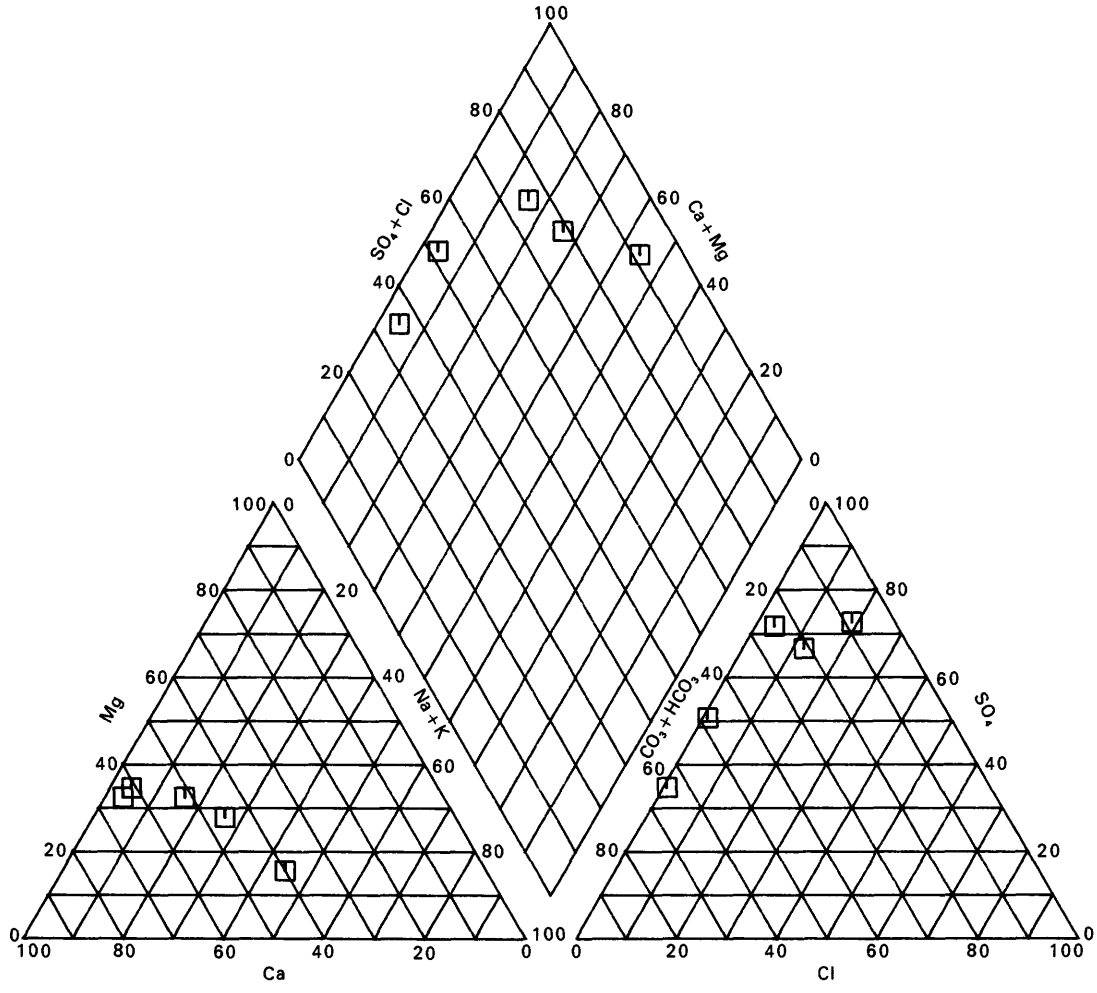

FIGURE 22.—Trilinear diagram showing chemical composition of water along flow path 1, in mole percent of cations and anions.

(H_2CO_3) in solution and thus increases the calculated P_{CO_2} (fig. 33). The shift in the carbonate system with lesser pH causes the water to be undersaturated with respect to dolomite, which in turn leads to dolomite dissolution and an increase in dissolved magnesium (fig. 31). Apparently the dissolution of anhydrite and dolomite exceeds the precipitation of calcite, resulting in a net increase in total dissolved calcium (fig. 30). The data in figures 34 and 35 show that pH and P_{CO_2} are very strong functions of temperature. This relation is not well understood but is in part a function of the strong temperature dependence of the Henry's-law constant for CO_2 gas (Plummer and Busenberg, 1982).

Two trends are evident in total alkalinity as a function of dissolved sulfate (fig. 36). First, most waters show a decrease in alkalinity with increasing sulfate. Second, the waters associated primarily with flow paths 2 and 3 display an opposite trend, having some of the maximum alkalinity concentrations (>300 mg/L as HCO_3^-) with large concentrations of dissolved sulfate. The decrease in alkalinity is to be expected for evolutionary paths following the dedolomitization reaction, but large alkalinity concentrations are not expected with large sulfate concentrations. Based on this determination, additional reactions beyond those among calcite, dolomite, and anhydrite can be expected along flow paths 2 and 3.

To help understand what these reactions are, we display the variations in sodium, potassium, and chloride with sulfate in figures 37–39. Generally waters with large concentrations of sodium also have large concentrations of potassium and chloride, indicating evaporite sources (halite and sylvite) for these ions. Sodium and chloride concentrations are small and nearly independent of sulfate along flow paths 1, 4, 6, 7, and 8. Flow paths 2, 3, and 5 have much greater concentrations of sodium, potassium, and chloride (figs. 37–39). Because the concentrations of

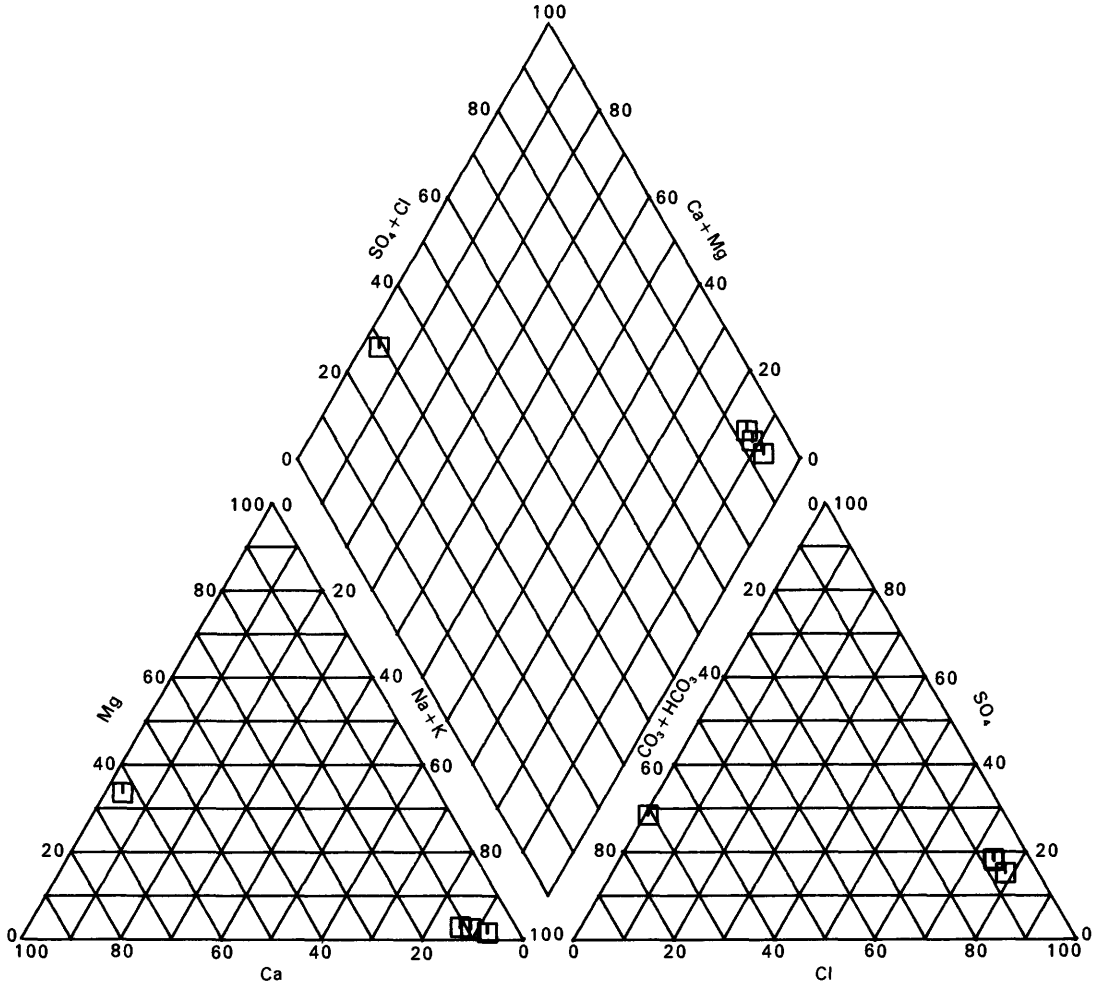

FIGURE 23.—Trilinear diagram showing chemical composition of water along flow path 2, in mole percent of cations and anions.

sodium plus potassium are similar to that of chloride for flow path 5, it is likely that evaporite minerals are the primary source for these ions along flow path 5. However, the concentrations of sodium plus potassium are nearly 10 mmol/kg of water greater than chloride for flow paths 2 and 3 (figs. 37–39). These are the same waters that contain unusually large concentrations of bicarbonate (fig. 36). Thus, there is a tendency to form sodium bicarbonate waters along flow paths 2 and 3.

Several reactions could lead to the formation of sodium bicarbonate waters, including (1) the dissolution of nahcolite ($NaHCO_3$), (2) the dissolution of carbonate minerals accompanying calcium and magnesium exchange for sodium on clay minerals, and (3) a reaction similar to case 2 above, but with the added possibility of incorporation of magnesium (and possibly calcium) in secondary clay minerals. Because nahcolite is not known or expected in the Madison aquifer, the possibility of its dissolution may be discounted. However, the data need to be examined more closely with mass-balance models in conjunction with the carbon-isotopic data in order to determine the reactions responsible for the excess sodium bicarbonate along flow paths 2 and 3.

Whereas flow paths 1, 4, 6, 7, and 8 show little variation in sodium and chloride, there is an indication of a progressive increase in potassium with increasing sulfate (fig. 38). This possibly is due to dissolution of trace quantities of detrital potassium silicate, such as orthoclase ($KAlSi_3O_8$), in the system.

Based on analysis of the chemical trends, the reactions along each flow path are summarized as follows. Flow paths 1, 4, 7, and 8 are examples of the dedolomitization reaction caused irreversibly by anhydrite dissolution at calcite-dolomite saturation. Flow paths 2 and 3, which combine the dedolomitization reaction with dissolution of halite and sylvite and possibly exchange (Ca^{2+} and

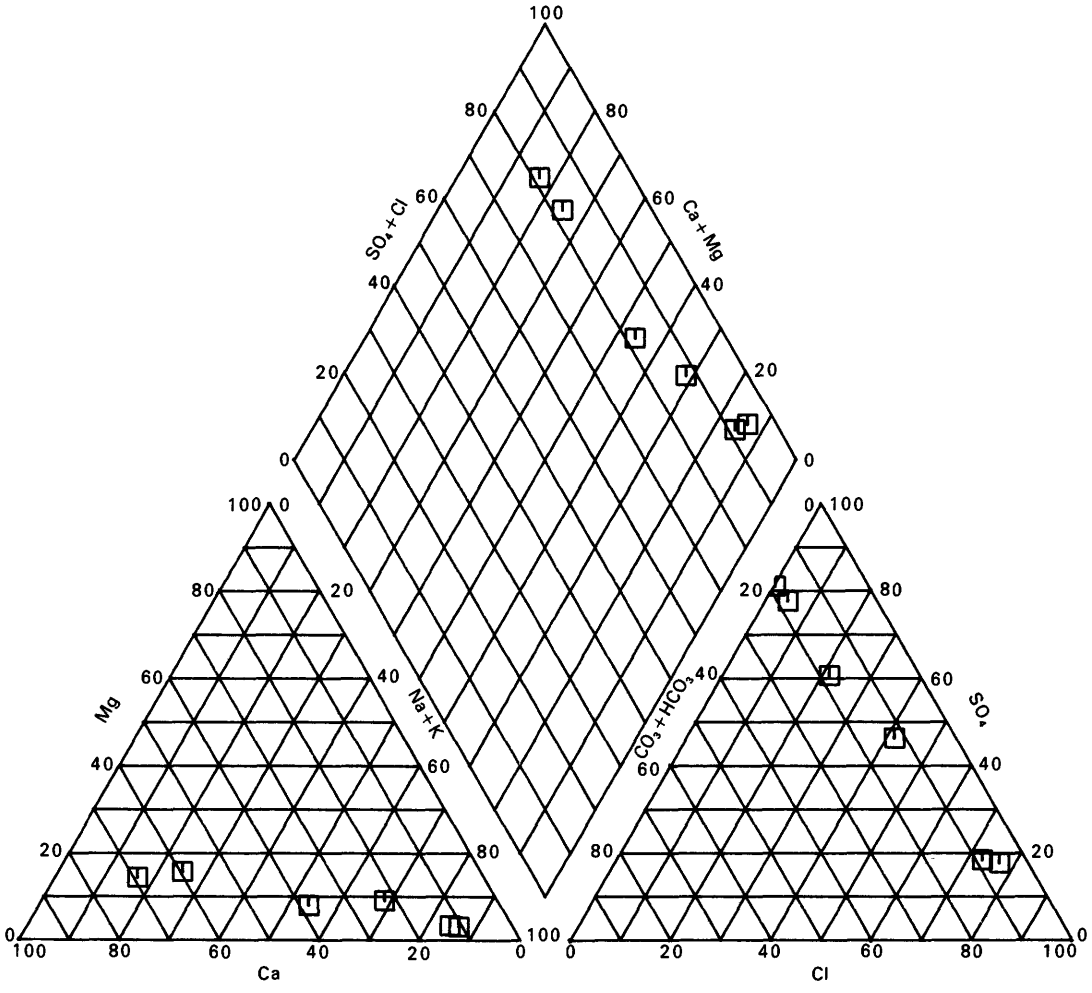

FIGURE 24.—Trilinear diagram showing chemical composition of water along flow path 3, in mole percent of cations and anions.

Mg^{2+} for Na^{+}), are the most complex chemically. Flow path 5 also shows evidence for the dedolomitization reaction accompanied by halite dissolution. Flow path 6 is controlled primarily by CO_2-carbonate mineral reactions with only small quantities of anhydrite dissolution.

ANALYSIS OF SULFUR-ISOTOPE DATA

Most of the waters downgradient from recharge areas contain traces of hydrogen sulfide, and, at least along flow path 2, H_2S concentrations larger than 100 mg/L have been determined (table 8). Therefore, in addition to the dissolution and precipitation reactions discussed above, the possibility of redox reactions (especially sulfate reduction) must also be considered.

In order to quantify redox reactions, it is necessary to evaluate mass-balance models, incorporating changes in the redox state of the waters in conjunction with the sulfur-isotope data as discussed by Plummer and others (1983).

Because the only likely sources of sulfate are gypsum ($CaSO_4 \cdot 2H_2O$) or anhydrite, dissolved sulfate was selected as the reaction-progress variable for the analysis of the chemical trends. Because the sulfate reduction process occurring in much of the ground-water system removes sulfate ion from solution, the quantity of anhydrite dissolved may be significantly larger than the quantity of sulfate in solution. Additionally, the quantity of hydrogen sulfide in solution is not always a good indication of the extent of sulfate reduction because of the negligible solubility of iron sulfides such as pyrite:

$$8SO_4^{2-} + 4FeOOH + 15CH_2O \rightarrow 4FeS_2 + 15HCO_3^- + 9H_2O + OH^-. \quad (12)$$

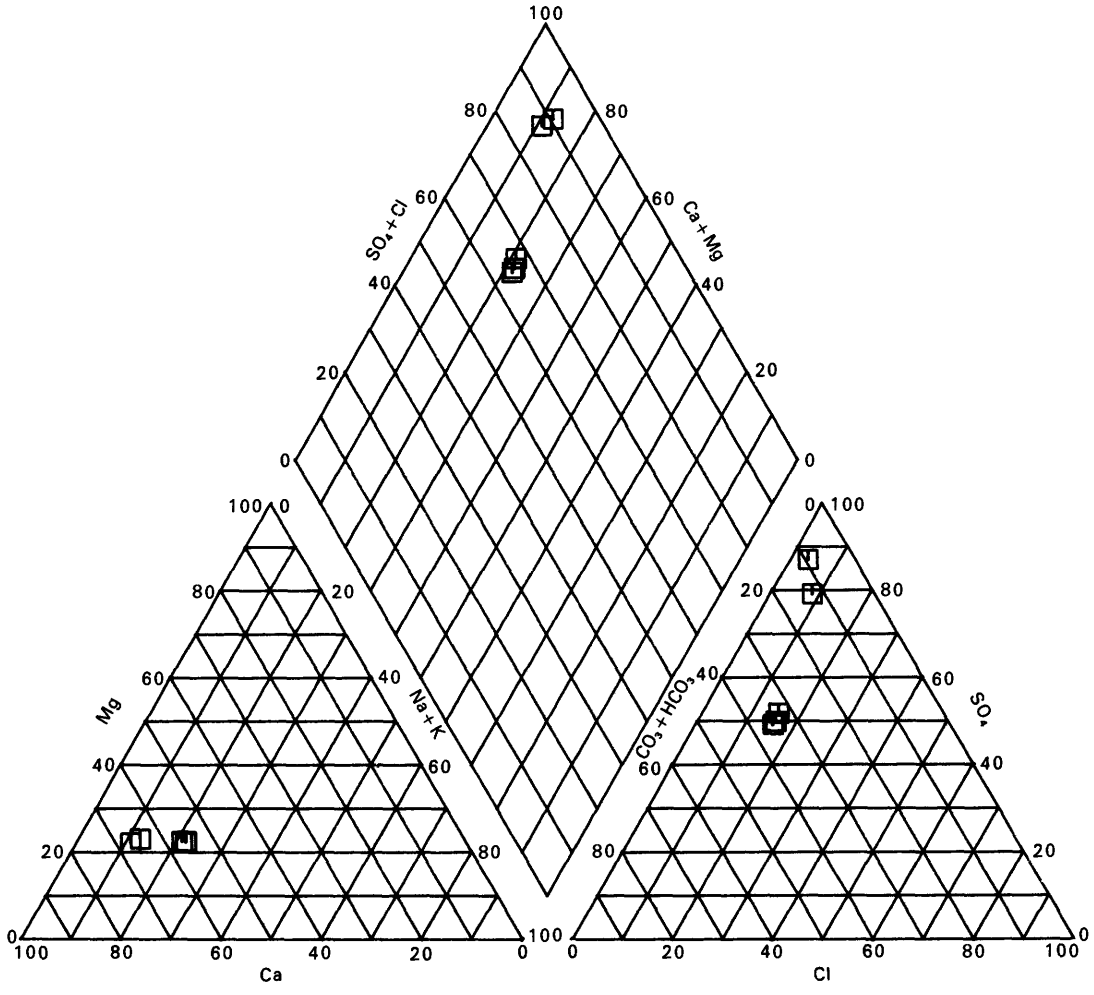

FIGURE 25.—Trilinear diagram showing chemical composition of water along flow path 4, in mole percent of cations and anions.

If a source of iron is available, it is possible for considerable sulfate reduction to occur with only traces of dissolved-sulfide species remaining in solution. In cases of abundant hydrogen sulfide, it can be concluded that sufficient sources of dissolved iron are not available to remove all the dissolved sulfide:

$$SO_4^{2-} + 2CH_2O \rightarrow H_2S + 2HCO_3^- . \quad (13)$$

Therefore, unless it is known that sulfate reduction is not occurring, it is not possible to calculate the anhydrite mass transfer directly from the change in sulfate concentration. Two methods of estimating the quantities of anhydrite dissolved and of pyrite precipitated have been considered. Each involves the sulfur-isotope compositions of dissolved-sulfur species (table 11). The first method is similar to that used by Plummer and others (1983) and assumes that the degree of sulfate reduction is sufficiently small so that the process can be treated as a problem in isotope dilution. The second method is more rigorous and treats the problem as one of Rayleigh distillation. This method is more accurate in cases of extensive sulfate reduction.

SULFUR-ISOTOPE DILUTION

The required information in treating the problem of the anhydrite and pyrite mass transfers as a case of isotope dilution included the sulfur-isotopic compositions of the dissolving anhydrite ($\delta^{34}S_{anhydrite}$) and of total dissolved sulfate and sulfide ($\delta^{34}S_T$). These data were then used to solve simultaneously a mass-balance equation for sulfur and a mass-balance equation for the sulfur isotope. In using a mass-balance equation for the sulfur isotope, the assumption was made that the degree of sulfate reduc-

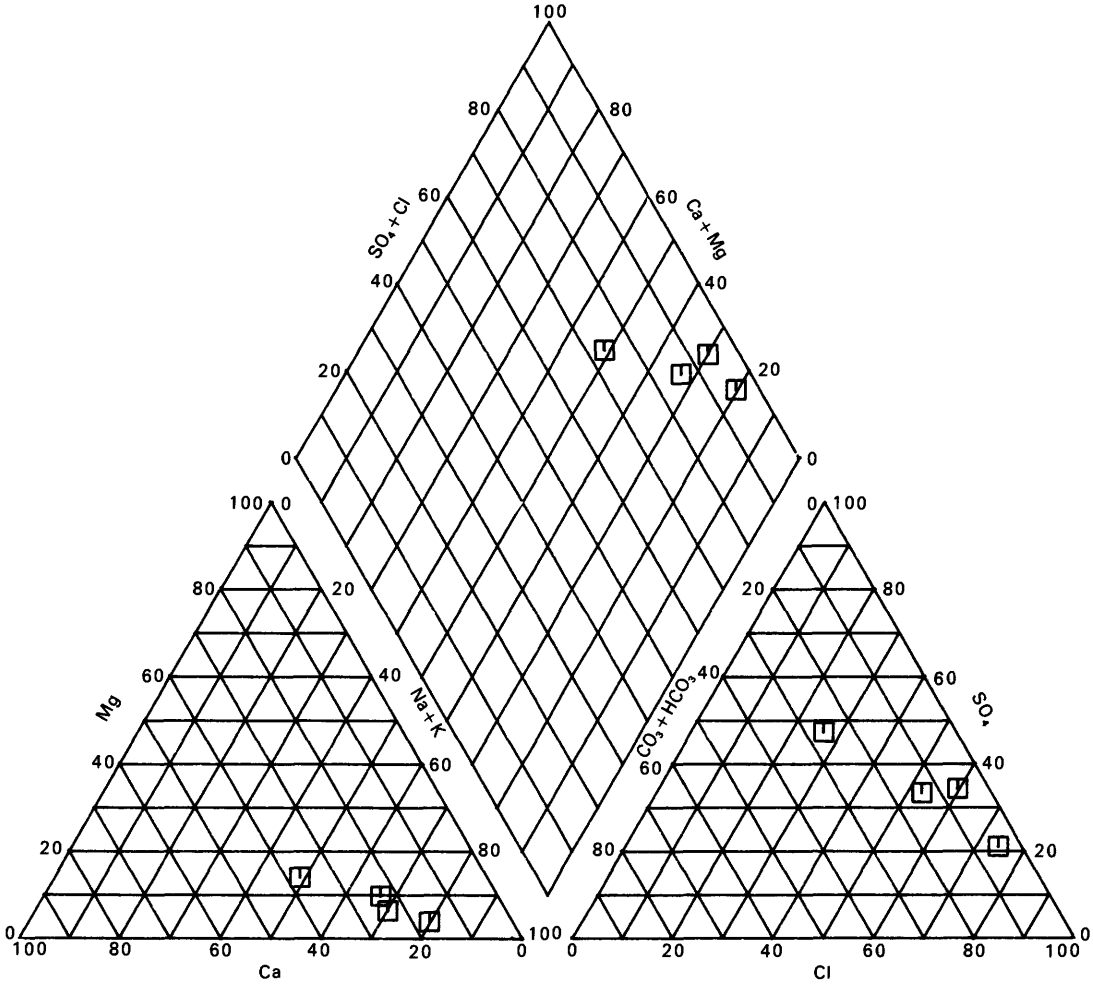

FIGURE 26.—Trilinear diagram showing chemical composition of water along flow path 5, in mole percent of cations and anions.

tion was small enough that the effects of Rayleigh distillation could be ignored. The sulfur mass-balance equation is

$$S_{T(\text{initial})} + \alpha_{\text{anhydrite}} + 2\alpha_{\text{pyrite}} = S_{T(\text{final})}, \quad (14)$$

where $S_{T(\text{initial})}$ and $S_{T(\text{final})}$ are the total molalities of sulfur (sulfate plus total sulfide) in the initial (recharge) water and the final (downgradient) water, respectively. The mass transfers of anhydrite ($\alpha_{\text{anhydrite}}$) and pyrite ($\alpha_{\text{pyrite}}$) have positive signs for dissolution and negative signs for precipitation.

The sulfur-isotope mass-balance equation is

$$S_{T(\text{initial})}\ \delta^{34}S_{(\text{initial})} + \alpha_{\text{anhydrite}}\ \delta^{34}S_{\text{anhydrite}} + 2\alpha_{\text{pyrite}}\ \delta^{34}S_{\text{pyrite}} = S_{T(\text{final})}\ \delta^{34}S_{(\text{final})}, \quad (15)$$

where $\delta^{34}S_{(\text{initial})}$, $\delta^{34}S_{\text{anhydrite}}$, $\delta^{34}S_{\text{pyrite}}$, and $\delta^{34}S_{(\text{final})}$ denote the isotopic compositions of sulfur in the initial water, anhydrite, pyrite, and the final water, respectively. It is assumed that $\delta^{34}S_{\text{pyrite}}$ is that of the dissolved sulfide (ignoring the small fractionation between dissolved sulfide and pyrite). If both sulfate and sulfide species are present, then we have

$$\delta^{34}S_{(\text{final})} = \frac{m_{SO_4}\ \delta^{34}S_{SO_4} + m_{H_2S}\ \delta^{34}S_{H_2S}}{m_{SO_4} + m_{H_2S}}, \quad (16)$$

where m_{SO_4} and m_{H_2S} are the molalities of sulfate and hydrogen sulfide, respectively; and $\delta^{34}S_{SO_4}$ and $\delta^{34}S_{H_2S}$ are the isotopic compositions of sulfate and hydrogen sulfide, respectively.

Only limited data on the sulfur-isotopic composition of anhydrite in the Madison aquifer were available. R.G. Deike (U.S. Geological Survey, oral commun., 1984) reported two values of $\delta^{34}S_{\text{anhydrite}}$ of 12.8 and 13.9 per mil from the HTH No. 1 well and six values at the HTH

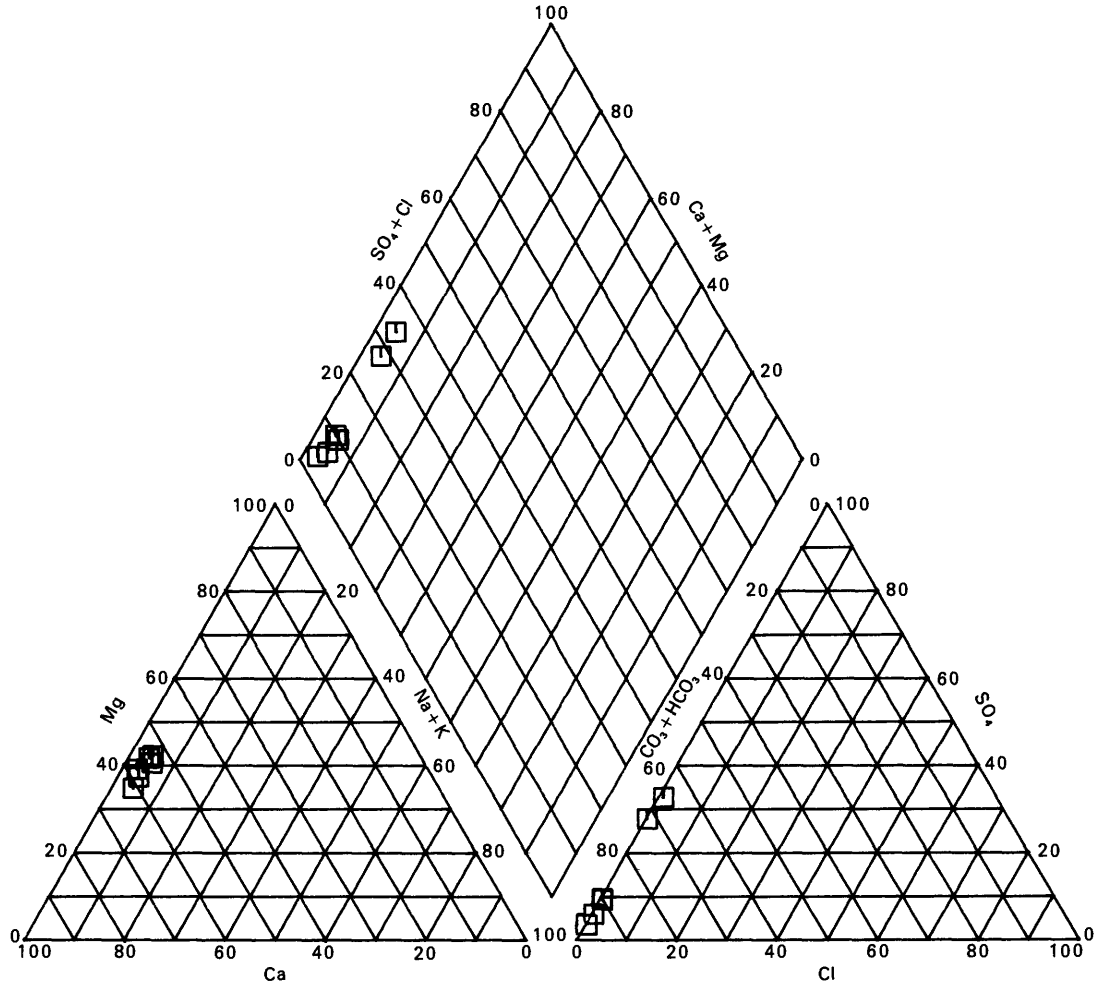

FIGURE 27.—Trilinear diagram showing chemical composition of water along flow path 6, in mole percent of cations and anions.

No. 2 well between 14.6 and 22.6 per mil. Most of these values are considerably lighter than that expected for open marine evaporites of Mississippian age (Claypool and others, 1980), indicating a terrigenous source, such as pyrite, for some of the sulfur. This source was subsequently oxidized, precipitated as gypsum, and diagenetically altered to the anhydrite, as now found in the Madison Limestone.

In the absence of abundant isotopic data for anhydrite, the isotopic composition of dissolved sulfate as a function of the sulfate concentration for each flow path has been examined. Assuming a nearly constant (average) isotopic composition of the anhydrite dissolving along a flow path, no change in $\delta^{34}S_{SO_4}$ would be observed if no sulfate reduction were occurring. Alternatively, if there was sulfate reduction, a trend to heavier $\delta^{34}S_{SO_4}$ with increased concentration of sulfate (reaction progress) would be determined as a result of the large sulfur isotope fractionation involved in the bacterially mediated reduction of sulfate. In either case, the $\delta^{34}S_{SO_4}$ trend should extrapolate back to the isotopic composition of anhydrite when no sulfate is present in solution. This method was used to approximate $\delta^{34}S_{anhydrite}$ for each flow path. The $\delta^{34}S_{anhydrite}$ derived by this method is reported to the nearest 0.1 per mil.

Although all eight flow paths show significant trends to heavier $\delta^{34}S_{SO_4}$ with increasing concentrations of dissolved sulfate (fig. 40*A–H*), it is clear that there are distinct differences between flow paths: For example, all $\delta^{34}S_{SO_4}$ values along flow path 1 (fig. 40*A*) are two to three times heavier than those along flow path 5 (fig. 40*E*). Because the data for several of the flow paths (notably 3, 4, 5, 6, and 8) indicate that $\delta^{34}S_{SO_4}$ increases linearly with sulfate concentration, the assumption has been made that all trends of figure 40 may be approximated with a linear relation.

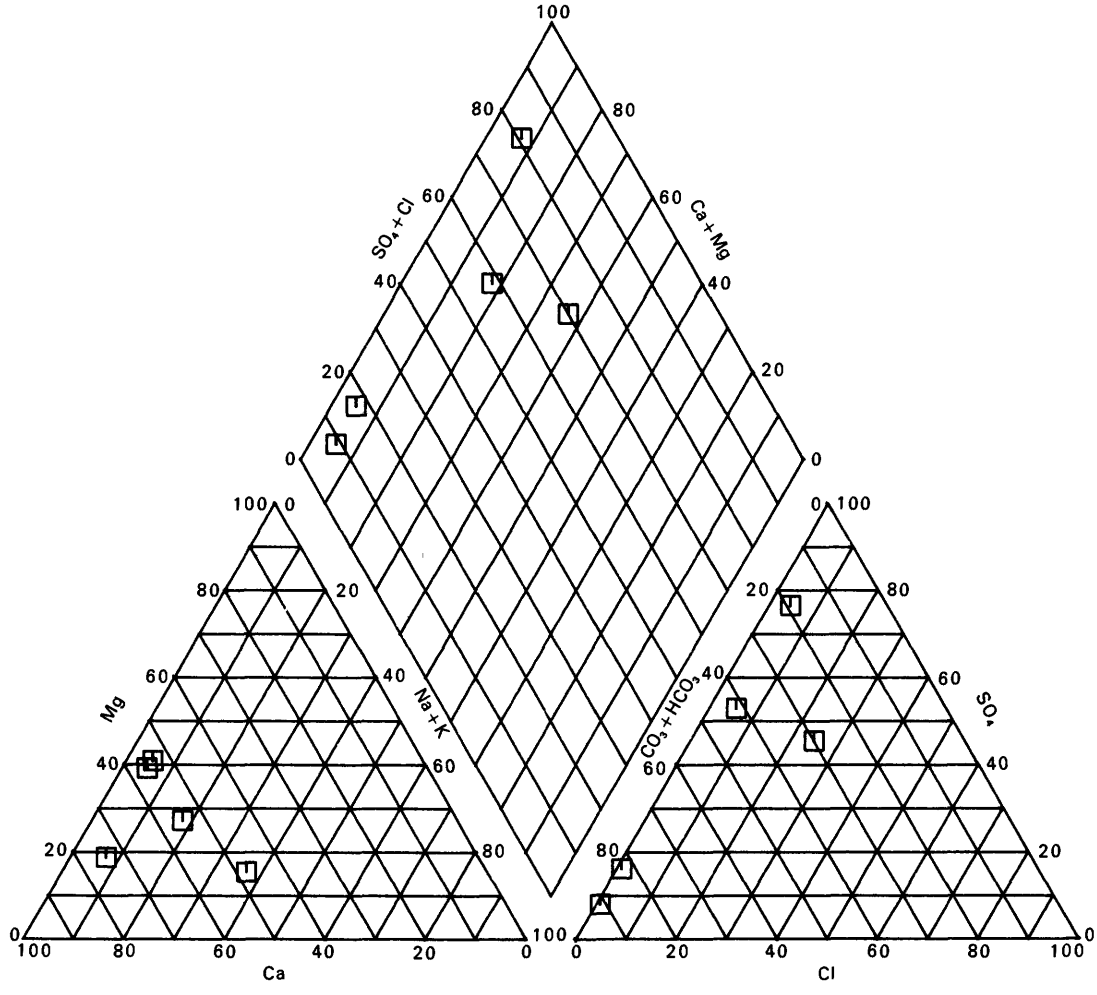

FIGURE 28.—Trilinear diagram showing chemical composition of water along flow path 7, in mole percent of cations and anions.

Several flow paths (such as 1, 2, and 7) contain some values of $\delta^{34}S_{SO_4}$ that deviate significantly from the selected linear trend (fig. 40). These may be due to regional variation in the anhydrite isotopic composition, or result from differences in the extent of sulfate reduction along the flow paths, or indicate that these wells do not lie entirely on the given flow path. In the preliminary mass-balance modeling discussed in a later section of this report, it was assumed that deviations from the selected linear trends of figure 40 are due to variations in the extent of sulfate reduction along the flow path.

The estimated initial isotopic compositions of anhydrite for flow paths 1 to 8, as indicated by the linear trends in figure 40, are summarized in table 12. The derived $\delta^{34}S_{anhydrite}$ values appear to be mappable, with lightest values (7.9 to 10.0 per mil) along flow paths 5, 6, and 7 in northeastern Wyoming and the adjacent southwestern corner of South Dakota. Moving northeast from these light values into South Dakota, and north and northwest into Montana, a progressive increase to heavier estimated values of the initial isotopic composition of dissolving anhydrite is found, with a maximum value of 17.1 per mil reached in north-central Montana. This pattern in estimated anhydrite isotopic composition may reflect the depositional environment of the Madison Limestone and surrounding exposed topography during the time of its emplacement (Sando, 1976b), indicating more abundant terrestrial sources of sediment, enriched in sulfide, in northeastern Wyoming and the area surrounding the Black Hills than in the rest of the area.

Presumably, the environment of anhydrite deposition in the Madison Limestone was affected by both marine and terrestrial sources of sulfate, with a greater abundance of terrigenous sulfate being introduced in northeastern Wyoming.

Returning to equations 14 and 15, we can use the data for $\delta^{34}S_{anhydrite}$ (table 12) with the concentrations and

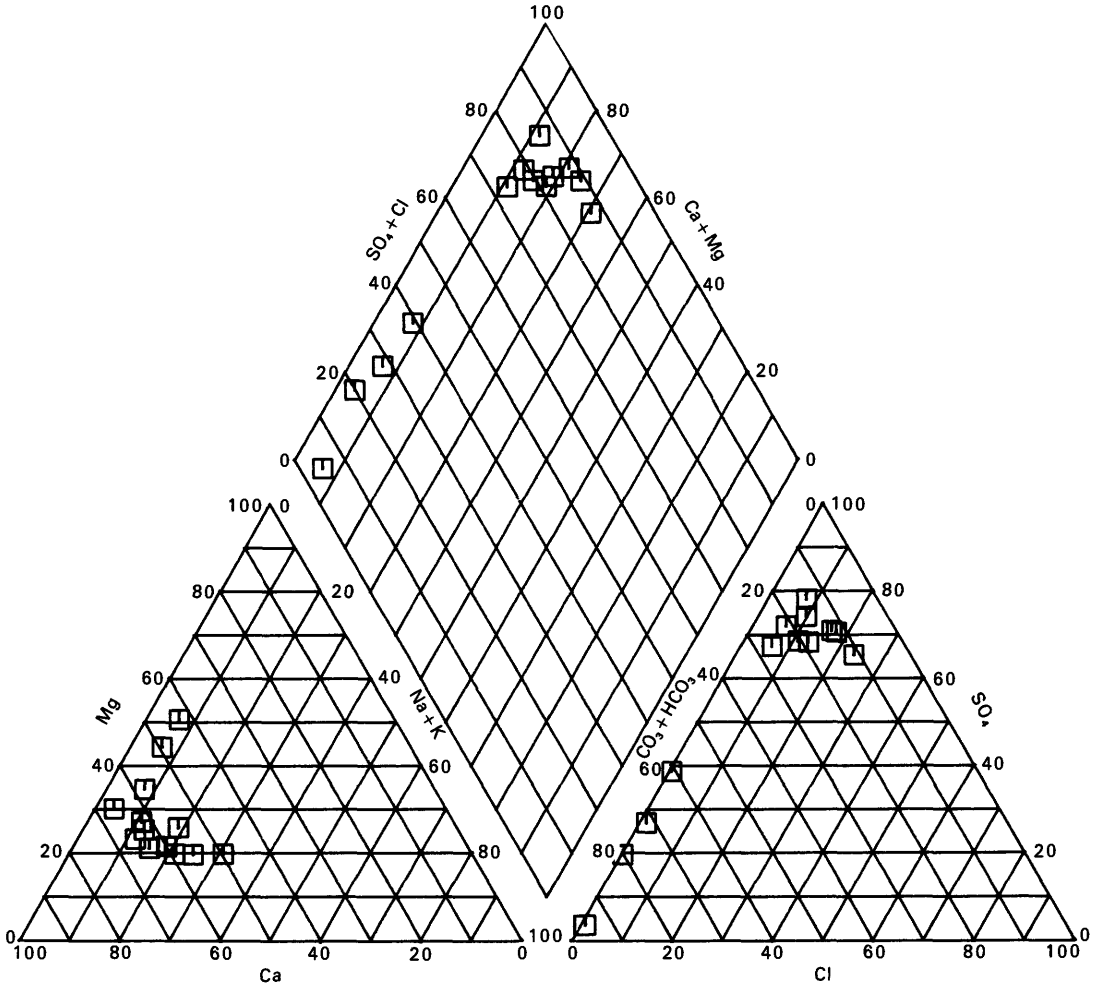

FIGURE 29.—Trilinear diagram showing chemical composition of water along flow path 8, in mole percent of cations and anions.

isotopic compositions of dissolved sulfate and total sulfide to estimate the anhydrite and pyrite mass transfers at the 12 wells in the Madison aquifer (table 13) for which sufficient analytical and isotopic data are available.

From equations (14) and (15), we have

$$\alpha_{\text{anhydrite}} = \frac{\Delta^{34}S_T - \Delta S_T\, \delta^{34}S_{\text{pyrite}}}{(\delta^{34}S_{\text{anhydrite}} - \delta^{34}S_{\text{pyrite}})}, \quad (17)$$

$$\alpha_{\text{pyrite}} = \frac{1}{2}(\Delta S_T - \alpha_{\text{anhydrite}}), \quad (18)$$

$$\Delta^{34}S_T = (S_T\, \delta^{34}S)_{\text{final}} - (S_T\, \delta^{34}S)_{\text{initial}}, \quad (19)$$

$$\Delta S_T = S_{T(\text{final})} - S_{T(\text{initial})}$$

The average concentration and isotopic composition of sulfate in the recharge water associated with each well (tables 10 and 11) were used in calculating the pyrite and anhydrite mass transfers in table 13. As discussed by Plummer and others (1983), although the computed mass transfer is not very sensitive to uncertainties of several parts per thousand in the isotopic composition of dissolved sulfide, it does depend significantly on the selected value for the isotopic composition of dissolving anhydrite. For example, if we assign an uncertainty of ± 1 per mil to the isotopic composition of dissolving anhydrite along flow path 2, the anhydrite and pyrite mass transfers along the flow path to the Sumatra well are 14.22 ± 0.83 and -0.22 ± 0.41 mmol/kg of water, respectively. Variations of several parts per thousand in $\delta^{34}S_{\text{anhydrite}}$ of individual anhydrite samples are likely along each flow path, but these variations are moderated somewhat because the values of $\delta^{34}S_{\text{anhydrite}}$ derived in figure 40 can be interpreted as average values for the flow path.

SULFUR ISOTOPES AS A RAYLEIGH-DISTILLATION PROBLEM

The results in table 13 show that for at least several wells, such as Dupree, relatively substantial sulfate reduction may be occurring. Therefore, the estimation of the anhydrite and pyrite mass transfers via the isotope-dilution equation may not be justified. A more precise method of estimating the anhydrite and pyrite mass transfers is to account for the fact that the sulfur-isotopic compositions of dissolved sulfate, dissolved sulfide, and pyrite vary with the extent of sulfate reduction. This is accounted for by treating the sulfur-isotope data as a problem in Rayleigh distillation.

In this particular case sulfate reduction involves the dissolution of anhydrite with an assumed constant isotopic composition, the reduction of dissolved-sulfate to dissolved-sulfide species with a fractionation that averages about 30 per mil (table 13), and the precipitation of a proportion of this dissolved sulfide as pyrite, involving only a small (but unknown) fractionation. By assuming that the sulfur-isotopic composition of pyrite is equal to that of the dissolved-sulfide species, the sulfate-reduction

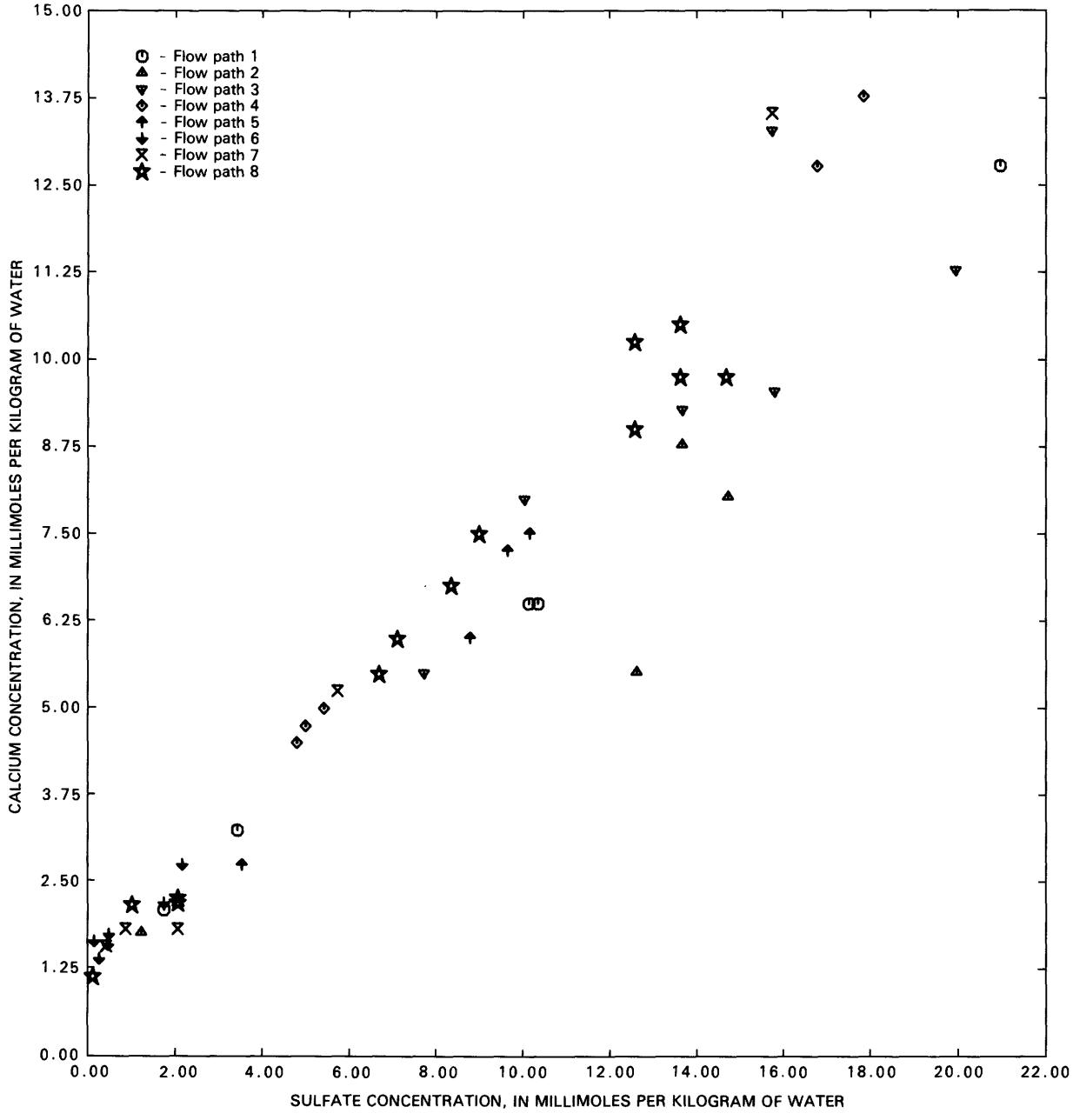

FIGURE 30.—Trend in dissolved-calcium concentration as a function of dissolved-sulfate concentration along flow paths 1 to 8.

process can be treated as one input (anhydrite) and one fractionating output (dissolved-sulfide species and pyrite) of the Rayleigh-distillation problem. The analytical solution to the Rayleigh-distillation problem in terms of the sulfur-isotopic composition of dissolved sulfate is adopted from Wigley and others (1978, 1979) and is

$$\delta^{34}S_{SO_4} = \frac{\left(\beta\,\delta^{34}S^{\circ}_{SO_4} - \delta^{34}S^{*}_{SO_4} + \frac{\varepsilon_{ps}}{\Gamma}\right)\left[\frac{m_{SO_4}}{m^{\circ}_{SO_4}}\right]^{\left(\frac{\beta\Gamma}{1-\Gamma}\right)} + \delta^{34}S^{*}_{SO_4} - \frac{\varepsilon_{ps}}{\Gamma}}{\beta}. \quad (20)$$

Equation 20 describes the isotopic composition of dissolved sulfate, $\delta^{34}S_{SO_4}$, as a function of reaction progress. The notation of equation 20 is defined as follows:

$\delta^{34}S^{\circ}_{SO_4}$ is the isotopic composition of sulfur in dissolved sulfate of the starting water;
$\delta^{34}S^{*}_{SO_4}$ is the isotopic composition of sulfur in anhydrite;
ε_{ps} is the additive fractionation factor – $^{34}\Delta = \delta^{34}S_{H_2S} - \delta^{34}S_{SO_4}$;
Γ is $|dI/dO|$, the absolute value of the ratio of moles of incoming sulfur to outgoing sulfur (as dissolved-sulfide species and pyrite);
$m^{\circ}_{SO_4}$ is the molality of sulfate in the starting water;
m_{SO_4} is the molality of sulfate in the final water; and
β is the parameter defined as $(1 + \frac{\varepsilon_{ps}}{1{,}000\ \Gamma})$.

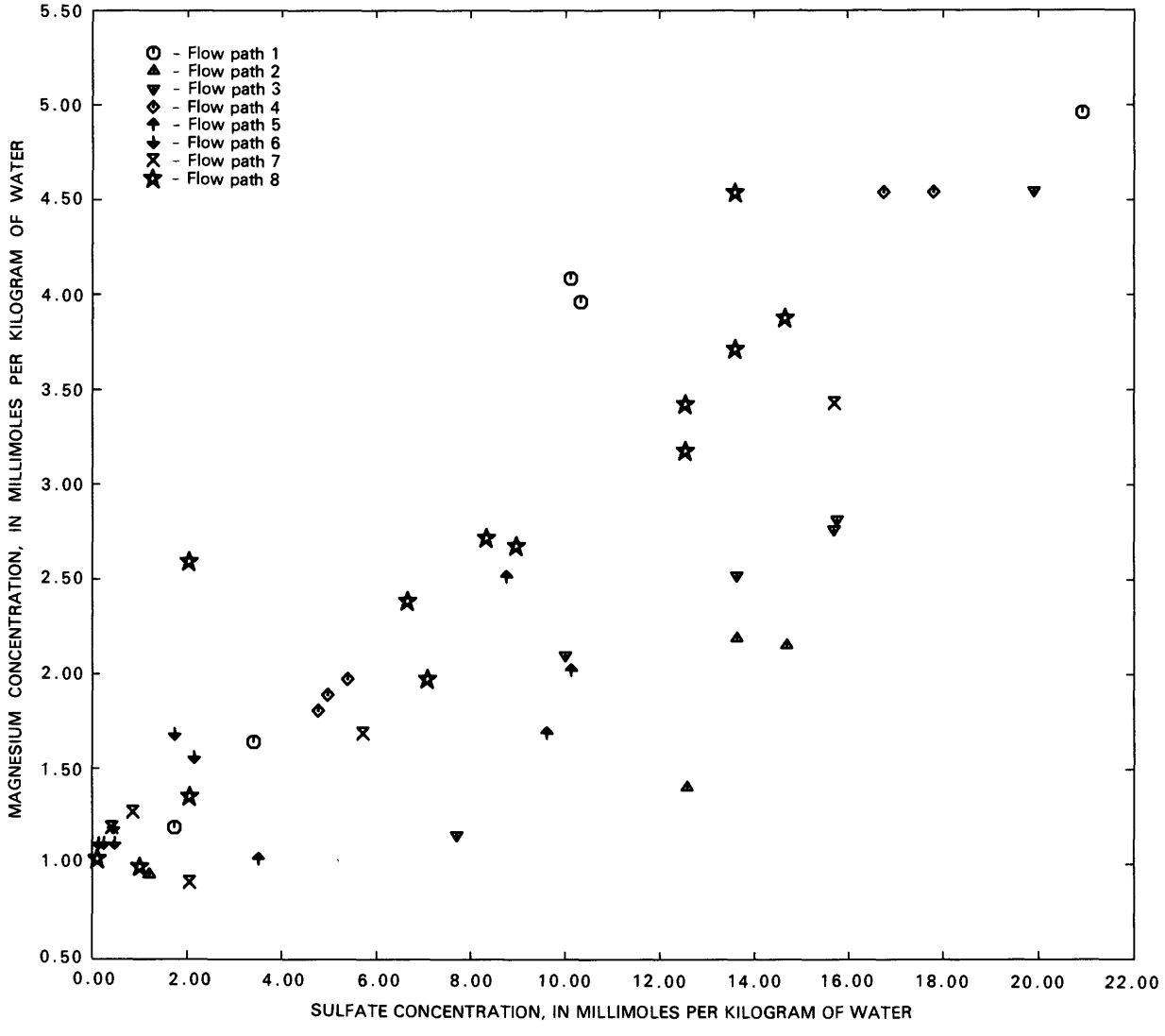

FIGURE 31.—Trend in dissolved-magnesium concentration as a function of dissolved-sulfate concentration along flow paths 1 to 8.

Equation 20 has been used to solve iteratively for Γ (the sulfur input to output ratio). Here we take ε_{ps} as the measured value, $\varepsilon_{ps} = -{}^{34}\Delta = \delta^{34}S_{H_2S} - \delta^{34}S_{SO_4}$, which is summarized in table 14 along with the rest of the measured parameters required by equation 20. The values of Γ calculated using equation 20 are also presented in table 14.

The calculated value of Γ is then combined with the mass-balance equation for sulfur and analytical data for dissolved sulfide to determine the anhydrite and pyrite mass transfers. The following two equations were used:

$$\Gamma = \left| \frac{\alpha_{\text{anhydrite}}}{H_2S_T + 2\alpha_{\text{pyrite}}} \right| \tag{21}$$

and

$$\Delta S_T = \alpha_{\text{anhydrite}} - 2\alpha_{\text{pyrite}}. \tag{22}$$

In equations 21 and 22, the mass transfers of anhydrite and pyrite, $\alpha_{\text{anhydrite}}$ and α_{pyrite}, are both treated as positive numbers because Γ is defined as the absolute value of the ratio of moles. Solving equations 21 and 22 for the anhydrite mass transfer, we obtain

$$\alpha_{\text{anhydrite}} = \Gamma \frac{(H_2S_T - \Delta S_T)}{(1 - \Gamma)}, \tag{23}$$

$$\alpha_{\text{pyrite}} = \frac{\alpha_{\text{anhydrite}} - \Delta S_T}{2}, \tag{24}$$

where H_2S_T is the total concentration of dissolved-sulfide species, and ΔS_T is the change in the total concentration of dissolved-sulfur species (sulfate plus sulfide species). The anhydrite and pyrite mass transfers are in millimoles per kilogram of water, the unit of concentration.

Comparison of the calculated anhydrite and pyrite mass transfers of table 14 with those calculated by the isotope-dilution method (table 13) shows only minor differences between the results from the two methods (table 15). For example, the anhydrite mass transfers differ by less than 4 percent between the two methods, which is probably better than the overall accuracy of the data. Therefore,

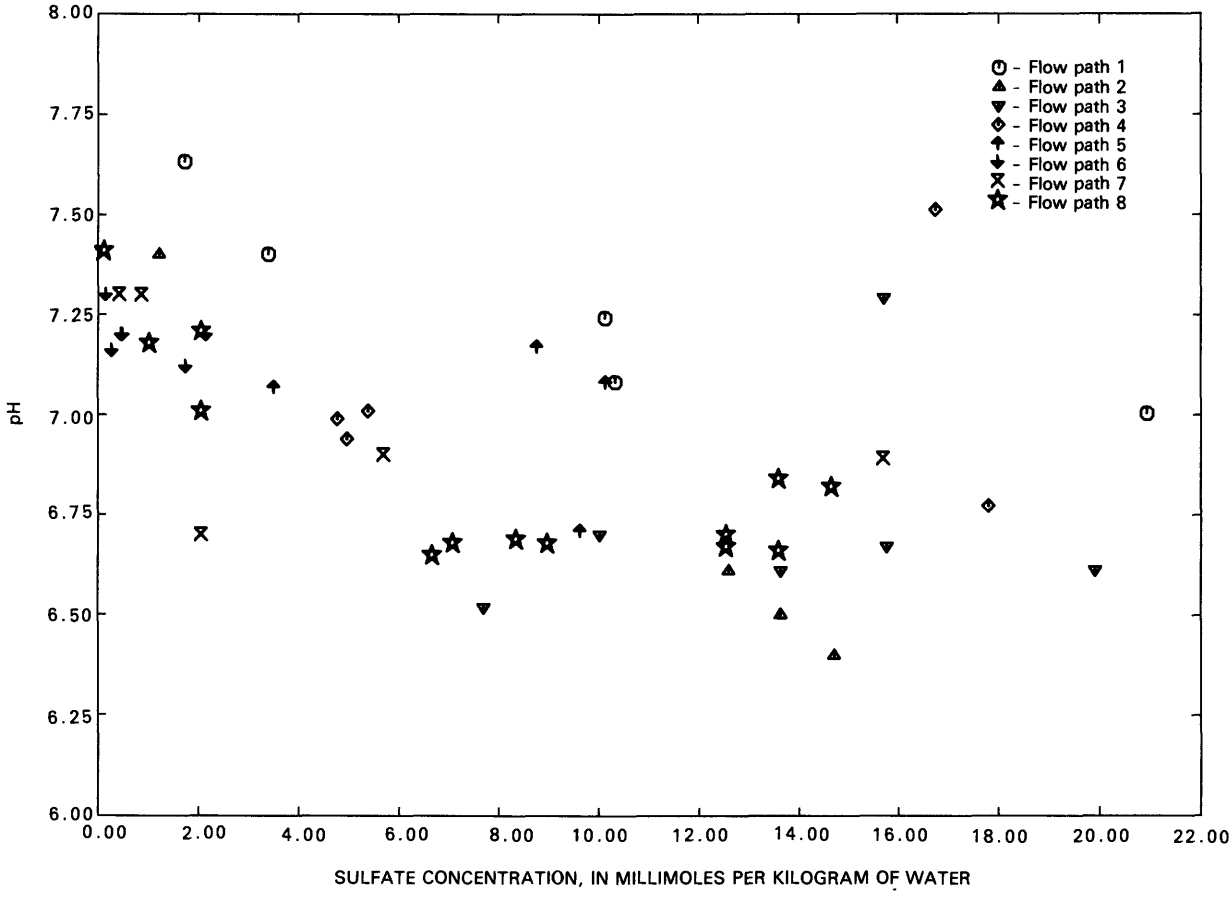

FIGURE 32.—Variation in pH as a function of dissolved-sulfate concentration along flow paths 1 to 8.

we conclude that negligible uncertainty is introduced in the anhydrite and pyrite mass transfers by treating sulfate reduction as a simple isotope-dilution problem.

The results in table 13 show that the quantity of anhydrite dissolved exceeds the sulfate concentration by values that range between 0.81 mmol/kg of water (at Sarpy Mine, well No. 19 in Montana) and 4.8 mmol/kg of water (at Dupree, well No. 20 in South Dakota). Wells in central Montana, which contain relatively large quantities of dissolved-sulfide species, indicate only minor pyrite precipitation, whereas wells in South Dakota, which show relatively small quantities of dissolved-sulfide species, indicate relatively substantial pyrite precipitation. Based on this determination and the discussion in the section "Depositional Environment," it is likely that sources of dissolved iron, such as detrital FeOOH, are more abundant in the Madison aquifer in South Dakota than in central Montana. Detrital FeOOH would be expected to be more prevalent near the source area of the sediments. This further supports the earlier hypothesis regarding the source of terrigenous sulfur in the vicinity of South Dakota and northeastern Wyoming.

Although the sulfur-isotopic composition of dissolved sulfate is known for nearly all the wells or springs sam-

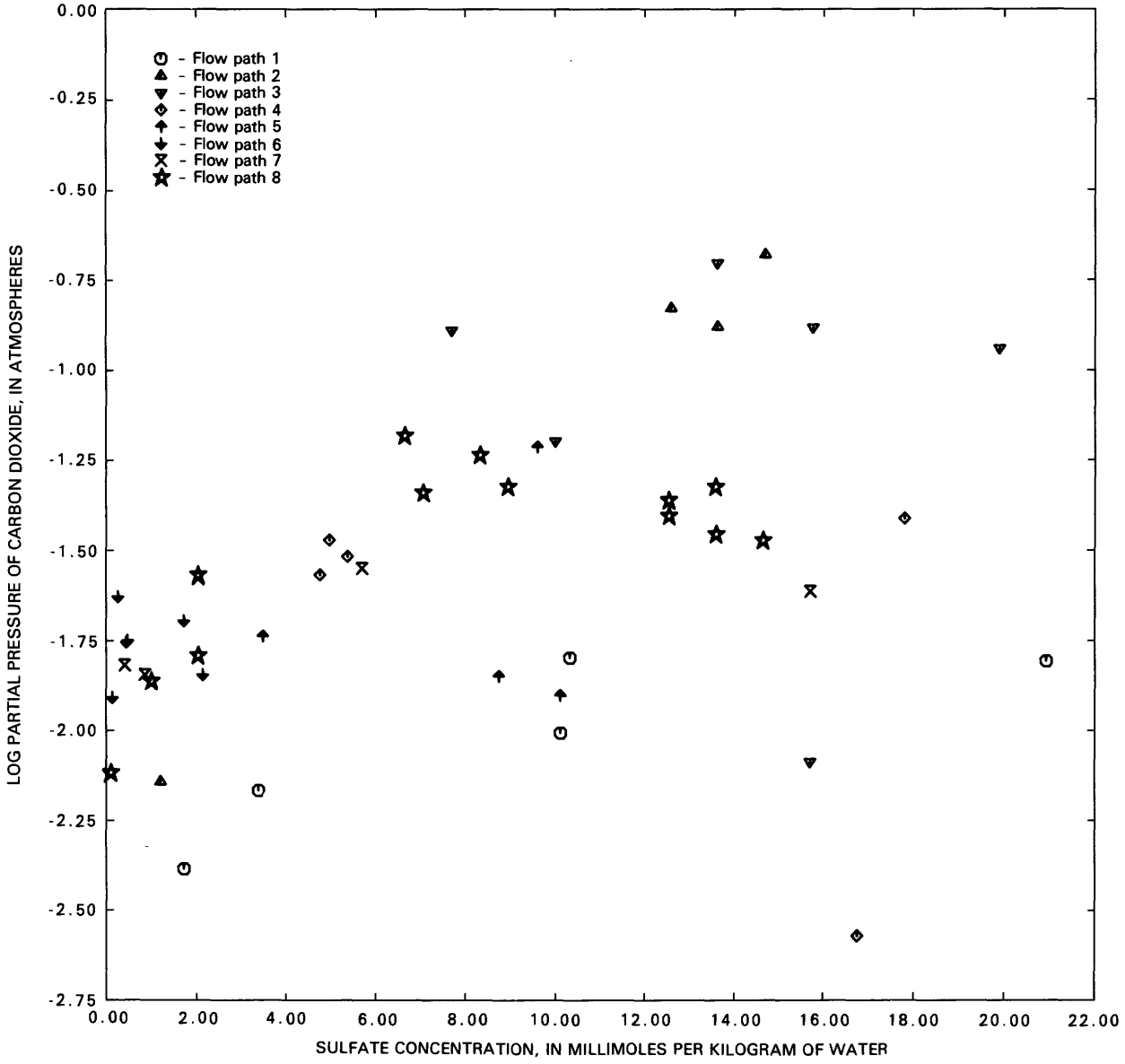

FIGURE 33.—Variation in log partial pressure of carbon dioxide (atmospheres) as a function of dissolved-sulfate concentration along flow paths 1 to 8.

pled in the Madison aquifer, the sulfur-isotopic composition of dissolved sulfide was obtained for only 12 wells (table 11). As a result, it was necessary to use an estimation procedure to calculate the anhydrite and pyrite mass transfers elsewhere in the Madison aquifer. This procedure was based on the parameter $^{34}\Delta$ (Pearson and Rightmire, 1980), where

$$^{34}\Delta = \delta^{34}S_{SO_4} - \delta^{34}S_{H_2S}. \quad (25)$$

An approximately linear correlation with temperature among $^{34}\Delta$ data from the Madison aquifer (table 13) and the Edwards aquifer in the Cretaceous Edwards Limestone of Texas (F.J. Pearson, Jr. and P.L. Rettman, U.S. Geological Survey, unpublished data) is shown in figure 41. As shown by Rye and others (1981) for the limestones of the Floridan aquifer of Florida, $^{34}\Delta$ approaches that expected for isotopic equilibrium [based on experimental data of Ohmoto and Rye (1979) at 200 to 350 °C].

Values of $^{34}\Delta$ in the Edwards and Madison aquifers probably result from kinetic fractionation during biologically mediated sulfate reduction. The kinetic fractionation in the Edwards and Madison aquifers appears to be a linear function of temperature (fig. 41) and is approximated by

$$^{34}\Delta = 54 - 0.40t, \quad (26)$$

where t is the temperature, in degrees Celsius.

Based on the scatter of values in figure 41, values of $^{34}\Delta$ estimated from equation 26 have uncertainties of ± 10 per mil. In the absence of additional data on the isotopic composition of dissolved sulfide in the Madison aquifer, the measured temperature, the isotopic composition of dissolved sulfate, and the correlation of equation 26 have been used to estimate $\delta^{34}S_{H_2S}$, which equals $\delta^{34}S_{pyrite}$, in the remaining wells sampled in the Madison aquifer. These estimates have then been used in the mass-balance models to calculate the anhydrite and pyrite mass transfers elsewhere in the Madison aquifer.

As a test of the magnitude of potential uncertainties due to the use of equation 26 (in lieu of actual data on the

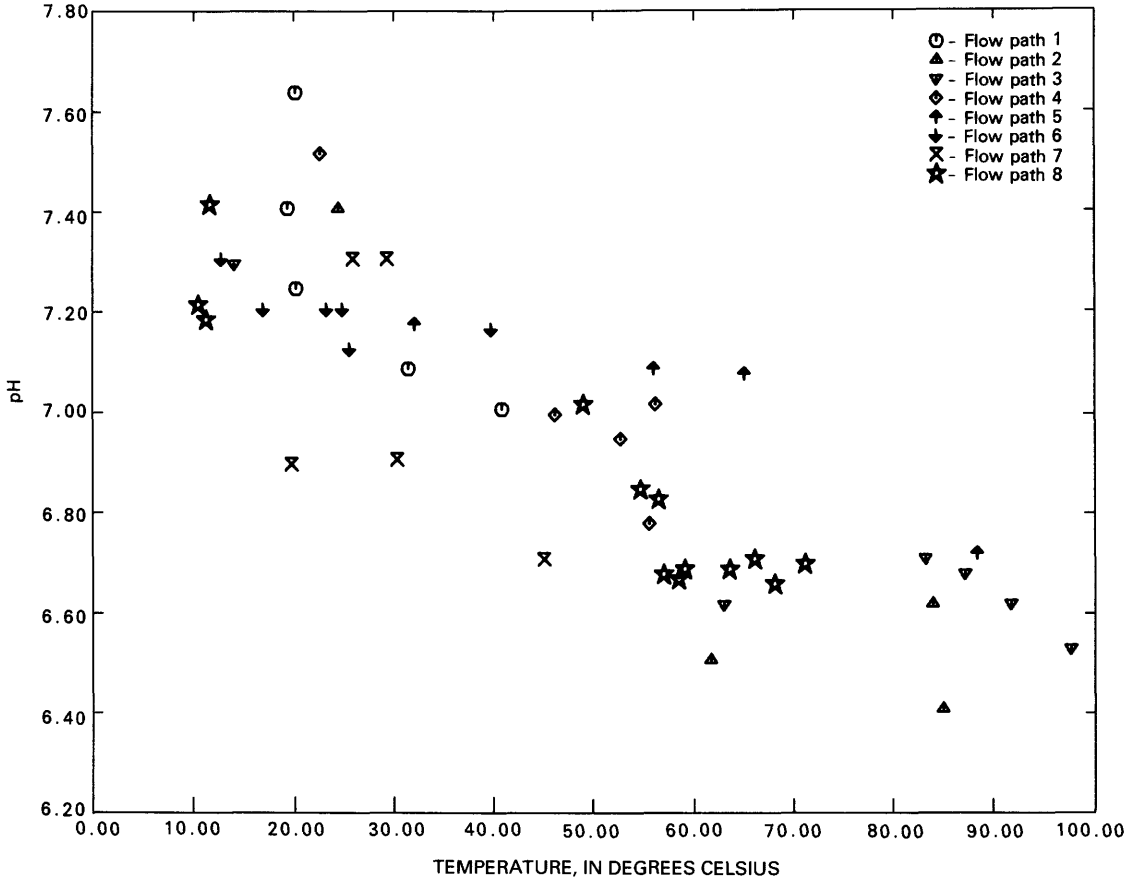

FIGURE 34.—Variation in pH as a function of temperature along flow paths 1 to 8.

sulfur-isotopic composition of dissolved sulfide), the isotope-dilution calculation of the anhydrite and pyrite mass transfers shown in table 13 was repeated using values of $\delta^{34}S_{H_2S}$ (which equals $\delta^{34}S_{pyrite}$) derived from equation 26. These mass-transfer values are compared with those derived from the measured $\delta^{34}S_{H_2S}$ data via the isotope-dilution and Rayleigh-distillation methods in table 15. The largest deviations of values derived from equation 26, from the measured values (±10 per mil uncertainty in $\delta^{34}S_{H_2S}$) lead to a 9 percent underestimation of the anhydrite mass transfer at the Dupree well and an 8 percent overestimation of the anhydrite mass transfer at the Moore well. All other anhydrite mass-transfer values calculated using equation 26 agree significantly more closely with the measured values (table 15). Uncertainties of less than 1.0 mmol/kg of water in the pyrite mass-transfer result from the approximation of equation 26.

MASS-BALANCE REACTION MODELS

EQUATIONS

Mass-balance reaction models are used to help define the net masses of minerals dissolved or precipitated along each flow path between the recharge area and each downgradient well. This type of modeling has been considered in detail by Plummer and others (1983). As shown by these authors, the chemical evolution of the water along the flow path is constrained by relations of conservation of mass and electrons that are represented by the equations

$$\sum_{p=1}^{P} \alpha_p b_{p,k} = \Delta m_{T,k},\ k = 1, \ldots, j \qquad (27)$$

and

$$\sum_{p=1}^{P} u_p \alpha_p = \Delta RS. \qquad (28)$$

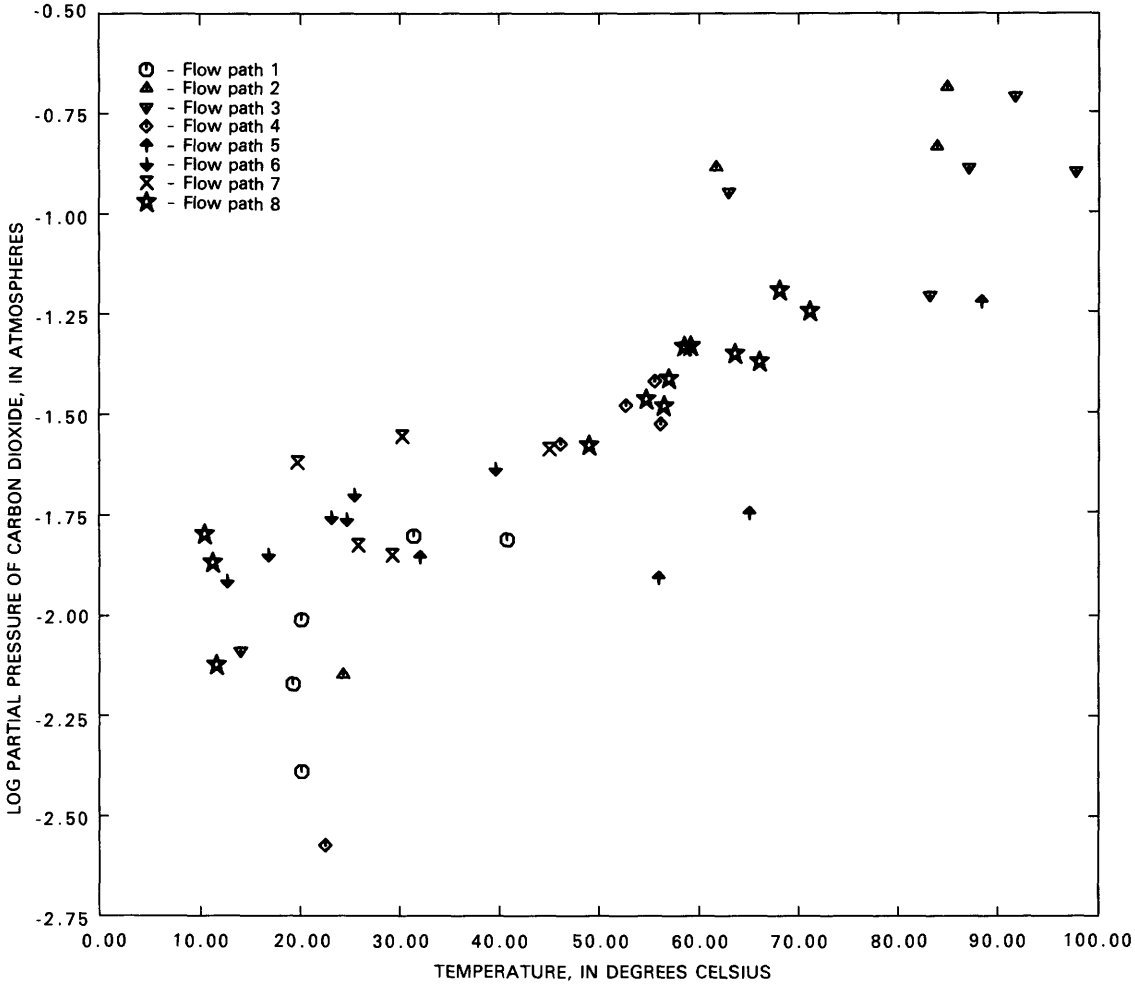

FIGURE 35.—Variation in log partial pressure of carbon dioxide (atmospheres) as a function of temperature along flow paths 1 to 8.

Equation 27 requires that the change in total moles of the kth element in solution along the flow path, $\Delta m_{T,k}$ (final water minus initial water), be equal to the sum of the net moles of that element entering or leaving solution as a result of dissolution, precipitation, biological degradation, gas transfer, and so forth of P phases along the flow path. Here the mass-transfer coefficient a_p is the number of moles of the pth mineral entering (positive) or leaving (negative) the solution, and $b_{p,k}$ is the stoichiometric coefficient of the kth element in the pth mineral. There are j equations of the form of equation 27, one for each of the j elements (excluding hydrogen and oxygen) required to define the composition of the P phases (minerals) considered in the model. Thus a reaction model

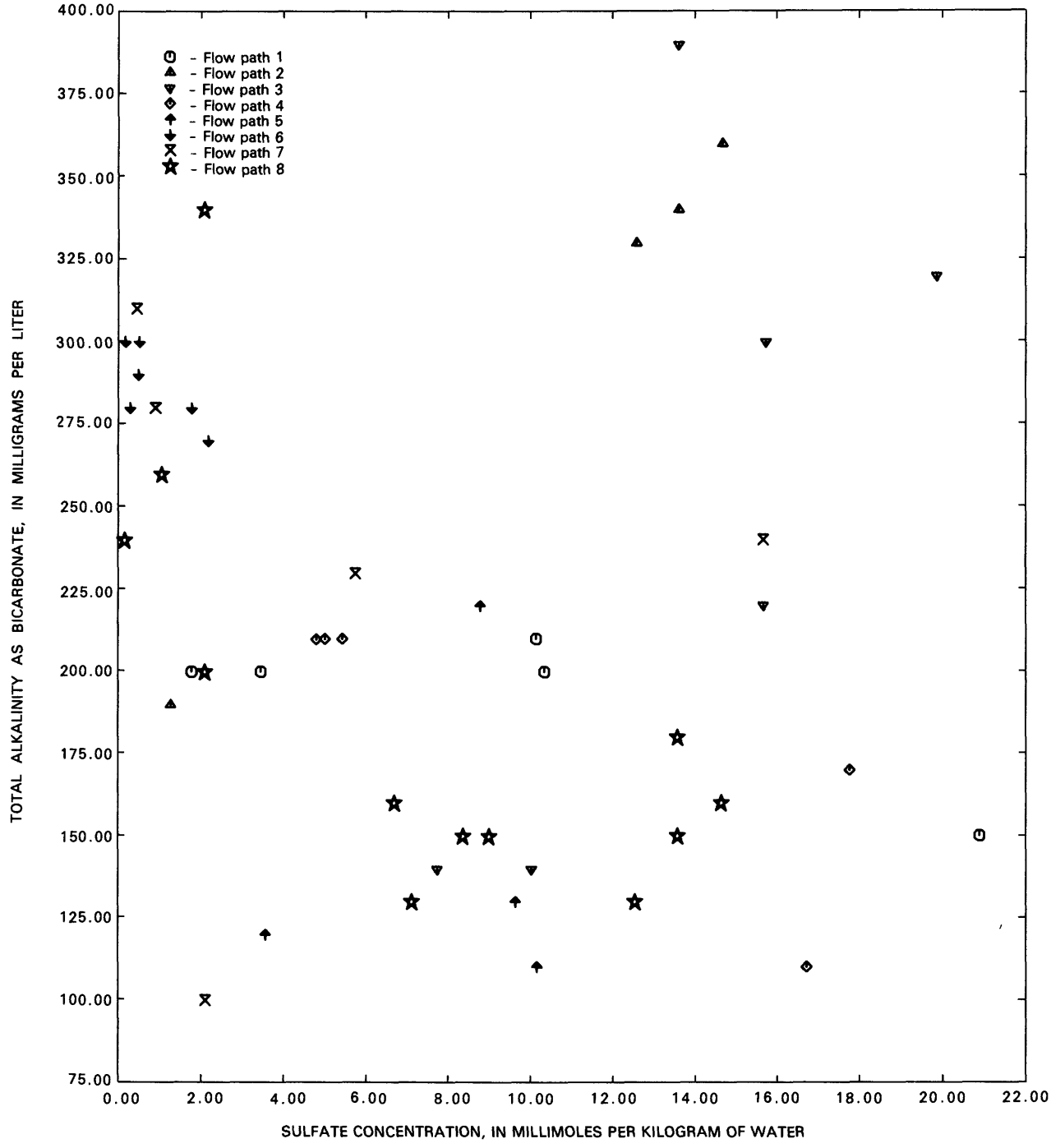

FIGURE 36.—Variation in total alkalinity as a function of dissolved-sulfate concentration along flow paths 1 to 8.

is a particular choice of phases that react to give the actual final-water composition.

If the reaction also includes changes in the oxidation state, equation 28 provides an additional constraint on the reaction. Equation 28 follows from the fact that hydrated electrons do not exist in aqueous solution. If electron transfer does take place (that is, there is a redox reaction), the electrons transferred are conserved among the dissolved species and the masses (α_p) of the P phases in the model. Equation 28 relates the sum of operational valences of the constituents in the pth plausible phase (u_p) and the stoichiometric coefficient of the pth plausible phase in the mass-balance calculation to ΔRS (the difference in redox state between the initial and final waters).

In equation 28 the change in the redox state of the solution (ΔRS) is calculated from the analytical data, as is Δm_T, and includes the (operational) valence v_i of the ith species in solution. The operational valence is defined by Plummer and others (1983) and in some cases differs by convention from the recognized oxidation state. Using those conventions, the term ΔRS is defined as

$$\Delta RS = \sum_{i=1}^{I} v_i m_i \text{ (final)} - \sum_{i=1}^{I} v_i m_i \text{ (initial)}, \qquad (29)$$

where m_i is the molality of the ith species in solution. (The initial condition refers to the recharge area, and the final condition indicates the downgradient well). The change in the redox state is then set equal to the number of electrons transferred among the P phases.

The data required to solve a mass-balance reaction model are (1) the set of phases thought to be reacting along the flow path, and (2) the concentrations of the elements in the initial and final waters that correspond to the composition of the chosen phases. The analytical

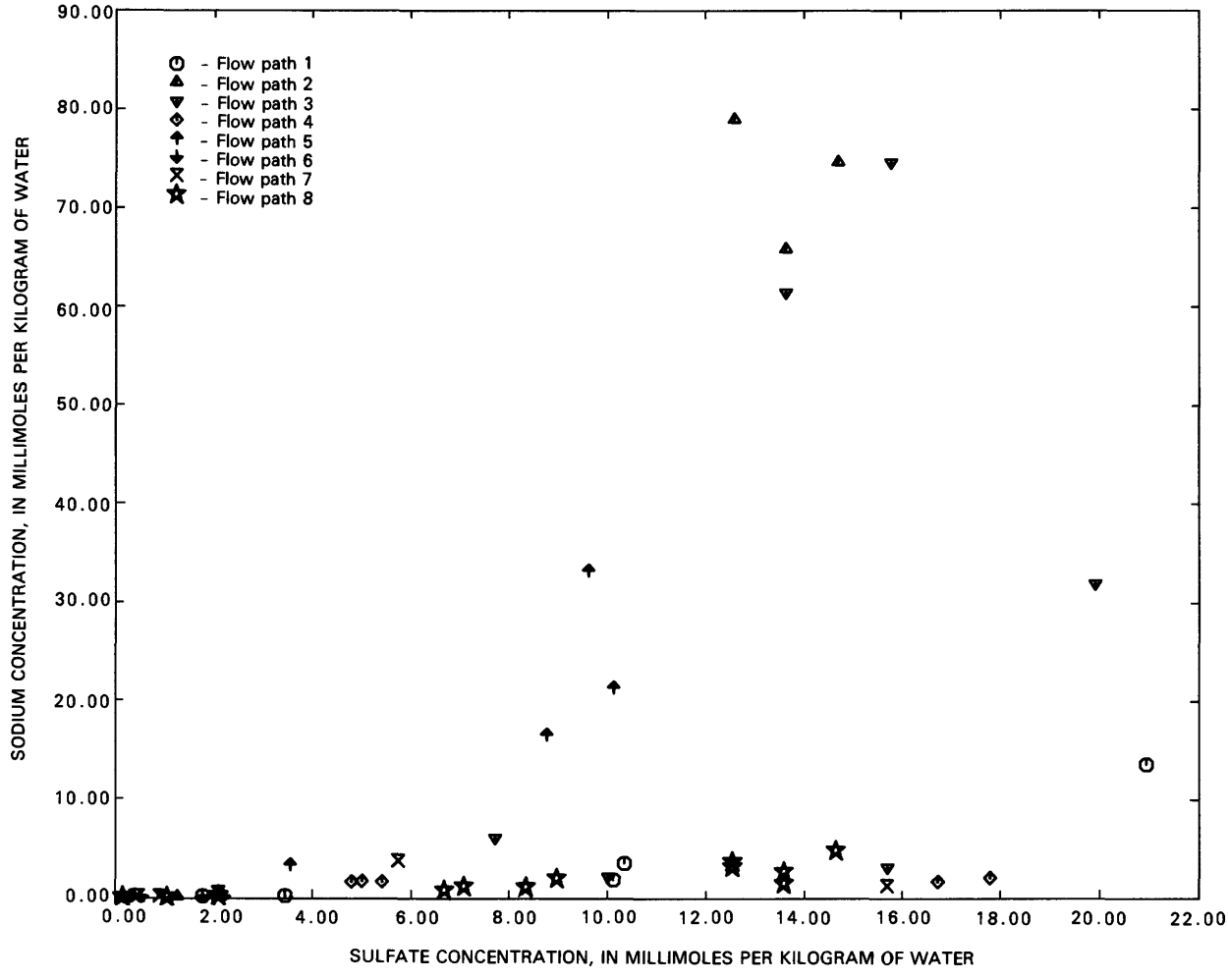

FIGURE 37.—Variation in dissolved sodium as a function of dissolved-sulfate concentration along flow paths 1 to 8.

data and redox states used in mass-balance modeling of the Madison aquifer are summarized in table 10.

The most obvious phases to include in the mass-balance modeling, based on the analysis of the chemical trends, the calculated values of *SI*, and the mineralogy, are summarized in table 16. Organic matter (CH_2O) is included as the most likely electron donor for bacterially mediated sulfate reduction. The formula CH_2O is used only to denote carbon of valence zero. Sulfate reduction is known to occur because of the presence of dissolved-sulfide species in many wells (table 8) and of the occurrence of sulfate-reducing bacteria as facultative thermophiles in one of the test wells drilled during the Madison Limestone Project (Olson and others, 1982; Blankennagel and others, 1979). As discussed in the previous section, if sufficient sources of dissolved iron are available for precipitation of pyrite, sulfate reduction need not be associated with large concentrations of dissolved-sulfide species. Therefore, ferric hydroxide and pyrite have been included in the mass-balance models. Dolomite, calcite, and anhydrite are included to quantify the dedolomitization reaction. Dissolution of halite was indicated by the earlier analysis of trends, and excess sodium is attributed to sodium-calcium ion exchange according to the reaction

$$Na_2X + Ca^{2+} = CaX + 2Na^{+}. \quad (30)$$

Carbon dioxide gas is included to account for the possibility of the exchange of CO_2 between the waters from the Madison aquifer and other reservoirs. Near-zero values for the CO_2 gas mass transfer indicate that ground-water conditions approximate a closed system. The deep ground-water system, with the exceptions of a small area along flow path 2 in Montana (the area of extensive faulting associated with the Little Rocky and Big Snowy Mountains) and the extreme eastern edge of the project area at the subcrop of the Madison aquifer, is expected to be virtually closed. Nonzero values of CO_2 gas mass transfer in other areas probably indicate errors in the analytical data or in the choice of mineral phases.

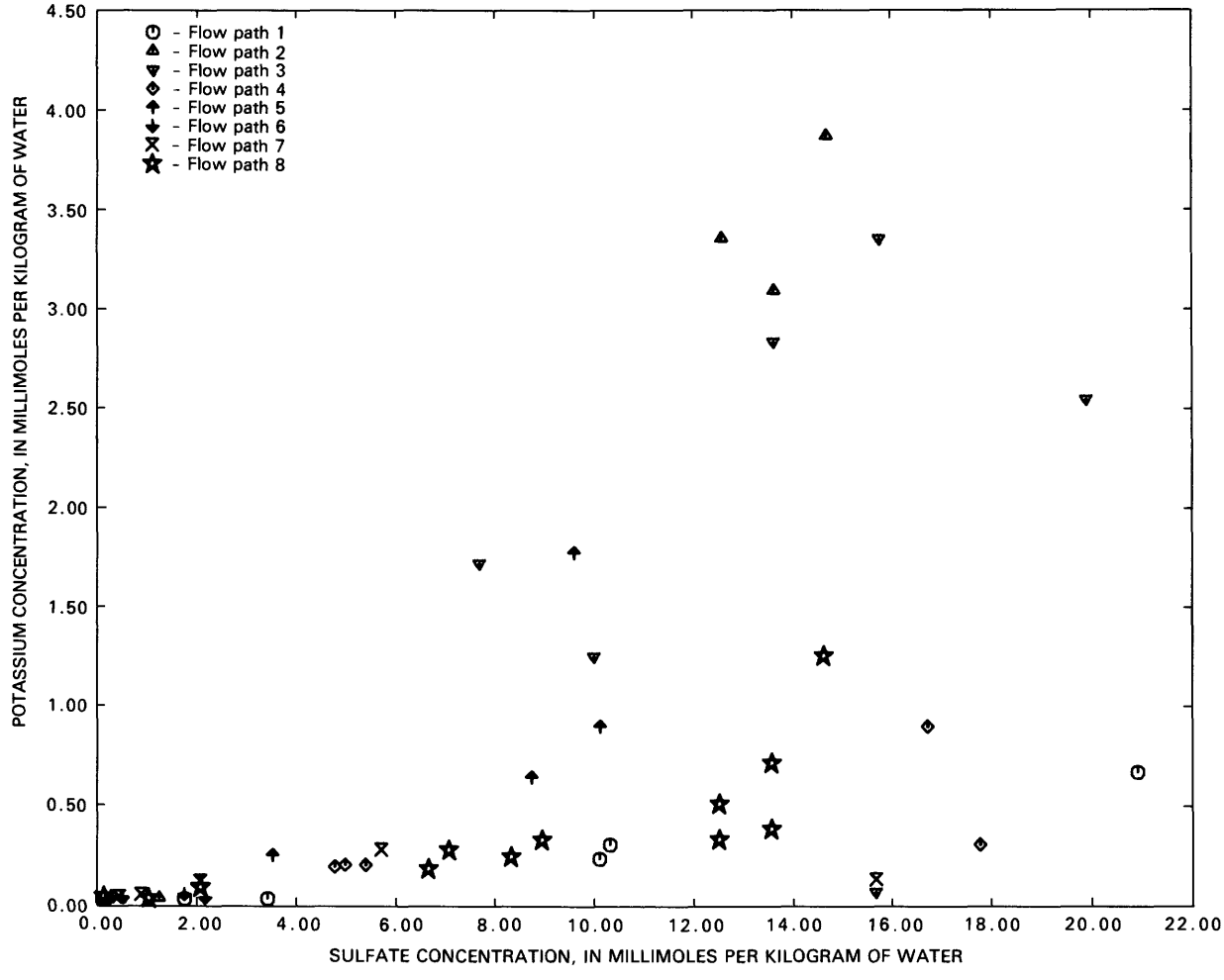

FIGURE 38.—Variation in dissolved potassium as a function of dissolved-sulfate concentration along flow paths 1 to 8.

As discussed in the previous section, the anhydrite and pyrite mass transfers probably can be estimated accurately by the sulfur mass-balance equation (eq 27 for sulfur) and an isotope-dilution equation for $\Delta^{34}S_T$. In the form of equations 27 and 28, the sulfur-isotope balance equation is

$$\sum_{p=1}^{P} \alpha_p b_{p,S}\, \delta^{34}S_p = \Delta^{34}S_T, \quad (31)$$

where

$\Delta^{34}S_T$ is $(S_T\, \delta^{34}S_T)_{final} - (S_T\, \delta^{34}S_T)_{initial}$;

$b_{p,S}$ is the stoichiometric coefficient of sulfur of the pth phase;

$\delta^{34}S_p$ is the sulfur-isotopic composition, in parts per thousand, of the pth phase;

S_T and $\delta^{34}S_T$ denote the total molality of sulfur in solution (sulfate plus sulfide species) and the average isotopic composition, in parts per thousand, of total dissolved sulfur, respectively; and

α_p is the mass transfer of the pth phase.

Values of $\delta^{34}S$ for sulfate and sulfide are required in the solution of the mass transfers of anhydrite and pyrite. Measured values have been used where available (12 wells, table 11). For the other wells, $\Delta^{34}S_T$ was estimated using equation 26 in conjunction with the measured temperature and $\delta^{34}S$ of the dissolved sulfate. Apparent values of $\delta^{34}S$ for anhydrite are summarized in table 12 for each flow path.

For the 10 plausible phases listed in table 16, 10 equations of the form of equations 27, 28, and 31 are needed to calculate the mass-transfer coefficients (α_p). These equations are

1. Mass balance (eq 27):

$$\alpha_{calcite} + 2\alpha_{dolomite} + \alpha_{CH_2O} + \alpha_{CO_2(gas)} = \Delta m_{T,C}, \quad (32)$$

$$\alpha_{anhydrite} + 2\alpha_{pyrite} = \Delta m_{T,S}, \quad (33)$$

$$\alpha_{calcite} + \alpha_{dolomite} + \alpha_{anhydrite} - \alpha_{exchange} = \Delta m_{T,Ca}, \quad (34)$$

$$\alpha_{dolomite} = \Delta m_{T,Mg}, \quad (35)$$

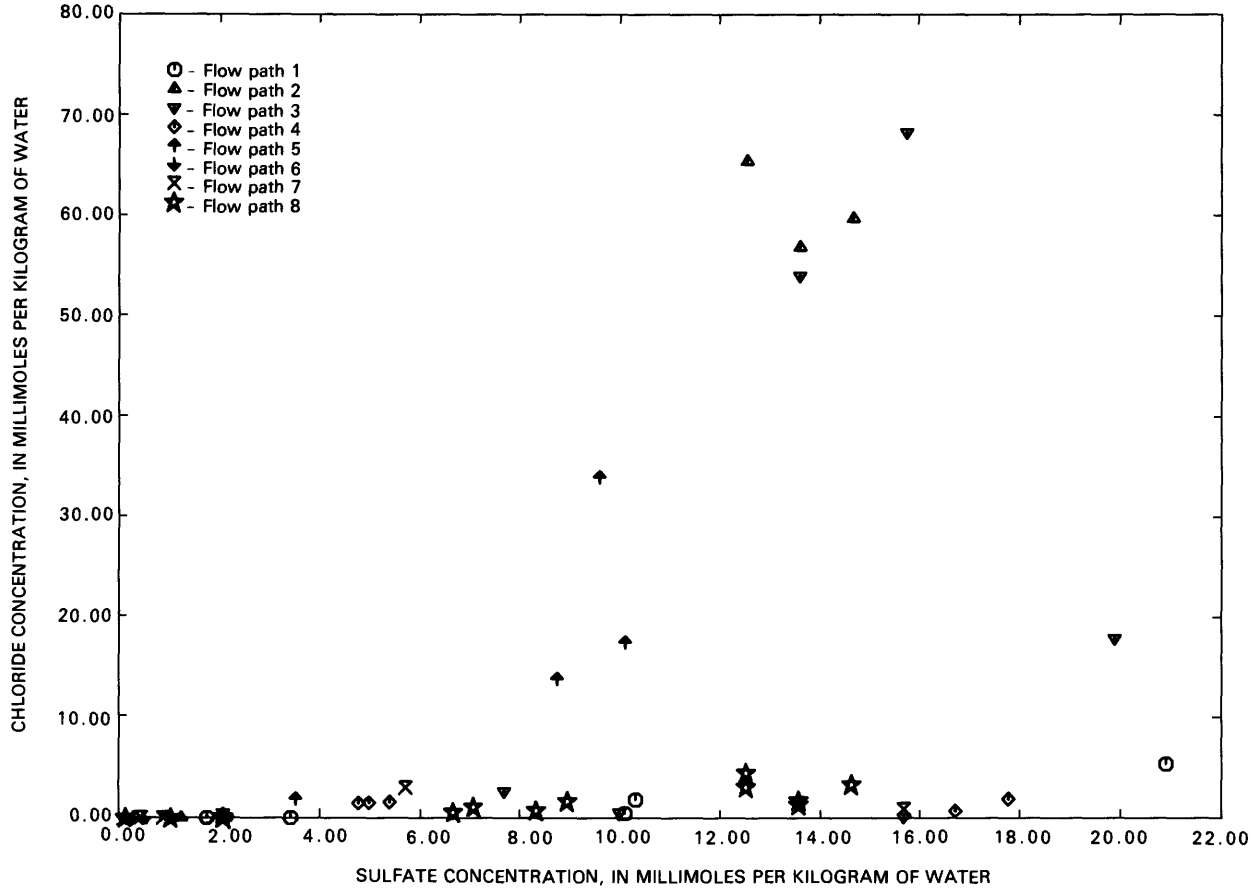

FIGURE 39.—Variation in dissolved chloride as a function of dissolved-sulfate concentration along flow paths 1 to 8.

TABLE 11.—*Isotopic data*

[Letter in front of flow-path number indicates whether the spring or well was used as recharge (R) or on the flow path (F); TU, tritium units]

Spring or well	Spring or well number	State	Flow path	Tritium (TU)	$\delta^{18}O$ (per mil)	δD (per mil)	$\delta^{34}S$ (sulfate) (per mil)	$\delta^{34}S$ (sulfide) (per mil)	$\delta^{13}C$ (per mil)	Carbon-14 (percent modern)
Lewistown Big Spring	10	Mont.	R1	0.8	-18.25	-139.20	14.93	--	-4.97	35.8
Hanover Flowing Well	8	Mont.	F1	.0	-18.25	-140.45	17.48	--	-5.32	25.4
Vanek Warm Spring	9	Mont.	F1	5.3	-18.35	-139.65	17.78	--	-5.18	29.3
Landusky Spring	12	Mont.	F1	21.9	-18.25	-138.75	21.33	--	-7.46	--
Lodgepole Warm Spring	13	Mont.	F1	31.8	-17.80	-134.75	23.86	--	-7.04	28.0
Sleeping Buffalo	18	Mont.	F1	--	-18.40	-138.35	21.95	--	-3.22	4.2
Bozeman Fish Hatchery	4	Mont.	R2	115.0	-18.90	-143.70	3.34	--	-8.98	84.1
Big Timber Fish Hatchery	7	Mont.	R2	124.0	-18.60	-142.65	-4.46	--	-14.11	103.9
McLeod Warm Spring	6	Mont.	F2	45.5	-18.50	-140.70	17.95	--	-7.57	52.5
Sumatra	17	Mont.	F2	--	-16.90	-136.15	17.01	-2.60	-3.61	--
Keg Coulee	15	Mont.	F2	--	-16.80	-136.40	17.75	--	-1.68	1.0
Texaco C115X	16	Mont.	F2	--	--	--	18.69	-.22	--	--
Mock Ranch	1	Wyo.	R3, R4	35.4	-18.35	-138.00	--	--	-7.10	57.7
Denius No. 1	2	Wyo.	R3, R4	19.8	-18.50	-137.85	9.73	--	-6.88	8.4
Colstrip	21	Mont.	F3	--	-19.05	-146.05	14.67	--	-2.67	--
Sarpy Mine	19	Mont.	F3	--	-19.80	-151.40	13.79	-9.20	-2.33	3.3
Gas City	26	Mont.	F3	--	--	--	--	--	--	--
Bluewater Spring	11	Mont.	F3	.5	-19.35	-146.90	--	--	-9.51	--
Moore	22	Mont.	F3	--	-18.00	-141.75	17.06	-7.73	-2.40	1.6
Mysse Flowing Well	20	Mont.	F3	--	-18.25	-141.50	16.30	-22.09	-2.34	.8
Storey Fish Hatchery	6	Wyo.	R4	107.0	-18.35	-138.95	--	--	-7.82	88.8
Mobil	7	Wyo.	R4	56.7	-17.45	-132.00	11.51	--	-9.75	62.2
HTH No. 1	14	Wyo.	F4	5.4	--	--	11.60	--	-6.63	12.7
Ranch Creek	23	Mont.	F4	--	-18.10	-137.60	11.75	--	-6.17	10.0
Belle Creek	24	Mont.	F4	--	-18.25	-137.90	11.71	--	-6.02	9.5
Delzer No. 1	7	S.Dak.	F4	.0	-19.66	--	15.20	--	-4.60	4.6
Delzer No. 2	8	S.Dak.	F4	.0	-18.13	--	14.67	-17.37	-2.61	2.8
Hole in the Wall	5	Wyo.	R5	.5	-18.30	-139.10	--	--	-10.77	87.4
Barber Ranch Spring	12	Wyo.	R5	53.0	-18.20	-137.65	7.75	--	-11.74	83.7
Conoco No. 175	11	Wyo.	F5	.8	-19.25	-145.50	8.23	--	-6.23	13.9
MKM	10	Wyo.	F5	.2	-19.70	-152.05	8.52	--	-4.66	2.6
Shidler	9	Wyo.	F5	1.2	-20.15	-153.65	8.64	--	--	6.2
Conoco No. 44	8	Wyo.	F5	.0	-20.10	-154.05	8.41	--	-5.14	1.8
Mallo Camp	24	Wyo.	R6	--	--	--	--	--	-8.00	92.9
Rhoads Fork	4	S.Dak.	R6, R7	62.2	-17.22	-125.00	6.22	--	-11.00	92.9
Seeley	19	Wyo.	F6	.8	--	-133.50	9.94	--	-7.82	61.4
Coronado No. 2	16	Wyo.	F6	.0	-17.60	-133.30	--	--	-7.51	36.0
Newcastle	21	Wyo.	F6	.1	-17.66	-130.00	9.84	--	-10.40	46.2
Osage	17	Wyo.	F6	.5	-18.15	-135.00	10.44	--	-10.00	54.7
Upton	15	Wyo.	F6	--	-18.18	-133.00	12.16	--	-8.20	14.7
Devils Tower	13	Wyo.	F6	1.5	-17.85	-139.95	11.68	--	-6.80	59.0
Voss	20	Wyo.	F7	2.3	-17.40	-130.65	10.09	--	-7.26	44.5
Self	22	Wyo.	F7	.0	-17.60	-131.80	10.49	--	-6.60	31.2
JBJ	18	Wyo.	F7	.3	-17.95	-130.65	11.68	--	-4.24	4.8
Evans Plunge	10	S.Dak.	F7	--	-16.71	-121.00	11.62	--	-9.70	28.5
Cascade Spring	9	S.Dak.	F7	--	-15.48	-118.00	12.50	--	-9.10	19.4
Jones Spring	12	S.Dak.	R8	276.0	-14.61	-110.00	6.67	--	-11.60	100.0
Kaiser	11	S.Dak.	R8	27.7	-12.13	--	9.00	--	-8.36	81.1
Cleghorn Spring	16	S.Dak.	R8	182.0	-13.23	-103.00	5.75	--	-9.60	91.6
Lien	17	S.Dak.	F8	16.6	-14.19	--	-3.20	--	-8.03	68.5
McNenney	2	S.Dak.	F8	11.4	-17.43	-127.00	11.36	--	-11.50	79.6
Ellsworth AFB	18	S.Dak.	F8	--	-14.13	-107.00	--	--	-9.10	5.8
Fuhs	6	S.Dak.	F8	65.6	-16.13	--	4.50	--	-9.96	53.8
Kosken	1	S.Dak.	F8	.1	-16.75	-126.60	12.93	--	-6.20	7.8
Philip	19	S.Dak.	F8	--	-17.55	-125.00	14.52	--	-7.20	2.8

TABLE 11.—*Isotopic data*—Continued

Spring or well	Spring or well number	State	Flow path	Tritium (TU)	$\delta^{18}O$ (per mil)	δD (per mil)	$\delta^{34}S$ (sulfate) (per mil)	$\delta^{34}S$ (sulfide) (per mil)	$\delta^{13}C$ (per mil)	Carbon-14 (percent modern)
Midland	24	S.Dak.	F8	--	-17.62	-128.00	14.96	--	-6.20	2.4
Murdo	25	S.Dak.	F8	1.3	-17.35	-131.45	14.56	-19.12	-5.50	3.2
Hilltop Ranch	22	S.Dak.	F8	.0	-17.60	-132.40	12.96	--	-6.63	4.6
Prince	26	S.Dak.	F8	--	-17.87	--	15.58	--	-4.72	4.0
Hamilton	21	S.Dak.	F8	--	-17.74	--	15.22	-12.22	-3.50	2.4
Eagle Butte	23	S.Dak.	F8	.6	-18.25	-137.10	15.99	-7.21	-2.40	2.2
Dupree	20	S.Dak.	F8	10.2	-19.00	-143.65	16.31	-4.77	-2.05	2.8
Gore Hill	2	Mont.	--	1.0	-19.35	-148.75	22.91	--	-3.18	3.6
Great Falls High School	3	Mont.	--	16.1	-19.00	-146.20	7.71	--	-7.20	24.2
Bough Ranch	5	Mont.	--	.0	-18.15	-141.25	19.99	-26.21	-3.80	1.3
HTH No. 3	14	Mont.	--	.1	--	--	--	--	-3.68	--
Buckhorn Exeter	27	Mont.	--	--	--	--	17.38	-4.23	--	--
Provo	3	S.Dak.	--	--	-17.09	-131.00	10.89	--	-9.40	7.3
Spearfish	5	S.Dak.	--	87.5	-17.06	-126.00	3.19	--	-10.20	74.3
Black Hills Cemetery	13	S.Dak.	--	--	-15.04	--	-5.10	--	-9.88	69.1
Streeter Ranch	14	S.Dak.	--	10.6	-12.05	-88.40	--	--	-6.65	52.2
Bean	27	S.Dak.	--	--	--	--	11.50	--	-6.73	3.3
Denius No. 2	3	Wyo.	--	--	--	--	--	--	--	--
Denius No. 3	4	Wyo.	--	--	--	--	--	--	--	--
Martens Madison	23	Wyo.	--	--	-17.45	-130.95	--	--	-9.56	61.9
Ranch A	25	Wyo.	--	41.6	-17.49	--	11.20	--	-10.81	74.4

$$\alpha_{halite} + 2\alpha_{exchange} = \Delta m_{T,Na}, \quad (36)$$

$$\alpha_{sylvite} = \Delta m_{T,K}, \quad (37)$$

$$\alpha_{halite} + \alpha_{sylvite} = \Delta m_{T,Cl}, \quad (38)$$

$$\alpha_{FeOOH} + \alpha_{pyrite} = \Delta m_{T,Fe}. \quad (39)$$

2. Conservation of electrons (eq 28):

$$4\alpha_{calcite} + 8\alpha_{dolomite} + 6\alpha_{anhydrite} + 4\alpha_{CO_2(gas)} + 3\alpha_{FeOOH} = \Delta RS. \quad (40)$$

Note that terms for CH_2O and pyrite do not appear in equation 40 because their operational valence is zero.

3. Sulfur-isotope balance (eq 31):

$$\alpha_{anhydrite}\,\delta^{34}S_{anhydrite} + 2\alpha_{pyrite}\,\delta^{34}S_{pyrite} = \Delta^{34}S_T \quad (41)$$

Equations 32 to 41 provide the 10 independent equations required to solve for the unknown mass-transfer coefficients (α_p). The following are algebraic solutions to equations 32 to 41, which define the mass transfers of anhydrite, pyrite, sylvite, halite, Ca^{2+}/Na^+ ion exchange, dolomite, goethite, calcite, CO_2 gas, and CH_2O.

$$\alpha_{anhydrite} = \frac{\Delta^{34}S_T - \delta^{34}S_{pyrite}\Delta m_{T,S}}{\delta^{34}S_{anhydrite} - \delta^{34}S_{pyrite}}, \quad (42)$$

$$\alpha_{pyrite} = (\Delta m_{T,S} - \alpha_{anhydrite})/2, \quad (43)$$

$$\alpha_{sylvite} = \Delta m_{T,K}, \quad (44)$$

$$\alpha_{halite} = \Delta m_{T,Cl} - \alpha_{sylvite}, \quad (45)$$

$$\alpha_{exchange} = (\Delta m_{T,Na} - \alpha_{halite})/2, \quad (46)$$

$$\alpha_{dolomite} = \Delta m_{T,Mg}, \quad (47)$$

$$\alpha_{FeOOH} = \Delta m_{T,Fe} - \alpha_{pyrite}, \quad (48)$$

$$\alpha_{calcite} = \Delta m_{T,Ca} + \alpha_{exchange} - \alpha_{anhydrite} - \alpha_{dolomite}, \quad (49)$$

$$\alpha_{CH_2O} = \Delta m_{T,C} - \alpha_{CO_2(gas)} - 2\alpha_{dolomite} - \alpha_{calcite}, \quad (50)$$

$$\alpha_{CO_2(gas)} = \frac{(\Delta RS - 3\alpha_{FeOOH} - 4\alpha_{calcite} - 8\alpha_{dolomite} - 6\alpha_{anhydrite})}{4} \quad (51)$$

To facilitate the calculations, equations 32 to 41 were solved using the computer program BALANCE (Parkhurst and others, 1982).

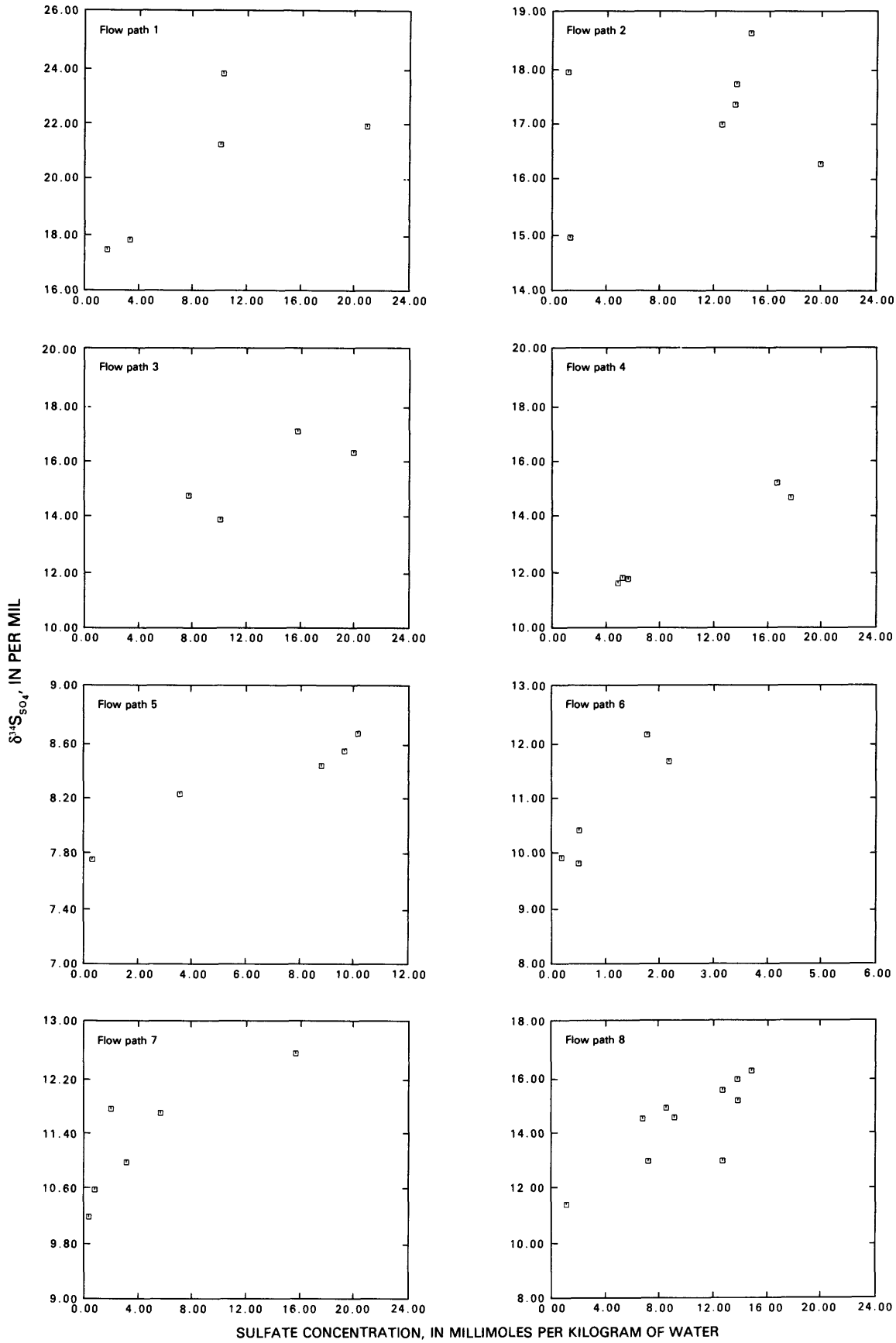
Flow path 1
Flow path 2
Flow path 3
Flow path 4
Flow path 5
Flow path 6
Flow path 7
Flow path 8
$\delta^{34}S_{SO_4}$, IN PER MIL
SULFATE CONCENTRATION, IN MILLIMOLES PER KILOGRAM OF WATER

TABLE 12.—*Initial estimate of sulfur-isotopic composition of dissolving anhydrite along flow paths*

Flow path	State	$\delta^{34}S_{anhydrite}$ (per mil)
1	Mont.	17.1
2	Mont.	14.7
3	Mont.	11.8
4	Wyo.	10.3
5	Wyo.	7.9
6	Wyo.	9.5
7	Wyo.	10.0
8	S. Dak.	11.0

PRELIMINARY MASS-TRANSFER RESULTS

Preliminary mass-transfer coefficients, in millimoles per kilogram of water, calculated for 42 waters along the 8 selected flow paths are summarized in table 17. Waters not included either do not fall on any of the eight flow paths, do not have a $\delta^{34}S$ value for dissolved sulfate, or were judged to be from multiple sources.

The computed mass transfer in table 17 represents the net millimoles of each phase entering (positive sign) or leaving (negative sign) a kilogram of water by dissolution or precipitation as that kilogram of water flows from the recharge area to the downgradient well. For example, according to the preliminary results in table 17, a kilogram of water moving along flow path 8 from the recharge area in the Black Hills eastward into South Dakota, some 106 miles to the Hamilton well, evolves according to the following net reaction:

$$\begin{aligned}\text{recharge water} &+ 2.90\ CaMg(CO_3)_2 + 15.90\ CaSO_4 \\ &+ 4.68\ CH_2O + 1.28\ FeOOH + 0.14\ Na_2X \\ &+ 0.97\ NaCl + 0.33\ KCl = 9.49\ CaCO_3 \\ &+ 1.22\ FeS_2 + 0.14\ CaX + 2.45\ CO_2 \\ &+ \text{Hamilton well water},\end{aligned} \qquad (52)$$

where the mass-transfer coefficients are in millimoles per kilogram of water. Similar net reactions can be written for each downgradient well using the preliminary results from table 17.

FIGURE 40.—Trends in $\delta^{34}S_{SO_4}$ with dissolved-sulfate concentration along flow paths 1 to 8.

INDICATIONS OF UNCERTAINTIES IN THE PRELIMINARY MODELING RESULTS

The validity of the preliminary mass-transfer results given in table 17 depends on many factors, including the choice of plausible phases, the accuracy of the correlation of $^{34}\Delta$ with temperature described by equation 26, the assumed constant sulfur-isotopic composition of anhydrite along each flow path (table 12), and the accuracy of the analytical data. One particularly uncertain aspect of the preliminary modeling results in table 17 is the required outgassing of significant quantities of CO_2 gas from many of the wells. About one-half of the wells modeled indicate CO_2 outgassing of 1.0 to 4.0 mmol/kg of water.

One way of checking the modeled mass transfer is to use the preliminary mass-transfer results in table 17 and the Rayleigh-distillation equations of Wigley and others (1978, 1979) to predict the measured values of $\delta^{13}C$ ($\delta^{13}C_{meas}$) of each downgradient water. A detailed example of how these calculations are made is given by Plummer and others (1983). If $\delta^{13}C_{meas}$ cannot be predicted within reasonable uncertainties of $\delta^{13}C$ values of the carbon sources (CH_2O and dolomite), then this is a strong indication of modeling error. In making such a calculation, we have used the average $\delta^{13}C_{meas}$ value for each recharge area of each flow path (table 11) as the starting point.

In the carbon-isotope modeling, computed positive values of CO_2 gas mass transfer (table 17) were interpreted as dissolution of soil gas CO_2 associated with the recharge process. The values of $\delta^{13}C$ (table 18) were calculated from the recharge waters and assumed to be representative of the average soil gas. The ^{14}C content of the downgradient well also was calculated, assuming no radioactive decay. The prenuclear-detonation ^{14}C content of the recharge waters, shown in table 18, was computed from mass-balance calculations assuming a 100 percent modern source for soil gas CO_2 and 0 percent modern sources of dissolving calcite and dolomite. Along each flow path, the ^{13}C content of reacting dolomite ($\delta^{13}C_{dolomite}$) and of CH_2O ($\delta^{13}C_{CH_2O}$) was taken as 2.0 and −20 per mil, respectively. The ^{14}C content of calcite and of CH_2O was assumed to be 0 percent modern. The $\delta^{13}C$ and ^{14}C content of the downgradient well, shown in table 19, was computed using the Rayleigh-distillation equations of Wigley and others (1978, 1979).

Cases involving possible CO_2 outgassing were treated with the one input (dolomite, CH_2O) and two fractionating output (CO_2 gas, calcite) equations. The case of apparent ingassing of CO_2 was solved with the one input (dolomite, CH_2O, CO_2 gas) and one fractionating output (calcite) equations. Carbon-isotope fractionation factors were those used by Plummer and others (1983), taking into account variation in temperature along the flow path.

TABLE 13.—*Calculation of anhydrite and pyrite mass transfers using the isotope-dilution method*

[°C, degrees Celsius; mmol/kg, millimoles per kilogram of water]

Spring or well	Spring or well number	State	Flow path	$\delta^{34}S$ anhydrite (per mil)	Temperature (°C)	Sulfate		Total sulfide		$^{34}\Delta = \delta^{34}S_{SO4} - \delta^{34}S_{H2S}$ (per mil)	Mass transfer[1]		
						mmol/kg	$\delta^{34}S$ (per mil)	mmol/kg	$\delta^{34}S$ (per mil)		Anhydrite	Pyrite	Sulfate (reduced)
Bough Ranch[2]	5	Mont.	--	17.1	17.9	16.67	19.99	0.24	-26.21	46.20	17.78	-0.44	1.11
Sumatra	17	Mont.	2	14.7	83.7	12.57	17.01	1.36	-2.60	19.61	14.22	-.22	1.65
Buckhorn Exeter[3]	27	Mont.	--	14.7	80.0	13.54	17.38	1.00	-4.23	21.61	15.41	-.56	1.87
Texaco C115X	16	Mont.	2	14.7	84.7	14.67	18.69	3.90	-.22	18.91	18.59	-.15	3.92
Sarpy Mine	19	Mont.	3	11.8	83.0	10.01	13.79	.09	-9.20	22.99	10.82	-.44	.81
Moore	22	Mont.	3	11.8	86.9	15.72	17.06	.56	-7.73	24.79	19.81	-1.84	4.09
Mysee Flowing Well	20	Mont.	3	11.8	63.0	19.86	16.30	.26	-22.09	38.39	22.35	-1.19	2.49
Delzer No. 2	8	S.Dak	4	10.3	55.6	17.74	14.67	.01	-17.37	32.04	20.44	-1.40	2.70
Murdo	25	S.Dak	8	11.0	59.1	8.97	14.56	.004	-19.12	33.68	9.89	-.54	.92
Hamilton	21	S.Dak.	8	11.0	58.5	13.56	15.22	.04	-12.22	27.44	15.90	-1.22	2.34
Eagle Butte	23	S.Dak.	8	11.0	54.7	13.56	15.99	.03	-7.21	23.20	17.16	-1.86	3.60
Dupree	20	S.Dak.	8	11.0	56.5	14.61	16.31	.03	-4.77	21.08	19.41	-2.46	4.80

[1]Positive for dissolution, negative for precipitation.
[2]Assuming zero sulfate in the recharge water and that the dissolving anhydrite is similar in isotopic composition to that of flow path 1.
[3]Assumed to be on flow path 2.

TABLE 14.—*Calculation of anhydrite and pyrite mass transfers using the Rayleigh-distillation method*

[mmol/kg, millimoles per kilogram of water]

Spring or well	Spring or well number	State	Flow path	$\delta^{34}S_{SO4}$			Dissolved sulfate (mmol/kg)		ε_{ps} (per mil)	Calculated Γ	Dissolved concentration (mmol/kg)		Mass transfer (mmol/kg)		
				$CaSO_4$	Starting water	Final water	Starting water	Final water			Sulfide species	ΔS_T	Anhydrite	Pyrite	Sulfate reduced
Bough Ranch	5	Mont.	--	17.1	3.34	19.99	0.26	16.67	-46.20	15.25	0.24	16.65	17.56	-0.46	1.15
Sumatra	17	Mont.	2	14.7	3.34	17.01	.26	12.57	-19.61	8.05	1.36	13.67	14.06	-.19	1.75
Buckhorn Exeter	27	Mont.	--	14.7	3.34	17.38	.26	13.54	-21.61	7.75	1.00	14.28	15.25	-.48	1.97
Texaco C115X	16	Mont.	2	14.7	3.34	18.69	.26	14.67	-18.91	4.72	3.90	18.31	18.28	.01	3.87
Sarpy Mine	19	Mont.	3	11.8	9.73	13.79	.16	10.01	-22.99	11.45	.09	9.94	10.79	-.43	.94
Moore	22	Mont.	3	11.8	9.73	17.06	.16	15.72	-24.79	4.77	.56	16.12	19.69	-1.78	4.13
Mysee Flowing Well	20	Mont.	3	11.8	9.73	16.30	.16	19.86	-38.39	8.62	.26	19.96	22.29	-1.16	2.59
Delzer No. 2	8	S.Dak.	4	10.3	10.62	14.67	.11	17.74	-32.04	7.42	.01	17.64	20.38	-1.37	2.75
Murdo	25	S.Dak.	8	11.0	7.14	14.56	.15	8.97	-33.68	9.40	.004	8.82	9.87	-.52	1.05
Hamilton	21	S.Dak.	8	11.0	7.14	15.22	.15	13.56	-27.44	5.83	.04	13.45	16.19	-1.37	2.78
Eagle Butte	23	S.Dak.	8	11.0	7.14	15.99	.15	13.56	-23.20	5.26	.03	13.44	16.56	-1.56	3.15
Dupree	20	S.Dak.	8	11.0	7.14	16.31	.15	14.61	-21.08	4.02	.03	14.49	19.25	-2.38	4.79

The data in figure 42 show that there is a systematic variation to heavier values in the measured $\delta^{13}C$ of waters in the Madison aquifer with increasing concentration of dissolved sulfate. The preliminary modeling results in table 19 show that, typically, the calculated $\delta^{13}C$ is 5 to 10 per mil lighter than the measured value. Six samples of Madison dolomite had an average $\delta^{13}C$ value of 1.8 ± 1.5 per mil (R.G. Deike, U.S. Geological Survey, written commun., 1982). The value of 2.0 per mil for $\delta^{13}C$ of dolomite has been used in modeling the calculated $\delta^{13}C$ of the water. Organic-carbon sources are expected to be light isotopically and are typically near −25 per mil. The modeling results of table 19 were obtained using a heavier $\delta^{13}C$ for organic matter (−20 per mil), but even in this case, the calculated values of $\delta^{13}C$ are systematically too light. Sensitivity analysis showed that no reasonable values of $\delta^{13}C$ for dolomite or organic matter were capable of predicting values of $\delta^{13}C$ similar to the

TABLE 15.—*Evaluation of uncertainties in anhydrite and pyrite mass transfers*

[°C, degrees Celsius; mmol/kg, millimoles per kilogram of water]

Spring or well	Spring or well number	State	Flow path	Temperature (°C)	$\delta^{34}S_{H2S}$ (per mil)		Anhydrite mass transfer (mmol/kg)			Pyrite mass transfer (mmol/kg)		
					Measured	Equation 26	Isotope dilution	Rayleigh distillation	Isotope dilution and equation 26	Isotope dilution	Rayleigh distillation	Isotope dilution and equation 26
Bough Ranch	5	Mont.	--	17.9	-26.21	-26.85	17.78	17.56	17.61	-0.44	-0.46	-0.48
Sumatra	17	Mont.	2	83.7	-2.60	-3.51	14.22	14.06	14.19	-.22	-.19	-.26
Buckhorn Exeter	27	Mont.	--	80.0	-4.23	-4.62	15.41	15.25	15.38	-.56	-.48	-.55
Texaco C115X	16	Mont.	2	84.7	-.22	-1.43	18.59	18.28	18.58	-.15	.01	-.13
Sarpy Mine	19	Mont.	3	83.0	-9.20	-7.01	10.82	10.79	10.92	-.44	-.43	-.49
Moore	22	Mont.	3	86.9	-7.73	-2.18	19.81	19.69	21.28	-1.84	-1.78	-2.58
Mysee Flowing Well	20	Mont.	3	63.0	-22.09	-12.50	22.35	22.29	23.29	-1.19	-1.16	-1.66
Delzer No. 2	8	S.Dak.	4	55.6	-17.37	-17.09	20.44	20.38	20.46	-1.40	-1.37	-1.41
Murdo	25	S.Dak.	8	59.1	-19.12	-15.80	9.89	9.87	10.03	-.54	-.52	-.60
Hamilton	21	S.Dak.	8	58.5	-12.22	-15.38	15.90	16.19	15.61	-1.22	-1.37	-1.08
Eagle Butte	23	S.Dak.	8	54.7	-7.21	-16.81	17.16	16.56	15.54	-1.86	-1.56	-1.05
Dupree	20	S.Dak.	8	56.5	-4.77	-15.09	19.41	19.25	17.47	-2.46	-2.38	-1.49

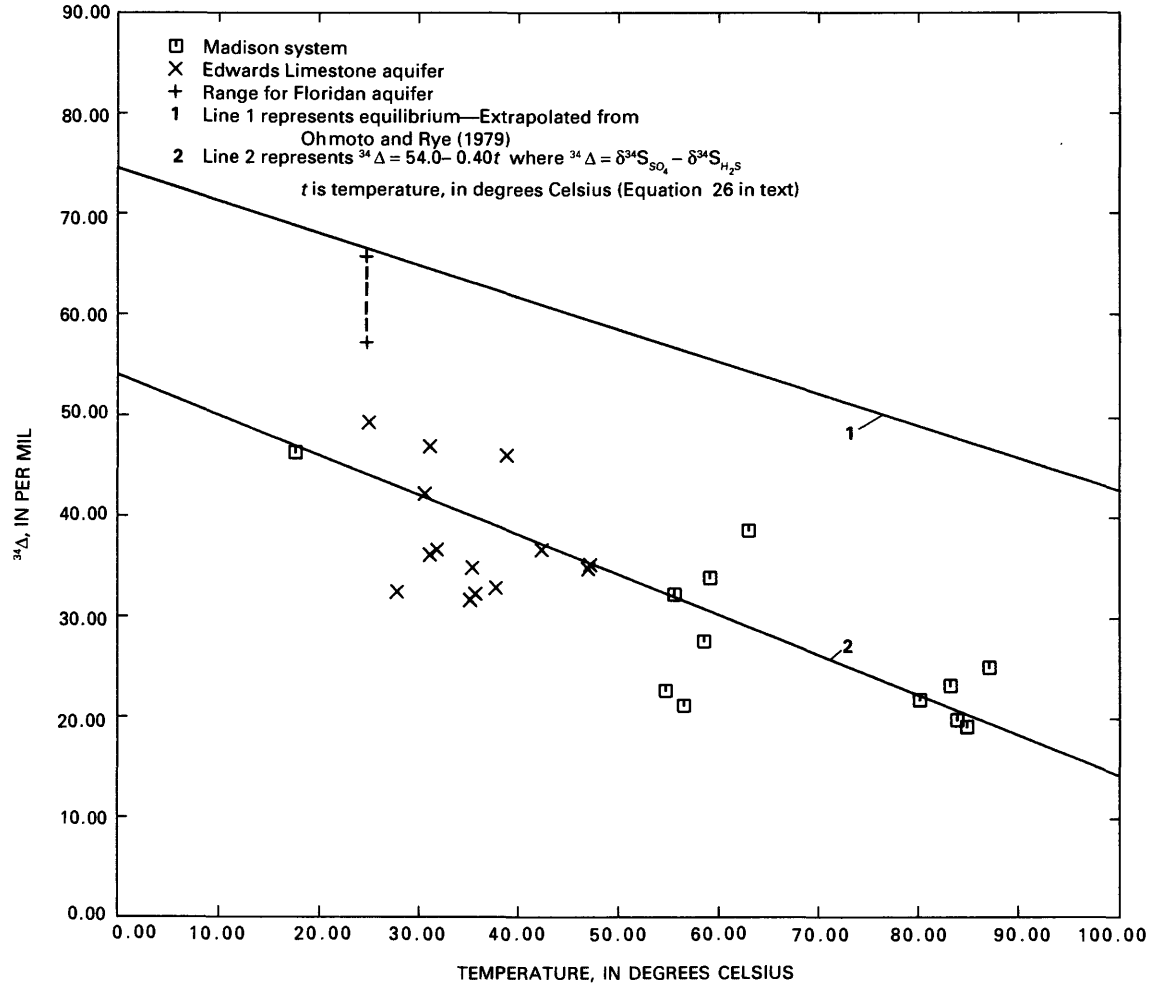

FIGURE 41.—Variation in $^{34}\Delta = \delta^{34}S_{SO_4} - \delta^{34}S_{H_2S}$ as a function of temperature for water in Madison aquifer compared with waters from Edwards and Floridan aquifers.

TABLE 16.—*Selected phases for mass-balance modeling*

Phase	Composition	Redox state (u_p)
Calcite (aragonite)	$CaCO_3$	4.0
Dolomite	$CaMg(CO_3)_2$	8.0
Anhydrite	$CaSO_4$	6.0
Organic matter	CH_2O	.0
Carbon dioxide gas	CO_2	4.0
Ferric hydroxide (goethite)	FeOOH	3.0
Pyrite	FeS_2	.0
Cation exchange	$(Ca\text{-}Na_2)X$	.0
Halite	NaCl	.0
Sylvite	KCl	.0

measured values for many of the wells or springs. For example, if $\delta^{13}C$ for dolomite and organic matter were 2.0 and −20.0 per mil, respectively, the calculated $\delta^{13}C$ at Dupree (well No. 20 in South Dakota) is −11.58 per mil. Even if $\delta^{13}C$ for organic matter is increased to −15 per mil and $\delta^{13}C$ for dolomite to +4.0 per mil, the calculated $\delta^{13}C$ at Dupree is still only −7.85 per mil, which compares with the measured $\delta^{13}C$ value of −2.05 per mil.

Another indicator of modeling error is based on the calculated ^{14}C activity. This activity is corrected for reaction effects only, and because radioactive decay is not applied to the calculated value, the calculated ^{14}C is expected to be larger than the measured. The age of the water is a function of the ratio of calculated to measured ^{14}C. Modern samples will have ratios of about 1.0 with the ratio increasing with age. Ratios less than 1.0 are impossible and indicate errors in the modeling process. Many of the calculated ^{14}C activities for wells downgradient are about equal to or less than the measured ^{14}C activities, indicating very young to impossibly young waters at points where, based on ground-water flow modeling, the ages of the waters are expected to be in excess of 10,000 to 20,000 yr. For example, the calculated ^{14}C activity at Dupree is 1.07 percent modern, which is less than the measured 2.80 percent modern. As the water at Dupree is expected to be in excess of 10,000 yr in age, the calculated ^{14}C activity is expected to be greater than 11 percent modern. Again, a serious flaw is indicated in the modeling process.

SOURCES OF ERROR

Many sources of error have been considered. These include (1) uncertainties in the analytical data, (2) uncertainties in defining the chemical and isotopic compositions of the recharge waters, (3) uncertainties in the ^{13}C fractionation factors as a function of temperature, (4) uncertainties in the ^{13}C content of dolomite and organic matter, (5) uncertainties in the estimation of $\delta^{34}S$ of dissolved sulfide (pyrite), (6) uncertainties in the estimation of the sulfur-isotopic composition of dissolving anhydrite, (7) the possibility of other reactions such as magnesium-sodium ion exchange and the in situ generation of methane (methanogenesis), and (8) uncertainties in determining the flow paths. Certainly all of these factors contribute to the modeling uncertainties, but only a few affect the results significantly.

From inspection of equations 42 to 51, it can be seen how errors in the analytical data propagate through the computed mass transfer, with the CO_2 gas and CH_2O mass transfers most sensitive to combined analytical error. Because most of the waters balance in charge within 1 percent or less, it is unlikely that there are large errors in the analytical data. Uncertainties in defining the chemical and isotopic compositions of recharge areas are real and probably contribute to modeling errors of ground waters near recharge areas which have not been affected by significant chemical reaction. Test calculations show, however, that differences in recharge-water composition have little effect on modeling results. Uncertainties in the ^{13}C fractionation factors have only minor effect on the modeling. For example, assuming that there is no fractionation between the bicarbonate ion and calcite, the calculated value of $\delta^{13}C$ at Dupree (well No. 20 in South Dakota) was changed by only 0.5 per mil. The calculated ^{14}C content (in percent modern) is even less dependent on uncertainties in the fractionation factors (Wigley and others, 1978, 1979). It already has been shown that even for unrealistic choices of $\delta^{13}C$ for organic matter and dolomite, large modeling errors remain.

Uncertainties in the compositions of the sulfur isotopes are likely and contribute to modeling errors. For example, the correlation described by equation 26 has been used to estimate $\delta^{34}S_{H_2S}$, using the measured temperature and $\delta^{34}S_{SO_4}$, where no value of $\delta^{34}S_{H_2S}$ was available. Deviations of ±10 per mil in the calculated $\delta^{34}S_{H_2S}$ values are likely (fig. 42). The Dupree well is used as an example. Here the measured $\delta^{34}S_{H_2S}$ is −4.77 per mil. Using this value, the preliminary modeling results of table 17 indicate oxidation of 9.29 millimoles of CH_2O per kilogram of water, outgassing of 4.08 millimoles of CO_2 per kilogram of water, and a calculated $\delta^{13}C$ of −11.58 per mil (table 19). Using the calculated $\delta^{34}S_{H_2S}$ of 15.09 per mil (eq 26) and otherwise identical modeling conditions, the quantity of CH_2O oxidized is decreased to 5.8 mmol/kg of water, the quantity of CO_2 outgassed is lessened to 2.4 mmol/kg of water, and the calculated $\delta^{13}C$ is −9.6 per mil. Although a 10 per mil difference in $\delta^{34}S_{H_2S}$ can significantly alter the modeled mass transfer, in this case the shift is far from sufficient to

TABLE 17.—*Preliminary results from mass-transfer model*

[All mineral and gas mass transfers are in millimoles per kilogram of water. Negative for precipitation, positive for dissolution]

Spring or well	Spring or well number	State	Flow path	Dolomite	Calcite	Anhydrite	Organic matter	Goethite	Pyrite	Ion exchange	Halite	Sylvite	Carbon dioxide gas
Hanover Flowing Well	8	Mont.	1	0.04	-0.20	0.40	0.16	0.04	-0.04	0.02	-0.02	0.01	0.06
Vanek Warm Spring	9	Mont.	1	.49	-1.20	2.10	.23	.06	-.06	.02	.01	.01	.21
Landusky Spring	12	Mont.	1	2.93	-7.36	9.76	2.07	.55	-.55	.70	.27	.21	-.07
Lodgepole Warm Spring	13	Mont.	1	2.80	-8.26	10.97	3.95	1.05	-1.05	.89	1.56	.28	-.89
Sleeping Buffalo	18	Mont.	1	3.80	-11.15	22.62	5.98	1.60	-1.59	4.37	4.68	.64	-2.93
McLeod Warm Spring	6	Mont.	2	.27	-1.01	1.18	.37	.10	-.10	-.07	-.02	-.01	-.39
Sumatra	17	Mont.	2	.73	-2.36	14.22	3.75	.22	-.22	8.32	61.92	3.30	-.38
Keg Coulee	15	Mont.	2	1.51	-3.19	15.08	3.46	.03	-.03	5.88	53.65	3.04	-.36
Texaco C115X	16	Mont.	2	1.47	-4.07	18.59	8.34	.14	-.15	9.23	55.74	3.82	-4.70
Colstrip	21	Mont.	3	.14	-2.72	9.41	3.49	.87	-.87	2.54	1.00	1.69	-1.78
Sarpy Mine	19	Mont.	3	1.09	-3.75	10.82	1.82	.45	-.44	1.36	-.66	1.23	-1.57
Moore	22	Mont.	3	1.81	-8.47	19.81	8.04	1.84	-1.84	4.81	64.80	3.32	-1.47
Mysse Flowing Well	20	Mont.	3	3.54	-7.53	22.35	4.99	1.19	-1.19	8.28	15.31	2.52	-1.97
HTH No. 1	14	Wyo.	4	.96	-2.36	4.87	.36	.19	-.09	.09	1.33	.17	.01
Ranch Creek	23	Mont.	4	1.04	-2.43	5.12	.43	.11	-.12	.12	1.37	.18	-.09
Belle Creek	24	Mont.	4	1.12	-2.72	5.56	.47	.13	-.13	.10	1.40	.18	-.11
Delzer No. 1	7	S.Dak.	4	3.68	-9.83	18.64	3.87	1.16	-1.02	.86	-.20	.88	-3.58
Delzer No. 2	8	S.Dak.	4	3.68	-11.32	20.44	5.28	1.50	-1.40	.16	1.58	.29	-1.93
Conoco No. 175	11	Wyo.	5	-.02	-1.02	3.38	.09	.06	-.02	.72	1.69	.21	-1.26
MKM	10	Wyo.	5	.64	-3.85	9.73	.65	.29	-.16	.40	32.16	1.73	.26
Shidler	9	Wyo.	5	.97	-2.48	10.16	.47	.16	-.12	2.28	16.60	.86	-2.38
Conoco No. 44	8	Wyo.	5	1.47	-3.68	8.67	.21	.07	-.05	1.59	13.17	.60	.06
Seeley	19	Wyo.	6	.14	-.18	.15	.01	.00	.00	.01	-.01	.01	-.07
Newcastle	21	Wyo.	6	.23	-.60	.47	.01	.00	.00	.04	-.01	.03	.01
Osage	17	Wyo.	6	.14	-.41	.51	.02	.01	-.01	.03	-.02	.02	.17
Upton	15	Wyo.	6	.72	-1.87	1.86	.22	.06	-.06	.05	-.04	.04	.00
Devils Tower	13	Wyo.	6	.60	-1.62	2.27	.20	.05	-.05	.04	.03	.02	-.21
Voss	20	Wyo.	7	.25	-.71	.42	.01	.00	.00	.03	.01	.03	.04
Self	22	Wyo.	7	.33	-1.00	.88	.02	.01	-.01	.03	.01	.04	-.41
JBJ	18	Wyo.	7	-.04	-1.77	2.16	.20	.05	-.05	.17	.10	.11	-1.88
Evans Plunge	10	S.Dak.	7	.74	-2.64	5.93	.44	.12	-.12	.44	2.83	.27	-.42
Cascade Spring	9	S.Dak.	7	2.48	-6.95	16.52	1.69	.45	-.45	.19	.75	.12	-.56
McNenney	2	S.Dak.	8	.18	-.31	.91	.03	.01	-.01	-.06	-.03	-.02	.20
Kosken	1	S.Dak.	8	1.17	-3.92	7.47	1.00	.26	-.27	.05	.84	.23	-1.26
Philip	19	S.Dak.	8	1.58	-4.91	7.55	1.93	.51	-.52	.06	.43	.13	-1.29
Midland	24	S.Dak.	8	1.91	-6.08	9.74	2.91	.77	-.78	.16	.54	.19	-2.07
Murdo	25	S.Dak.	8	1.87	-5.40	9.89	2.03	.56	-.54	.19	1.38	.28	-1.79
Hilltop Ranch	22	S.Dak.	8	2.36	-8.40	13.35	1.84	.50	-.49	-.36	4.18	.28	-.07
Prince	26	S.Dak.	8	2.61	-8.08	14.54	4.08	1.09	-1.09	.16	2.59	.46	-3.10
Hamilton	21	S.Dak.	8	2.90	-9.49	15.90	4.68	1.28	-1.22	.14	.97	.33	-2.45
Eagle Butte	23	S.Dak.	8	3.72	-11.80	17.16	7.04	1.91	-1.86	.66	1.06	.66	-3.82
Dupree	20	S.Dak.	8	3.07	-12.84	19.41	9.29	2.47	-2.46	1.22	2.13	1.20	-4.08

account for the lack of agreement between calculated (−9.6 per mil) and measured (−2.05 per mil) $\delta^{13}C$ at Dupree.

In summary, the main indicators of modeling errors in the preliminary results (tables 17 and 19) are (1) the tendency for unreasonable quantities of CO_2 outgassing, (2) calculated $\delta^{13}C$ values that are significantly lighter than the measured values, and (3) calculated ^{14}C activities that are about equal to or less than the measured values when they are expected to be significantly larger than these values. Factors or processes that, if applied uniformly to the modeling exercise, could systematically improve the discrepancies in calculated $\delta^{13}C$, ^{14}C, and CO_2 outgassing were examined and are discussed below.

TABLE 18.—*Summary of average carbon-isotope values for recharge waters used for modeling carbon isotopes at downgradient wells*

	$\delta^{13}C_{(water)}$ (per mil)[1]	$\delta^{13}C_{CO2(gas)}$ (per mil)[2]	^{14}C (percent modern)[3]
Recharge 1	-4.97	-9.44	52.68
Recharge 2	-11.55	-20.49	56.37
Recharge 3	-6.99	-13.36	52.34
Recharge 4	-7.89	-14.64	53.88
Recharge 5	-11.26	-20.24	55.63
Recharge 6	-9.50	-17.39	54.64
Recharge 7	-11.00	-19.90	55.29
Recharge 8	-9.85	-17.16	57.39

[1]Average of wells defined as recharge water for each flow path.
[2]Estimated, assuming recharge water evolved from reaction of rain with soil carbon dioxide, calcite, and dolomite where del carbon-13 of calcite and dolomite is taken as 0.
[3]Estimated, prenuclear-detonation carbon-14 content of recharge waters calculated assuming a 100 percent modern source of carbon dioxide gas and 0 percent modern carbonate mineral sources.

As the preliminary model results show (tables 17 and 19), only two sources of carbon are expected: a light source (CH_2O), and a heavy source (dolomite). The modeling discrepancies in calculated $\delta^{13}C$ values indicate a need to either decrease the quantity of CH_2O reacting, increase the quantity of dolomite dissolving, or find a sink for light $\delta^{13}C$. Three modeling alternatives that can improve the results are (1) a mineral sink for magnesium such as Mg^{2+}/Na^+ ion exchange or formation of a magnesium-silicate phase, (2) methanogenesis, and (3) variation in $\delta^{34}S_{anhydrite}$.

An added sink for magnesium will increase the quantity of dolomite that can dissolve, leading to heavier values of calculated $\delta^{13}C$. Likely sinks for magnesium include ion exchange of Mg^{2+} for Na^+ and the formation of authigenic magnesium-silicate minerals such as sepiolite [$Mg_2Si_3O_{7.5}(OH)\cdot 3H_2O$] and stevensite [$Na_{0.67}Mg_{2.67}Si_4O_{10}(OH)_2$], which are significant weathering products of pyroclastic rocks (Jones and Weir, 1983). Calculations using various additional sinks for magnesium show that heavier $\delta^{13}C$ values can be calculated. However, the mass transfer is confined to the calcite-dolomite phases, with more calcite precipitated as more dolomite dissolves. The CO_2 outgassing term is not a function of noncarbonate magnesium sinks. Furthermore, by increasing the quantity of dolomite dissolved and calcite precipitated, the calculated ^{14}C content is significantly decreased, as required by incorporation of ^{14}C in precipitated calcite.

To demonstrate this point and other modeling options, an example using several modeling alternatives at the Mysse Flowing Well (well No. 20 in Montana) was made. The data in table 20 show, for the modeling conditions of Ca^{2+}/Na^+ exchange, no methanogenesis, $\delta^{34}S_{anhydrite}$ equal to that derived for flow path 3 (table 12), $\delta^{13}C_{dolomite}$ equal to 2.0 per mil, and $\delta^{13}C_{CH_2O}$ equal to −25.0 per mil, that the calculated value of $\delta^{13}C$ (−9.39 per mil) is substantially different from the measured value (−2.34 per mil) and that a significant quantity of CO_2 outgassing (1.97 mmol/kg of water) is indicated (case 1, table 20). By providing a sink for magnesium, for example, as a pure Mg^{2+}/Na^+ exchange reaction in place of pure Ca^{2+}/Na^+ exchange, the dolomite and calcite mass transfers are almost tripled (case 2, table 20), but there is no change in the large calculated quantity of CO_2 outgassed. Although the calculated value of $\delta^{13}C$ (−4.31 per mil) is now closer to the measured value (−2.34 per mil), the added magnesium sink still leads to a calculated ^{14}C value less than the measured value (case 2, table 20).

Analysis of the chemical trends indicates that excess bicarbonate is found primarily along flow paths 2 and 3, indicating significant ion exchange. The preliminary mass-transfer results confirm this trend because values of about zero for the ion-exchange mass-transfer coefficient were determined almost everywhere in the Madison aquifer system (table 17) except along flow paths 2 and 3. Thus, Mg^{2+}/Na^+ exchange or combined $(Ca^{2+} + Mg^{2+})/Na^+$ exchange cannot be invoked to account for the ^{13}C discrepancy throughout the Madison aquifer. Furthermore, by adding the magnesium sink, the CO_2-outgassing problem is not affected and the ^{14}C discrepancy is even larger.

Another modeling alternative is the possibility of methanogenesis. A large biological fractionation accompanies methanogenesis, resulting in the formation of CH_4, which is typically 40 ± 20 per mil lighter in ^{13}C than the CH_2O from which it was derived. Methane as light as −80 per mil is not uncommon (Hoefs, 1973). The CO_2-CH_4 equilibrium fractionation factor is about 70 per mil at 25 °C and decreases to 50 per mil at about 90 °C (Bottinga, 1969).

Only traces of dissolved CH_4 were found in the dissolved gases of 12 wells completed in the Madison aquifer (Busby and others, 1983). The maximum concentrations (0.45 to 0.87 mg/L) were in water from wells along flow paths 2 and 3. The modeling of the mass transfer along these flow paths indicates that such concentrations of methane are insufficient to significantly affect the calculated value of $\delta^{13}C$. Larger concentrations of CH_4 are required to increase the calculated value of $\delta^{13}C$, which would necessitate a system open to both CO_2 and CH_4 outgassing.

Returning to the modeling example of the Mysse Flowing Well, the mass transfer to this well was calculated assuming the formation of a gas containing 20 percent of CH_4 and 80 percent of CO_2. The CH_4 produced was assumed to be 60 per mil lighter than the $\delta^{13}C$ of the aqueous solution. The remainder of the modeling parameters were as before: Ca^{2+}/Na^+ exchange, $\delta^{34}S_{anhydrite}$

TABLE 19.—*Summary of preliminary model parameters and carbon-isotope results*

[Calculated carbon-14 assumes no radioactive decay]

Spring or well	Spring or well number	State	Flow path	$\delta^{34}S$ anhydrite (per mil)	$\delta^{13}C$ (per mil)		$\delta^{13}C$, water (per mil)		Carbon-14, water (percent modern)		Apparent age (years)
					Organic matter	Dolomite	Calculated	Measured	Calculated	Measured	
Hanover Flowing Well	8	Mont.	1	17.10	-20.00	2.00	-5.62	-5.32	49.09	25.40	5,446
Vanek Warm Spring	9	Mont.	1	17.10	-20.00	2.00	-4.68	-5.18	37.38	29.30	2,013
Landusky Spring	12	Mont.	1	17.10	-20.00	2.00	-4.85	-7.46	5.66	--	--
Lodgepole Warm Spring	13	Mont.	1	17.10	-20.00	2.00	-7.55	-7.04	3.46	28.00	modern
Sleeping Buffalo	18	Mont.	1	17.10	-20.00	2.00	-7.52	-3.22	.61	4.20	modern
McLeod Warm Spring	6	Mont	2	14.70	-20.00	2.00	-10.01	-7.57	43.82	52.50	modern
Sumatra	17	Mont.	2	14.70	-20.00	2.00	-13.49	-3.61	19.81	--	--
Keg Coulee	15	Mont.	2	14.70	-20.00	2.00	-10.84	-1.68	16.10	1.00	22,970
Texaco C115X	16	Mont.	2	14.70	-20.00	2.00	-12.89	--	5.90	--	--
Colstrip	21	Mont.	3	11.80	-20.00	2.00	-13.81	-2.67	20.02	--	--
Sarpy Mine	19	Mont.	3	11.80	-20.00	2.00	-7.84	-2.33	17.22	3.30	13,659
Moore	22	Mont.	3	11.80	-20.00	2.00	-13.59	-2.40	5.35	1.60	9,986
Mysse Flowing Well	20	Mont.	3	11.80	-20.00	2.00	-7.55	-2.34	5.79	.80	16,368
HTH No. 1	14	Wyo.	4	10.30	-20.00	2.00	-6.02	-6.63	30.59	12.70	7,266
Ranch Creek	23	Mont.	4	10.30	-20.00	2.00	-5.85	-6.17	28.70	10.00	8,716
Belle Creek	24	Mont.	4	10.30	-20.00	2.00	-5.78	-6.02	27.28	9.50	8,720
Delzer No. 1	7	S.Dak.	4	10.30	-20.00	2.00	-4.08	-4.60	1.02	4.60	modern
Delzer No. 2	8	S.Dak.	4	10.30	-20.00	2.00	-8.21	-2.61	1.84	2.80	modern
Conoco No. 175	11	Wyo.	5	7.90	-20.00	2.00	-10.10	-6.23	54.73	13.90	11,329
MKM	10	Wyo.	5	7.90	-20.00	2.00	-11.59	-4.66	33.08	2.60	21,026
Shidler	9	Wyo.	5	7.90	-20.00	2.00	-4.16	--	25.32	6.20	11,631
Conoco No. 44	8	Wyo.	5	7.90	-20.00	2.00	-6.23	-5.14	26.56	1.80	22,252
Seeley	19	Wyo.	6	9.50	-20.00	2.00	-8.86	-7.82	51.80	61.40	modern
Newcastle	21	Wyo.	6	9.50	-20.00	2.00	-8.76	-10.40	50.14	46.20	677
Osage	17	Wyo.	6	9.50	-20.00	2.00	-9.31	-10.00	51.68	54.70	modern
Upton	15	Wyo.	6	9.50	-20.00	2.00	-7.67	-8.20	40.09	14.70	8,294
Devils Tower	13	Wyo.	6	9.50	-20.00	2.00	-7.62	-6.80	41.85	59.00	modern
Voss	20	Wyo.	7	10.00	-20.00	2.00	-10.17	-7.26	50.62	44.50	1,065
Self	22	Wyo.	7	10.00	-20.00	2.00	-9.26	-6.60	48.68	31.20	3,677
JBJ	18	Wyo.	7	10.00	-20.00	2.00	-9.65	-4.24	53.57	4.80	19,942
Evans Plunge	10	S.Dak.	7	10.00	-20.00	2.00	-8.84	-9.70	38.04	28.50	2,386
Cascade Spring	9	S.Dak.	7	10.00	-20.00	2.00	-6.63	-9.10	15.75	19.40	modern
Lien	17	S.Dak.	8	11.00	-20.00	2.00	-8.20	-8.03	52.62	68.50	modern
McNenney	2	S.Dak.	8	11.00	-20.00	2.00	-9.47	-11.50	53.02	79.60	modern
Fuhs	6	S.Dak.	8	11.00	-20.00	2.00	-5.59	-9.96	34.80	53.80	modern
Kosken	1	S.Dak.	8	11.00	-20.00	2.00	-7.28	-6.20	23.15	7.80	8,995
Philip	19	S.Dak.	8	11.00	-20.00	2.00	-8.22	-7.20	16.55	2.80	14,689
Midland	24	S.Dak.	8	11.00	-20.00	2.00	-8.55	-6.20	10.32	2.40	12,059
Murdo	25	S.Dak.	8	11.00	-20.00	2.00	-7.14	-5.50	13.14	3.20	11,679
Hilltop Ranch	22	S.Dak.	8	11.00	-20.00	2.00	-7.78	-6.63	9.44	4.60	5,944
Prince	26	S.Dak.	8	11.00	-20.00	2.00	-8.05	-4.72	4.50	4.00	981
Hamilton	21	S.Dak.	8	11.00	-20.00	2.00	-8.86	-3.50	3.91	2.40	4,026
Eagle Butte	23	S.Dak.	8	11.00	-20.00	2.00	-8.99	-2.40	1.65	2.20	modern
Dupree	20	S.Dak.	8	11.00	-20.00	2.00	-11.58	-2.05	1.07	2.80	modern

equal to the average flow-path value (11.8 per mil), and $\delta^{13}C_{CH_2O}$ and $\delta^{13}C_{dolomite}$ of -25.0 and 2.0 per mil, respectively.

The mass-transfer and carbon-isotope calculations are summarized in table 20 (case 3). Inclusion of methanogenesis significantly increases the calculated quantity of outgassing. As expected, the quantity of organic matter oxidized is increased and there is only minor improvement in the calculated value of $\delta^{13}C$ compared with case 1. The combined effect of pure Mg^{2+}/Na^{+} exchange and methanogenesis (case 4, table 20) differs little from that of Mg^{2+}/Na^{+} exchange alone (case 2).

Substantial methanogenesis is not known to occur when dissolved sulfate is present (Fenchel and Blackburn, 1979). Because many of the waters are almost saturated with respect to anhydrite, methanogenesis is not expected to be an important process in the Madison aquifer.

One final and potentially more likely modeling alternative considered was the possibility that the sulfur-isotopic composition of dissolving anhydrite may differ from that derived for each flow path (table 12) and may vary along the flow path. If, for example, $\delta^{34}S_{anhydrite}$ were heavier than previously estimated (table 12), less sulfate reduction would be calculated, the quantity of isotopically light CH_2O reacting would decrease, and the value of $\delta^{13}C$ would be heavier. In addition, the decrease in CH_2O mass transfer would decrease the quantity of CO_2 outgassed, and thus it may be possible to find a "reasonable" value of $\delta^{34}S_{anhydrite}$ that indicates a system closed to CO_2 gas. Finally, decreased CH_2O mass

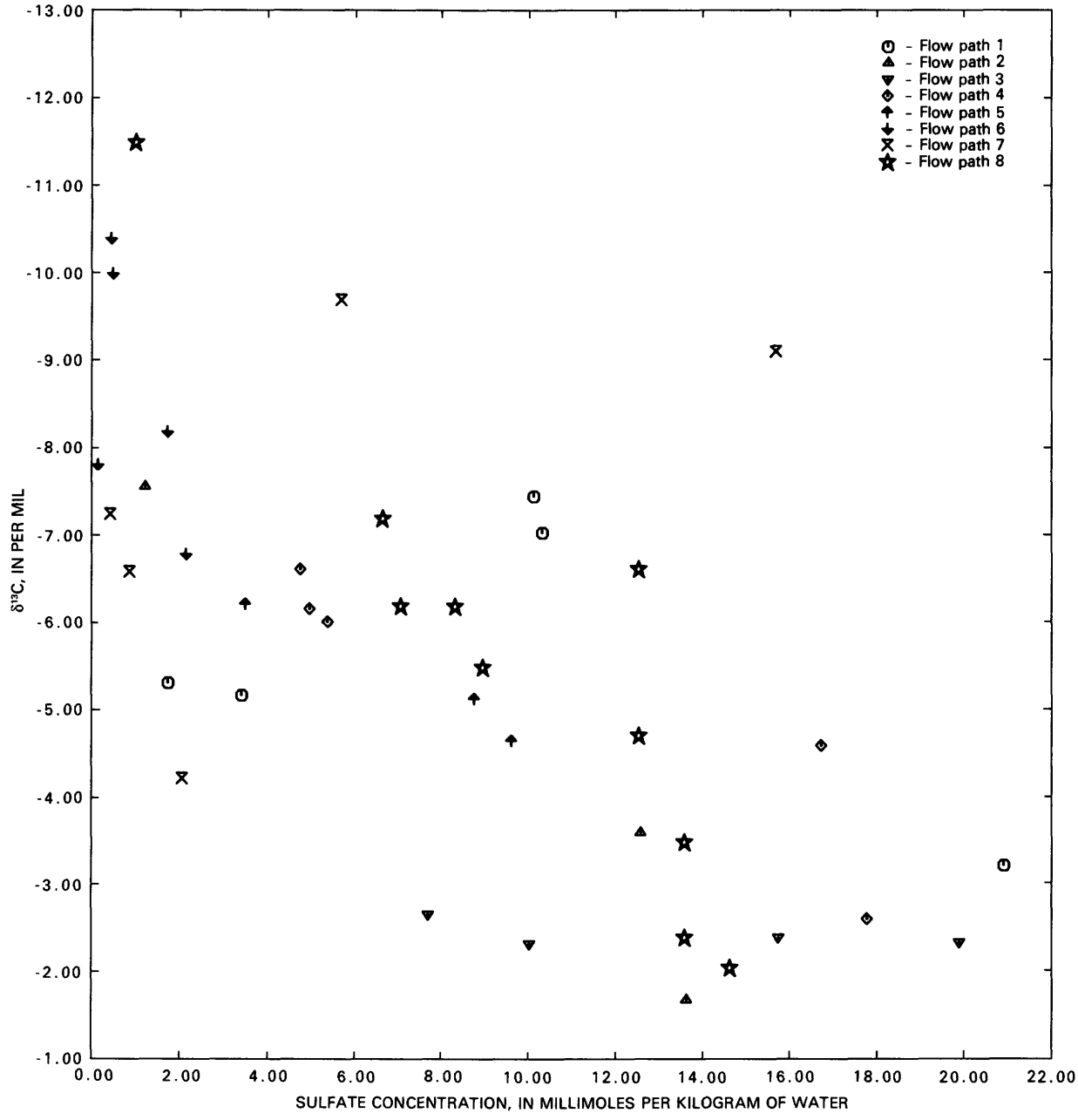

FIGURE 42.—Variation in measured $\delta^{13}C$ as a function of dissolved-sulfate concentration in Madison aquifer system.

TABLE 20.—*Summary of modeling alternatives applied to the Mysse Flowing Well (well No. 20 in Montana)*

[mmol/kg, millimoles per kilogram of water]

Modeling parameters

Case	$\delta^{34}S$ (per mil)[1]	Ion exchange XMg[2]	Proportion of carbon dioxide in gas[3]	Solution-methane fractionation (per mil)	$\delta^{13}C$ (per mil)	
					Organic matter	Dolomite
1	11.8	0.0	1.0	--	-25.0	+2.0
2	11.8	1.0	1.0	--	-25.0	+2.0
3	11.8	.0	.8	-60.	-25.0	+2.0
4	11.8	1.0	.8	-60.	-25.0	+2.0
5	15.5	.0	1.0	--	-25.0	+2.0
6	15.5	.0	1.0	--	-25.0	+4.0

Calculated results

Case	Mass transfer (mmol/kg)					$\delta^{13}C$ (per mil)		Carbon-14 activity (percent modern)[4]	
	Dolomite	Calcite	Anhydrite	Organic matter	Gas	Calculated	Measured	Calculated	Measured
1	3.54	-7.53	22.35	5.00	-1.97	-9.39	-2.34	5.79	0.80
2	11.82	-24.09	22.35	5.00	-1.97	-4.31	-2.34	.28	.80
3	3.54	-7.53	22.35	6.31	-3.28	-7.90	-2.34	4.56	.80
4	11.82	-24.09	22.35	6.31	-3.28	-3.78	-2.34	.22	.80
5	3.54	-7.53	20.15	0.87	-0.04	-3.57	-2.34	12.30	.80
6	3.54	-7.53	20.15	0.87	-0.04	-2.20	-2.34	12.30	.80

[1]Dissolving anhydrite.

[2]XMg is the fraction of magnesium/sodium ion exchange;
0.0 = pure calcium/sodium ion exchange,
1.0 = pure magnesium/sodium ion exchange.

[3]Proportion of carbon dioxide gas in a carbon dioxide-methane mixture;
1.0 = pure carbon dioxide gas,
0.0 = pure methane gas.

[4]Content corrected for reaction effects but not radioactive decay.

$$\text{Calculated age} = \frac{5730}{\ln 2} \ln\left[\frac{\text{carbon-14 (calculated)}}{\text{carbon-14 (measured)}}\right], \text{ in years.}$$

transfer, caused by increasing $\delta^{34}S_{anhydrite}$, would result in less dilution of ^{14}C by ^{14}C-depleted carbon, and thus older ages would be calculated.

The data in table 20 show that for the Mysse Flowing Well (case 5), the calculated CO_2 outgassing is about 0.0 mmol/kg of water if $\delta^{34}S_{anhydrite}$ is 15.5 per mil rather than the extrapolated value of 11.8 per mil (table 12), which resulted in CO_2 outgassing of 1.97 mmol/kg of water. If we use this heavier value of $\delta^{34}S_{anhydrite}$, the CH_2O mass transfer is decreased from 5.00 to 0.87 mmol/kg of water. The quantity of anhydrite dissolved is decreased from 22.35 to 20.15 mmol/kg of water, and the calculated value of $\delta^{13}C$ is only 1.23 per mil lighter than the measured value.

Minor variations in many of the other modeling parameters can lead to almost identical calculated and measured values of $\delta^{13}C$. For example, if $\delta^{13}C$ of the dissolving dolomite is about 4.0 per mil rather than 2.0 per mil (case 6, table 20), the calculated $\delta^{13}C$ value is similar to the measured value. Other factors, which separately or combined would result in similar calculated and measured values of $\delta^{13}C$, are (1) lighter $\delta^{34}S_{H_2S}$, (2) variation in $\delta^{13}C_{dolomite}$, (3) variation in $\delta^{13}C_{CH_2O}$, (4) $(Ca^{2+} + Mg^{2+})/Na^{+}$ ion exchange, and (5) minor uncertainties in the analytical data. It is apparent that an almost unlimited number of minor variations in reaction parameters can lead to close agreement in calculated and measured values of $\delta^{13}C$. But, through all of these changes, the overall

mass-transfer results are changed only slightly and are similar to those of case 5 (table 20).

Of the three modeling alternatives investigated (Mg^{2+}/Na^+ ion exchange, methanogenesis, and variation in $\delta^{34}S_{anhydrite}$), only by increasing the value of $\delta^{34}S_{anhydrite}$ can all major model discrepancies be resolved. That is, by increasing $\delta^{34}S_{anhydrite}$, the calculated CO_2 outgassing is minimized, indicating the expected closed system; the calculated $\delta^{13}C$ value is heavier and similar to the measured values; and the calculated ^{14}C activity, corrected for reaction effects, is now significantly larger than the measured value, which results in more reasonable age estimates.

For example, at the Mysse Flowing Well (case 5, table 20) the calculated ^{14}C activity of 12.30 percent modern, when used with the measured ^{14}C activity (0.80 percent modern), indicates a water age in excess of 22,000 yr, which is within the reasonable range as determined from ground-water flow models (Downey, 1984). None of the other modeling alternatives considered (Mg^{2+}/Na^+ ion exchange and methanogenesis) can yield the same reasonable results.

Based on this analysis of modeling uncertainties, the single most significant factor contributing to modeling errors in the preliminary results (tables 17 and 19) is uncertainty in the sulfur-isotopic composition of dissolving anhydrite. Unfortunately, almost no data are available for $\delta^{34}S_{anhydrite}$ in the Madison aquifer. As mentioned earlier, R.G. Deike (U.S. Geological Survey, written commun., 1984) reported values of $\delta^{34}S_{anhydrite}$ in HTH No. 1 (well No. 14 in Wyoming) on flow path 4 of 12.8 and 13.9 per mil, and six values at HTH No. 2 were between 14.6 and 22.6 per mil. Claypool and others (1980) reported marine evaporites of Mississippian age with $\delta^{34}S_{anhydrite}$ in the range of 16 per mil (Upper Mississippian) to 25 per mil (Lower Mississippian). Because the $\delta^{34}S_{SO_4}$ of gypsum or anhydrite formed by oxidation of a terrigenous sulfide with subsequent precipitation of anhydrite would be lighter than that from a marine evaporite, the measured values are reasonable.

CRITERIA USED IN REACTION MODELING

In preparing the final mass-transfer models, the initial set of plausible reactants and products was virtually maintained (table 16), whereas the isotopic composition of dissolving anhydrite was varied. The following requirements were met in preparing the final mass-transfer models:

1. It was assumed that different values of $\delta^{34}S$ of anhydrite may be appropriate for different wells or springs on the same flow path.

2. The value of $\delta^{34}S_{anhydrite}$ needs to be equal to or less than the value of $\delta^{34}S_{SO_4}$ for each well or spring. That is, if there were no sulfate reduction, $\delta^{34}S_{SO_4}$ would be equal to $\delta^{34}S_{anhydrite}$.

3. The value of $\delta^{34}S_{anhydrite}$ was varied (usually increased) in order to minimize (and decrease to zero, if possible) the CO_2 gas mass transfer.

4. Only wells or springs with measured values of $\delta^{34}S_{SO_4}$ were modeled. The value of $\delta^{34}S_{H_2S}$ used was either the measured value or, if missing, the calculated value using equation 26.

5. Pyrite always was maintained as a product and goethite as a reactant. For example, in some cases in order to decrease the $\alpha_{CO_2(gas)}$ term to zero, the value of $\delta^{34}S_{anhydrite}$ was increased to the point that mass-balance calculations showed pyrite as a reactant and goethite as a product. In these cases the value of $\delta^{34}S_{anhydrite}$ was decreased until pyrite appeared as a product and FeOOH as a reactant. Pyrite is a product because of the presence of H_2S.

6. For wells or springs where the CO_2 gas and pyrite mass transfers are not sensitive to $\delta^{34}S_{anhydrite}$, the selected criterion for $\delta^{34}S_{anhydrite}$ was that the measured and calculated values of $\delta^{13}C$ agree in the final solution.

7. The value of $\delta^{13}C_{CH_2O}$ was varied between -20 to -27 per mil but usually chosen to be -25 per mil.

8. The value of $\delta^{13}C_{dolomite}$ was varied between 0.0 and 6.7 per mil but usually chosen as 2.0 per mil.

9. Magnesium/sodium ion exchange was found necessary for wells or springs along flow paths 2 and 3, where ion exchange is an important reaction, based on the analysis of the chemical trends. A variable ($Ca^{2+} + Mg^{2+})/Na^+$ ion-exchange reaction was considered in which the fraction of magnesium exchange, XMg, was adjusted in the range $0 \leqslant X\text{Mg} \leqslant 1.0$. The value of XMg equal to 1.0 corresponds to pure Mg^{2+}/Na^+ exchange, and the value of XMg equal to 0.0 represents pure Ca^{2+}/Na^+ exchange. Cases of extensive Mg^{2+}/Na^+ ion exchange indicate formation of magnesium-enriched minerals such as sepiolite or stevensite.

10. In a few cases, the magnitude of the ion-exchange term was not sufficient to increase the calculated value of $\delta^{13}C$ to a value similar to the measured value, and for these cases, the possibility of methanogenesis was investigated.

The data in table 21 are the best estimates of the mass transfers of dolomite, calcite, anhydrite, CH_2O, goethite, pyrite, ion exchange, halite, sylvite, and CO_2 gas, in mmol/kg of water, for 42 wells or springs in the Madison aquifer. The carbon- and sulfur-isotopic values used and the nature of the ion-exchange reaction considered are summarized in table 22. The calculated and measured $\delta^{13}C$ values also are compared in table 22. The few examples of dissimilarity between calculated and measured values of $\delta^{13}C$, such as the Voss well (well No. 20 in Wyoming), usually correspond to wells near recharge

TABLE 21.—*Summary of final mass-transfer model results*

[All mineral and gas mass transfers are in millimoles per kilogram of water. Negative for precipitation, positive for dissolution]

Spring or well	Spring or well number	State	Flow path	Dolomite	Calcite	Anhydrite	Organic matter	Goethite	Pyrite	Ion exchange	Halite	Sylvite	Carbon dioxide
Hanover Flowing Well	8	Mont.	1	0.04	-0.20	0.40	0.16	0.04	-0.04	0.02	-0.02	0.01	0.06
Vanek Warm Spring	9	Mont.	1	.49	-1.20	2.10	.23	.06	-.06	.02	.01	.01	.21
Landusky Spring	12	Mont.	1	2.93	-7.36	9.76	2.07	.55	-.55	.70	.27	.21	-.07
Lodgepole Warm Spring	13	Mont.	1	2.80	-7.41	10.13	2.36	.63	-.63	.89	1.56	.28	-.14
Sleeping Buffalo	18	Mont.	1	3.80	-8.26	19.73	.56	.15	-.15	4.37	4.68	.64	-.40
McLeod Warm Spring	6	Mont.	2	.27	-.95	1.12	.25	.07	-.07	-.07	-.02	-.01	-.33
Sumatra	17	Mont.	2	5.72	-12.10	13.97	3.29	.15	-.15	8.32	61.92	3.30	-.17
Keg Coulee	15	Mont.	2	7.39	-14.95	15.08	3.46	.03	-.03	5.88	53.65	3.04	-.36
Texaco C115X	16	Mont.	2	10.70	-22.52	18.59	8.34	.14	-.15	9.23	55.74	3.82	-4.70
Colstrip	21	Mont.	3	2.68	-6.35	7.97	.78	.15	-.15	2.54	1.00	1.69	-.52
Sarpy Mine	19	Mont.	3	2.18	-5.35	10.23	.72	.16	-.15	1.36	-.66	1.23	-1.06
Moore	22	Mont.	3	6.61	-16.07	17.81	4.28	.84	-.84	4.81	64.80	3.32	.29
Mysse Flowing Well	20	Mont.	3	3.54	-5.33	20.15	.87	.09	-.09	8.28	15.31	2.52	-.04
HTH No. 1	14	Wyo.	4	.96	-2.36	4.87	.36	.19	-.09	.09	1.33	.17	.01
Ranch Creek	23	Mont.	4	1.04	-2.33	5.03	.25	.07	-.07	.12	1.37	.18	-.01
Belle Creek	24	Mont.	4	1.12	-2.61	5.46	.27	.07	-.07	.10	1.40	.18	-.02
Delzer No. 1	7	S.Dak.	4	3.68	-8.81	17.62	1.97	.66	-.52	.86	-.20	.88	-2.70
Delzer No. 2	8	S.Dak.	4	3.68	-9.14	18.26	1.19	.41	-.31	.16	1.58	.29	-.02
Conoco No. 175	11	Wyo.	5	.70	-2.47	3.38	.09	.06	-.02	.72	1.69	.21	-1.26
MKM	10	Wyo.	5	.64	-3.85	9.73	.65	.29	-.16	.40	32.16	1.73	.26
Shidler	9	Wyo.	5	.97	-2.48	10.16	.47	.16	-.12	2.28	16.60	.86	-2.38
Conoco No. 44	8	Wyo.	5	1.47	-3.59	8.58	.05	.02	-.01	1.59	13.17	.60	.14
Seeley	19	Wyo.	6	.14	-.18	.15	.01	.00	.00	.01	-.01	.01	-.07
Newcastle	21	Wyo.	6	.23	-.60	.47	.01	.00	.00	.04	-.01	.03	.01
Osage	17	Wyo.	6	.14	-.41	.51	.02	.01	-.01	.03	-.02	.02	.17
Upton	15	Wyo.	6	.72	-1.87	1.86	.22	.06	-.06	.05	-.04	.04	.00
Devils Tower	13	Wyo.	6	.60	-1.62	2.27	.20	.05	-.05	.04	.03	.02	-.21
Voss	20	Wyo.	7	.25	-.71	.42	.01	.00	.00	.03	.01	.03	.04
Self	22	Wyo.	7	.33	-1.00	.88	.02	.01	-.01	.03	.01	.04	-.41
JBJ	18	Wyo.	7	-.04	-1.77	2.16	.20	.05	-.05	.17	.10	.11	-1.88
Evans Plunge	10	S.Dak.	7	.74	-2.64	5.93	.44	.12	-.12	.44	2.83	.27	-.42
Cascade Spring	9	S.Dak.	7	2.48	-7.33	16.91	2.42	.65	-.65	.19	.75	.12	-.90
McNenney	2	S.Dak.	8	.18	-.31	.91	.03	.01	-.01	-.06	-.03	-.02	.20
Kosken	1	S.Dak.	8	1.17	-3.35	7.10	.30	.08	-.08	.05	.84	.23	-.93
Philip	19	S.Dak.	8	1.58	-4.34	6.98	.86	.23	-.23	.06	.43	.13	-.79
Midland	24	S.Dak.	8	1.91	-5.00	8.66	.88	.23	-.24	.16	.54	.19	-1.12
Murdo	25	S.Dak.	8	1.87	-4.70	9.19	.71	.21	-.19	.19	1.38	.28	-1.18
Hilltop Ranch	22	S.Dak.	8	2.36	-7.75	12.70	.63	.18	-.17	-.36	4.18	.28	.49
Prince	26	S.Dak.	8	2.61	-6.47	12.94	1.07	.29	-.28	.16	2.59	.46	-1.70
Hamilton	21	S.Dak.	8	2.90	-7.15	13.56	.30	.11	-.06	.14	.97	.33	-.40
Eagle Butte	23	S.Dak.	8	3.72	-8.22	13.58	.33	.12	-.07	.66	1.06	.66	-.69
Dupree	20	S.Dak.	8	3.07	-8.17	14.74	.53	.13	-.13	1.22	2.13	1.20	.00

areas where modeling is particularly sensitive to the starting $\delta^{13}C$ conditions. As previously discussed, the similarity in calculated and measured values of $\delta^{13}C$ was a modeling requirement and dependent on the choice of modeling parameters.

Although methanogenesis was investigated for many of the wells or springs, none of the final modeling results included this process. The calculated (adjusted for reaction) ^{14}C content and measured ^{14}C content (percent modern) also are included in table 22 along with an age estimate calculated by the following equation:

$$\Delta t = \frac{5730}{\ln 2} \ln \left[\frac{^{14}C_{calc}}{^{14}C_{meas}} \right], \quad (53)$$

where Δt is the travel time, in years, since the ground water became isolated from the soil ^{14}C reservoir (Wigley and Muller, 1981), and $^{14}C_{calc}$ and $^{14}C_{meas}$ are in percent modern (table 22).

TABLE 22.—*Summary of final model parameters and carbon-isotope results*

[Calculated carbon-14 assumes no radioactive decay]

Spring or well	Spring or well number	State	Flow path	$\delta^{34}S$ anhydrite (per mil)	$\delta^{13}C$ (per mil)		Ion exchange (X_{Mg})	$\delta^{13}C$ (per mil)		Carbon-14 (percent modern)		Adjusted age (years)
					Organic matter	Dolomite		Calculated	Measured	Calculated	Measured	
Hanover Flowing Well	8	Mont.	1	17.10	-25.00	2.00	0.0	-5.84	-5.32	49.09	25.40	5,446
Vanek Warm Spring	9	Mont.	1	17.10	-25.00	1.00	.0	-5.19	-5.18	37.38	29.30	2,013
Landusky Spring	12	Mont.	1	17.10	-25.00	.00	.0	-7.33	-7.46	5.66	--	--
Lodgepole Warm Spring	13	Mont.	1	20.00	-25.00	2.00	.0	-7.05	-7.04	5.45	28.00	modern
Sleeping Buffalo	18	Mont.	1	21.90	-25.00	.00	.0	-3.22	-3.22	3.63	4.20	modern
McLeod Warm Spring	6	Mont.	2	17.00	-25.00	2.00	.0	-10.15	-7.57	45.29	52.50	modern
Sumatra	17	Mont.	2	15.00	-20.00	4.00	.6	-3.72	-3.61	2.92	--	--
Keg Coulee	15	Mont.	2	14.70	-20.00	5.00	1.0	-1.85	-1.68	1.66	1.00	[1]4,185
Texaco C115X	16	Mont.	2	14.70	-20.00	5.00	1.0	-3.19	--	.15	--	--
Colstrip	21	Mont.	3	14.00	-20.00	4.00	1.0	-2.64	-2.67	10.97	--	--
Sarpy Mine	19	Mont.	3	13.00	-20.00	4.00	.8	-2.41	-2.33	12.75	3.30	11,173
Moore	22	Mont.	3	14.00	-20.00	6.70	1.0	-2.47	-2.40	2.43	1.60	3,448
Mysse Flowing Well	20	Mont.	3	15.50	-25.00	4.00	.0	-2.21	-2.34	12.30	.80	22,588
HTH No. 1	14	Wyo.	4	10.30	-25.00	1.20	.0	-6.66	-6.63	30.59	12.70	7,266
Ranch Creek	23	Mont.	4	10.90	-25.00	.90	.0	-6.18	-6.17	30.61	10.00	9,247
Belle Creek	24	Mont.	4	10.90	-25.00	1.00	.0	-6.01	-6.02	28.72	9.50	9,147
Delzer No. 1	7	S.Dak.	4	12.60	-27.00	.00	.0	-4.58	-4.60	1.99	4.60	modern
Delzer No. 2	8	S.Dak.	4	13.60	-22.00	4.00	.0	-2.60	-2.61	5.49	2.80	5,560
Conoco No. 175	11	Wyo.	5	7.90	-25.00	2.50	.0	-6.29	-6.23	34.84	13.90	7,597
MKM	10	Wyo.	5	7.90	-20.00	2.00	.0	-11.59	-4.66	33.08	2.60	21,026
Shidler	9	Wyo.	5	7.90	-25.00	2.00	.0	-4.69	--	25.32	6.20	11,631
Conoco No. 44	8	Wyo.	5	8.30	-25.00	4.00	.0	-5.10	-5.14	27.79	1.80	22,624
Seeley	19	Wyo.	6	9.50	-25.00	2.00	.0	-8.86	-7.82	51.80	61.40	modern
Newcastle	21	Wyo.	6	9.50	-25.00	2.00	.0	-8.77	-10.40	50.14	46.20	677
Osage	17	Wyo.	6	9.50	-25.00	2.00	.0	-9.33	-10.00	51.68	54.70	modern
Upton	15	Wyo.	6	9.50	-25.00	.50	.0	-8.19	-8.20	40.09	14.70	8,294
Devils Tower	13	Wyo.	6	9.50	-25.00	2.00	.0	-7.79	-6.80	41.85	59.00	modern
Voss	20	Wyo.	7	10.00	-25.00	2.00	.0	-10.17	-7.26	50.62	44.50	1,065
Self	22	Wyo.	7	10.00	-25.00	2.00	.0	-9.28	-6.60	48.68	31.20	3,677
JBJ	18	Wyo.	7	10.00	-25.00	2.00	.0	-9.92	-4.24	53.57	4.80	19,942
Evans Plunge	10	S.Dak.	7	10.00	-25.00	.00	.0	-9.67	-9.70	38.04	28.50	2,386
Cascade Spring	9	S.Dak.	7	9.00	-25.00	1.00	.0	-9.08	-9.10	13.72	19.40	modern
McNenney	2	S.Dak.	8	11.00	-25.00	2.00	.0	-9.51	-11.50	53.02	79.60	modern
Kosken	1	S.Dak.	8	12.40	-25.00	2.00	.0	-6.14	-6.20	28.01	7.80	10,568
Philip	19	S.Dak.	8	12.90	-25.00	2.00	.0	-7.20	-7.20	21.49	2.80	16,847
Midland	24	S.Dak.	8	13.70	-25.00	2.00	.0	-6.18	-6.20	17.31	2.40	16,332
Murdo	25	S.Dak.	8	13.30	-25.00	2.00	.0	-5.52	-5.50	18.40	3.20	14,461
Hilltop Ranch	22	S.Dak.	8	12.30	-25.00	2.00	.0	-6.72	-6.63	15.35	4.60	9,960
Prince	26	S.Dak.	8	14.30	-25.00	2.00	.0	-4.73	-4.72	10.26	4.00	7,784
Hamilton	21	S.Dak.	8	15.00	-25.00	2.00	.0	-3.59	-3.50	12.01	2.40	13,310
Eagle Butte	23	S.Dak.	8	15.80	-25.00	2.00	.0	-2.35	-2.40	8.53	2.20	11,203
Dupree	20	S.Dak.	8	16.00	-25.00	4.90	.0	-2.07	-2.05	10.29	2.80	10,763

[1]An adjusted carbon-14 age of 23,000 years is found if H_2S is introduced by crossformational leakage (see text).

SELECTION OF MODELING PARAMETERS FOR EACH FLOW PATH

FLOW PATH 1

As modeling progressed, it became evident that the five wells and springs selected for flow path 1 do not approximate a single flow path but are instead all relatively young waters affected primarily by varying quantities of anhydrite dissolution and local recharge conditions. The Hanover Flowing Well (well No. 8 in Montana) appears to be nearest to recharge-water composition, with only 0.04 mmol of anhydrite dissolved per kilogram of water. The CO_2 outgassing is about zero and is insensitive to uncertainties in $\delta^{34}S_{anhydrite}$. As the dolomite and CH_2O

mass transfers are about zero (table 21) at the Hanover Flowing Well, the calculated value of $\delta^{13}C$ is insensitive to values selected for $\delta^{13}C_{dolomite}$ and $\delta^{13}C_{CH_2O}$. The small differences in calculated and measured $\delta^{13}C$ probably are due to differences in the $\delta^{13}C$ value of the recharge area.

The Vanek Warm Spring water (spring No. 9 in Montana) is similar to water from the Hanover Flowing Well except that more anhydrite has dissolved and the dedolomitization reaction has begun. The CO_2 outgassing is again small and insensitive to $\delta^{34}S_{anhydrite}$. The previously defined value of $\delta^{34}S_{anhydrite}$ (17.10 per mil) was used (table 12) for both the Hanover Flowing Well and Vanek Warm Spring. The calculated and measured $\delta^{13}C$ agree if $\delta^{13}C$ of the reacting dolomite is 1.00 per mil rather than 2.00 per mil.

Landusky Spring (spring No. 12 in Montana) is approximately half-saturated with anhydrite, and the mass-transfer calculations indicate a moderate dedolomitization reaction (table 21). The CO_2 outgassing term is about zero if 17.10 per mil is again used for $\delta^{34}S_{anhydrite}$. The calculated value of $\delta^{13}C$ agrees with the measured value if $\delta^{13}C_{dolomite}$ is about 0.0. The spring water is affected by moderate ion exchange (0.70 mmol/kg of water) and significant sulfate reduction (2.07 mmol of CH_2O oxidized per kilogram of water).

The two remaining waters along flow path 1, Lodgepole Warm Spring (spring No. 13 in Montana) and Sleeping Buffalo (well No. 18 in Montana), probably dissolve isotopically heavier anhydrite. Using 17.10 per mil for $\delta^{34}S_{anhydrite}$, the preliminary modeling indicated 0.9 and 2.9 mmol of CO_2 outgassing per kilogram of water for Lodgepole Warm Spring and Sleeping Buffalo well, respectively, which is unlikely. Furthermore, the calculated value of $\delta^{13}C$ was too light at Sleeping Buffalo well, consistent with excessive calculated sulfate reduction and CH_2O oxidation. The adjustment procedure was as follows: First $\delta^{34}S_{anhydrite}$ was increased to minimize the CO_2 outgassing term. Estimated values of 20.0 and 21.9 per mil were used for $\delta^{34}S_{anhydrite}$ at Lodgepole Warm Spring and Sleeping Buffalo well, respectively.

At Lodgepole Warm Spring, CO_2 outgassing changes to ingassing of 0.09 mmol/kg of water if $\delta^{34}S_{anhydrite}$ is 21.0 per mil rather than 20.0 per mil (corresponding to 0.14 mmol of CO_2 outgassing per kilogram of water). Considering the magnitude of the uncertainties in total inorganic carbon in the recharge water, further refinement of the $\delta^{34}S_{anhydrite}$ parameter is not warranted at Lodgepole Warm Spring. The calculated value of $\delta^{13}C$ is similar to the measured value at Lodgepole Warm Spring if dolomite with $\delta^{13}C$ of 2.0 per mil and CH_2O with $\delta^{13}C$ of -25.0 per mil are reacting.

The CO_2 outgassing at Sleeping Buffalo well cannot be decreased to zero without using $\delta^{34}S_{anhydrite}$ values greater than $\delta^{34}S_{SO_4}$ (21.95 per mil). The value of 21.90 per mil for $\delta^{34}S_{anhydrite}$ was selected, resulting in 0.40 mmol of CO_2 outgassing per kilogram of water, which again could be due to uncertainties in total inorganic carbon of the recharge water. Using 21.9 per mil for $\delta^{34}S_{anhydrite}$, the measured $\delta^{13}C$ at Sleeping Buffalo well is then matched if $\delta^{13}C_{CH_2O}$ is -25.0 per mil and $\delta^{13}C_{dolomite}$ is 0.0 per mil.

The ^{14}C age estimates are summarized in table 22. All waters along flow path 1 appear to be younger than about 6,000 yr. The Hanover Flowing Well and Vanek Warm Spring water ages are relatively well defined because of the smaller mass transfer involved in calculating the adjusted ^{14}C content. No ^{14}C data were available for Landusky Spring. Water from Lodgepole Warm Spring is likely contaminated with a modern source, because the measured ^{14}C value is significantly larger than the calculated value. This indication of a modern component in water from Lodgepole Warm Spring is further supported by a tritium content of 31.8 TU (table 11).

The importance of reaction corrections in ^{14}C age dating is demonstrated by water from the Sleeping Buffalo well, which has a relatively small ^{14}C content (4.2 percent modern) that is equivalent to an unadjusted ^{14}C age (assuming a recharge water of 50 percent modern ^{14}C) in excess of 20,000 yr. After correction for extensive dedolomitization, the age is, within the uncertainties of the calculation, virtually modern. The short residence time along flow path 1 in Montana, caused by a local cell of recharge-discharge, results in water of virtually modern age at the Sleeping Buffalo well (Downey, 1984).

FLOW PATH 2

The McLeod Warm Spring (spring No. 6 in Montana) is located nearest the recharge area of flow path 2, and the water composition indicates that only minor reactions have occurred. Water from this spring is similar in composition to the average recharge water along flow path 2, except that an additional 1.1 mmol of anhydrite per kilogram of water have dissolved. The calculated mass transfer is not sensitive to $\delta^{34}S_{anhydrite}$ or reasonable estimates of $\delta^{13}C$ for CH_2O and dolomite. For example, using 14.7 per mil for $\delta^{34}S_{anhydrite}$, -25.0 for $\delta^{13}C_{CH_2O}$, and 2.0 per mil for $\delta^{13}C_{dolomite}$, the calculated value of $\delta^{13}C$ is -10.47 per mil. Increasing $\delta^{34}S_{anhydrite}$ to 17.0 per mil increases the calculated value of $\delta^{13}C$ to -10.15 per mil. If $\delta^{34}S_{anhydrite}$ is increased to 17.5 per mil (approximately that of dissolved SO_4^{2-} at McLeod Warm Spring) and $\delta^{13}C_{dolomite}$ is increased to 4.0 per mil, the calculated value of $\delta^{13}C$ is increased to -9.81 per mil. The difference in calculated and measured $\delta^{13}C$ probably is due to differences in $\delta^{13}C$ of the recharge water, as the measured $\delta^{13}C$ is -7.57 per mil.

The recharge waters used to define the average recharge of flow path 2 (Bozeman Fish Hatchery, well No. 4 in Montana; Big Timber Fish Hatchery, spring No. 7 in Montana) have a considerable variation in $\delta^{13}C$ of -8.98 and -14.11 per mil, respectively. The calculations along flow path 2 included the average $\delta^{13}C$ of -11.55 per mil for the recharge area. The final values used at McLeod Warm Spring were 17.00 per mil for $\delta^{34}S_{anhydrite}$, -25.0 per mil for $\delta^{13}C_{CH_2O}$, and 2.0 per mil for $\delta^{13}C_{dolomite}$. The calculated ^{14}C is not a function of uncertainty in the $\delta^{34}S$ and $\delta^{13}C$ values and indicates that water from McLeod Warm Spring is virtually modern.

The remaining three wells along flow path 2—Sumatra (well No. 17 in Montana), Keg Coulee (well No. 15 in Montana), and Texaco C115X (well No. 16 in Montana)—pose far more difficult problems in interpretation of chemical reactions. Because of the presence of significant concentrations of H_2S in these waters (as much as 132 mg/L at Texaco C115X), pyrite would be expected to precipitate as a product if it was included in the model. This places a severe constraint on modeling because the $\delta^{34}S_{anhydrite}$ cannot be much heavier than the estimated flow-path value of 14.70 per mil without resulting in a calculated dissolution of pyrite. But if a value of $\delta^{34}S_{anhydrite}$ of 14.70 per mil is used, the calculated values of $\delta^{13}C$ are very light (ranging from -12 to -15 per mil) when the measured values are -1.68 and -3.61 per mil, respectively, at Keg Coulee and Sumatra. No carbon-isotope data are available for Texaco C115X, but because of its close proximity to Sumatra and Keg Coulee, similar values are expected.

In order to calculate heavy $\delta^{13}C$ values at these three wells, it was necessary to assume an additional sink for magnesium so that additional dissolution of dolomite would increase the calculated $\delta^{13}C$ values. For modeling purposes, this was done in the form of Mg^{2+}/Na^{+} exchange, although, as discussed earlier, other authigenic magnesium-silicate minerals may be forming along flow path 2. Methanogenesis also was considered along flow path 2, but it had only a minor effect on the calculated value of $\delta^{13}C$. As an example, some of the modeling parameters investigated for Sumatra are shown in table 23 along with the resulting calculated value of $\delta^{13}C$.

Only by including substantial Mg^{2+}/Na^{+} exchange ($XMg = 0.6$) and relatively heavy sources of ^{13}C (-20.00 per mil for CH_2O and 4.00 per mil for dolomite) was the calculated $\delta^{13}C$ value at Sumatra similar to the measured value. Even more extensive magnesium ion exchange ($XMg = 1.0$) and a $\delta^{13}C$ value for dolomite of 5.00 per mil are required to calculate heavy values of $\delta^{13}C$ at Keg Coulee and Texaco C115X (table 22). The calculated dolomite mass transfer was significantly increased in obtaining the heavy values. For example, without the added magnesium sink, only 1.51 mmol of dolomite is dissolved per kilogram of water at Keg Coulee (table 17), but by adding Mg^{2+}/Na^{+} ion exchange, dissolution of 7.39 mmol of dolomite per kilogram of water is indicated (table 21).

Although the increased dolomite dissolution resulted in reasonable agreement between calculated and measured values of $\delta^{13}C$, the calculated ^{14}C content decreased significantly. Without Mg^{2+}/Na^{+} ion exchange, the calculated ^{14}C age at Keg Coulee (table 19) is about 23,000 yr (but there is little agreement with the measured value of $\delta^{13}C$). With the magnesium sink, the additional dolomite dissolution at Keg Coulee decreased the calculated ^{14}C age to about 4,000 yr (table 22), but the calculated and measured values of $\delta^{13}C$ showed agreement.

Based on distance from the recharge area in central Montana, the waters are expected to be old along flow path 2, and the 23,000-yr age for water at Keg Coulee is not unreasonable. Other possibilities that can result in relatively old water with a heavy calculated value of $\delta^{13}C$ were considered. One is that the large concentrations of dissolved H_2S along flow path 2 were introduced by leakage from other formations and are not the product of in situ sulfate reduction. To investigate this possibility, the mass-balance calculations were repeated, but H_2S was treated as a separate phase. Significant improvements in the modeling results were found, but an adjustment was required for the total inorganic carbon of the recharge water along flow path 2. If (1) the water recharging flow path 2 contains about 1.5 mmol of CO_2 per kilogram of water more than that at Big Timber Fish Hatchery and Bozeman Fish Hatchery (average total inorganic carbon of 3.8 mmol/kg of water); (2) the H_2S found along flow path 2 formed in other formations and migrated into the Madison aquifer; and (3) the $\delta^{13}C_{dolomite}$ value along flow path 2 is 4.0 per mil, then there is similarity between the calculated and measured $\delta^{13}C$ values of the water. The calculated value of ^{14}C is then 16.5 percent modern, giving an age of 23,000 yr at Keg Coulee.

Measured ^{14}C data at the Sumatra and Texaco C115X wells are not available because organic-corrosion-prevention additives were present in the wells. Calculated values are 27.1 and 9.0 percent modern, respectively, for the same assumptions as at Keg Coulee. In addition to resulting in more reasonable age estimates along flow path 2, the calculations indicate that $\delta^{34}S_{anhydrite}$ varies between 18.0 and 18.6 per mil for Sumatra, Keg Coulee, and Texaco C115X; these values are similar to the reported values for Mississippian evaporite deposits (Claypool and others, 1980). The hypothesis of an extra-formational source for the H_2S along flow path 2 results in reasonably good agreement with the analytical data.

TABLE 23.—*Summary of selected modeling parameters evaluated at Sumatra (well No. 17 in Montana) on flow path 2*

[X_{CO_2}, fraction of carbon dioxide gas in carbon dioxide-methane mixture; X_{Mg}, fraction of magnesium ion exchange]

$\delta^{34}S$ anhydrite (per mil)	Ion exchange (X_{Mg})	Gas composition (X_{CO_2})	$\delta^{13}C$ (per mil)					Pyrite dissolution (+) or precipitation (-)
			Methane	Organic matter	Dolomite	Calculated	Measured	
17.0	0.0	1.0	--	-25.0	2.0	-11.5	-3.61	+
14.7	.0	1.0	--	-25.0	2.0	-15.8	-3.61	-
16.0	.0	1.0	--	-25.0	2.0	-13.4	-3.61	+
15.0	.0	1.0	--	-25.0	2.0	-15.3	-3.61	-
15.0	1.0	1.0	--	-25.0	2.0	-4.3	-3.61	-
15.0	.5	1.0	--	-25.0	4.0	-5.6	-3.61	-
15.0	.5	.9	-80.0	-25.0	4.0	-5.6	-3.61	-
15.0	1.0	1.0	--	-20.0	4.0	-1.9	-3.61	-
15.0	.6	1.0	--	-20.0	4.0	-3.7	-3.61	-

FLOW PATH 3

Problems in modeling reactions along flow path 3 are similar to those of flow path 2 except that concentrations of H_2S in most waters are less. As along flow path 2, it was necessary to resort to sinks for magnesium (treated as Mg^{2+}/Na^+ exchange), to isotopically heavy dolomite ($\delta^{13}C_{dolomite}$ of 4.0 per mil), and to relatively heavy organic matter ($\delta^{13}C_{CH_2O}$ of −20 per mil) in order to obtain the calculated values of $\delta^{13}C$. In minimizing the CO_2 mass transfer, values of $\delta^{34}S_{anhydrite}$ of 13.0 to 15.5 per mil were used rather than the estimated value of 11.8 per mil (table 12).

The measured value of $\delta^{13}C$ (−2.67 per mil) at Colstrip (well No. 21 in Montana) is almost matched if $\delta^{34}S_{anhydrite}$ is 14.0 per mil, pure Mg^{2+}/Na^+ exchange is included, $\delta^{13}C_{CH_2O}$ is −20.0 per mil, and $\delta^{13}C_{dolomite}$ is 4.0 per mil. No data are available for the measured ^{14}C, but the adjusted ^{14}C is 10.97 percent modern. If the measured ^{14}C of Colstrip is similar to that at the nearby Sarpy Mine well (well No. 19 in Montana) (3.30 percent modern), the water at Colstrip is at least 10,000 yr old.

Modeling of the Sarpy Mine well yields results similar to those at Colstrip. The measured value of $\delta^{13}C$ (−2.33 per mil) is almost matched if $\delta^{34}S_{anhydrite}$ is 13 per mil, predominantly Mg^{2+}/Na^+ ion exchange (XMg = 0.8) is included, $\delta^{13}C_{CH_2O}$ is −20 per mil, and $\delta^{13}C_{dolomite}$ is 4.0 per mil. The calculated ^{14}C age is about 11,000 yr.

The Moore Flowing Well (well No. 22 in Montana) posed the most difficult modeling problems along flow path 3. The CO_2 mass transfer was minimized using a $\delta^{34}S_{anhydrite}$ value of 14.0 per mil. Taking this value, and including pure Mg^{2+}/Na^+ exchange, a $\delta^{13}C_{CH_2O}$ value of −20.0 per mil, and a $\delta^{13}C_{dolomite}$ value of 4.0 per mil, the calculated value of $\delta^{13}C$ was −4.40 per mil, which is similar to the measured value of −2.40 per mil. By varying the $\delta^{13}C$ of dolomite, but holding the other parameters constant, a value of 6.70 per mil for $\delta^{13}C_{dolomite}$ is required to match the measured value of $\delta^{13}C$. This probably is unrealistic and indicates further uncertainties in the modeling exercise. It is noted that the Moore Flowing Well has a relatively large concentration of dissolved H_2S (table 8) and may be affected by leakage of H_2S from other formations, as was suggested earlier for waters along flow path 2. A further indication of problems in modeling the Moore Flowing Well is a calculated ^{14}C age of about 3,000 yr in an area where the age of the water likely ranges from 10,000 to 20,000 yr old.

Contrary to the previous three wells modeled along flow path 3, the Mysse Flowing Well (well No. 20 in Montana) is relatively less complicated to model and was treated in the same fashion as wells along flow path 1. The CO_2 mass transfer is minimized at Mysse if $\delta^{34}S_{anhydrite}$ is near 15.5 per mil, and a calculated $\delta^{13}C$ value similar to the measured value is determined if $\delta^{13}C_{dolomite}$ is 4.0 per mil and $\delta^{13}C_{CH_2O}$ is −25.0 per mil. No Mg^{2+}/Na^+ exchange was required. The calculated ^{14}C age is about 23,000 yr, similar to that indicated for flow path 2.

FLOW PATH 4

Most of the wells along flow path 4 were modeled using the dedolomitization reaction and by making small adjustments to values of $\delta^{34}S$ of reacting anhydrite. The estimated flow-path value of $\delta^{34}S_{anhydrite}$ along flow path 4 used in the preliminary modeling was 10.3 per mil. Values between 10.3 and 13.6 per mil were found to minimize the CO_2 outgassing term. Ion exchange is not an important reaction along flow path 4.

The CO_2 outgassing term is not sensitive to $\delta^{34}S_{anhydrite}$ at HTH No. 1 (well No. 14 in Wyoming), and similar calculated and measured $\delta^{13}C$ values were determined by changing $\delta^{13}C_{dolomite}$ to 1.2 per mil. Calculated and measured values of $\delta^{13}C$ at Ranch Creek (well No. 23 in Montana) were matched with a $\delta^{34}S_{anhydrite}$ of 10.9 per mil, a $\delta^{13}C_{CH_2O}$ of −25.00 per mil, and a $\delta^{13}C_{dolomite}$ of 0.90 per mil. Belle Creek (well No. 24 in Montana) is located within 13 miles of Ranch Creek, and very similar modeling results were obtained there. The values for $\delta^{34}S_{anhydrite}$, $\delta^{13}C_{CH_2O}$, and $\delta^{13}C_{dolomite}$ were 10.9, −25.0, and 1.0 per mil, respectively.

The calculated ^{14}C ages of Belle Creek and Ranch Creek differ by only 100 yr (9,200 versus 9,100 yr) even though the measured and adjusted ^{14}C contents differ somewhat.

Delzer No. 1 (well No. 7 in South Dakota) and Delzer No. 2 (well No. 8 in South Dakota) are very near each other, yet in this case the models do not agree. Reasonable results were found for Delzer No. 2 if $\delta^{34}S_{anhydrite}$ is 13.6 per mil, $\delta^{13}C_{CH_2O}$ is −22.0 per mil, and $\delta^{13}C_{dolomite}$ is 4.0 per mil, resulting in a ^{14}C age of 5,560 yr.

The data for Delzer No. 2 are considered more reliable than those for Delzer No. 1. The unusually low flow at Delzer No. 1 apparently resulted in collection of a less reliable sample, as evidenced by a 20 °C temperature difference between the reported bottom-hole and wellhead temperatures and the observed evolution of CO_2 gas. A comparison of the analytical data for Delzer No. 1 and No. 2 shows a significant difference in total inorganic carbon for the two wells, a result consistent with the field observations. The modeling results also were consistent with the field observations; a large transfer of CO_2 gas from the system was required regardless of the value chosen for $\delta^{34}S_{anhydrite}$. The modeling results in tables 21 and 22 are based on the reported analytical data and show what modeling parameters were required to match the measured $\delta^{13}C$ value. These results indicate a modern age for the waters at Delzer No. 1, a result inconsistent with the conceptual model of the flow system. Results in better agreement with the conceptual model of the flow system are obtained for Delzer No. 1 if a value for total inorganic carbon similar to the value measured for Delzer No. 2 is used.

FLOW PATH 5

Waters along flow path 5 are unusual in that they have the lightest values of $\delta^{34}S_{SO_4}$ in the Madison system (8.2 to 8.6 per mil with an extrapolated lower limit of 7.90 per mil). Each well on flow path 5 posed special modeling problems, particularly in determining modeling alternatives that match the measured, relatively heavy values of $\delta^{13}C$.

The preliminary results in table 17 are based on a model that does not incorporate Mg^{2+}/Na^{+} exchange. These results show no net dissolution along the flow path to Conoco No. 175 (well No. 11 in Wyoming). Because there is no mass transfer of dolomite, the relatively heavy $\delta^{13}C$ value of −6.23 per mil cannot be calculated even with a $\delta^{13}C_{CH_2O}$ value of −20.00. Thus, it was necessary to propose either a magnesium sink or methanogenesis in modeling Conoco No. 175. In addition, it was determined that the sulfur-isotopic composition of dissolving anhydrite could not be heavier than 8.2 per mil or else dissolution of pyrite would be predicted. By increasing the $\delta^{34}S_{anhydrite}$ value from 7.9 to 8.2 per mil, the quantity of CO_2 outgassed is decreased by only 0.03 mmol/kg of water. Thus, Conoco No. 175 poses an additional problem in the carbon balance. Differences in total inorganic carbon in the recharge area are suspected. Using the average flow-path value of $\delta^{34}S_{anhydrite}$ (7.9 per mil), Conoco No. 175 has been modeled two ways: (1) by assuming methanogenesis, and (2) by assuming a magnesium sink.

The model incorporating methanogenesis includes Ca^{2+}/Na^{+} exchange, dedolomitization, and outgassing of a gas containing 14 percent of CH_4 ($\delta^{13}C_{CH_4}$ of −80.00 per mil). If, in addition, $\delta^{13}C_{CH_2O}$ and $\delta^{13}C_{dolomite}$ have values of −25.00 and 2.00 per mil respectively, then the measured $\delta^{13}C$ value is almost matched. Using the model incorporating methanogenesis, the calculated ^{14}C age is 10,300 yr. Conoco No. 175 also can be modeled by assuming there that there is a sink for magnesium. Treating this as pure Mg^{2+}/Na^{+} exchange, the measured $\delta^{13}C$ value at Conoco No. 175 is almost matched if $\delta^{13}C_{CH_2O}$ is −25.0 per mil and $\delta^{13}C_{dolomite}$ is 2.5 per mil. The calculated dissolution of an additional 0.70 mmol/kg of dolomite per kilogram of water dilutes the ^{14}C reservoir somewhat, leading to a slightly younger calculated age (7,600 yr).

Of the two modeling alternatives, the choice incorporating pure magnesium ion exchange is preferred. Methanogenesis is not thought to be an important mechanism in the presence of dissolved sulfate (3.47 mmol of sulfate per kilogram of water), and small concentrations of CH_4 (less than 1.88×10^{-5} mmol/kg of water) have been measured in the Madison aquifer system (Busby and others, 1983).

Even more difficult problems are encountered in modeling the MKM well (well No. 10 in Wyoming) on flow path 5. Using the value of 7.9 per mil for $\delta^{34}S_{anhydrite}$, dissolution of 0.26 mmol of CO_2 gas per kilogram of water was computed. This can be decreased to the expected zero value (closed system) if the $\delta^{34}S_{anhydrite}$ value is 7.4 per mil. It is, however, more likely that the carbon imbalance is due to the difference in total inorganic carbon in the recharge water for the MKM well. Using −25.0 per mil for $\delta^{13}C_{CH_2O}$, 2.0 per mil for $\delta^{13}C_{dolomite}$, and 7.9 per

mil for $\delta^{34}S_{anhydrite}$, the calculated value of $\delta^{13}C$ (−12.27 per mil) was significantly lighter than the measured value (−4.66 per mil). Furthermore, only 0.4 mmol of ion exchange per kilogram of water are calculated, so that even with pure Mg^{2+}/Na^{+} ion exchange, and using heavy CH_2O and dolomite (−20.0 and 4.0 per mil, respectively), the calculated value of $\delta^{13}C$ only increased to −9.17 per mil compared with the value of −11.59 per mil in the preliminary model results (table 19). Thus, either there are serious errors in the analytical data for MKM or else the process of methanogenesis needs to be considered as a cause of the measured heavy value of $\delta^{13}C$. But in order to compute significant methanogenesis, the carbon balance needs to be corrected in order for the mass balance to calculate a net loss of gas. Because the magnitude of the required adjustments to the carbon balance are unknown, the mass transfer to the MKM well cannot be finalized, and thus the preliminary results have been retained in the final mass-transfer results (table 21). Because most of the mass transfer is accounted for by the dedolomitization reaction, there probably are no large errors in the calculated ^{14}C age, which, based on the preliminary results, is about 21,000 yr.

A measured $\delta^{13}C$ value is not available for the Shidler well (well No. 9 in Wyoming), but it is assumed to be in the range of −4.0 to −6.0 per mil, similar to that for the other wells along flow path 5. The large, calculated CO_2 outgassing is probably due to uncertainties in the composition of recharge water. Using 7.9 per mil for $\delta^{34}S_{anhydrite}$, −25.0 per mil for $\delta^{13}C_{CH_2O}$, 2.0 per mil for $\delta^{13}C_{dolomite}$, and Ca^{2+}/Na^{+} exchange, a reasonable value of $\delta^{13}C$ (−4.69 per mil) was calculated for the Shidler well.

The Conoco No. 44 well (well No. 8 in Wyoming) was modeled using 8.30 per mil for $\delta^{34}S_{anhydrite}$, Ca^{2+}/Na^{+} ion exchange, and −25.0 and 4.0 per mil for $\delta^{13}C_{CH_2O}$ and $\delta^{13}C_{dolomite}$, respectively. Some CO_2 dissolution was calculated but probably is due to differences in recharge waters. If the carbon balance is adjusted to obtain a system closed to CO_2, lighter values of $\delta^{13}C_{dolomite}$ can be included in the model. Carbon-dioxide dissolution was treated as input of soil gas using the average calculated recharge-area soil gas $\delta^{13}C$ value (table 18) of −20.24 per mil for flow path 5. If the carbon balance were adjusted to calculate zero CO_2 mass transfer, no net input of −20.24 per mil soil CO_2 gas would be included in the ^{13}C calculation and a lighter $\delta^{13}C_{dolomite}$ would be indicated.

FLOW PATH 6

The water along flow path 6 has the least quantities of mass transfer of the entire Madison aquifer. This can probably be attributed to rapid ground-water flow on the west side of the Black Hills, which has removed most of the reactants, CH_2O, and anhydrite, thereby limiting the driving force for reaction. If this is the case, a relatively younger age would be expected for water along flow path 6.

Using the value of 9.5 per mil for $\delta^{34}S_{anhydrite}$ (table 12), all wells along flow path 6 are found to be virtually closed to CO_2 gas. Ion exchange does not occur and minor sulfate reduction is calculated only for the wells at Upton (well No. 15 in Wyoming) and Devils Tower (well No. 13 in Wyoming). Because the dolomite mass transfer also is very small, particularly at Seeley (well No. 19 in Wyoming), Newcastle (well No. 21 in Wyoming), and Osage (well No. 17 in Wyoming), there is only a minor carbon source, and thus the calculated $\delta^{13}C$ value depends significantly on the starting (recharge water) $\delta^{13}C$ value. Calculated and measured $\delta^{13}C$ values differ by about 1.00 per mil, (except at Upton), but this probably is not an indication of mass-transfer errors.

The calculated ^{14}C age at Upton is about 8,000 yr, and its water is the oldest along flow path 6. Three other waters (Seeley, Osage, and Devils Tower) probably are less than 1,000 yr old but cannot be dated more closely because the measured ^{14}C value is slightly larger than the calculated value. Tritium concentrations range from 0.0 to 0.8 TU along flow path 6, so a large modern component is not expected. The Newcastle well has 0.10 TU, and the corrected ^{14}C age there is about 700 yr.

FLOW PATH 7

Reactions along flow path 7 are similar to those along flow path 6, but with somewhat more reaction progress. The calculated $\delta^{13}C$ values at three of the wells (Voss, well No. 20 in Wyoming; Self, well No. 22 in Wyoming; and JBJ, well No. 18 in Wyoming) could not be matched closely to the measured $\delta^{13}C$ values, probably because of relatively light ^{13}C in the recharge area. Rhoads Fork (well No. 4 in South Dakota) has been used as the recharge water for flow path 7 and has a measured $\delta^{13}C$ value of −11.0 per mil. A recharge water with a $\delta^{13}C$ value of about −8.0 per mil is indicated by the modeling results of table 21. Waters at Voss and Self evolved by relatively slight dedolomitization (0.42 and 0.88 mmol of anhydrite dissolved per kilogram of water). Neither water is sensitive to variation in $\delta^{34}S_{anhydrite}$, and both appear, within reasonable uncertainties in the recharge-water composition, to be closed to CO_2. A large calculated CO_2 outgassing at the JBJ well is not sensitive to $\delta^{34}S_{anhydrite}$ and probably indicates uncertainties in the recharge composition.

Significantly larger quantities of anhydrite have dissolved in the Evans Plunge and particularly the Cascade Spring waters. The CO_2 mass transfer at Evans Plunge

is minimized to −0.20 mmol/kg of water if $\delta^{34}S_{anhydrite}$ is 11.6 per mil, but in this case the measured $\delta^{13}C$ value cannot be exactly matched. Using −25.0 per mil and 0.0 per mil for $\delta^{13}C_{CH_2O}$, and $\delta^{13}C_{dolomite}$, respectively, the calculated value of $\delta^{13}C$ at Evans Plunge is about 1.00 per mil heavier than the measured value (−9.70 per mil). In order to obtain the best match between calculated and measured $\delta^{13}C$ values, a smaller average value for $\delta^{34}S_{anhydrite}$ (10.0 per mil) has been used, resulting in more sulfate reduction and lighter calculated values of $\delta^{13}C$.

A similar determination was made for the Cascade Spring water. The measured $\delta^{13}C$ value (−9.10 per mil) is very light, particularly for a water almost saturated with anhydrite and dolomite, which likely is the result of substantial calcite precipitation. For example, using 11.5 per mil for $\delta^{34}S_{anhydrite}$, the CO_2 mass transfer is decreased to zero at Cascade Spring, but even values of −25.0 per mil for $\delta^{13}C_{CH_2O}$ and 0.0 per mil for $\delta^{13}C_{dolomite}$ result in a calculated ^{13}C value that is too heavy (−7.00 per mil). In order to match the measured $\delta^{13}C$ value, an isotopically lighter anhydrite source is required. Calculated and measured values of $\delta^{13}C$ are almost matched if $\delta^{34}S_{anhydrite}$ is 9.0 per mil, $\delta^{13}C_{CH_2O}$ is −25.0 per mil, and $\delta^{13}C_{dolomite}$ is 1.0 per mil. The computed CO_2 gas mass transfer (−0.90 mmol/kg of water) may be due to differences in recharge composition.

Because these waters flow along a path consisting of highly transmissive rocks, it is not surprising that all of these waters (table 22) are less than 4,000 yr old, except for the JBJ well. Water from the latter well, which is located on the western side of the flow-controlling structure on the western side of the Black Hills in Wyoming (Downey, 1984), has an age of about 20,000 yr before present.

FLOW PATH 8

From the preliminary modeling, several serious problems were evident along flow path 8. In addition to difficulties in matching the measured $\delta^{13}C$ values and unreasonably large calculated CO_2 outgassing, the calculated ^{14}C ages increase with increasing reaction progress. Waters with the most extensive reaction progress were found to be impossibly young (calculated ^{14}C content less than the measured content). Varying the sulfur-isotopic composition of anhydrite, however, generally improved model results.

As with many of the previously modeled wells that are associated with recharge areas, calculated and measured $\delta^{13}C$ values at the McNenney well (well No. 2 in South Dakota) could not be exactly matched; the calculated $\delta^{13}C$ value was several parts per thousand heavier than the measured value and insensitive to variation in $\delta^{34}S_{anhydrite}$, $\delta^{13}C_{CH_2O}$, and $\delta^{13}C_{dolomite}$. The data in table 11 show that the McNenney well contains tritium (11.4 TU), and the calculated ^{14}C content was found to be less than the measured content. It was concluded, therefore, that the McNenney well is not completely isolated from the recharge process. The remaining wells along flow path 8 have anhydrite mass transfers of 6.98 to 14.74 mmol/kg of water. For these, the modeling results were improved by increasing $\delta^{34}S_{anhydrite}$ from the estimated value of 11.0 per mil.

The largest value of $\delta^{34}S_{anhydrite}$ tested for the Kosken well (well 1 in South Dakota) was 12.9 per mil; this minimized the quantity of CH_2O reacted. The CO_2 outgassing could not be decreased to zero by further increasing $\delta^{34}S_{anhydrite}$ without leading to impossible reactions such as the formation of CH_2O. Using 12.9 per mil for $\delta^{34}S_{anhydrite}$, −25.00 per mil for $\delta^{13}C_{CH_2O}$, and 0.30 per mil for $\delta^{13}C_{dolomite}$, the calculated $\delta^{13}C$ value almost matches the measured value. If $\delta^{13}C_{dolomite}$ were 2.0 per mil, then the measured $\delta^{13}C$ value would almost be matched if $\delta^{34}S_{anhydrite}$ were 12.4 per mil. This latter result for Kosken has been retained in tables 21 and 22.

Modeling of the remaining wells along flow path 8 followed a similar pattern. The sulfur-isotopic composition of dissolving anhydrite used in the modeling process was varied from 12.3 per mil at Hilltop Ranch (well No. 22 in South Dakota) to 16.0 per mil at Dupree (well No. 20 in South Dakota). By varying $\delta^{34}S_{anhydrite}$, all but one of the wells along flow path 8 could be modeled using −25.0 per mil for $\delta^{13}C_{CH_2O}$ and 2.0 per mil for $\delta^{13}C_{dolomite}$. Dupree required a heavier dolomite (4.9 per mil) to obtain a match between calculated and measured values of $\delta^{13}C$.

Most of the wells along flow path 8 indicated an outgassing of less than 1.0 mmol of CO_2 per kilogram of water, probably indicating a smaller dissolved CO_2 concentration in the recharge area than was used in the calculations.

The calculated ^{14}C ages indicate that the modeling results in tables 21 and 22 are correct. Unlike the preliminary modeling results (table 19), the final modeling results (table 22) are relatively constant with respect to the ages of the waters. Because most of the wells are located along a north-trending line normal to the direction of flow along flow path 8, generally similar ages are expected. Excluding McNenney, which has been shown to be associated with the recharge process, the average age of waters along flow path 8 is 12,300 ± 2,900 yr.

SUMMARY OF FINAL MASS-TRANSFER RESULTS FOR EACH FLOW PATH

The mass-transfer results of the modeling excercises for each flow path are summarized below and detailed in tables 21 and 22.

FLOW PATH 1

The evolution of waters at five wells and springs in north-central Montana was modeled using the composition of Lewistown Big Spring (spring No. 10 in Montana) as the starting point. The mass-transfer results in table 21 show that water at sites nearest the recharge area, the Hanover Flowing Well (well No. 8 in Montana) and Vanek Warm Spring (spring No. 9 in Montana), is affected by some anhydrite dissolution accompanying the dissolution of dolomite and the precipitation of calcite. No other reactions are important for these two waters. At Landusky Spring (spring No. 12 in Montana), Lodgepole Warm Spring (spring No. 13 in Montana), and Sleeping Buffalo (well No. 18 in Montana), further progress in the anhydrite-driven dedolomitization reaction is determined with more than 19 mmol of anhydrite dissolved per kilogram of water at Sleeping Buffalo. Accompanying the extensive dedolomitization reaction is substantial sulfate reduction (about 0.56 mmol CH_2O oxidized per kilogram of water), pyrite formation balanced by dissolution of FeOOH (as much as 0.15 mmol/kg of water), Ca^{2+}/Na^{+} exchange (4.37 mmol/kg of water), and dissolution of halite and sylvite (4.68 and 0.64 mmol/kg of water, respectively).

All of the waters along flow path 1 appear to be young (about 5,000 yr to modern), and it is likely that the water from the five wells and springs selected is primarily affected by local recharge conditions and probably is not part of a regional flow system.

FLOW PATH 2

Data from wells at Bozeman Fish Hatchery (well No. 4 in Montana) and Big Timber Fish Hatchery (well No. 7 in Montana) were averaged to define the recharge water for flow path 2. Water at McLeod Warm Spring (spring No. 6 in Montana), nearest the recharge area, is affected by dedolomitization (with 1.12 mmol of anhydrite dissolved per kilogram of water) and sulfate reduction (0.25 mmol CH_2O oxidized per kilogram of water). Proceeding downgradient some 124 miles to oilfield waterflood wells at Sumatra (well No. 17 in Montana), Keg Coulee (well No. 15 in Montana), and Texaco C115X (well No. 16 in Montana), which are all within 23 miles of each other, all reactions except pyrite formation and goethite dissolution are significant. Anhydrite mass transfer varies between 13.97 and 18.59 mmol/kg of water between these three wells and the recharge area.

Large modeling uncertainties remain along flow path 2 concerning primarily the calcite and dolomite mass transfers. If there is a major sink for magnesium (such as Mg^{2+}/Na^{+} exchange), then substantial dolomite dissolution (as much as 10.70 mmol/kg of water) and calcite precipitation (to 22.5 mmol/kg of water) are indicated. Although this model results in agreement between calculated and measured $\delta^{13}C$ values, the calculated ^{14}C activity indicates very young ages (about 4,000 yr) for waters with ages likely ranging from 10,000 to 20,000 yr.

Based on the indications of leakage and the extensive faulting in the area around flow path 2 (fig. 9), it is likely that the H_2S found along flow path 2 has migrated into the Madison aquifer from the underlying Cambrian-Ordovician aquifer and is not really a product of in situ sulfate reduction. The hypothesis of an external source of hydrogen sulfide gives reasonable model results. If this is the case, much of the calcium from anhydrite dissolution is removed from the water by ion exchange, with 5.88 to 9.23 mmol of calcium exchanged per kilogram of water. The removal of calcium results in decreased calcite precipitation (2.36 to 4.07 mmol/kg of water) and dolomite dissolution (0.73 to 1.51 mmol/kg of water). This modeling alternative almost results in a match between calculated and measured $\delta^{13}C$ values and ^{14}C ages of about 23,000 yr.

Regardless of the source of H_2S, as much as 61.92 mmol of halite and 3.82 mmol sylvite dissolve in each kilogram of water along flow path 2. Exchange of Ca^{2+} for Na^{+}, producing excess sodium bicarbonate, is more significant along flow path 2 than for any other flow path in the Madison aquifer.

FLOW PATH 3

The wells used to define the composition of the recharge water for flow path 3 were at Mock Ranch (well No. 1 in Wyoming) and Denius No. 1 (well No. 2 in Wyoming), some 31 miles south of flow path 3 in north-central Wyoming. No $\delta^{34}S$ data were obtained for HTH No. 3 (well No. 14 in Montana) and Gas City (well No. 26 in Montana), which precluded mass-transfer modeling of water from these wells. Water from the remaining four wells, Colstrip (well No. 21 in Montana), Sarpy Mine (well No. 19 in Montana), Moore (well No. 22 in Montana), and Mysse Flowing Well (well No. 20 in Montana), is dominated by a considerable range of reactions, including extensive dedolomitization driven by dissolution of more than 20 mmol of anhydrite per kilogram of water. Halite dissolution is significant at the Moore and Gas City wells (the latter was calculated independent of the lack of sulfur-isotope data) and of little importance at the Colstrip and Sarpy Mine wells. Varying degrees of ion exchange are present, with between 1.36 and 8.28 mmol of calcium exchanged per kilogram of water along flow path 3.

Ages along flow path 3 ranged from about 3,000 yr at the Moore well to about 23,000 yr at the Mysse Flowing Well. The latter value probably is more reasonable for flow path 3, and the younger ages probably are due to uncertainties in the mass transfer used to correct the calculated ^{14}C value.

FLOW PATH 4

The recharge area of flow path 4 is well defined by four wells in north-eastern Wyoming: Storey Fish Hatchery (well No. 6 in Wyoming), Mobil (well No. 7 in Wyoming), Mock Ranch (well No. 1 in Wyoming), and Denius No. 1 (well No. 2 in Wyoming). Five wells were modeled along flow path 4, which has a length of more than 155 miles through northeast Wyoming, southeast Montana, and northwest South Dakota; the wells modeled were HTH No. 1 (well No. 14 in Wyoming), Ranch Creek (well No. 23 in Montana), Belle Creek (well No. 24 in Montana), Delzer No. 1 (well No. 7 in South Dakota), and Delzer No. 2 (well No. 8 in South Dakota). Very similar mass transfers were found for the HTH No. 1, Ranch Creek, and Belle Creek wells, which are within 31 miles of each other and midway along the flow path. The mean anhydrite mass transfer at this point is 5.12 mmol/kg of water, with an average of 2.43 mmol of calcite precipitated and an average of 1.04 mmol of dolomite dissolved per kilogram of water. Only minor sulfate reduction has occurred (0.30 mmol CH_2O oxidized per kilogram of water) with formation of traces of pyrite. Halite dissolution and ion exchange are not significant, at least to the midpoint of flow path 4. Farther downgradient at the Delzer No. 1 and No. 2 wells, which are less than 0.62 miles apart, more extensive dedolomitization caused by dissolution of 17.94 mmol of anhydrite per kilogram of water was determimed. Sulfate reduction is more significant at this farthest point sampled along flow path 4 (1.19 to 1.97 mmol of CH_2O oxidized per kilogram of water) with acompanying formation of 0.31 to 0.52 mmol of pyrite per kilogram of water. Neither ion exchange nor halite dissolution contribute significantly to the mass transfer throughout the entire 155-mile distance sampled along flow path 4.

Some of the more reliable ^{14}C age dates are calculated along flow path 4, particularly in the vicinity of the HTH No. 1, Ranch Creek, and Belle Creek wells; the ages for the latter three wells range between about 7,300 and 9,200 yr.

FLOW PATH 5

Waters at the Hole in the Wall well (well No. 5 in Wyoming) and Barber Ranch Spring (spring No. 12 in Wyoming) were averaged to define the recharge composition for flow path 5. Four wells were modeled along a 62-mile flow path in northeast Wyoming: Conoco No. 175 (well No. 11 in Wyoming), MKM (well 10 in Wyoming), Shidler (well No. 9 in Wyoming), and Conoco No. 44 (well No. 8 in Wyoming). In spite of difficulties experienced in modeling waters along flow path 5 (see previous section), a similar pattern in mass transfer resulted for all four wells. Waters from these wells are affected by moderately extensive dedolomitization, with as much as 10.16 mmol of anhydrite dissolved per kilogram of water, and only minor sulfate reduction and pyrite formation. Halite dissolution is a major contributor to the water quality along flow path 5 (as much as 32.16 mmol dissolved per kilogram of water), and moderate ion exchange was detected (as much as 2.28 mmol of calcium exchanged per kilogram of water). Carbon-14 ages of about 8,000 to about 23,000 yr were calculated.

FLOW PATH 6

The Mallo Camp (well No. 24 in Wyoming) and Rhoads Fork (well No. 4 in South Dakota) wells were selected to define the average recharge-water composition of flow path 6. Five wells in northeastern Wyoming were modeled along flow path 6, a distance of about 50 miles. These are the Seeley (well No. 19 in Wyoming), Newcastle (well No. 21 in Wyoming), and Osage (well No. 17 in Wyoming) wells clustered within 19 miles of each other on the west side of the Black Hills, and the Upton (well No. 15 in Wyoming) and Devils Tower (well No. 13 in Wyoming) wells at the end of the flow path. The mass transfers listed in table 21 show that very little, if any, reaction takes place along flow path 6.

The three wells nearest the recharge area (Seeley, Newcastle, and Osage) averaged only 0.38 mmol of anhydrite dissolved per kilogram of water, with some dolomite dissolution and calcite precipitation. No other reactions were detected at these wells. At the Upton and Devils Tower wells, more extensive dedolomitization was evidenced by as much as 2.27 mmol of anhydrite dissolved per kilogram of water and small increases in the dolomite and calcite mass transfers.

Some sulfate reduction probably occurs near the end of flow path 6, as about 0.20 mmol of CH_2O was oxidized per kilogram of water. Ion exchange and halite dissolution are not significant, and all waters appear to be modern to 1,000 yr old except water from the Upton well, which is about 8,000 yr old.

FLOW PATH 7

Water from the Rhoads Fork well (well No. 4 in South Dakota) was selected as representative of the recharge composition of flow path 7 on the southwest side of the Black Hills. Reactions were modeled for water from 4 wells and 1 spring along flow path 7, a distance of more than 50 miles. Waters from the three wells nearest the recharge area, Voss (well No. 20 in Wyoming), Self (well No. 22 in Wyoming), and JBJ (well No. 18 in Wyoming), are effected almost exclusively by some dedolomitization. Water at JBJ well indicated some amount of dolomite precipitation (−0.04 mmol/kg of

water), which probably indicates either that there are errors in the water analysis or that water from the Rhoads Fork well is not representative of recharge for the JBJ well. No other reactions are significant near the recharge area of flow path 7.

Farther downgradient along flow path 7 to Evans Plunge (well No. 10 in South Dakota) and Cascade Springs (spring No. 9 in South Dakota) the calculations show significant increases in the extent of dedolomitization (16.91 mmol of anhydrite dissolved per kilogram of water at Cascade Spring). In addition, sulfate reduction was inferred based on 2.42 mmol of CH_2O oxidized per kilogram of water with accompanying pyrite precipitation at Cascade Spring. Some ion exchange and halite dissolution were indicated near the end of flow path 7. Excluding water from well JBJ, which may not be part of the flow system, the waters along flow path 7 are young, ranging between modern and 4,000 yr old.

FLOW PATH 8

The average recharge for flow path 8 was defined using the composition of waters at Jones Spring (spring No. 12 in South Dakota), the Kaiser well (well No. 11 in South Dakota), and Cleghorn Spring (spring No. 16 in South Dakota) on the east side of the Black Hills. From here, reactions were modeled to 10 wells east and northeast of the Black Hills for a distance of about 124 miles. Water from the McNenney well (well No. 2 in South Dakota) near the recharge area is slightly affected by dedolomitization, with 0.91 mmol of anhydrite dissolved per kilogram of water. No other reactions were important at this site.

The remaining nine wells are all located along the farthest part of the flow path in western South Dakota. Modeling of waters from those wells showed a progressive increase in mass transfer along a line normal to the direction of flow extending from the Kosken well (well No. 1 in South Dakota) in south-central South Dakota to the Dupree well (well No. 20 in South Dakota) about 106 miles to the north-northwest in northwestern South Dakota. Along this line, progressive increases in the quantities of anhydrite dissolved (increasing from 7.10 to 14.74 mmol/kg of water), calcite precipitated (increasing from 3.35 to 8.22 mmol/kg of water), and dolomite dissolved (increasing from 1.17 to 3.72 mmol/kg of water) were determined. This trend in mass transfer probably is due to regional variations in the abundance of anhydrite in the Madison aquifer system, with availability of anhydrite for reaction increasing northward in western South Dakota toward the Williston basin. No trends in any other reactions were evident. The quantity of CH_2O oxidized ranged between 0.30 and 1.07 mmol/kg of water, and pyrite formation and ion exchange generally were of minor significance.

Ion exchange was more significant at the Dupree well and the Eagle Butte well (well No. 23 in South Dakota) (0.66 and 1.22 mmol Ca^{2+} exchanged per kilogram of water, respectively). Some halite dissolution (0.97 to 4.18 mmol dissolved per kilogram of water) was found at the Murdo (well No. 25 in South Dakota), Hilltop Ranch (well No. 22 in South Dakota), Prince (well No. 26 in South Dakota), Hamilton (well No. 21 in South Dakota), Eagle Butte, and Dupree wells.

Trends in ^{14}C age were neither expected nor found for the nine wells near the end of flow path 8. Calculated ages vary between about 8,000 and about 17,000 yr and average $12{,}400 \pm 3{,}000$ yr.

OVERVIEW OF CHEMICAL REACTIONS IN THE MADISON AQUIFER

Complete reaction models were developed at wells for which carbon- and sulfur-isotope data were available (table 21). Partial reaction information for the mass transfers of anhydrite, dolomite, halite, and ion exchange was obtained from the chemical analyses in cases of limited isotopic data. In addition, results from some wells in the vicinity of the Black Hills not previously modeled have been added to the mass-transfer maps (figs. 43 and 47–50) to improve control.

Some estimated values of anhydrite mass transfer are displayed in figure 43. In the absence of sulfur-isotope data, anhydrite mass transfer was estimated from the difference between recharge and final dissolved sulfate content, ignoring sulfate reduction. The total amount of anhydrite dissolved will be larger than the change in dissolved sulfate content by the amount reduced to hydrogen sulfide. The extent of sulfate reduction has been found to be relatively small in the Madison aquifer system where sulfur-isotope data have permitted a more complete evaluation (table 21).

The mass transfer of dolomite is defined (eq 47) by the change in magnesium content independently of the sulfur- and carbon-isotope data and may, therefore, be compared with all other modeled results. The mass transfers of sylvite, halite, and ion exchange are also defined independently of the carbon- and sulfur-isotope data through mass-balance relations involving changes in dissolved sodium, potassium, and chloride (eqs 44–46).

The data in table 21 indicate that dedolomitization—that is, dissolution of anhydrite and dolomite accompanying precipitation of calcite—is the predominant reaction throughout the entire Madison aquifer. The extent to which this reaction proceeds appears to be both a function of flow distance (age) and availability of anhydrite for reaction. The anhydrite mass transfer is about 20 mmol dissolved per kilogram of water along flow paths 1, 2, 3, and 4. Along flow path 8 the quantity of

anhydrite dissolved increases northward normal to the eastward direction of flow, indicating that the increased availability of anhydrite northward toward the Williston basin is a more dominant cause of reaction progress than distance down the flow path. Other waters show little or no anhydrite dissolution (flow path 6), indicating little abundance of the mineral there and more rapid flow velocities. The importance of mineral availability for reactions is further demonstrated by the fact that some of the largest quantities of anhydrite dissolution are found in some of the youngest (flow paths 1 and 7) and oldest (flow paths 2 and 3) waters.

There are systematic variations in the regional pattern of anhydrite dissolution in the Madison aquifer based on mass-transfer calculations (fig. 44). The quantity of anhydrite dissolved is affected by distance from recharge

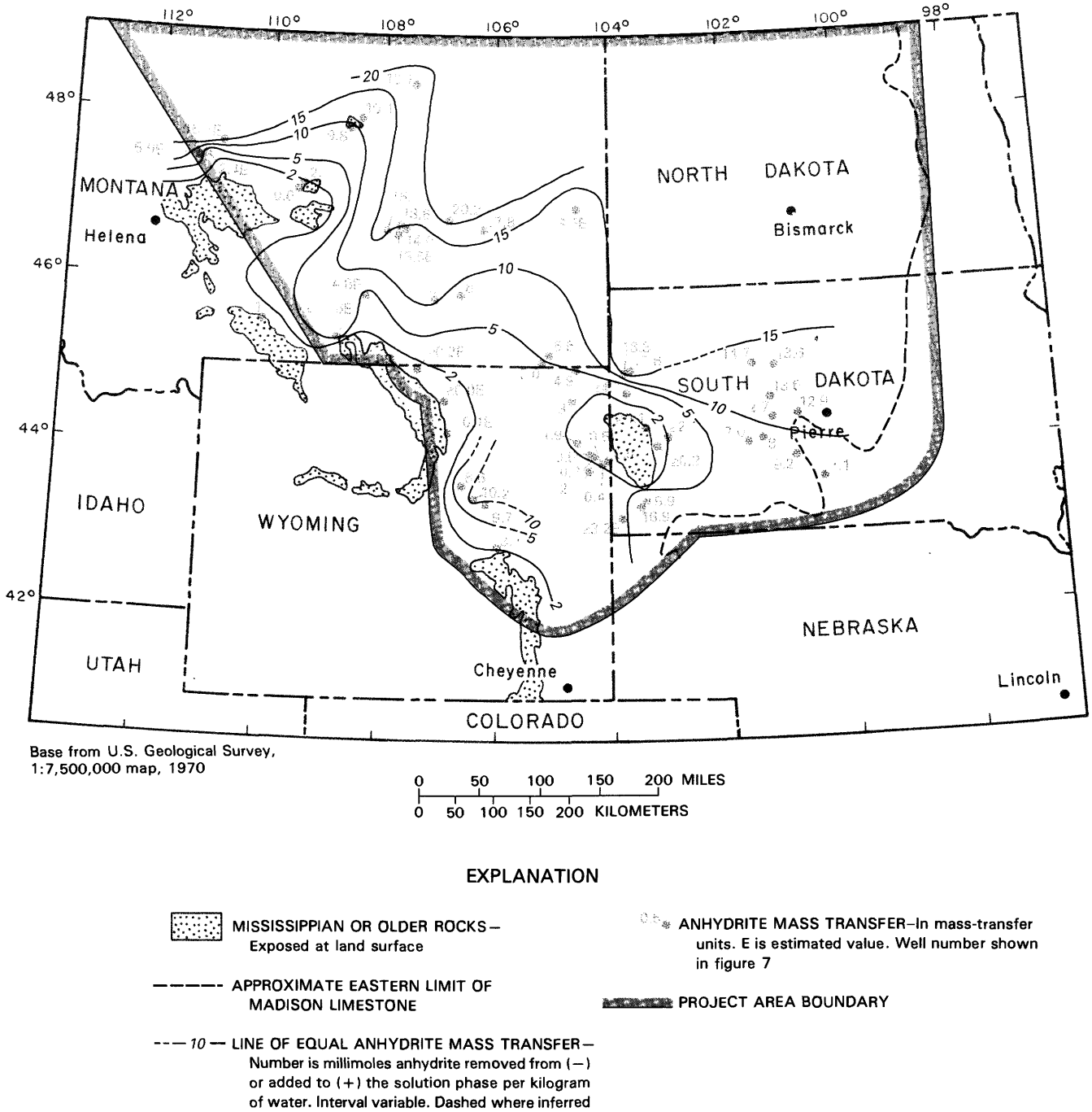

FIGURE 43.—Regional variation in anhydrite mass transfer (per kilogram of water) for all wells and springs sampled.

areas; progressive increases in anhydrite dissolution occur with distance downgradient. This is most noticeable for the Madison aquifer in the area surrounding the Black Hills.

As expected for dedolomitization, the dolomite and calcite mass-transfer patterns are similar to the anhydrite mass-transfer results. The data in figures 44 and 45 indicate nearly linear relations between the mass transfers of anhydrite and dolomite, and between anhydrite and calcite. The slopes of points in figures 44 and 45 indicate that for flow paths 1 to 8, about 0.2 mmol/kg of water of dolomite dissolves for every millimole per kilogram of water of anhydrite dissolved, causing the precipitation of approximately 0.5 mmol/kg of water of calcite. These mass transfers are similar to those calculated from thermodynamic simulations of hypothetical dedolomitization using the geochemical mass-transfer program PHREEQE (Parkhurst and others, 1980).

In a simulation of the dedolomitization reaction, 14.74 mmol/kg of water of anhydrite was dissolved in a hypothetical recharge water saturated with calcite and dolomite at 10^{-2} atm P_{CO_2} and 12 °C. Temperature was increased in the calculation to 56.5 °C while maintaining equilibrium with calcite and dolomite. The calculated mass transfer showed that for each millimole of anhydrite dissolved, an average of 0.26 mmol/kg of water of

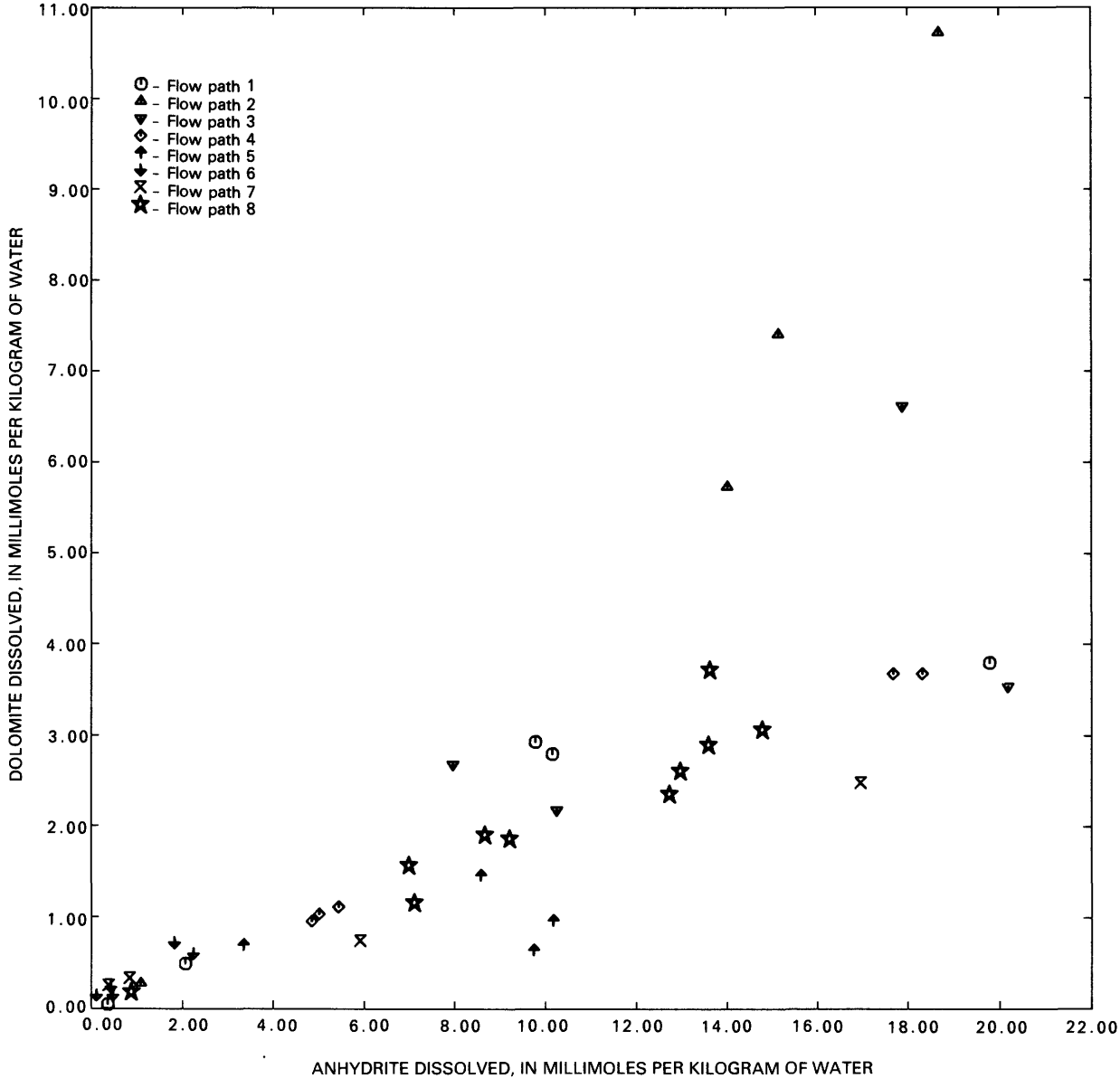

FIGURE 44.—Trend in quantity of dolomite dissolved (per kilogram of water) as a function of anhydrite dissolution along flow paths 1 to 8.

dolomite dissolved and 0.58 mmol/kg of water of calcite precipitated. These hypothetical mass transfers are similar to the mass-balance results (table 21) for the Dupree well (well No. 20 in South Dakota). The only significant exceptions to these determinations in the calcite and dolomite mass transfers are several wells along flow paths 2 and 3 where substantial ion exchange was indicated. Here the dissolved-dolomite and precipitated-calcite mass transfers were larger than the trend shown for the rest of the Madison aquifer.

Regionally, the dolomite mass-transfer pattern (fig. 46*A*) generally parallels the anhydrite dissolution pattern (fig. 43). The quantity of dolomite dissolved also is found to increase normal to the direction of flow along flow path 8, in response to the irreversible dissolution of anhydrite. Similar variations exist for the calcite mass transfer (fig. 46*B*).

Occurring with the dedolomitization reaction generally is some lesser organic-matter oxidation, dissolution of ferric hydroxide, and pyrite formation. Several flow paths,

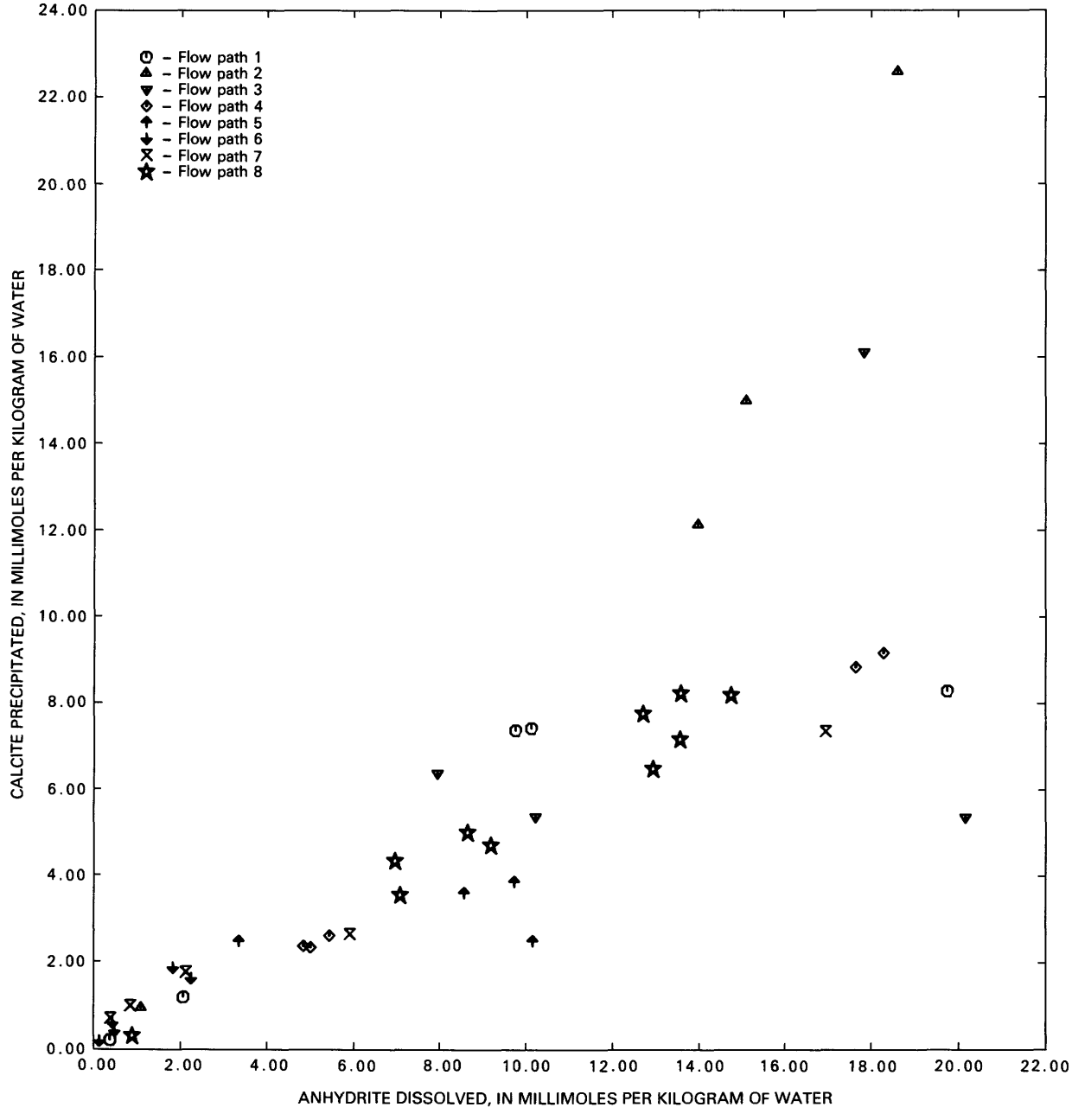

FIGURE 45.—Trend in quantity of calcite precipitated (per kilogram of water) as a function of anhydrite dissolution along flow paths 1 to 8.

notably 5, 6 and 7, show little or no evidence of sulfate reduction, whereas water from wells in the Central Montana trough (flow paths 2 and 3) and points along flow paths 4 and 8 indicate greater sulfate reduction. For example, in water from wells in the Central Montana trough, as much as 4 to 8 mmol of organic matter is oxidized per kilogram of water. The mass-balance calculations indicate that less than 0.50 mmol of organic matter oxidized is typical of much of the Madison aquifer.

Accompanying the relatively substantial sulfate reduction along flow path 2 generally is some lesser pyrite precipitation and dissolution of FeOOH. As discussed earlier, this probably reflects lesser quantities of detrital FeOOH deposited in the Central Montana trough. Here most of the reduced sulfur species remain in solution. As a result of the modeling exercise it appears that the H_2S found in wells along flow path 2 may have been introduced from other formations. Elsewhere in the Madison aquifer, sulfate reduction accompanies proportionately larger quantities of FeOOH and greater pyrite mass transfer.

Halite dissolution and ion exchange are significant only in limited parts of Montana and Wyoming, presumably reflecting availability of halite and clay minerals there.

Ion exchange is important along flow paths 2 and 3 and begins to contribute significantly to the mass transfer at points along flow paths 1, 5, and 8, but except for flow paths 2 and 3, ion exchange is not important throughout most of the Madison aquifer. There are systematic variations in the degree of ion exchange (as calculated from eq 46), increasing significantly northeastward from central Montana (fig. 47). Dissolution of halite is very important along flow paths 2, 3, and 5 and minor to absent throughout the rest of the Madison aquifer. Halite dissolution generally contributes 1 mmol of chloride per kilogram of water or less to most of the waters of the Madison aquifer, except in east-central Montana where, very abruptly, waters from most wells have more than 50 millimoles of halite dissolved per kilogram of water (fig. 48). The dissolution of a sylvitelike phase always accompanies halite dissolution but at mass-transfer levels of only 5 percent that of halite.

As discussed earlier, the CO_2 gas mass transfer is expected to be near zero, and the magnitude of this term has been used as a criterion in refining the mass-balance models. For most of the wells modeled, the CO_2 gas mass transfer is 0.0 ± 0.5 mmol/kg of water, which, taking into account the many modeling assumptions, reasonably supports the conclusion of a closed system. Other wells show larger CO_2 gas mass transfers that are attributed to uncertainties in the composition of recharge waters or other errors in the modeling exercise.

The thermodynamic calculations in table 9 show that most of the waters are undersaturated with anhydrite, asymptotically approaching anhydrite saturation farther downgradient. For those few waters in equilibrium with anhydrite, dissolution of anhydrite can take place in response to the exchange of Ca^{2+} for Na^{+} and sulfate reduction; these reactions decrease the anhydrite saturation state. The calcite, dolomite, pyrite, and FeOOH mass transfers are directly linked thermodynamically to the irreversible dissolution of anhydrite and sulfate reduction. Halite dissolution also responds irreversibly, but its mass transfer is a function of halite availability. The ion-exchange reaction probably proceeds reversibly, but the degree of the reaction probably is related to the abundance of sites available for exchange.

REGIONAL PATTERNS IN $\delta^{34}S_{anhydrite}$

The best estimates of the sulfur-isotopic composition of dissolving anhydrite in the Madison aquifer are given in table 22. The lightest values (about 8 per mil) are found in northeast Wyoming and eastward through the Black Hills (9 to 10 per mil). As shown in figure 49, these model-derived values of $\delta^{34}S_{anhydrite}$ increase progressively to heavier values northward into east-central Montana and northward through western South Dakota. The lighter sulfur-isotopic values in northeastern Wyoming previously have been interpreted as indicating leakage of waters from overlying Pennsylvanian and Permian rocks in response to extensive pumpage from the Madison aquifer (Busby and others, 1983). The values in northeast Wyoming (fig. 49) are not necessarily anomalous; they may instead be part of a regional pattern in the Madison aquifer.

If the sulfur-isotope variation in figure 49 reflects that of the in situ anhydrite, then the pattern indicates a terrigenous source of sulfur in northeast Wyoming and southwest South Dakota. According to Sando (1976b), land masses associated with the transcontinental arch were emergent in southeast Wyoming and northeast Nebraska throughout the Mississippian and could have contributed light sulfur (presumably from pyrite) to deposits in northeastern Wyoming and southwestern South Dakota. The inferred trend to heavier sulfur-isotopic composition of anhydrite northward through western South Dakota and through east-central Montana probably corresponds to a decrease in deposition of terrigenous sulfur and the increasing effect of a marine evaporite facies.

CARBON-14 AGES

Carbon-14 ages are reaction-model dependent. The calculation of ^{14}C age requires a detailed knowledge both of all mass transfers of carbon into and out of solution and of the ^{14}C content of the incoming carbon. It is like-

ly that all sources of carbon (dolomite, CH_2O) contain no ^{14}C, so the primary concern in ^{14}C dating is the accuracy of the derived mass transfers. The ^{14}C ages in table 22 may be used with varying degrees of confidence. The most reliable ages were determined from waters that have undergone only the dedolomitization reaction. The tritium data (table 11) indicate that some waters, particularly those near recharge areas, may be partially contaminated with modern ^{14}C.

As discussed earlier, the ^{14}C ages are particularly sensitive to the sulfur-isotopic composition of dissolving anhydrite and to the extent to which a magnesium sink,

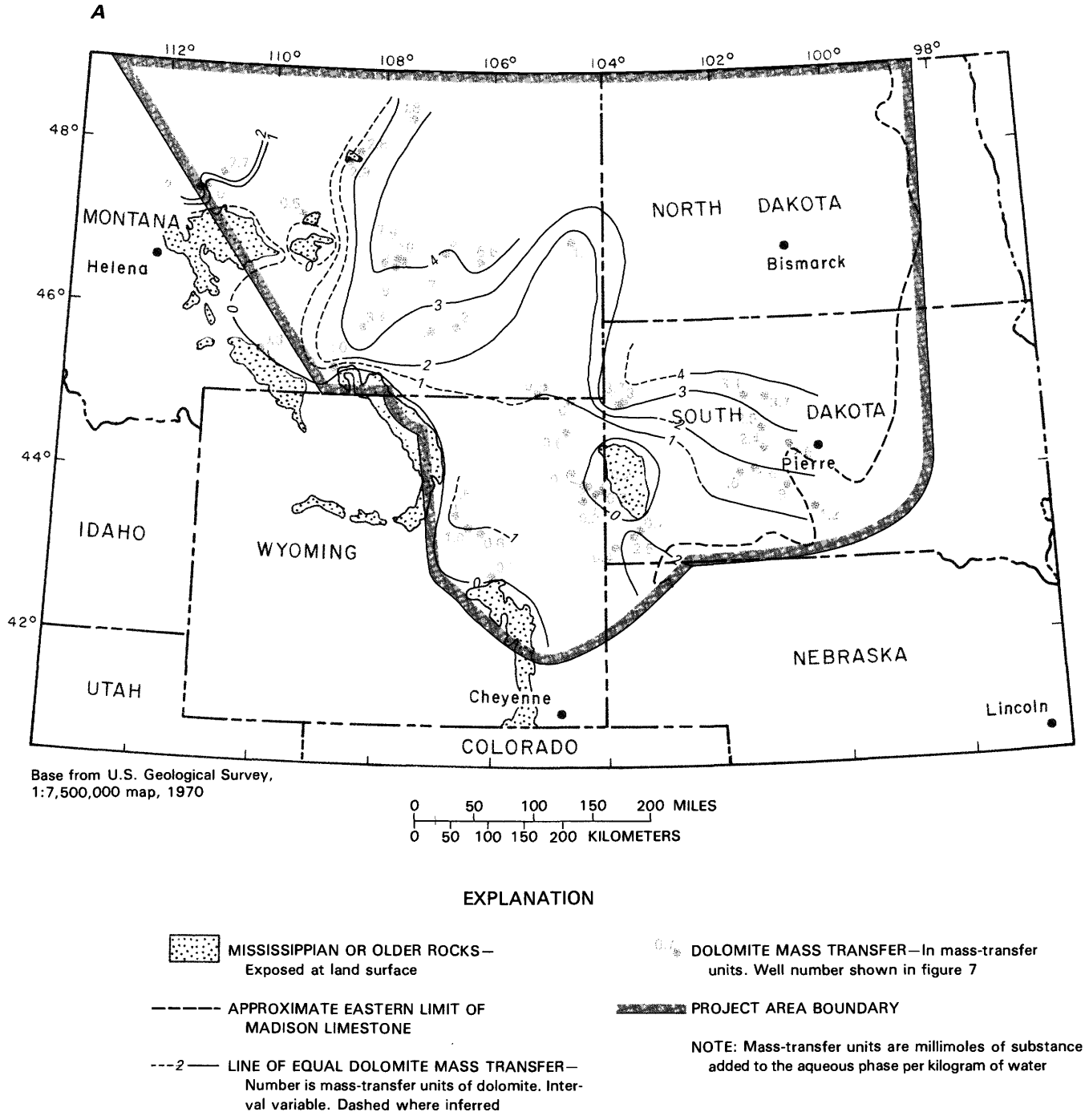

FIGURE 46.—Regional variation in millimoles of (*A*) dolomite dissolved and of (*B*) calcite transferred (per kilogram of water) for all wells and springs sampled.

such as Mg^{2+}/Na^{+} exchange, is present. Through the modeling process, lighter values of $\delta^{34}S_{anhydrite}$ cause calculation of more sulfate reduction and thus oxidation of more (^{14}C-depleted) organic matter. This additional dilution of the ^{14}C leads to smaller calculated (reaction-corrected) ^{14}C values and younger ages. Similarly, an additional sink for magnesium causes calculation of more extensive dissolution of ^{14}C-depleted dolomite, which again results in younger ages. Consequently, some of the more uncertain ^{14}C ages are those along flow paths 2 and 3, where extensive sulfate reduction and Mg^{2+}/Na^{+} exchange have been included in the reaction models.

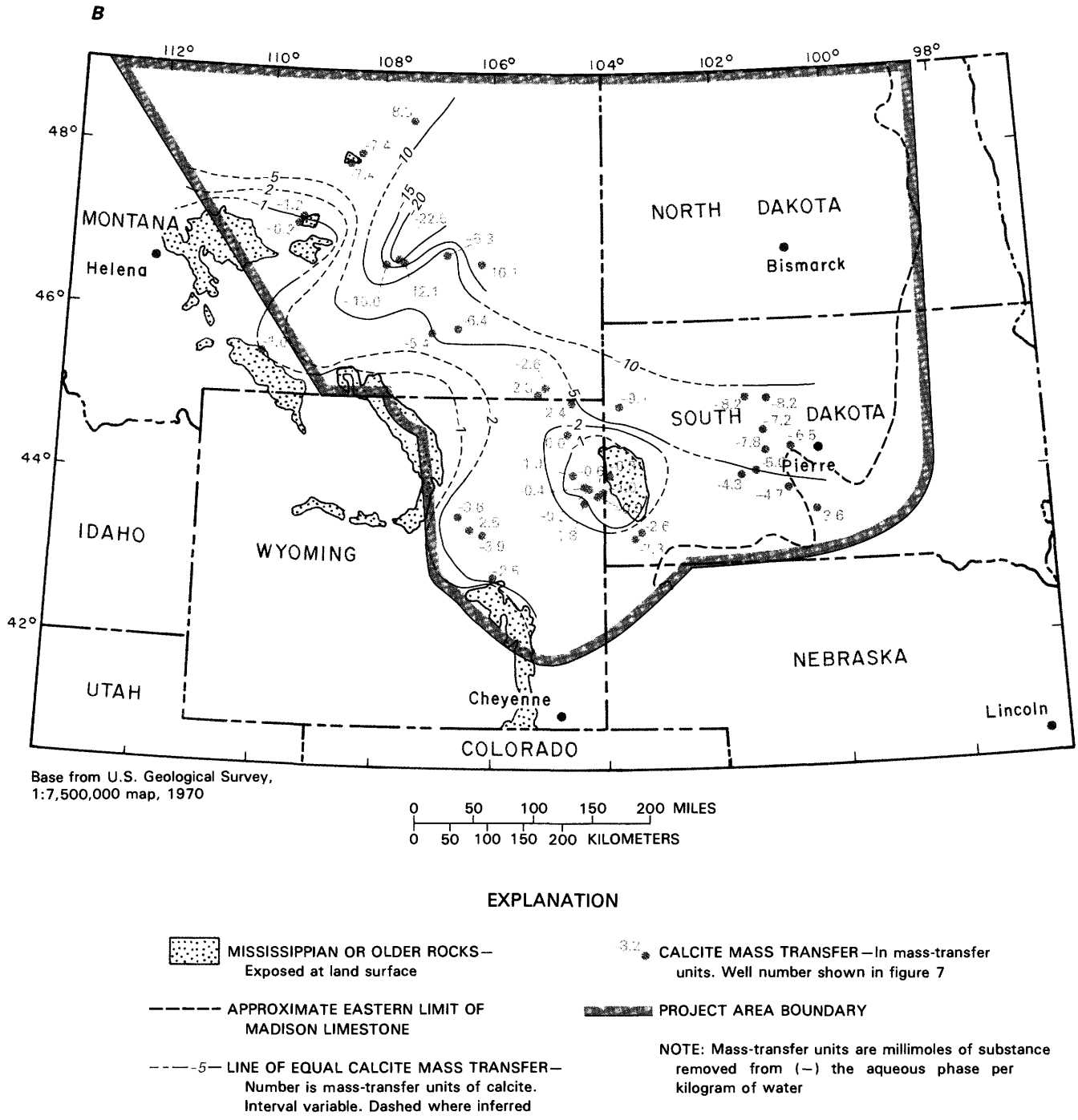

FIGURE 46.—Continued.

The importance of the reaction-model corrections to ^{14}C dating of the waters, however, cannot be overlooked. The variation in the measured ^{14}C content of all wells and springs along flow paths 1 to 8 as a function of the computed molal scale sulfate concentration is shown in figure 50. An abrupt and systematic decrease is seen in the ^{14}C content as anhydrite dissolves. This decrease is in part due to radioactive decay because the older waters generally have greater concentrations of dissolved anhydrite. The measured ^{14}C values are further decreased by dilution

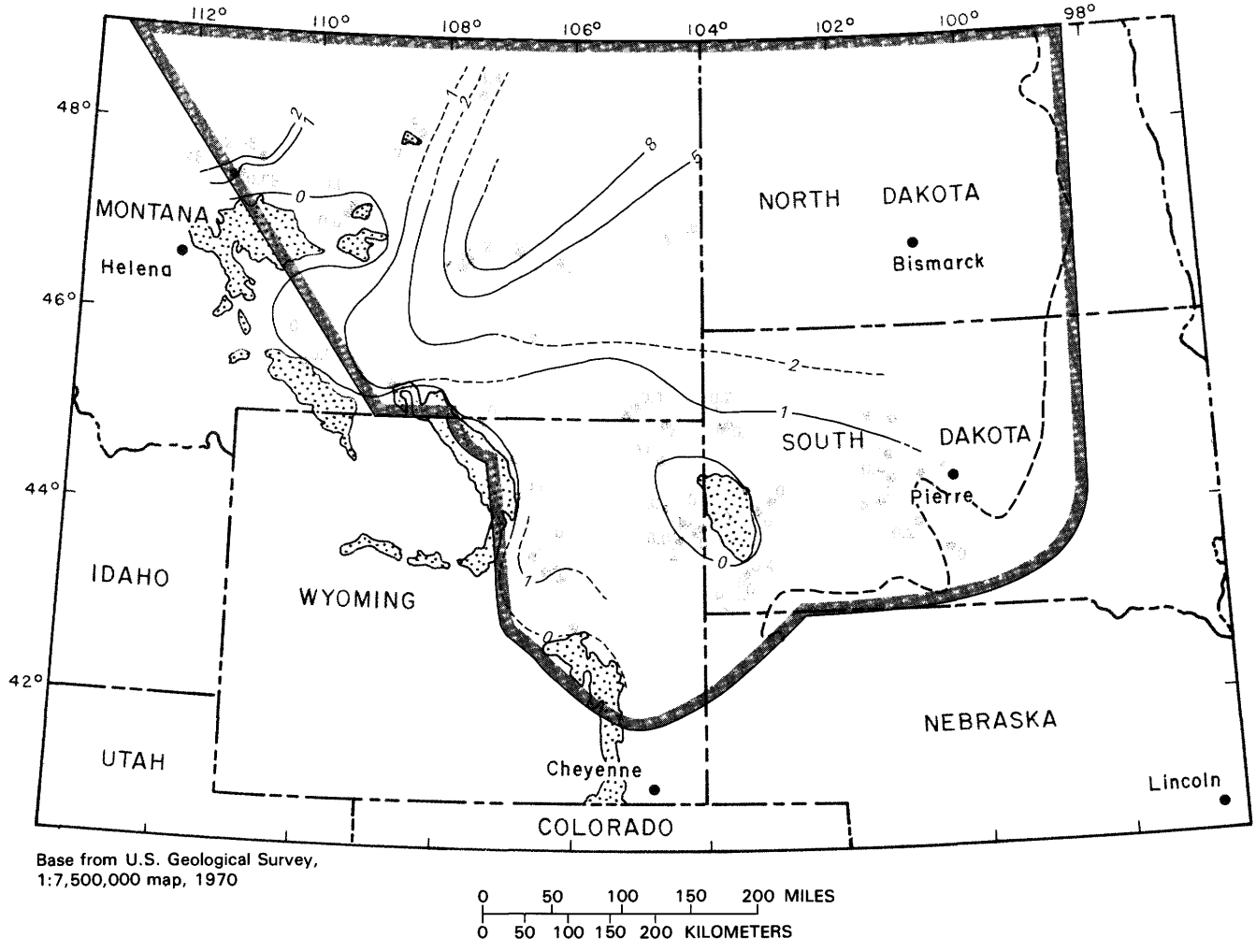

EXPLANATION

MISSISSIPPIAN OR OLDER ROCKS—Exposed at land surface

APPROXIMATE EASTERN LIMIT OF MADISON LIMESTONE

----2— LINE OF EQUAL ION EXCHANGE—Number is mass-transfer units of exchange. Interval variable. Dashed where inferred

ION EXCHANGE—In mass-transfer units. Well number shown in figure 7

PROJECT AREA BOUNDARY

NOTE: Mass-transfer units are millimoles of substance added to the aqueous phase per kilogram of water

FIGURE 47.—Regional variation in degree of ion exchange (divalent cation exchanged for sodium per kilogram of water) for all wells and springs sampled.

from dissolution of dolomite and oxidation of CH_2O as well as by incorporation of ^{14}C in secondary calcite precipitated via the dedolomitization reaction.

Taking Sleeping Buffalo (well No. 18 in Montana) as an example, the measured ^{14}C content of 4.20 percent modern is equivalent to an age of 26,000 yr if no corrections for reaction are made; that is, the unadjusted age is equal to (5730/ln 2) (100/measured percent modern). Correcting for an assumed congruent dissolution of carbonate minerals in an original CO_2-H_2O solution, the model of Pearson and White (1967) results in an age for water from the Sleeping Buffalo well of about 17,000 yr

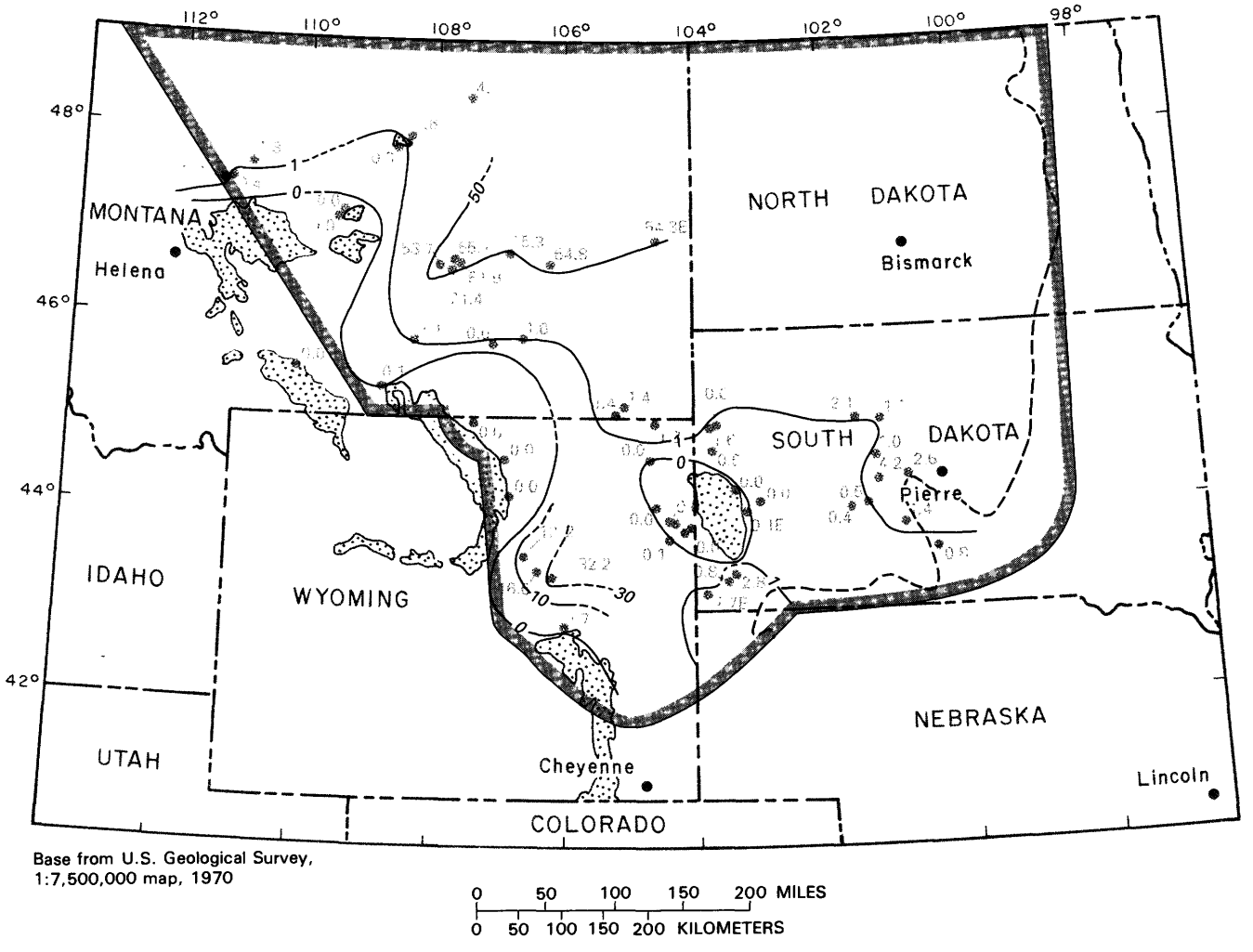

FIGURE 48.—Regional variation in millimoles of halite dissolved (per kilogram of water) for all wells and springs sampled.

(assuming $\delta^{13}C_{dolomite}$ is 0 per mil and $\delta^{13}C_{CO_2gas}$ is −9.44 per mil; see table 18). When the data are corrected for incongruent dissolution of carbonate minerals and sulfate reduction using the Rayleigh-distillation equations of Wigley and others (1978, 1979)—that is, the final calculated mass transfer (table 21)—the water at Sleeping Buffalo is found to be approximately modern (probably less than 5,000 yr old). Not all examples are as extreme as the water from the Sleeping Buffalo well. For example, the Mysse Flowing Well (well No. 20 in Montana) has an unadjusted ^{14}C age of 40,000 yr. By correcting for assumed congruent reaction (Pearson and White, 1967),

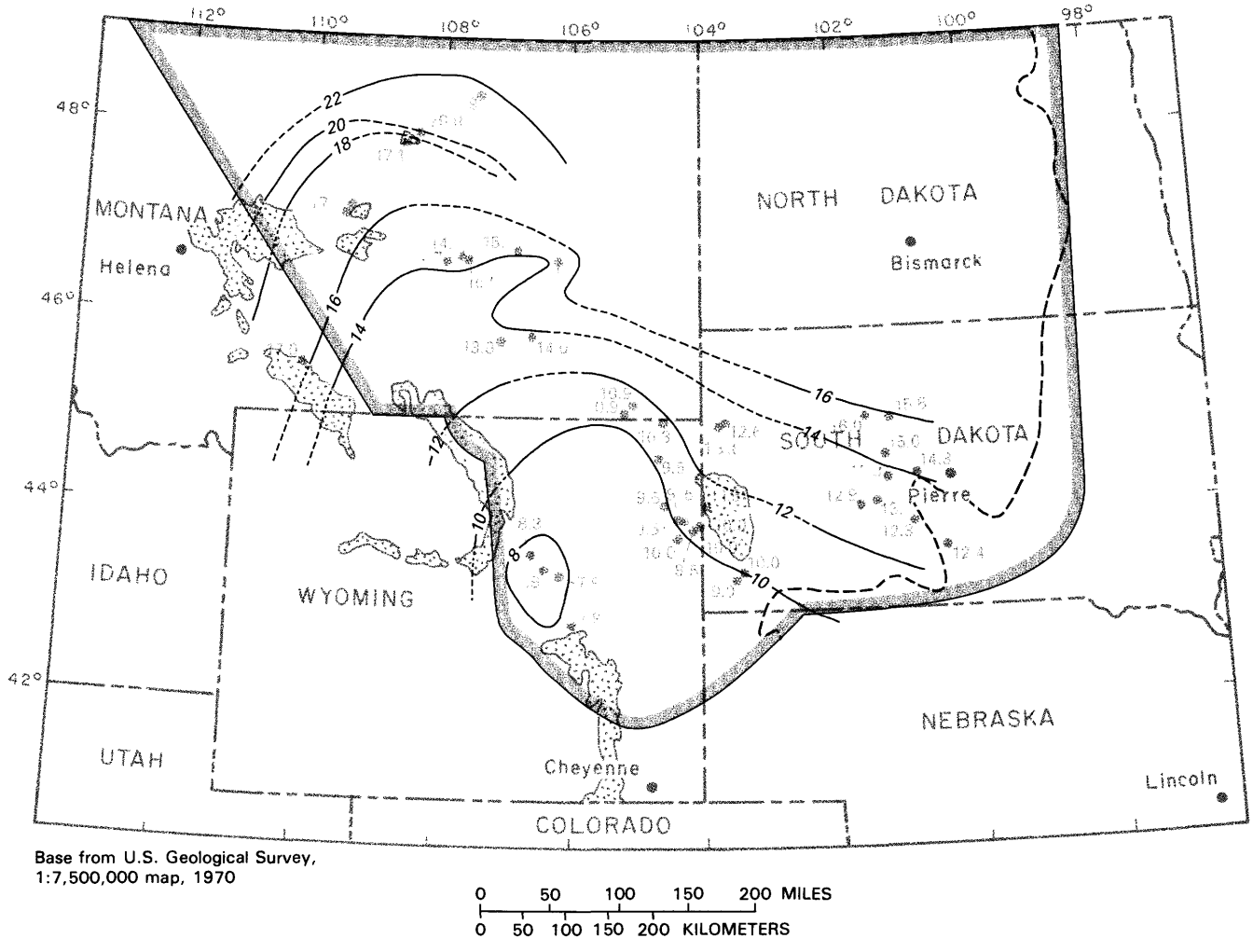

FIGURE 49.—Regional variation in estimated sulfur-isotopic composition of dissolving anhydrite for all wells and springs sampled.

the ^{14}C age is decreased to 25,500 yr, which compares favorably with 22,600 yr (table 22) based on all corrections for reactions.

In an earlier publication (Back and others, 1983), several waters from the Madison aquifer in the vicinity of the Black Hills were ^{14}C-dated by correcting for incongruent dissolution only (the dedolomitization reaction). This led to a ^{14}C age at the Philip well (well No. 19 in South Dakota), for example, of 20,000 yr. When both the dedolomitization reaction and sulfate reduction were corrected, the water from the Philip well was found to be younger, about 16,800 yr old (table 22).

The curve in figure 50 shows the calculated ^{14}C content along a hypothetical flow path to the Dupree well (well No. 20 in South Dakota). The ^{14}C content was calculated using the computed mass transfer to the Dupree well and by assuming constant relative rates of reaction in proportion to the computed mass transfer. Although the curve in figure 50 is based on the mass transfer to the Dupree well, similar variation is expected for other waters that are affected predominantly by the dedolomitization reaction. Modern waters will have measured ^{14}C contents similar to those along the curve as a function of anhydrite dissolution. Older waters have ^{14}C values that plot below the curve. The ratio of the calculated (corrected) and measured ^{14}C at the Dupree well results in an age of about 10,800 yr. Waters with large anhydrite mass transfers and relatively large values of measured ^{14}C, such as Cascade Spring and the Evans Plunge Spring (fig. 50), are interpreted to be either virtually modern or possibly mixtures of older waters that have been contaminated in part with modern soil CO_2 gas. Unfortunately, no tritium data are available for these two waters to check for contamination. Water from Lodgepole Warm Spring (fig. 50) is contaminated with tritium (31.8 TU; see table 11), indicating either a modern water or an older water mixed with a modern source.

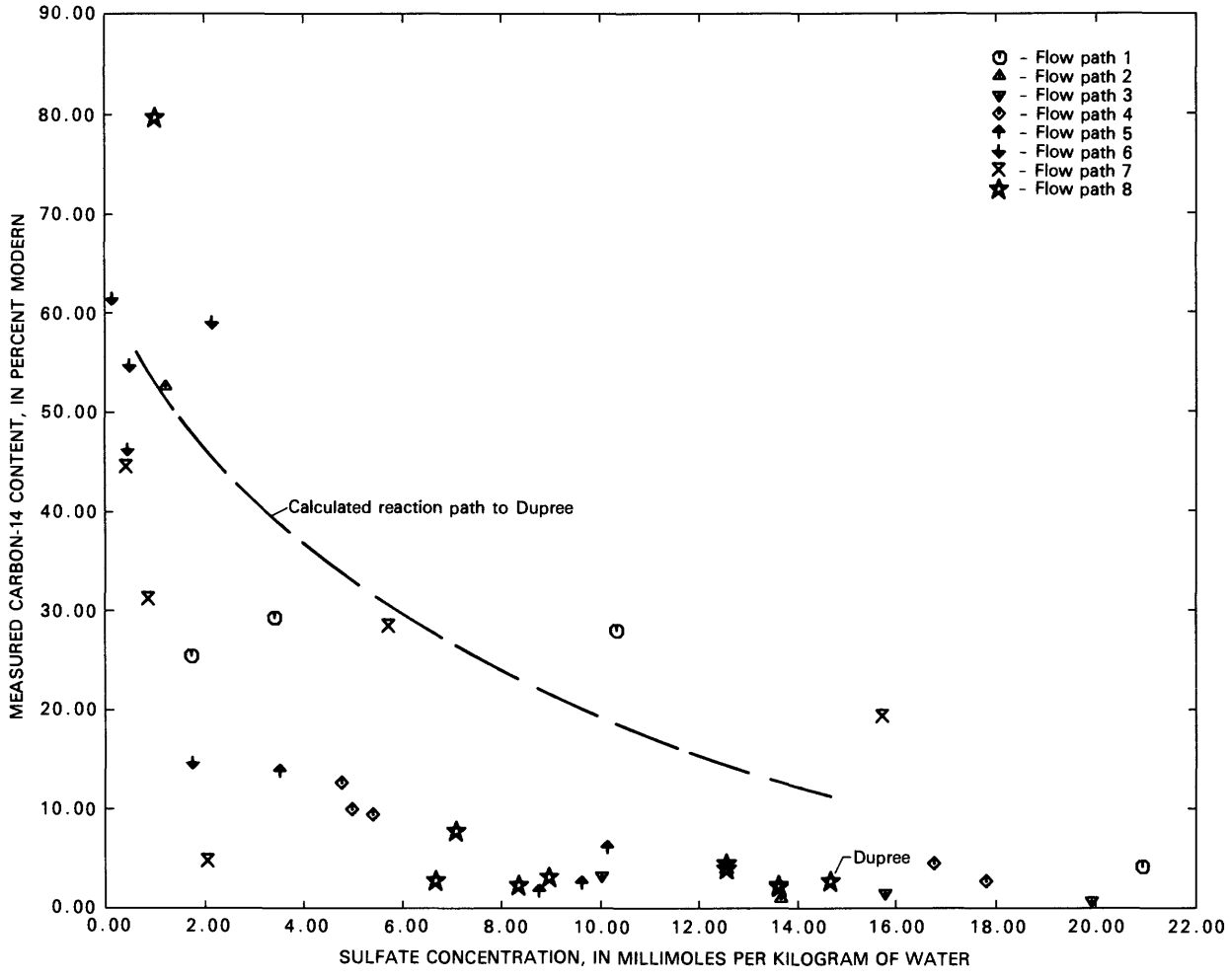

FIGURE 50.—Variation in measured carbon-14 content as a function of concentration of dissolved sulfate along flow paths 1 to 8.

FLOW VELOCITIES CALCULATED FROM CARBON-14 AGES

Calculated ^{14}C ages for selected waters from the Madison aquifer, as well as estimates of the length of the assumed horizontal, straight flow path from the recharge area to the well or spring, calculated flow velocities, and regional hydraulic-conductivity values are summarized in table 3. The flow velocities vary between 7.2 and 86.7 ft/yr, the average being about 43.3 ft/yr. The slowest velocities are found along flow path 5 in northeast Wyoming, where the average is 18.9 ft/yr. Waters along flow paths 2 and 3 have velocities ranging between 23.2 and 82.0 ft/yr. Flow velocities were calculated along flow path 4 to the Belle Creek and Ranch Creek wells and averaged about 39 ft/yr. The velocity to Evans Plunge on flow path 7 (68.2 ft/yr) is high, similar to that at the Sarpy Mine well (82.0 ft/yr), whereas the flow velocity at the Upton well (15.9 ft/yr) on flow path 6 indicates a retardation in flow similar to that suggested by L.F. Konikow (U.S. Geological Survey, written commun., 1984). A greater range of velocities is calculated along flow path 8 (33.3 to 86.7 ft/yr). An average velocity of 57.8 ft/yr probably is most representative of waters along flow path 8.

RATES OF REACTIONS

Average net rates of reaction (table 24) were calculated for the same set of wells or springs for which average flow velocities were calculated (table 3). The average net rate of reaction was calculated using the net mass transfer given in table 21 and the ^{14}C age (table 3). The unit of the rate of the reaction is millimoles per kilogram of water per year and has not been corrected to unit mineral-surface area, as the mineral-surface area in contact with a kilogram of water is not known for the Madison aquifer.

The reactions involving dissolution of anhydrite and halite and organic-matter oxidation are regarded as irreversible in the Madison aquifer, with the exception of a few waters that appear to be anhydrite saturated (fig. 11). The dissolution of dolomite and precipitation of calcite, in contrast, are reversible and are linked to the dissolution of anhydrite. The rates of anhydrite dissolution vary from 2.2 to 32.6×10^{-4} mmol/kg of water per year. The rate variability probably is a function of the availability of anhydrite for dissolution. From laboratory studies, the rate of dissolution of gypsum (Liu and Nancollas, 1971) and presumably anhydrite is expected to be rapid. In the laboratory, stirred suspensions of gypsum crystals reach equilibrium within hours to days depending on the solid surface area/solution ratio. Because waters throughout the Madison aquifer are not in equilibrium with anhydrite, it is evident that mineral abundance is rate limiting. Several waters that indicate very rapid anhydrite dissolution, such as Delzer No. 2 (well No. 8 in South Dakota) and Evans Plunge (spring No. 10 in South Dakota) probably flow in part through bedded evaporites or are receiving waters from other formations. Waters with very slow rates of anhydrite dissolution probably flow through areas where much of the anhydrite has already been dissolved. The slow rates probably represent the dissolution of nodules or pockets of anhydrite within the dolostone that, through dolomite dissolution, occasionally come into contact with the ground water. Once the anhydrite is exposed, dissolution probably is very rapid. From a regional perspective the average effect is one of slow anhydrite dissolution.

As shown in figures 44 and 45, the dolomite and calcite mass transfers are approximately linear functions of the anhydrite mass transfer, and thus a significant correlation among calcite, dolomite, and anhydrite rates is expected. The calculated rates of calcite precipitation vary between 1.6 and 16.3×10^{-4} mmol/kg of water per year, whereas the dolomite dissolution rate varies from 0.3 to 6.6×10^{-4} mmol/kg of water per year.

SUMMARY AND CONCLUSIONS

In interpreting the water chemistry of the Madison aquifer, extensive use has been made of thermodynamic-speciation calculations, mass-balance calculations, and carbon- and sulfur-isotopic data. The major conclusions are as follows:

1. The predominant ground-water reaction in the Madison aquifer is dedolomitization (calcite or aragonite precipitation accompanying dolomite dissolution), which is driven by the irreversible dissolution of anhydrite. Sulfate reduction, $[Ca^{2+}+Mg^{2+}]/Na^{+}$ exchange, and halite dissolution are locally important, particularly in central Montana.

2. The carbon-isotope data, coupled with the mass-balance calculations, indicate that incorporation of magnesium in a secondary mineral, such as through ion exchange or formation of authigenic magnesium-silicate minerals, is an important reaction in parts of central Montana and northeast Wyoming. The indicated loss of magnesium causes additional dissolution of dolomite in accounting for the measured heavy $\delta^{13}C$ values (about -2.0 per mil).

3. With the possible exception of flow path 2 and the beginning of flow path 3, the ground-water system was assumed to be closed to CO_2 gas.

4. The sulfur-isotopic composition of dissolving anhydrite in northeastern Wyoming and western South Dakota, estimated through the modeling process, appears to be significantly lighter than that of Mississippian marine evaporites, indicating, in part, a terrigenous source of sulfur. The lighter sulfur-isotopic values in

TABLE 24.—*Summary of average net rates of reactions*

Spring or well	Spring or well number	State	Flow path	Rate (millimoles per kilogram of water per year)				
				Anhydrite dissolution (10^{-4})	Calcite precipitation (10^{-4})	Dolomite dissolution (10^{-4})	CH_2O oxidation (10^{-4})	Halite dissolution (10^{-4})
Keg Coulee	15	Mont.	2	6.6	6.5	3.2	15.0	23.3
Sarpy Mine	19	Mont.	3	9.1	4.8	2.0	6.4	--
Mysse Flowing Well	20	Mont.	3	9.0	2.4	1.6	4.4	6.8
HTH No. 1	14	Wyo.	4	6.7	3.2	1.3	4.9	1.8
Ranch Creek	23	Mont.	4	5.5	2.5	1.1	2.7	1.5
Belle Creek	24	Mont.	4	6.0	2.9	1.2	3.0	1.5
Delzer No. 2	8	S.Dak.	4	32.6	16.3	6.6	21.3	2.8
Conoco No. 175	11	Wyo.	5	4.5	3.3	.9	1.2	2.2
MKM	10	Wyo.	5	4.6	1.8	.3	3.1	15.3
Shidler	9	Wyo.	5	8.8	2.1	.8	4.1	14.3
Conoco No. 44	8	Wyo.	5	3.8	1.6	.7	.2	5.8
Upton	15	Wyo.	6	2.2	2.3	.9	2.7	--
Evans Plunge	10	S.Dak.	7	24.7	11.0	3.1	18.3	11.8
Kosken	1	S.Dak.	8	6.7	3.4	1.1	2.8	.8
Philip	19	S.Dak.	8	4.2	2.6	.9	5.1	.3
Midland	24	S.Dak.	8	5.3	3.1	1.2	5.4	.3
Murdo	25	S.Dak.	8	6.3	3.2	1.3	4.9	1.0
Hilltop Ranch	22	S.Dak.	8	12.7	7.8	2.4	6.3	4.2
Prince	26	S.Dak.	8	16.6	8.3	3.4	13.7	3.3
Hamilton	21	S.Dak.	8	10.2	5.4	2.2	2.3	.7
Eagle Butte	23	S.Dak.	8	12.1	7.4	3.3	3.0	.9
Dupree	20	S.Dak.	8	13.7	7.6	2.8	4.9	1.9

northeastern Wyoming are thought to be part of a regional depositional pattern for the Madison aquifer, rather than the result of a withdrawal-induced leakage from the Pennsylvanian and Permian Minnelusa Formation.

5. Ground-water ages vary from virtually modern to about 23,000 yr. The ^{14}C ages indicate flow velocities of between 7 to 87 ft/yr. Hydraulic conductivities based on average carbon-14 flow velocities are similar to those based on digital simulation of the flow system (Downey, 1984).

SELECTED REFERENCES

Agnew, A.F., and Tychsen, P.C., 1965, A guide to the stratigraphy of South Dakota: South Dakota State Geological Survey Bulletin 14, 195 p.

Back, William, Hanshaw, B.B., Plummer, L.N., Rahn, P.H., Rightmire, C.T., and Rubin, Meyer, 1983, Process and rate of dedolomitization—Mass transfer and ^{14}C dating in a regional carbonate aquifer: Geological Society of America Bulletin, v. 94, no. 12, p. 1415–1429.

Bischoff, J.L., 1968, Kinetics of calcite nucleation—Magnesium ion inhibition and ionic strength catalysis: Journal of Geophysical Research, v. 73, no. 10, p. 3315–3322.

Blankennagel, R.K., Howells, L.W., Miller, W.R., and Hansen, C.V., 1979, Preliminary data for Madison Limestone test well 3, NW¼SE¼ sec. 35, T. 2 N., R. 27 E., Yellowstone County, Montana: U.S. Geological Survey Open-File Report 79-745, 201 p.

Bottinga, Y., 1969, Calculated fractionation factors for carbon and hydrogen isotope exchange in the system calcite-CO_2-graphite-methane-hydrogen and water vapor: Geochimica et Cosmochimica Acta, v. 33, no. 1, p. 49–64.

Brown, D.L., Blakennagel, R.K., MacCary, L.M., Peterson, J.A., 1982, Correlation of paleostructure and sediment deposition in the Madison Limestone and associated rocks in parts of Montana, North Dakota, South Dakota, Wyoming, and Nebraska: U.S. Geological Survey Open-File Report 82-906, 80 p.

Brown, Eugene, Skougstad, M.W., and Fishman, M.J., 1970, Methods for collection and analysis of water samples for dissolved minerals and gases: U.S. Geological Survey, Techniques of Water-Resources Investigations, chap. C1, *in* book 5, Laboratory Analysis, 160 p.

Brown, P.M., Miller, J.A., and Swain, F.M., 1972, Structural and stratigraphic framework, and spatial distribution of permeability of the Atlantic Coastal Plain, North Carolina to New York: U.S. Geological Survey Professional Paper 796, 79 p.

Busby, J.F., Lee, R.W., and Hanshaw, B.B., 1983, Major geochemical processes related to the hydrology of the Madison Aquifer System and associated rocks in parts of Montana, South Dakota, and Wyoming: U.S. Geological Survey Water-Resources Investigations Report 83-4093, 180 p.

Busenberg, E., Plummer, L.N., and Parker, V.B., 1984, The solubility of strontianite ($SrCO_3$) in CO_2-H_2O solutions between 2 and 91 °C,

the association constants of $SrHCO_3^+$ (aq) and $SrCO_3^0$(aq) between 5 and 80 °C, and an evaluation of the thermodynamic properties of Sr^{2+} (aq) and $SrCO_{3(cr)}$ at 25 °C and 1 atm total pressure: Geochimica et Cosmochimica Acta, v. 48, no. 10, p. 2021–2035.

Claypool, G.E., Holser, W.T., Kaplan, I.R., Sakai, H., and Zak, I., 1980, The age curves of sulfur and oxygen isotopes in marine sulfate and their mutual interpretation: Chemical Geology, v. 28, no. 3–4, p. 199–260.

Downey, J.S., 1982, Machine-readable data files from the Madison Limestone and northern Great Plains Regional Aquifer System Analysis project, Montana, Nebraska, North Dakota, South Dakota, and Wyoming: U.S. Geological Survey Water-Resources Investigations Report 82-4107, 26 p.

_____ 1984, Geohydrology of the Madison and associated aquifers in parts of Montana, North Dakota, South Dakota, and Wyoming: U.S. Geological Survey Professional Paper 1273-G, 47 p.

_____ 1986, Geohydrology of bedrock aquifers of the Northern Great Plains in parts of Montana, North Dakota, South Dakota, and Wyoming: U.S. Geological Survey Professional Paper 1402-E, 87 p.

Fenchel, T., and Blackburn, T.H., 1979, Bacteria and mineral cycling: New York, Academic Press, 225 p.

Gallo, G., 1935, Equilibrio fra sulfato distronzio ed hequa alle varia temperatura—A: Annali di Chimica Applicata, v. 25, p. 628–631.

Grossman, I.G., 1968, Origin of the sodium sulfate deposits of the northern Great Plains of Canada and the United States, *in* Geological Survey Research 1968: U.S. Geological Survey Professional Paper 600-B, p. B104–B109.

Hach Chemical Co., 1982, Water analysis handbook: Ames, Iowa, 316 p.

Hanshaw, B.B., Back, William, and Deike, R.G., 1971, A geochemical hypothesis for dolomitization by ground water: Economic Geology, v. 66, no. 5, p. 710–724.

Hanshaw, B.B., Back, William, and Rubin, Meyer, 1964, Radiocarbon determinations for estimating ground-water flow velocities in central Florida: Science, v. 148, no. 3669, p. 494–495.

Harvie, C.E., and Weare, J.H., 1980, The prediction of mineral solubilities in natural waters—The Na-K-Mg-Ca-Cl-SO_4-H_2O system from zero to higher concentrations at 25 °C: Geochimica et Cosmochimica Acta, v. 44, no. 7, p. 981–997.

Hoefs, J., 1973, Stable isotope geochemistry: New York, Springer-Verlag, 140 p.

Jones, B.F., and Weir, A.H., 1983, Clay minerals of Lake Abert, an alkaline, saline lake: Clays and Clay Minerals, v. 31, no. 3, p 161–172.

Kinsman, D.J., 1969, Modes of formation, sedimentary associations, and diagnostic features of shallow-water and supratidal evaporites: Bulletin of the American Association of Petroleum Geologists, v. 53, no. 4, p. 830–841.

Konikow, L.F., 1976, Preliminary digital model of ground-water flow in the Madison Group, Powder River basin and adjacent areas, Wyoming, Montana, South Dakota, North Dakota, and Nebraska: U.S. Geological Survey Water Resources Investigations Report 63-75, 44 p.

Linke, W.F., and Seidell, A., 1965, Solubilities, inorganic and metal-organic compounds, v. 2, K–Z: Washington, D.C., American Chemical Society, 1914 p.

Liu, S.T., and Nancollas, G.H., 1971, The kinetics of dissolution of calcium sulfate dihydrate: Journal of Inorganic Nuclear Chemistry, v. 33, p. 2311–2316.

MacCary, L.M., 1981, Apparent water resistivity, porosity and groundwater temperature of the Madison Limestone and underlying rocks in parts of Montana, North Dakota, and Wyoming: U.S. Geological Survey Open-File Report 81-269, 35 p.

MacCary, L.M., Cushing, E.M., and Brown, D.L., 1983, Potentially favorable areas for large-yield wells in the Red River Formation and Madison Limestone in parts of Montana, North Dakota, South Dakota, Wyoming, and Nebraska: U.S. Geological Survey Professional Paper 1273-E, p. E1–E13.

Marshall, W.L., and Slusher, R., 1966, Thermodynamics of calcium sulfate dihydrate in aqueous sodium chloride solutions, 0–110°: Journal of Physical Chemistry, v. 70, no. 12, p. 4015–4027.

Ohmoto, H., and Rye, R.O., 1979, Carbon and sulfur isotopes, *in* Barnes, A. L., ed., Geochemistry of hydrothermal ore deposits (2d ed.): New York, Wiley-Interscience, p. 509–567.

Olson, G.J., Dockins, W.S., McFeters, G.A., and Iverson, W.P., 1982, Sulfate reducing bacteria from deep aquifers in Montana: Geomicrobiology Journal, v. 2, no. 4, p. 327–340.

Parker, V.B., Wagman, D.D., and Evans, W.H., 1976, Selected values of chemical thermodynamic properties: National Bureau of Standards, Technical Note 270-6, 106 p.

Parkhurst, D.L., Plummer, L.N., and Thorstenson, D.C., 1982, BALANCE—A computer program for calculating mass transfer for geochemical reactions in ground water: U.S. Geological Survey Water-Resources Investigation Report 82-14, 29 p.

Parkhurst, D.L., Thorstenson, D.C., and Plummer, L.N., 1980, PHREEQE—A computer program for geochemical calculations: U.S. Geological Survey Water-Resources Investigations Report 80-96, 210 p.

Pearson, F.J., Jr., Fisher, S.W., and Plummer, L.N., 1978, Correction of ground-water chemistry and carbon isotopic composition for effects of CO_2 outgassing: Geochimica et Cosmochimica Acta, v. 42., no. 12, p. 1799–1807.

Pearson, F.J., Jr., and Rightmire, C.T., 1980, Sulfur and oxygen isotopes in aqueous sulfur compounds, *in* P. Fritz and J. Ch. Fontes, eds., Handbook of environmental isotope geochemistry: New York, Elsevier Scientific Publishing Co., p. 227–258.

Pearson, F.J., Jr., and White, D.E., 1967, Carbon-14 ages and flow rates of water in Carrizo Sand, Atascosa County, Texas: Water Resources Research, v. 3, no. 1, p. 251–261.

Peterson, J.A., 1978, Subsurface geology and porosity distribution, Madison Limestone and underlying formations, Powder River basins, northeastern Wyoming, and southeastern Montana and adjacent areas: U.S. Geological Survey Open-File Report 78-783, 32 p.

_____ 1981, Stratigraphy and sedimentary facies of the Madison Limestone and associated rocks in parts of Montana, Nebraska, North Dakota, South Dakota, and Wyoming: U.S. Geological Survey Professional Paper 1273-A, 34 p.

Plummer, L.N., and Busenberg, Eurybiades, 1982, The solubilities of calcite, aragonite and vaterite in CO_2-H_2O solutions between 0 and 90 °C, and an evaluation of the aqueous model for the system $CaCO_3$-CO_2-H_2O: Geochimica et Cosmochimica Acta, v. 46, no. 6, p. 1011–1040.

Plummer, L.N., Jones, B.F., and Truesdell, A.H., 1976, WATEQF—A FORTRAN IV version of WATEQ, a computer program for calculating chemical equilibria of natural waters: U.S. Geological Survey Water-Resources Investigations Report 76-13, 61 p., [available from National Technical Information Service, Springfield, Virginia 22161 as Report PB-261027].

Plummer, L.N., Parkhurst, D.L., and Thorstenson, D.C., 1983, Development of reaction models for groundwater systems: Geochimica et Cosmochimica Acta, v. 47, no. 4, p. 665–685.

Robie, R.A., Hemingway, B.S., and Fisher, J.R., 1978, Thermodynamic properties of minerals and related substances at 298.15 °K and 1 bar (10^5 pascal) pressure and at higher temperatures: U.S. Geological Survey Bulletin 1452, 456 p.

Rose, P.R., 1976, Mississippian carbonate shelf margins, western U.S.: U.S. Geological Survey Journal of Research, v. 4, no. 4, p. 449–466.

Rye, R.O., Back, William, Hanshaw, B.B., Rightmire, C.T., and Pearson, F.J., Jr., 1981, The origin and isotopic composition of dissolved sulfide in groundwater from carbonate aquifers in Florida

and Texas: Geochimica et Cosmochimica Acta, v. 45, no. 10, p. 1941–1950.

Sales, J.K., 1968, Crustal mechanics of Cordilleran foreland deformation—A regional and scale-model approach: Bulletin of the American Association of Petroleum Geologists, v. 52, no. 10. p. 2016–2044.

Sandberg, C.A., 1961, Distribution and thickness of Devonian rocks in Williston basin in central Montana and north-central Wyoming: U.S. Geological Survey Bulletin 112-D, p. 105–127.

_____ 1962, Geology of the Williston basin, North Dakota, Montana, and South Dakota, with reference to subsurface disposal of radioactive wastes: U.S. Geological Survey TEI-809, 148 p.

Sando, W.J., 1968, Mississippian depositional provinces in the northern Cordilleran region, *in* Geological Survey Research 1967: U.S. Geological Survey Professional Paper 575-D, p. D29–D38.

_____ 1974, Ancient solution phenomena in the Madison Limestone (Mississippian) of north-central Wyoming: U.S. Geological Survey Journal of Research, v. 2, no. 2, p. 133–141.

_____ 1976a, Madison Limestone, east flank of Bighorn Mountins, Wyoming: Wyoming Geological Association Annual Field Conference, 28th, 1976, Guidebook, p. 45–52.

_____ 1976b, Mississippian history of the northern Rocky Mountains region: U.S. Geological Survey Journal of Research, v. 4, no. 3, p. 317–338.

Sando, W.J., and Dutro, J.T., Jr., 1974, Type sections of the Madison Group (Mississippian) and its subdivisions in Montana: U.S. Geological Survey Professional Paper 842, 22 p.

Slack, P.B., 1981, Paleotectonics and hydrocarbon accumulation, Powder River basin, Wyoming: Bulletin of the American Association of Petroleum Geologists, v. 65, no. 4, p. 730–743.

Smith, D.L., 1972, Depositional cycles of the Lodgepole Formation (Mississippian) in central Montana: Montana Geological Society Annual Field Conference, 21st, 1972, Guidebook, p. 27–36.

Smith, H.J., 1918, On equilibrium in the system: Ferrous carbonate, carbon dioxide, and water: Journal of the American Chemical Society, v. 40, p. 879–885.

Smith, R.M., and Martell, A.E., 1976, Inorganic complexes, v. 4 *of* Critical stability constants: New York, Plenum Press, 257 p.

Stearns, D.W., Sacrison, W.R., and Hanson, R.C., 1975, Structural history of southwestern Wyoming as evidenced from outcrop and seismics, *in* Bolyard, D.W., ed., Symposium on Deep Drilling Frontiers in the Central Rocky Mountains, Steamboat Springs, Colo., 1975, Proceedings: Denver, Rocky Mountain Association of Geologists, p. 9–20.

Stone, D.S., 1969, Wrench faulting and Rocky Mountain tectonics: Wyoming Geological Association Earth Science Bulletin, v. 2, no. 2, p. 27–41.

Swenson, F.A., 1968, New theory of recharge in the artesian basin of the Dakotas: Geological Society of America Bulletin, v. 79, no. 1, p. 163–182.

Thayer, P.A., 1981, Petrology and petrography for U.S. Geological Survey test wells 1, 2, and 3 in the Madison Limestone in Montana and Wyoming: U.S. Geological Survey Open-File Report 81-221, 82 p., 3 pl.

Wigley, T.M.L., and Muller, A.B., 1981, Fractionation corrections in radiocarbon dating: Radiocarbon, v. 23, no. 2, p. 173–190.

Wigley, T.M.L., Plummer, L.N., and Pearson, F.J., 1978, Mass transfer and carbon isotope evolution in natural water systems: Geochimica et Cosmochimica Acta, v. 42, no. 8, p. 1117–1139.

_____ 1979, Errata: Geochimica et Cosmochimica Acta, v. 43, p. 1395.

Wood, W.W., 1976, Guidelines for collection and field analysis of groundwater samples for selected unstable constituents: U.S. Geological Survey Techniques of Water-Resources Investigations, chap. D2 *in* book 1, 24 p.

SELECTED SERIES OF U.S. GEOLOGICAL SURVEY PUBLICATIONS

Periodicals

Earthquakes & Volcanoes (issued bimonthly).
Preliminary Determination of Epicenters (issued monthly).

Technical Books and Reports

Professional Papers are mainly comprehensive scientific reports of wide and lasting interest and importance to professional scientists and engineers. Included are reports on the results of resource studies and of topographic, hydrologic, and geologic investigations. They also include collections of related papers addressing different aspects of a single scientific topic.

Bulletins contain significant data and interpretations that are of lasting scientific interest but are generally more limited in scope or geographic coverage than Professional Papers. They include the results of resource studies and of geologic and topographic investigations; as well as collections of short papers related to a specific topic.

Water-Supply Papers are comprehensive reports that present significant interpretive results of hydrologic investigations of wide interest to professional geologists, hydrologists, and engineers. The series covers investigations in all phases of hydrology, including hydrogeology, availability of water, quality of water, and use of water.

Circulars present administrative information or important scientific information of wide popular interest in a format designed for distribution at no cost to the public. Information is usually of short-term interest.

Water-Resources Investigations Reports are papers of an interpretive nature made available to the public outside the formal USGS publications series. Copies are reproduced on request unlike formal USGS publications, and they are also available for public inspection at depositories indicated in USGS catalogs.

Open-File Reports include unpublished manuscript reports, maps, and other material that are made available for public consultation at depositories. They are a nonpermanent form of publication that may be cited in other publications as sources of information.

Maps

Geologic Quadrangle Maps are multicolor geologic maps on topographic bases in 7 1/2- or 15-minute quadrangle formats (scales mainly 1:24,000 or 1:62,500) showing bedrock, surficial, or engineering geology. Maps generally include brief texts; some maps include structure and columnar sections only.

Geophysical Investigations Maps are on topographic or planimetric bases at various scales; they show results of surveys using geophysical techniques, such as gravity, magnetic, seismic, or radioactivity, which reflect subsurface structures that are of economic or geologic significance. Many maps include correlations with the geology.

Miscellaneous Investigations Series Maps are on planimetric or topographic bases of regular and irregular areas at various scales; they present a wide variety of format and subject matter. The series also includes 7 1/2-minute quadrangle photogeologic maps on planimetric bases which show geology as interpreted from aerial photographs. Series also includes maps of Mars and the Moon.

Coal Investigations Maps are geologic maps on topographic or planimetric bases at various scales showing bedrock or surficial geology, stratigraphy, and structural relations in certain coal-resource areas.

Oil and Gas Investigations Charts show stratigraphic information for certain oil and gas fields and other areas having petroleum potential.

Miscellaneous Field Studies Maps are multicolor or black-and-white maps on topographic or planimetric bases on quadrangle or irregular areas at various scales. Pre-1971 maps show bedrock geology in relation to specific mining or mineral-deposit problems; post-1971 maps are primarily black-and-white maps on various subjects such as environmental studies or wilderness mineral investigations.

Hydrologic Investigations Atlases are multicolored or black-and-white maps on topographic or planimetric bases presenting a wide range of geohydrologic data of both regular and irregular areas; principal scale is 1:24,000 and regional studies are at 1:250,000 scale or smaller.

Catalogs

Permanent catalogs, as well as some others, giving comprehensive listings of U.S. Geological Survey publications are available under the conditions indicated below from the U.S. Geological Survey, Books and Open-File Reports Section, Federal Center, Box 25425, Denver, CO 80225. (See latest Price and Availability List.)

"Publications of the Geological Survey, 1879- 1961" may be purchased by mail and over the counter in paperback book form and as a set of microfiche.

"Publications of the Geological Survey, 1962- 1970" may be purchased by mail and over the counter in paperback book form and as a set of microfiche.

"Publications of the U.S. Geological Survey, 1971- 1981" may be purchased by mail and over the counter in paperback book form (two volumes, publications listing and index) and as a set of microfiche.

Supplements for 1982, 1983, 1984, 1985, 1986, and for subsequent years since the last permanent catalog may be purchased by mail and over the counter in paperback book form.

State catalogs, "List of U.S. Geological Survey Geologic and Water-Supply Reports and Maps For (State)," may be purchased by mail and over the counter in paperback booklet form only.

"Price and Availability List of U.S. Geological Survey Publications," issued annually, is available free of charge in paperback booklet form only.

Selected copies of a monthly catalog "New Publications of the U.S. Geological Survey" available free of charge by mail or may be obtained over the counter in paperback booklet form only. Those wishing a free subscription to the monthly catalog "New Publications of the U.S. Geological Survey" should write to the U.S. Geological Survey, 582 National Center, Reston, VA 22092.

Note.--Prices of Government publications listed in older catalogs, announcements, and publications may be incorrect. Therefore, the prices charged may differ from the prices in catalogs, announcements, and publications.